The influence of early life nutrition on adipose tissue development is modulated by age in sheep

By

Ahmad Alhaddad

Division of Child Health, Obstetrics and Gynaecology

School of Medicine Faculty of Medicine and Health Sciences

University of Nottingham

August, 2018

Abstract

Introduction

Non-shivering thermogenesis in brown adipose tissue (BAT), mediated by a unique uncoupling protein (UCP1), is essential for metabolic adaptation birth in large mammals such as sheep. BAT then undergoes substantial changes as UCP1 is gradually lost and replaced with white adipose tissue (WAT) which mainly acts as a fat storage tissue. Given BAT can be retained into later life a better understanding of this process could enable the maintenance of BAT function by modifying its transition to WAT in early life. Ultimately this could provide a potential target to prevent obesity in adulthood.

Methods

It remains unclear as to whether anatomical location determines a fat depots response to changes in maternal diet during postnatal development. I, therefore, carried out a study that entailed the data mining of microarrays and lipidomic data generated from the major fat depots in young sheep. The sternal, perirenal and epicardial depots were studied, which all possess large amounts of UCP1 at birth and were compared with the subcutaneous depot which has little UCP1 and the omental depot which only appears after birth and does not contain UCP1. This investigation was undertaken by applying machine learning algorithms and weighted gene co-expression networks analyses, during the specific time period of 7 to 28 days of age, which is characterised by the transition of BAT into WAT in young sheep. In addition, I examined whether modifying the mother's milk fat content through fatty acid supplementation, could increase the fatty acid availability and delay the rate at which UCP1 was

lost. This was achieved by investigating the impact of supplementing the maternal diet with 3% of canola oil from the day of delivery through the first 28 days of lactation.

Results

By using the gene network analyses, I established that each depot exhibited different gene expression profiles during development. This further demonstrated that the anatomical location modulated this process as each depot displayed succinct arrays of modules consisting of co-expressed gene indicating their unique biological function. It included the capability of mitochondrial biogenesis which was associated with adipocyte differentiation in response to local environmental stimuli. Brown like depots were also distinguished functionally, for lipid metabolism in perirenal, angiogenesis in sternal, and cardiomyocyte cell differentiation in epicardial. In white adipocyte depots, i.e. omental and subcutaneous, high-lighted genes were mainly involved in growth and cell maturation function.

In addition, the result of supplementing the maternal diet with 3% of canola oil revealed a lower rate of loss of mitochondrial gene expression within the sternal, perirenal, omental and subcutaneous depots, specifically in BAT depots (i.e. perirenal and sternal), that enables a high capacity of non-shivering thermogenesis in early life. The lipidomic analyses further demonstrated that the perirenal depot was the only one to exhibit a modified lipid profile to the dietary intervention at 28 days of age when BAT was mostly converted into WAT.

Conclusion

In conclusion, manipulation of the maternal diet by enhancing milk fatty acid content in early life delays losing of mitochondrial genes expression, in the offsprings adipose tissue. This response is modulated by age and anatomical location. These findings suggest that modulating the maternal diet impacts on postnatal fat development, for which the longer term outcomes now need establishing.

Acknowledgements

Firstly, I thank my God who gave me the health, strength and patience to accomplish such great work. I also thank the Government of Kuwait, represented by the Ministry of Social Affairs and Work, for funding me during my PhD journey.

In addition to my name, there is a list of names who have made great contributions and helped me during all the PhD stages to accomplish this task.

At the top of this list, my main supervisor Professor Michael Symonds is the person that I would like to give sincere thanks and praise to in regard to what he had of great positive influence during my journey, through his faith in my abilities and kept motivating me until the last word in writing this thesis, providing all the means of support both in terms of academic and personal level.

I am also greatly indebted to my second supervisor, Professor Helen Budge, who offered me the care and guidance, and valuable tips and comments that helped me a lot to gain and develop new skills in the research felid, which make me more confident in overcoming many difficulties.

I can't forget the great and continuous efforts that have been made by Dr Hernan Fainberg, from the beginning of my first year, so I would like to thank him for all his assistance, and support in acquiring the basic skills in the principles of statistics by providing me with valuable tips during my scientific journey.

Dr Ian Bloor, Mr Mark Pope, Mrs Vicky Wilson, thanks for your technical support. And I would like to thank the camaraderie of my colleagues in the Division of Child Health, Obstetrics and Gynaecology for the atmosphere as one family.

And last but not least, I'm really thankful to my family, the people who mean the most to me, for their continued support in the worst of my circumstances. In particular my mother Jamila Alhaddad, who was praying to God to facilitate things even during her limited time and preoccupation with taking care of the other members of the family. And I would also like to thank my father Hamza Alhaddad for his faith in me. I would like to thank my brothers Abdallah and Abdulrahman and my dear sister Asma; the people that I can rely on and resort to in times of adversity, and I find them beside me in all cases and always urging me to succeed, excel and achieve all my dreams and aspirations.

And from the bottom of my heart, thanks to someone very special to me, the person without whose support I couldn't even have started my journey, the person who has done a great job and stayed behind the scenes, my wonderful wife, thanks for always believing in me, thanks for your endless love, and for all that you have done for us, for our comfort, all the happiness that you give to me and your care for our children, and I know how tiring it is looking after the kids alone, I'm proud of you.

I also thank my children Layan, Yousef, and Jawan who are the reason behind taking the decision to start my PhD, thanks for your encouragement, believing in me, and for being patient while I'm studying abroad, I can never say how grateful I am to all of you.

Declaration

The work in this thesis was performed within the Academic Division of Child Health, Obstetrics and Gynaecology at Nottingham University Hospital, Queens Medical Centre, Nottingham, between November 2013 and April 2018.

Unless otherwise stated, this thesis illustrates my own work completed under the supervision of Professor Michael Symonds, Professor Helen Budge of the University of Nottingham.

This thesis is an accurate representation of the work performed and no other study reproducing this work, to my knowledge, has been carried out within the University of Nottingham.

Ahmad Alhaddad

August 2018

Presentations

Alhaddad, A.; Symonds, M. and Budge, H. Effect of early life nutritional intervention on brown adipose tissue development. M&HS Faculty Postgraduate Research Forum, School of Medicine, University of Nottingham. June 2015.

Alhaddad, A.; Symonds, M. and Budge. The effects of maternal diet intervention on offering adipose tissue lipid profile. Division of Child Health, Obstetrics and Gynaecology, School of Medicine, University of Nottingham, March 2016.

Alhaddad, A.; Symonds, M. and Budge, H . the dynamic change in gene expression profile of brown adipose tissue in early life . Division of Child Health, Obstetrics and Gynaecology, School of Medicine, University of Nottingham December 2016.

Alhaddad , A.; Symonds, M. and Budge, H, the impact of canola oil on the perirenal adipose tissue .Division of Child Health, Obstetrics and Gynaecology, School of Medicine, University of Nottingham. March 2017.

Alhaddad, A.; Symonds, M. and Budge, H Gene expression profiling and function of brown adipose tissue. Sue Watson Postgraduate Presentation, School of Medicine, University of Nottingham. July 2017.

Alhaddad, A.; Symonds, M. and Budge, H,, .The effects of supplementing ewe diet during lactation with fatty acids on sternal gene expression profile. Division of Child Health, Obstetrics and Gynaecology, School of Medicine, University of Nottingham. December 2017.

Alhaddad, A.; Symonds, M. and Budge, H. The effects of supplementing the maternal diet during lactation on offspring's transcriptional landscape of the major brown adipose depots during early life. Division of Child Health, Obstetrics and Gynaecology, School of Medicine, University of Nottingham. February 2018.

Alhaddad , A.; Symonds, M. and Budge, H.the impact of anatomical location in early life of adipose tissue development. Division of Child Health, Obstetrics and Gynaecology, School of Medicine, University of Nottingham. April 2018.

Poster presentations

Alhaddad , A.; Symonds, M. and Budge, Effect of early life nutritional intervention on brown adipose tissue development. M&HS Faculty Postgraduate Research Forum, School of Medicine, University of Nottingham. June 2015.

Publications

Fainberg, H.; Ojha, S.; Alhaddad, A.; Alagal, R.; Birtwistle, M.; Davies, G.; Castellanos, M.; May, S.; Pelella, G.; Lotto, A.; Sacks, H.; Budge, H. and Symonds, M. Depot specific transcriptional signatures of adipose tissue in sheep and humans during early life. Endocrine Abstracts, 2016. ISSN 1470-3947 (print).

Fainberg, F.; Alhaddad, A.; Alagal, R.; Birtwistle, M.; Davies, G.; Castellanos, M.; May, S.; Sacks, H.; Budge, H. and Symonds, M. Transcriptional landscape of the major adipose depots during early life reveals unique pathways during development. The FASEB Journal, 2017. 31:1_supplement, 886.10-886.10.

Fainberg, F.; Birtwistle, M.; Alagal, R.; Alhaddad, A.; Davies, G.; Castellanos, M.; May, S.; Sacks, H.; Budge, H. and Symonds, M. Transcriptional

analyses of adipose tissue during development reveals depot-specific responsiveness to maternal dietary supplementation. Scientific Reports (Nature Publisher Group), 8, 1-11.

Table of contents

List of figures

List of tables

List of abbreviations

Abbreviation	Definition
AA	Arachidonic acid
aBAT	Axillary brown depot
AC	Adenylyl cyclase
ACC	Acetyl-coenzyme a carboxylase
ACOT11	Acyl-coenzyme A thioesterase 11
AL3+	Aluminium ions
ALA	α-linolenic acid
APS	Ammonium persulphate
ATP	Adenosine triphosphate
AUC	Area under the curve
BAT	Brown adipose tissue
BBB	Blood–brain barrier
BCA	Bicinchoninic acid
BH	Biohydrogenation
BLAST	Basic Local Alignment Search Tool

BMI	Body Mass Index
BMR	Basal metabolic rate
bp	Base pair
BRITE	Brown in white adipocytes
BSA	Bovine serum albumin
C	Catalytic subunits
cAMP	Cyclic adenosine monophosphate
cBAT	Cervical brown depot
cDNA	Complementary deoxyribonucleic acid
Cf	Final concentration
Ci	Initial concentration
CLA	Conjugated linoleic acid
COX1	Cytochrome c oxidase 1
COX2	Cytochrome c oxidase 2
Cp	Crossing point
CRAN	Comprehensive R Archive Network
Ct	Cycle threshold
CVD	Cardiovascular disease

DAB	3,3′-diaminobenzidine
DGLA	Dihomo-gamma-linolenic acid
DHA	Docosahexaenoic acid
DIT	Diet-induced thermogenesis
DNA	Deoxyribonucleic acid
dNTPs	Deoxyribonucleoside triphosphates
DOHaD	Developmental Origins of Health and Disease
E	Efficiency of the reaction
EAT	Epicardial adipose tissue
EDTA	Ethylenediaminetetraacetic acid
EFAs	Essential fatty acids
EFSA	European Food Safety Authority
ELOV3	Elongation of very long chain fatty acids 3
EPA	Eicosapentaenoic acid
eWAT	Epididymal adipose depot
FABP	Fatty acids binding proteins
FABP3	Fatty acid binding protein 3
FADS2	Fatty acid desaturase 2

FAS	fatty acid synthetase
FAs	Fatty acids
FDG	18 F-fludeoxyglucose
FDR	False discovery rate
FFAs	Free fatty acids
GC	Guanine/cytosine
gDNA	Genomic deoxyribonucleic acid
GWAS	Genome-wide association studies
H&E	Haematoxylin and Eosin
HIRE	Heat-induced epitope retrieval
HOXC9	Homeobox C9
HRP	Horseradish peroxidase
HSCIC	Health and Social Care Information Centre
HSE	Health Survey for England
HSL	Hormone sensitive lipase
iBAT	Interscapular brown depot
IGF-1	Insulin-like growth factor 1
IHC	Immunohistochemistry

LA	linoleic acid
LCFAs	Long-chain fatty acids
LCPUFAs	Long-chain polyunsaturated fatty acids
LEAR	Low erucic acid rapeseed
LPL	Lipoprotein lipase
M	Stability value
mBAT	Mediastinal brown depot
MCFAs	Medium-chain fatty acids
MG	Monoacylglycerol
ML	Machine learning
MSCs	Mesenchymal stem cells
MUFAs	Monounsaturated fatty acids
mWAT	Mesenteric adipose depot
MYF5-	Myogenic factor 5- progenitors
MYF5+	Myogenic factor 5+ progenitors
NASC	Nottingham Arabidopsis Stock Centre
NCBI	National Center for Biotechnology Information
NE	Norepinephrine

NEFAs	Non-esterified fatty acids
NICE	National Institute for Clinical Excellence
NRTC	No-reverse transcriptase control
NST	Nonshivering thermogenesis
NTC	No-template control
PAT	Perirenal adipose tissue
PCA	Principal component analysis
PCR	Polymerase chain reaction
PET	Positron emission tomography
PG	prostaglandins
PGC-1α	Peroxisome proliferator-activated receptor gamma coactivator 1-alpha
PIC	Preinitiation complex
PKA	Protein kinase
PPARγ	Peroxisome proliferator-activated receptor gamma
prBAT	Perirenal adipose depot
PRDM16	PR domain containing 16,
PRLR	Prolactin receptor

PSOL	Positive sample-only learning
PUFAs	Polyunsaturated fatty acids
QC	Quality control
qPCR	Quantitative polymerase chain reaction
R	Regulatory subunits
R2	Correlation coefficient
RF	Random forest
RIN	RNA integrity number
RIP140	Receptor-interacting protein 140
RT-	Non-reverse transcription enzyme control
RT+	Reverse transcription enzyme control
RT-PCR	Reverse transcriptase-polymerase chain reaction
SCD1	Stearoyl-CoA desaturase-1
SDS	Sodium dodecyl sulphate
SEM	Standard error of the mean
SFAs	Saturated fatty acids
SHFAs	Short-chain fatty acids
SHOX2	Short stature homeobox 2

SNS	Sympathetic nervous system
TEMED	Tetramethylethylenediamine
TFAs	trans fatty acids
TGs	Triglycerides
Tris	Tris(hydroxymethyl)aminomethane
TRPs	Transient receptor potential channels
TTBS	Tris-buffered saline with Tween® 20
UCP1	Uncoupling Protein 1
USFAs	Unsaturated fatty acids
VDAC	Voltage-dependent anion channels
Vf	Final volume
Vi	Initial volume
VLDL	Very low-density proteins
WAT	White adipose tissue
WGNCA	Weighted correlation network analysis
WHO	World Health Organization
WOF	World Obesity Federation
ω-3	Omega-3 fatty acids

ω-6	Omega-6 fatty acids
ZFP36L1	ZFP36 Ring Finger Protein Like

1 Introduction

Obesity is increasingly becoming a health issue worldwide. An individual with a body mass index (BMI) higher than 25 is defined as overweight, and those above 29.9 they are considered to be obese (WHO, 2015). I will now focus on reviewing recent literature regarding the topic of obesity, and more specifically the role of brown adipose tissue (BAT). The effects of early-life nutritional interventions on BAT development will also be considered as part of my thesis.

1.1 Overweight and obesity

According to the World Health Organisation (WHO, 2015), obesity is defined as an excessive accumulation of fat that presents a risk to health and this is now considered to be a major public health problem. There is a need to understand the consequences of being either overweight or obese in a detailed manner, as it is not limited to any specific country. It is an issue that has wide-ranging implications all over the world. The incidence of obesity worldwide tripled between 1975 and 2016 (WHO, 2016), and it has been estimated that up to 1.9 billion adults are now overweight (39% of all men and 40% of all women). Of these over 650 million adults were found to be obese according to the WHO classification (WHO, 2016). The number of overweight children under the age of five is estimated to be over 41 million; half of these children live in Asia and one quarter in Africa (WHO, 2016). India is considered, among countries of the developing world, the nation with the most significant proportion of obese people (WHO, 2016). Obesity is also an increasing issue in China, where 100 million people are considered to be obese. Other countries showing similar trends include Germany (Freemark, 2010), the United Kingdom (Wright and Harwood, 2012) and Brazil (Nee, 2013). Kuwait is another country showing a high risk of obesity, as the last record of the World Obesity Federation (WOF) static in 2014 indicated that almost half of men and around 30% of women over 18 were classified as overweight, with nearly the same percentage of men and woman classified as obese (see Figure 1-1).

During the last decade, the number of obese/overweight men and women in the United Kingdom has increased from 13.2% and 16.4% to 23.8% and 26% respectively (HSCIC, 2014). In 2014, 22.5% of children (aged 4–5) and 33.5% of children (aged 6) were categorised as obese or overweight. Moreover, obese children are more likely to become obese adults and have a higher risk of developing diseases such as hypertension, non-alcoholic fatty liver and type 2 diabetes (HSCIC, 2014).

BMI is not a suitable criterion for defining the relative weight of children because of the rapid growth rate they exhibit compared with mature adults. Additionally, there are differences in growth rates in children depending on their sex, and to get a better idea of potential obesity issues the use of sex-specific growth charts is recommended (Barlow and Dietz, 1998). In the UK, for example, the standard measure is the British Growth Chart that was established in 1990 (UK 1990). Different charts from the WHO and the Centre for Disease Control and Prevention (CDC) are commonly used in other countries (WHO, 2016). On the British growth chart, children above the 95th percentile or higher are classified as obese, while children between the 85 and 95th percentile are considered overweight (NICE and Care, 2006) (Lean, 1989).

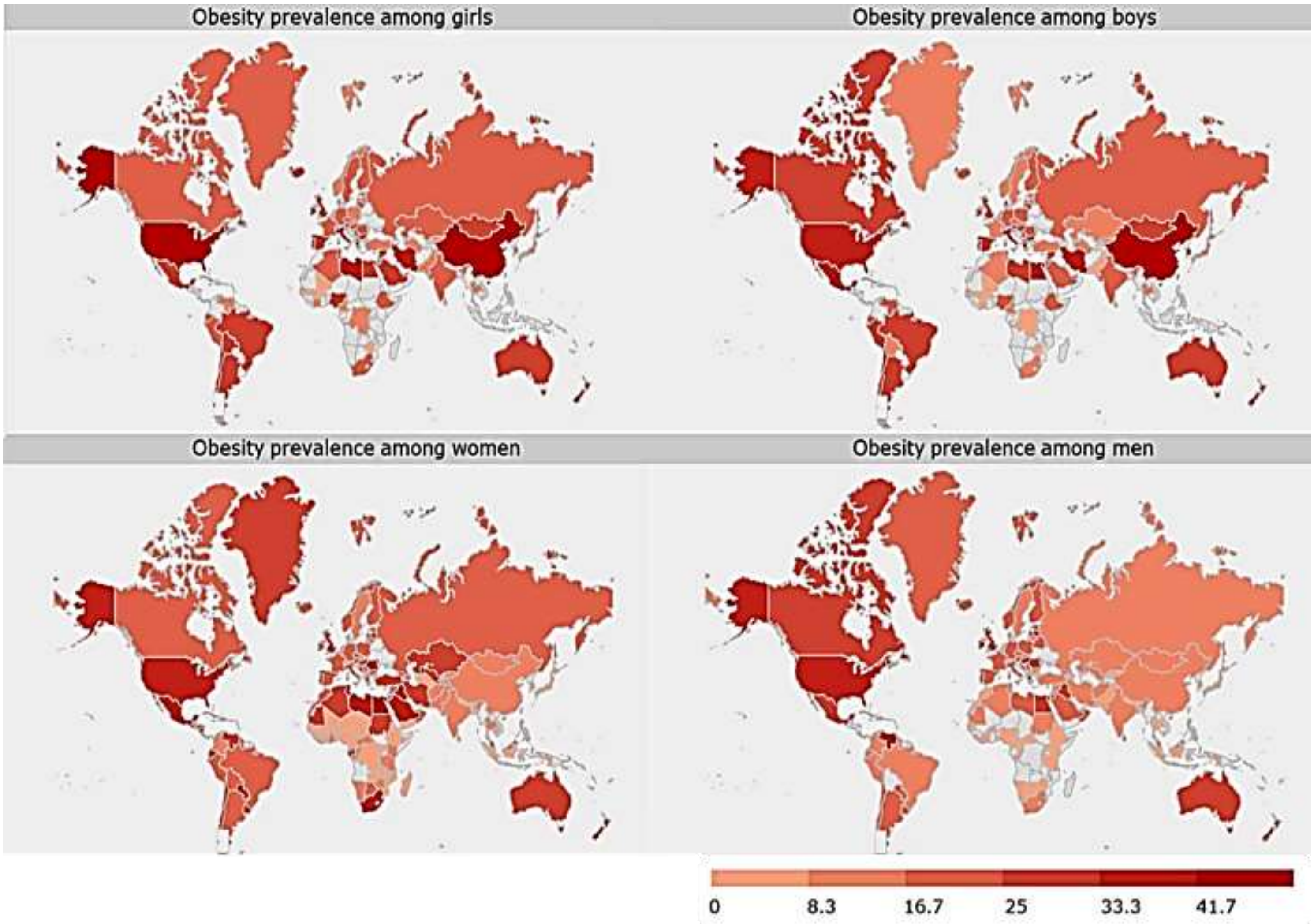

Figure 1-1: The universal distribution of obesity

Data obtained from the World Obesity Federation (WOF) representing the prevalence of obesity in more than 50 countries. Where the scale shows the percentage of individuals with obesity, grey shows no obesity data obtainable.

1.2 Causes and treatment

The World Health Organisation officially classified obesity as a disease in 1990. It is a chronic condition with a mortality rate of 6% (National Audit Office, 2011). Furthermore, the majority of people considered as obese have a higher risk of developing diseases by the age of 40, and most will need to undergo a medical intervention before they are aged 60 (Lean et al., 1998). However, obesity is a complicated condition, and its treatment cannot be as simple as telling someone to eat less (Sharma et al., 2009).

Obesity has been defined as an epidemic due to its potential impact on public health (Kelly et al., 2008, Gahagan, 2005). A greater understanding of the underlying causes could help to develop new treatments or interventions to promote weight loss. Several reasons for obesity and overweight have been identified, of which the main one is an energy imbalance between food intake that is too high and a low level of energy expenditure, which will lead to increased fat accumulation (Murano et al., 2005) see Figure 1-2.

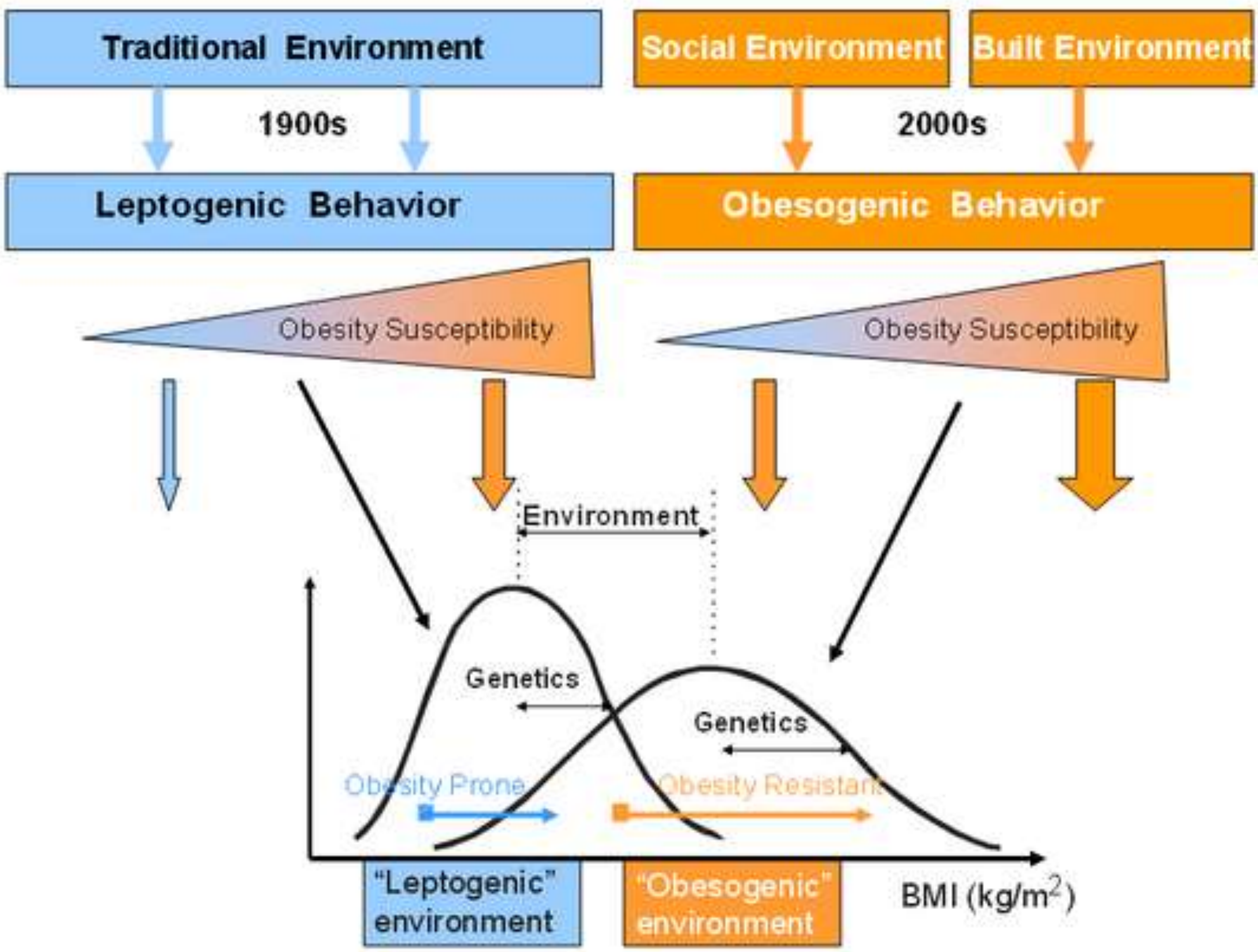

Figure 1-2: The potential effects of genes and environment on adiposity
Summary of the potential effect of genes and environment on adiposity assessed by body mass index (BMI): on the left the 'traditional environment', which shows low food intake and high energy expenditure (leptogenic) whereas the right part shows the (obesogenic). (Adapted from Bouchard, 2007).

1.3 Adipose tissue

Adipose tissue is a complex, metabolically active endocrine organ that produces a range of different molecules with profound local and systemic effects (Tiraby and Langin, 2003). When adipose tissue is formed, it results in the construction of a large endocrine organ that has a separate and distinct anatomy (Cinti, 2011). All mammals possess this endocrine organ, of which there are two main types of adipocyte, white and brown. They have different roles in the body and their function can vary depending on the environmental conditions. White adipose tissue (WAT) primarily acts as an energy source to be mobilised when food availability is restricted, while brown adipose tissue (BAT) is required to regulate body temperature during cold exposure (Enerbäck, 2010). These tissues are referred to as 'adipocytes' as they consist of lipid and triglycerides. However, they are classified differently depending on the cellular distribution of lipids in each cell, as WAT is considered unilocular, while BAT is multilocular (Cinti, 2006). They are present in different colours and locations around the body. If a brownish colour is observed when visually examining the depot, this indicates it is primarily BAT. If the colour is found to be white, then the depot is mostly WAT (Akabas et al., 2012). Those depots found immediately below the skin are defined as subcutaneous whereas depots present in the body trunk are described as visceral depots.

The performance and function of these two types of adipose tissue can be reorganised in the early stages of life (Budge et al., 2009). It is important to consider the process of adipose tissue formation as a process that continues throughout the life cycle. BAT could contribute to reducing obesity by reversing the excess WAT mass in overweight people (Budge et al., 2009). This will be discussed in more detail later on.

1.3.1 White adipose tissue (WAT)

WAT is a significant depot in the body in which excess energy is accumulated (Enerbäck, 2010). It consists of single large lipid droplets that can vary greatly in size (Cinti, 2006). The cytoplasm that bounds the nucleus is thicker than in other regions of the cell. Mitochondria in WAT are extended and contain more organelles that can be recognised under microscopic examination, and the cell is bound by a peripheral lamina (Cinti, 2006). WAT is considered the most abundant of adipose tissues, along with stromal vasculature tissue, another component of fatty tissue. It is distributed in subcutaneous and visceral depots (see Table 1-1).

The subcutaneous depot is found around the abdomen and under the skin, while the visceral depot surrounds organs in the perigonadal, retroperitoneal and intra-abdominal regions (Gesta et al., 2007). The primary role of WAT is to provide a source of energy storage, i.e. mobilising fat, when the body needs it, as an energy source that is dependent on food availability. Furthermore, in some organs, WAT has the capacity to regulate metabolic rate. It also plays a vital role in the overall regulation of substrate metabolism within the body and therefore contributes to energy homeostasis. In addition, WAT is responsible for the release of cytokines and other hormones, which can regulate the body's metabolism, insulin sensitivity, in other tissues such as muscle, liver and the brain (Gesta et al., 2007). For example, WAT regulates leptin secretion and can, therefore, regulate food intake (Cinti, 2006). WAT also plays a role in the inflammation process and glucose homeostasis (Cousin et al., 1999, Shimomura et al., 1998) but excessive accumulation results in obesity (see Table 1-1).

1.3.2 Brown adipose tissue (BAT)

BAT usually appears in newborn mammals and, in contrast with WAT, contains an abundance of smaller lipid droplets and a much higher amount of mitochondria (Sidossis and Kajimura, 2015). BAT has more blood vessels than WAT since it has a higher requirement for oxygen than most tissues (Cinti, 2006). It has an entirely different function from WAT as its primary function is to burn fat in order to generate heat. It is defined by the presence of a unique uncoupling protein, (UCP)1, located within the inner mitochondria, and it has the ability to rapidly increase energy expenditure by the oxidation of free fatty acids (FFA) and glucose (Cinti, 2006). More specifically, it uncouples respiration from Adenosine Triphosphate (ATP) synthesis (Cannon and Nedergaard, 2004).

In the majority of mammals studied to date, it appears that BAT plays a vital role in the body's defence system by regulating its temperature when exposed to cold and by increasing energy expenditure (Sidossis and Kajimura, 2015). It also enables the newborn to effectively adapt following cold exposure to the extrauterine environment (Saely et al., 2012). In adults, BAT has potential significance when it comes to regulating energy balance and the onset of obesity (Cannon and Nedergaard, 2004). In this respect, it is important to consider that BAT has the capacity to produce up to 300 W/kg of tissue, compared to all other tissues that can only produce 1 W/kg (Cannon and Nedergaard, 2004). In addition to BAT's presence is in both small (Kozak and Koza, 2009) and large mammals at birth (Symonds et al., 2012), it is perceived that it could play a possible role in energy expenditure in human adult (Nedergaard et al., 2007).

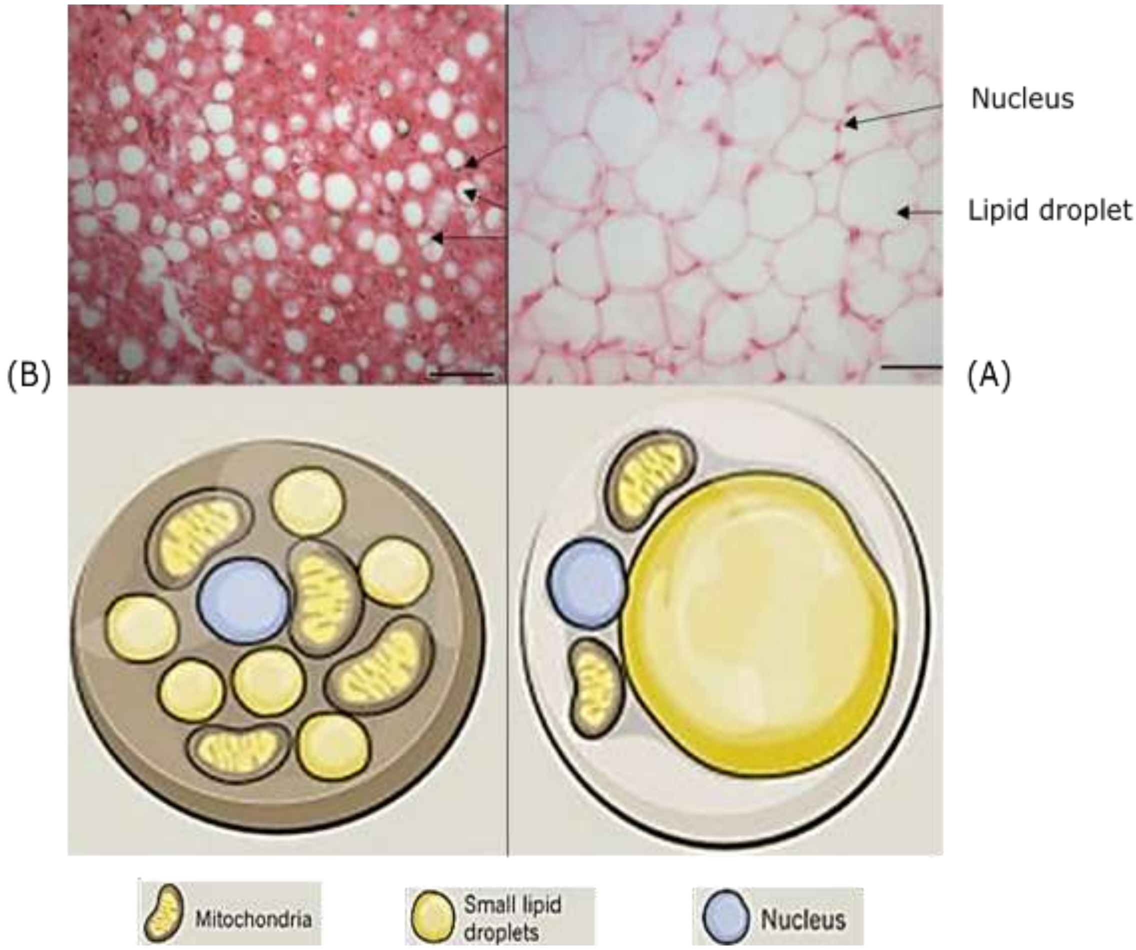

Figure 1-3: Histology of white (A) and brown (B) fat cells of sheep perirenal depot at 7 and 28 days of age

White adipocyte characterised by a single lipid droplet (unilocular) surrounded by cytoplasm containing a small number of mitochondria and nucleus. Brown adipocytes are smaller in size and have multiple lipid droplets (multilocular) holding the nucleus and a higher number of mitochondria within the cytoplasm.

Table 1-1: Differences between white and brown adipocytes
(adapted from Frühbeck et al., 2009).

Characteristic	White adipose tissue	Brown adipose tissue
Primary Function	-Depots of stored energy -Hormone release, such as leptin and adiponectin, which regulate	Heat generation
Main depot locations	Subcutaneous: abdominal, perirenal, gluteal region and inguinal, Visceral: intra-abdominal retroperitoneal, and perigonadal regions	Mediastinal Thyroid/tracheal perirenal supraclavicular
Colour	White, very variable from light to firm yellowish	Brown, from light pinkish to dark red
Vascularisation	Sufficient amount of vascularised	Highly vascularisation
The nervous system control	Sympathetic and parasympathetic	Sympathetic
Adipocyte shape	Variable from spherical to polyhedral	Polygonal
Size	Variable (25-200mm)	Much smaller (16-60mm)
Nucleus	Peripheral semilunar flattened only 2-3% of the cell volume	Oval or round shape Centrally located
Lipid droplets	Unilocular, in unusually large, lipid droplet occupies 90% of the cell volume	Multilocular, several small lipid droplets
Mitochondria	Less, small, elongated	More, large, round
Cytoplasm	Thin, stretched in the slim rim	Overextended around the cell

1.3.2.1 BAT and its role in obesity

As far as the role of BAT in obesity is concerned, its abundance is usually negatively correlated with the amount of WAT (Hamann et al., 1996) and with BMI (Vijgen et al., 2011). Maximally, the contribution of BAT to daily heat production, assuming 50g of BAT in an adult human, is 20% (Ouellet et al., 2012). Prevention or a reduction in the rate at which BAT is lost through adulthood could, therefore, increase energy expenditure (Tam et al., 2012).

1.3.2.2 BAT is present in small amounts in adults

It is assumed that BAT is present in the newborn, and disappears with age (Lean, 1989). More recently, significant metabolic activity within BAT has been found in adults (Saito et al., 2009) through the use of fludeoxyglucose (FDG) in positron emission tomography (PET). A number of research studies have subsequently examined possible methods of activating BAT in adult humans (Leff and Granneman, 2010).

1.3.2.3 BAT and the influence of variations in season and temperature

Cold temperatures play a primary role in the activation of BAT (Saito et al., 2009, Brine, 2006), which activates the sympathetic nervous system (SNS), thereby increasing norepinephrine (NE) concentration in plasma. Season also plays a vital role in stimulating BAT, which is higher in winter than in summer (Au-Yong et al., 2009). The effects and consequences of photoperiod can also be examined with ambient temperature, which fluctuates to a lesser extent (Saito et al., 2009). However, this process is sensitive and profoundly affected by both the magnitude of cold exposure and photoperiod. It has been shown that photoperiod in sheep (Bassett et al., 1988) and day length in humans (Steger et al., 1983) increases the plasma concentration of the hormone prolactin (Symonds, Budge et al., 2011) which is inversely associated with the abundance of its receptor (i.e. PRLR) (Auchtung et al., 2005). Another study found that the abundance of UCP1 declined in parallel with the loss of PRLR within one month after birth (Pearce et al., 2005). This finding supports the suggestion that PRLRs could play a role in foetal BAT development (Virtanen et al., 2009) and stimulate BAT function in the newborn (Viengchareun et al., 2008). Therefore, PRLP could be a key regulator of BAT development in the foetus (Symonds et al., 1998) and later adipose tissue composition (Symonds et al., 2011).

1.3.2.4 Age and brown adipose tissue

It is acknowledged that BAT activity decreases with age in adults (Yoneshiro et al., 2011). For example, in a study of 213 healthy participants aged 20-73 years, 50% of people in their twenties showed a BAT response to cold exposure, compared with 10% of in people aged 50-60 (Yoneshiro et al., 2011). These findings are in accord with those of Symonds et al. (2012), who used thermal imaging to measure supraclavicular BAT activity (Symonds et al., 2012). When comparing younger to older children by using positron emission tomography (PET)/computed tomography (CT) it was also found that BAT activity is much higher in children than adults under similar conditions, and the most significant activity of BAT was seen in 13 to 15-year-olds (Drubach et al., 2011, Gilsanz et al., 2012).

1.3.2.5 BMI and brown adipose tissue

Both BMI and BAT activity are inversely proportionate in children and adults (Saito, 2013). For example, in a study comprising 24 healthy people aged 18-32, 14 of whom were overweight or obese (BMI > 25), and 10 with a healthy BMI (< 25), BAT activity decreased with raised BMI (van Marken Lichtenbelt et al., 2009). In 2014 Robinson et al. used infrared thermography in 55 healthy children aged 6-11 years in a typical school environment and found that the temperature of the supraclavicular region, that is the primary site of BAT in humans, decreased with increased BMI centile (Robinson et al., 2014).

1.3.2.6 BAT markers

As far as BAT markers are concerned, the primary one is UCP1, which plays a significant part in thermogenesis (Cannon and Nedergaard, 2004). Other molecular markers include peroxisome proliferator-activated receptor gamma coactivator 1-alpha (PGC-1α), the master regulator of UCP1 transcription (Frühbeck et al., 2009), cell death-inducing DFFA-like effector; PR domain containing 16 (PRDM 16), which has a significant impact on brown fat (Kajimura et al., 2010); and potassium channel, subfamily K, member 3 (KCNK3) (Pope et al., 2014), which could be used as a gene marker of BAT when comparing with WAT (Svensson et al., 2011) (see Figure 1-4).

1.3.3 Transdifferentiation between BAT and WAT

The transdifferentiation of adipose tissue is the process of conversion adipocytes from brown to white fatty tissue (Cinti, 2006). After birth, it has been proposed that brown adipocytes gradually lose their specificity and turn to WAT, and thus lose UCP1, blood vessels and nerves. At the same time, BAT could gain the ability to activate the leptin gene (Cinti, 2006) which plays a role in WAT development (Mostyn et al., 2003), and considered to be the primary WAT marker (Cinti et al., 1997). The process of transdifferentiation seems to be reversible and has been termed the browning of WAT (Pope et al., 2014). This process could increase energy expenditure and, therefore, could help to prevent obesity; this has been illustrated in rodents (Wu et al., 2013). The distribution of white and brown adipocytes is affected by a range of environmental and other related conditions including age, species, and nutrition (Snitker et al., 2009). For example, one study shows that beiging of white adipose tissue could be induced by β3-adrenoceptor agonist pharmacologic treatment in obese diabetic mice (Himms-Hagen et al., 2000) (Jimenez et al., 2003). In addition, another study has suggested that a hormone called irisin, which is released following muscular contraction, may contribute to the process of browning (Lee et al., 2014). However, the mechanism of action by which irisin enhances the transdifferentiation process is still unclear and contentious (Aldiss et al., 2017). Other studies have found that cold exposure improves the transdifferentiation from white to BAT (Enerbäck, 2010, Murano et al., 2005). Overall this process is sensitive to which fat depot is studied (Sacks and Symonds, 2013), a factor that will be discussed in more detail later.

1.3.4 Beige adipose tissue

Beige adipocytes are another critical aspect to consider (Ishibashi and Seale, 2010, Clarke et al., 2007). Beige and brown adipocytes are similar in several ways. For instance, they have an enriched mitochondrion, and they express UCP1 and multilocular lipid droplets. However, the two depots (i.e. brown and beige) were found to be different in terms of cell size, gene markers (i.e. homeobox (HOX) C9 and short stature homeobox (SHOX) (Walden et al., 2012), and the amount of the UCP1 expressed (Bostrom et al., 2012). Furthermore, they develop from a different cell lineage (see Figure 1-4). It has been shown that classic BAT originates from the central dermomyotome that also produces epaxial muscle and dorsal demise (Atit et al., 2006). This result was confirmed by lineage-tracing studies, showing that myocytes and brown adipocytes alone originate from precursor cells that express Myogenic factor 5- progenitors (Myf5), a gene responsible for the formation of myogenic regulatory factor MYF-5. The development of brown adipocytes in WAT depots in adults, which facilitates thermogenic capacity, is usually a result of chronic adrenergic activation during exposure to cold (Cousin et al., 1992). In animals, who mainly depend on shivering to sustain a normal body temperature, it has been found that the expansion of BAT is accompanied by a gradual increase in non-shivering thermogenesis (Cannon and Nedergaard, 2004). BAT has been termed 'recruitable,' 'brite' (brown in white) or beige adipocytes, with the term 'recruitable,' being applied widely.

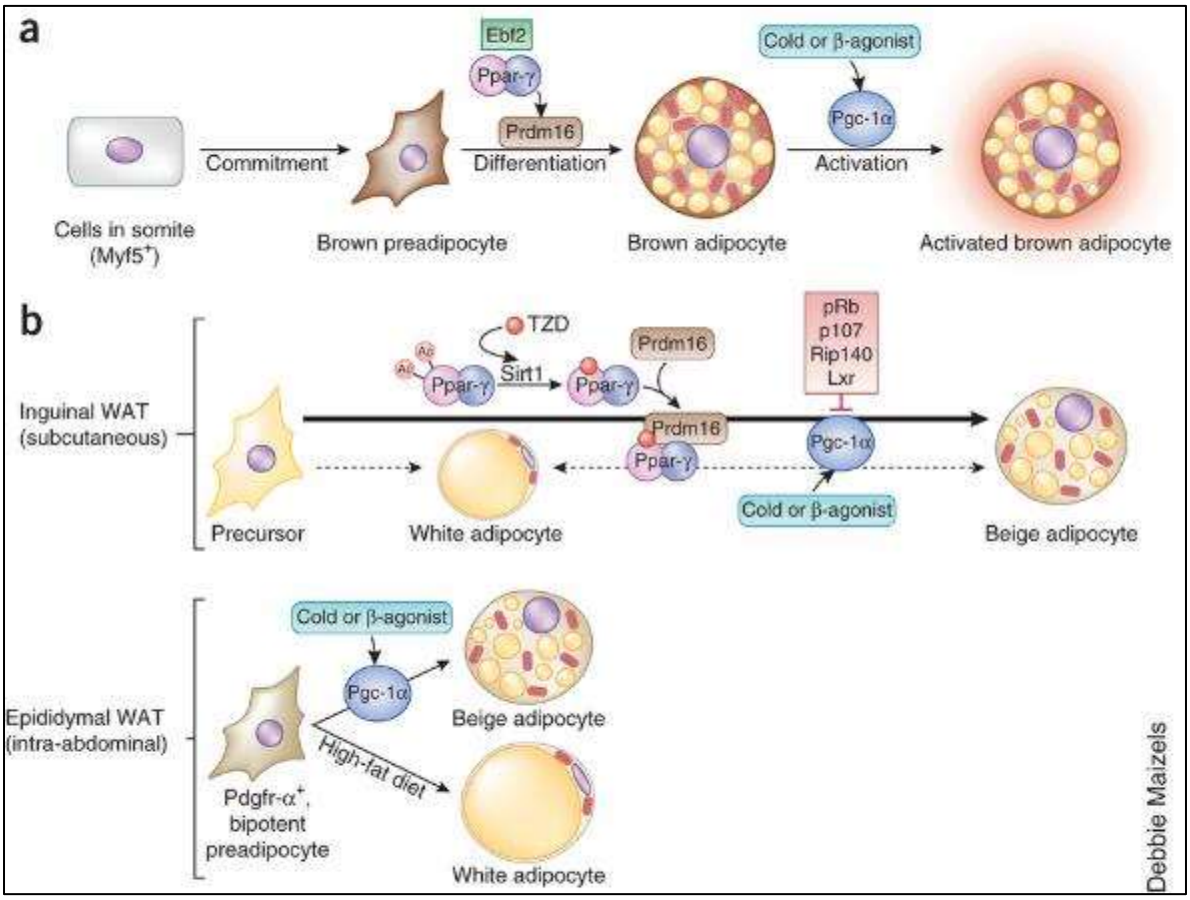

Figure 1-4: Brown and beige adipose tissue cell lineage

(a)Myf5 progenitor population produces the adipocytes. Ppar-γ cooperates with Ebf2 to enhance expression of PR domain containing 16 (Prdm16) which drives brown fat cell fate. Norepinephrine (NE) turns active the thermogenesis in mature adipocytes. A β3 agonist is secreted by sympathetic neurons. NE signals increase the reactions of PGC-1α, which is a coactivator, which helps carry out gene programming. (b) β-adrenergic stimulation in inguinal fat activates the denovo differentiation of precursor cells. There is a likelihood that mature white fat cells can turn into beige cells. Research has found that the caloric surplus in epididymal makes the bipotent progenitors break down into adipocytes and β-adrenergic activators stimulate the growth of adipocyte. In addition, Thiazolidinedione (TZD) agonists of Ppar-γ increasing the stability of Prdm 16 and also through the Sirt1-dependent deacetylation of Ppar-γ. This turns the Prdm16 into Ppar-γ target genes. β-adrenergic signals motivate the activities of Pgc-1α.several receptors targeting PGC-1α to inhibit beige adipocyte growth. (Harms and Seale, 2013)

1.3.5 Brown and beige stimulation factors

'Brite' ((Petrovic et al., 2010) or 'beige' (Ishibashi and Seale, 2010) adipocytes can only be detected in WAT following exposure to cold or other inducers (Cousin et al., 1992; Fukui et al., 2000; Guerra et al., 1998)). This dependency on external stimuli for induction of UCP1 is a unique characteristic of beige fat (Sidossis and Kajimura, 2015). As opposed to beige fat, UCP1 is expressed in brown fat cells in comparatively high amounts even without any stimulation. These individual difference can be attributed to finding that they arise through de novo differentiation from different precursors (Wang and Seale, 2016) which allow expression of UCP1 and tend to have increased amounts of mitochondria. Under the same conditions, precursors of beige fat undergo adipocyte conversion (Sidossis and Kajimura, 2015). However, they fail to activate the brown fat induction programme with Peroxisome proliferator-activated receptor gamma (PPARG) activators or b-adrenergic agonists (Ohno et al., 2012, Klaus et al., 1995, Wu et al., 2012, Petrovic et al., 2010). It is also important to note that wholly activated beige adipocytes express UCP1 at about 10% of that found in classical brown adipocytes and can undergo uncoupled respiration that is mediated by UCP1 (Okamatsu-Ogura et al., 2013, Long et al., 2014) (see Figure 1-5).

The following section will focus on how environmental changes affect cell fate specification and how maintenance can be increased while highlighting the endocrine factors that mediate the development and function of beige adipocyte triggered by the environment.

1.3.5.1 Exposure to chronic cold

The peroxisome proliferator-activated receptor γ coactivator-1α (PGC-1α) triggers mitochondrial biogenesis and oxidative metabolism and is essential for tolerating exposure to cold (Puigserver et al., 1998), which moderately increases its expression. Additionally, when it is knocked out in brown preadipocytes, this significantly blunts the UCP1 increase following adrenergic signalling (Uldry et al., 2006).

1.3.5.2 Environmental enrichment

Mice exposed to an enriched surrounding with complex social and physical stimuli show higher whole-body energy use and have elevated resistance to obesity induced by diet (Sidossis and Kajimura, 2015). Hypothalamic brain-derived neurotrophic factor (BDNF) mediates stimulation of the SNS, which is linked to the environment and differentiation of beige adipocytes. It has also been observed that BDNF hypothalamic overexpression is sufficient for the promotion of biogenesis of beige adipocyte and to increase levels of energy consumption (Cao et al., 2011).

1.3.5.3 Endocrine and metabolism

Previous studies have identified several endocrine mediators of beige and brown adipocytes, such as Fibroblast growth factor 19 (FGF19) (Fu et al., 2004), Bone morphogenetic protein 7 (BMP7) (Tseng et al., 2008), Fibroblast growth factor

21 (FGF21) (Kleiner et al., 2012), and growth differentiation factor-5 (GDF5) (Hinoi et al., 2013). In obese humans, a number of negative regulators have been shown to block beige and brown adipocytes (Sidossis and Kajimura, 2015). For instance, the expression of transforming growth factor beta (TGF-β) increases under obese conditions and inhibits the differentiation of beige adipocyte. On the other hand, inhibition of TGF-β signalling following genetic ablation of Mothers Against DPP Homolog 3 (*Smad3)*, or through the administration of TGF-β–neutralising antibody, facilitates browning of WAT and protects animals from insulin resistance and obesity triggered by diet (Yadav et al., 2011). In the same way, depletion of retaining aldehyde dehydrogenase 1 (*Aldh1*), an enzyme that produces retinoic acid or inhibits Notch signalling, (Kiefer et al., 2012) enhances WAT browning and elevates energy use in rodents.

1.3.5.4 Transcriptional mediators

Of the many transcription factors involved in BAT differentiation, two deserve particular attention. These are PR domain zinc finger protein 16 (PRDM16) and PGC-1a is known to activate the biogenesis of mitochondria and oxidative metabolism. It plays a significant role in tolerating cold exposure (Puigserver et al., 1998) when gene expression is usually elevated. Conversely, its knockout in brown pre-adipocytes significantly blunts the UCP1 increase following adrenergic stimulation (Uldry et al., 2006). PRDM16 has been shown to be highly expressed in brown adipocytes in comparison to white adipocytes. It functions as a transcription factor together with PGC-1α and euchromatic histone-lysine N-methyltransferase 1 (EHMT1). PRDM16 overexpression in preadipocytes from WAT depots (i.e. subcutaneous) resulted in an entirely brown adipocyte phenotype (Seale et al., 2007, Seale et al., 2011).

1.3.5.5 Genetic impact on brown, beige, and white adipocyte in association with obesity

Several studies in rodent animals that have shown that there is a significant association between propensity of browning in WAT and genetic vulnerability to obesity triggered by diet (Kozak, 2011). This genetic susceptibility is associated with changes in the expression of UCP1 in WAT but not in interscapular BAT, showing the biological role of beige adipose tissue in obesity (Xue et al., 2007).

Regarding humans, genetic links to the mass of BAT and energy use remain unclear. β3-adrenergic receptor (ADRB3) (64 Trp/Arg) and UCP1 polymorphisms (–3826 A/G) are linked to lower resting energy use and lowered cold-induced thermogenesis (Nagai et al., 2011). Additionally, in one study the prevalence of BAT was significantly reduced in older adults with polymorphisms in the β3-adrenergic receptor genes and UCP1 (Yoneshiro et al., 2013). According to two recent studies, genetic variations or mutations in humans affect the development and energy use in BAT. EHMT1 is a methyltransferase that is localised in the nucleus and is required for the development of beige and brown adipocytes (Sidossis and Kajimura, 2015). Lowering the level of whole-body energy use follows reduced EHMT1, leading to obesity, insulin resistance and hepatic steatosis in mice (Ohno et al., 2013). It has been shown that 40% to 50% of human patients with insufficient EHMT1 tend to develop obesity-related conditions (Willemsen et al., 2011). This trend reveals the significance of EHMT1 regarding energy homeostasis in humans.

In contrast, deletion of the gene that encodes for G-Protein-Coupled Receptor (GPCR) leucine-rich-repeat-containing GPCR4 (LGR4) encourages browning of WAT, partly by lowering the retinoblastoma 1 (Rb1) gene expression. Mice lacking the LGR4 gene are protected from dietary-induced obesity and insulin resistance (Wang et al., 2013). Interestingly, a gain-of-function variant (A750T) of LGR4 has been linked to obesity among Chinese people (Wang et al., 2013).

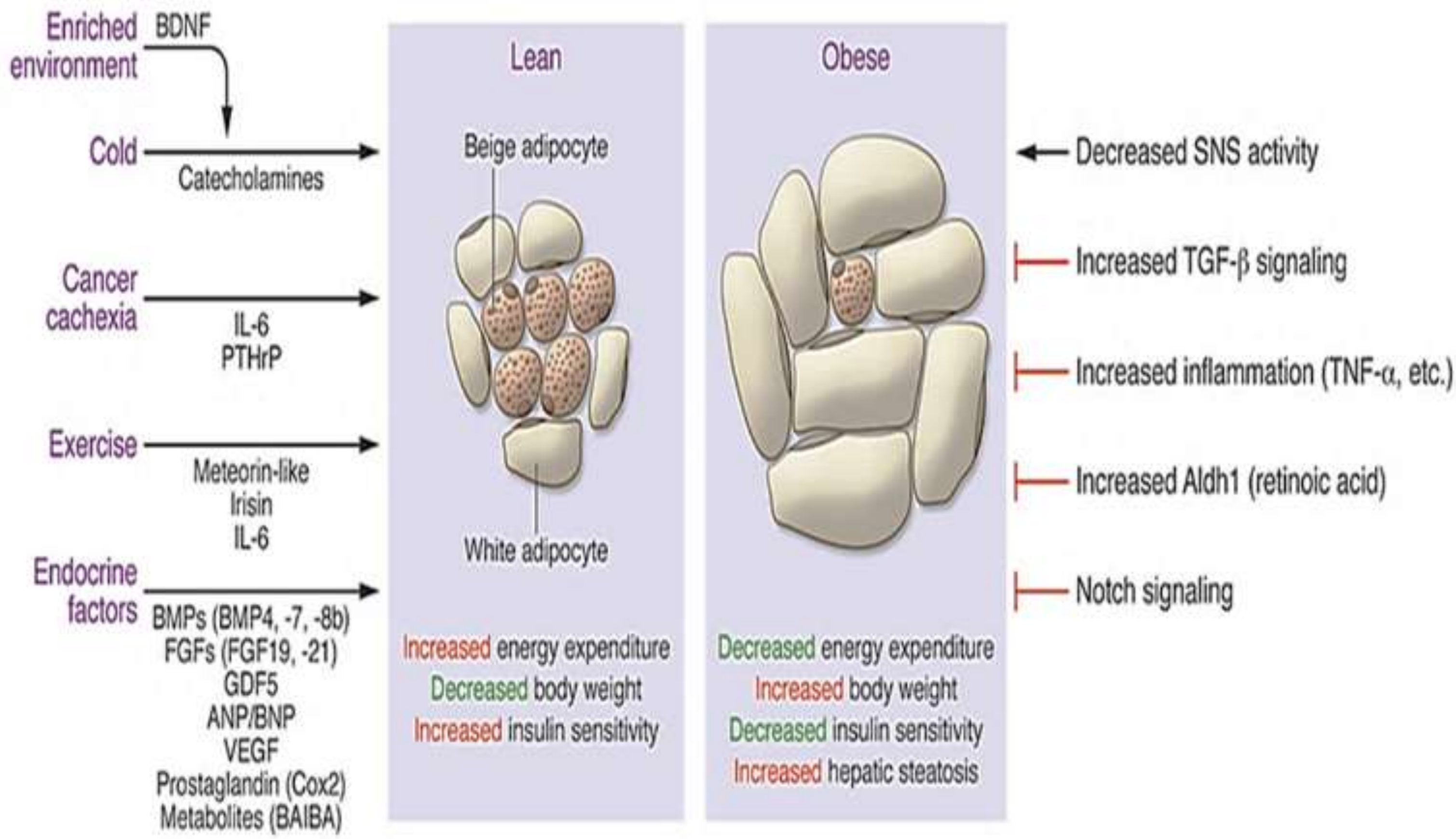

Figure 1-5: Summary of external stimulation causes that impact on beige adipose tissue development in obese and lean subjects
(Sidossis and Kajimura, 2015)

1.4 Brown, beige, and white adipose tissue location in different species

Figure 1-6, 1-7 and 1-8 below demonstrates the anatomical locations of BAT in different species, starting with a human in Figure 1-6, as determined using positron emission tomography and computed tomography. For example, a small amount of BAT can be seen in the neck, including the supraclavicular and auxiliary regions. It can also be found in the paravertebral, perirenal, adrenal and paraventral regions, and additionally in the area of the major blood vessels (e.g. the aorta, along with its main branches: carotid, subclavian, intercostal and renal arteries).

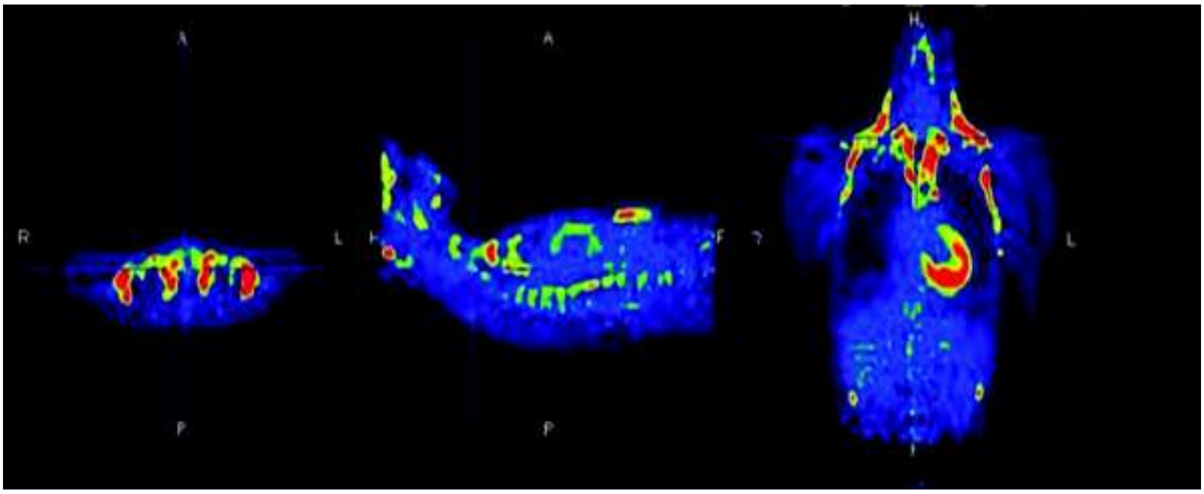

Figure 1-6: The anatomical location of discrete brown adipose tissue in a human
Measured by positron emission tomography and computed tomography (CT: Top), from right to left a coronal section of the thorax, in the middle sagittal section at the level of the spine, and left side representing a crosswise section at the level of the clavicles (adapted from Tam et al., 2012).

In rodents, as discussed previously in section 1.3.4, Myogenic factor 5+ progenitors (Myf5+) cells are known as early brown fat or muscle cell precursors. The anatomical locations for beige and BAT, in this regard, can be perceived as different when it comes to comparing between species. Major depots are present in humans in the supraclavicular area (Sacks and Symonds, 2013), which are not found in rodents, where the primary location of BAT markers is the interscapular region (Peirce et al., 2014) (see Figure 1-7).

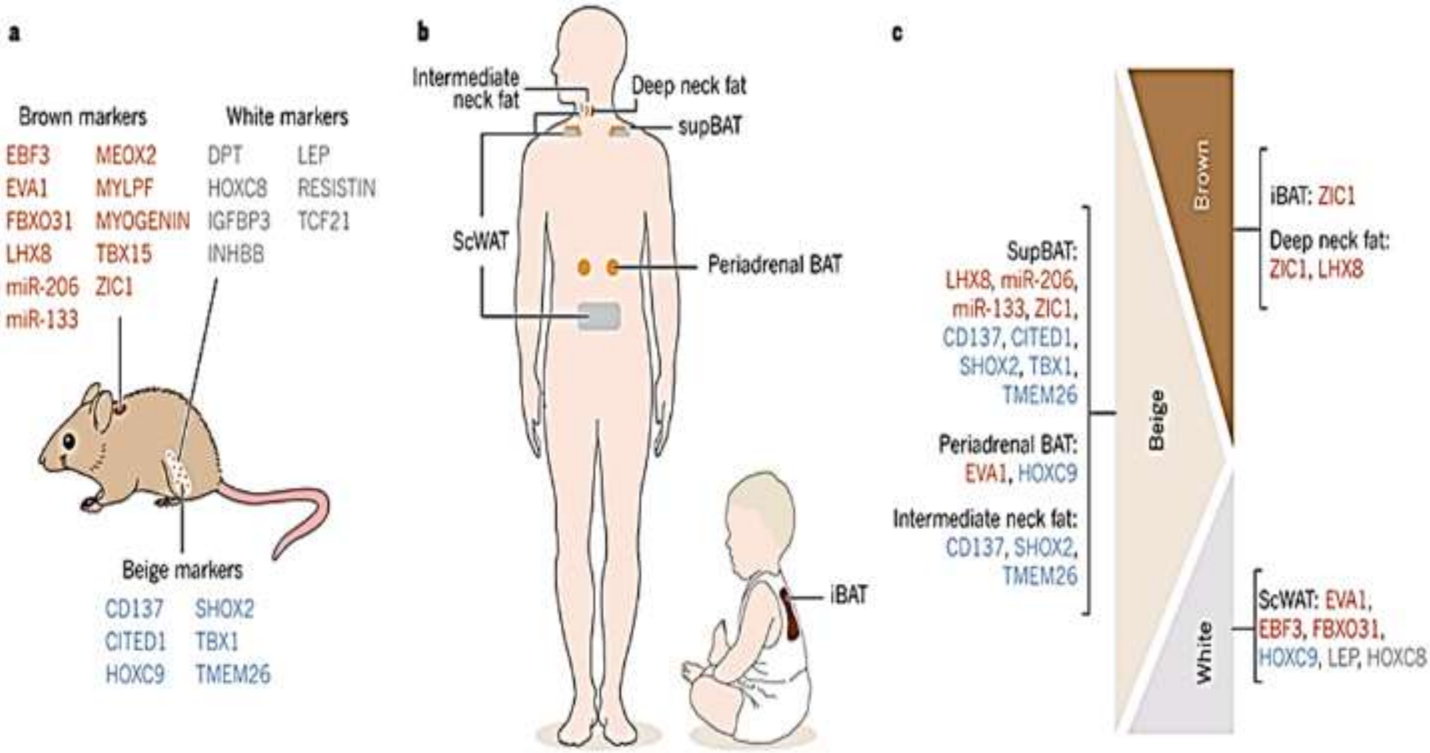

Figure 1-7: Assessment of brown, beige and white adipocyte genes markers

(a) Brown, beige and white adipocytes in rodent compared to (b) human adipose tissue, including (c) shared genes markers in the three different depots. (Adapted from Peirce et al., 2014).

In large mammals such as newborn humans and sheep (Figure 1-8), BAT is deposited mainly in late gestation (Lauritzen et al., 2001) and constitutes around 1-2% of birth weight (Merklin, 1974, Alexander and Bell, 1975). In addition, it seems that adipose tissue can be isolated physically and functionally in different anatomical locations. For example, the perirenal-abdominal area is the largest fat depot in young sheep (Symonds et al., 2012), accounting for up to 80% of total body fat. It is named perirenal because it originates and surrounds the kidney. The mass and size of perirenal adipose tissue (PAT) increase through late gestation by 30-40% (Alexander (1978), (Vernon et al., 1981), paralleled by an increase in UCP1 (Clarke et al., 1997a). During pregnancy, foetal PAT develops in order to be able to activate rapidly following cold exposure at birth.

The sternal depot, which is similar to the supraclavicular region and is located around the neck in humans (Virtanen et al., 2009), was found to be the second major fat depot in sheep after the perirenal (Henry et al., 2017). Furthermore , it has been shown that the sternal depot features a high capacity for a thermogenic response to a local stimulus including diet (Scotney et al., 2017), and cold exposure (van Marken Lichtenbelt et al., 2009) due to retaining a high amount of UCP1 in later life (Virtanen et al., 2009).

Another depot is the epicardial adipose tissue (EAT) which mainly appears after birth and is found to feature beige adipocyte characterisations in later life (Sacks et al., 2013). EAT accounts for about 80% of the heart's surface in adults and represents nearly a third of its total weight of the heart, with significant variation between sexes and individuals (Shirani et al., 1995). It is generally found in the interventricular and atrioventricular ridges (Willliams, 1995) and is involved in both energy and lipid metabolism. EAT differs from other fat depots in several ways including, but not limited to, its role as a buffer in terms of protecting the heart from fatty acid oxidation damage (Iacobellis et al., 2005). In addition, EAT is distinguished by exhibiting low rates of glucose utilisation and pronounced regression during weight loss (Sacks and Fain, 2007). EAT is also smaller in terms of total mass than other fat depots (Sons and Hoffmann, 1985). For example, in adult sheep, the mass of this tissue is the lowest compared to the other seven types of the depot; on the other hand, it is considered the greatest in term of adiposity cell ratio (i.e. the number of cells per gram) (Barber et al., 2000). EAT is a visceral depot that is used as an indicator of obesity (Sacks and Fain, 2007) and it has been suggested to be positively associated with body mass (Sons and Hoffmann, 1985). However, more recent autopsy and clinical studies have found that BMI and EAT were not well correlated (Shirani et al., 1995, Corradi et al., 2004, Rabkin, 2007).

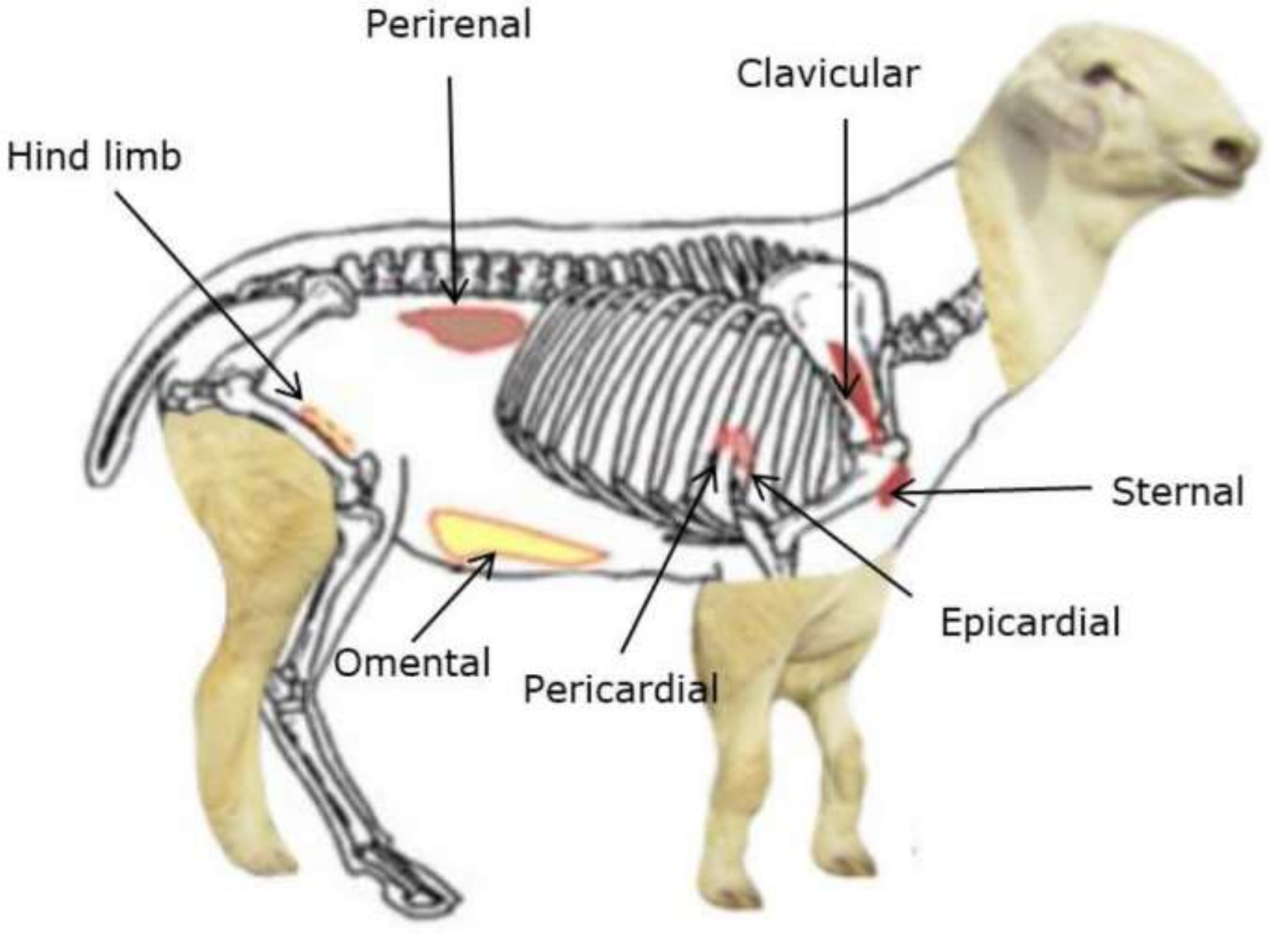

Figure 1-8: A summary of brown adipose tissue depots location in sheep
Adapted from Symonds et al., 2012)

1.5 Fatty acids

1.5.1 Overview

Fatty acids (FA) are long chains of lipid-carboxylic acid which are present in cell membranes and fat depots. They usually exist naturally and contain an unbranched chain of carbon atoms which are even in number (between four and 28). The unbranched chains may be saturated or unsaturated (Nic et al., 1997). FA arise from triglycerides or phospholipids and undergo metabolism to produce high amounts of ATP. Nonetheless, long chain Fatty acids (with 14 carbon molecules or more) are unable to move across the blood-brain barrier (BBB) and as a result, they cannot act as a fuel source for the central nervous system. On the other hand, medium- (6-12 carbon atoms) and short-chained (less than six atoms of carbon) FAs together with ketone bodies and glucose are capable of passing the BBB membrane (Vijay and Morris, 2007).

1.5.2 Classification of fatty acids

Fatty acids are named with respect to the number of carbons present, the degree of saturation, and if present, the geometrical structure and location of double bonds. The absence of double bonds in FA indicates that they are linearly configured and that they are saturated fatty acids (SFAs) that solidify at room temperature. Whenever the double bonds are present, the FAs are unsaturated (USFAs). USFAs can have a single, double bond (monounsaturated; MUFAs) or two or more double bonds (polyunsaturated; PUFAs) (Lobb and Chow, 2007). Unlike SFAs, unsaturated FAs exist in liquid form at room temperature. USFAs may also exist within a two-structural placement of *trans* and *cis* isomers. The position of the hydrogen atoms linked to the double bond of carbon determines the type of FA. FAs are *cis* if the hydrogen atoms occur on an identical side and are *trans* if the atoms occur on different sides (Figure 1-9). Fatty acids of the *trans* type do not usually occur naturally; they are usually created as a result of the industrial activity of hydrogenation (Katan et al., 1995).

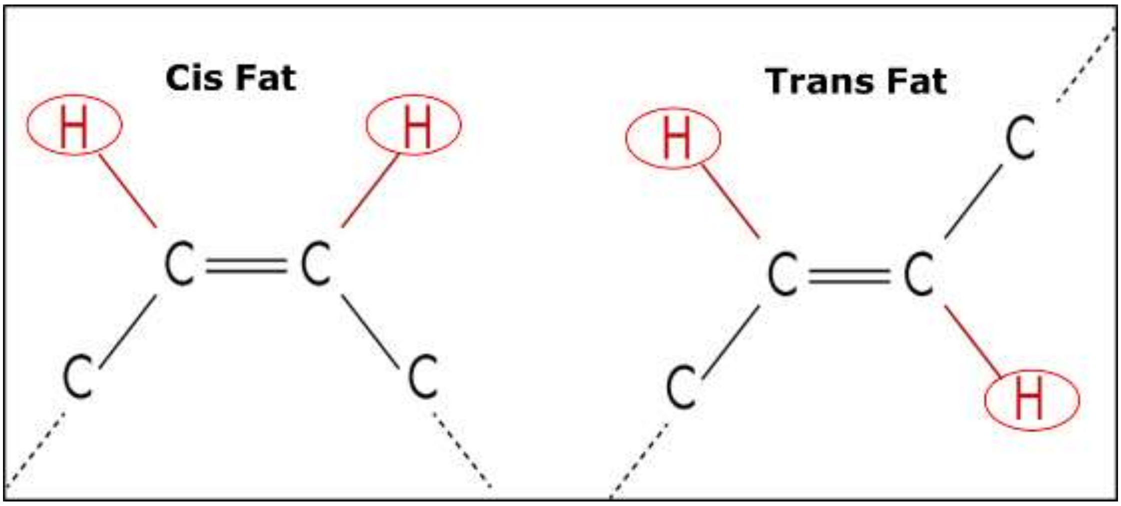

Figure 1-9: Structuring of *trans* and *cis* double bonds of carbon in fatty acids
Cis indicates that the functional groups are on the same side of the carbon chain while *trans* conveys them on opposing sides.

As illustrated in the above diagram, functional groups of *cis* occur on the same side of the carbon chain whereas those of *trans* occur on opposite sides. Carbon atoms in USFAs are numbered using two approaches; Δ approach or the n/ω numbering approach. In the Δ method, atoms from the carboxyl group are numbered, whereas, in the n/ω method, numbering starts with the carbon atom that is furthest from the carboxyl group (Katan et al., 1995). The Δ approach uses the format 'carbons number-double bonds number- Δ- location of double bonds with respect to carboxyl group terminal.' For example, 16:1 Δ9 means that the fatty acid has 16 carbons, a single, double bond and occurs nine carbon atoms from the carboxyl group (i.e. palmitoleic acid). The n/ω approach would number the same acid as 16:1 (n-7); this means that the double bond of the FA occurs in the seventh furthest carbon atom from the ω-carbon atom, which is the most distant carbon atom from the carboxyl group.

1.5.3 Trans fatty acids (TFAs)

Primarily, TFAs are UFAs. They have at least one double bond of carbon with hydrogen atoms in their chemical structure. According to Wanders et al. (2010), TFAs are produced through biohydrogenation within the rumen or due to incomplete hydrogenation of unsaturated oils. Ruminant TFAs, such as the vaccine and conjugated linoleic acids, occur in small quantities in the meat and milk of these animals (Ghafoorunissa, 2008, Iqbal, 2014). The consumption of TFAs across different nations is challenging to evaluate as the percentage found in the diet varies significantly. However, Sundram et al. (2003) suggested they contribute to 7% of the total energy consumption in the Middle East and Southern Asia and between 2-3% in the United States of America (USA). Several epidemiological studies indicate that industrial TFAs could contribute to the incidence of cardiovascular disease. However, no such correlation has been attributed to ruminant TFAs (Bolton-Smith et al., 1996, Weggemans et al., 2004, Lock et al., 2005, Van de Vijver et al., 2000).

1.5.4 Essential fatty acids

As suggested by the name, essential fatty acids (EFAs) are fundamentally important in maintaining and sustaining the development of bodily growth and function. Since desaturases are not present in mammalian cells, EFAs cannot be synthesised from simple precursors of carbon atoms. Instead, they are acquired through the diet (Christie, 1982, Le et al., 2009). The synthesis of downstream FAs mainly occurs by means of two EFAs, linoleic (LA, omega-6) and α-linolenic (ALA, omega-3) acids (Das, 2006, Le et al., 2009). Mammals lack the Δ12 and Δ15 desaturases which inhibit the formation of double bonds beyond the ninth carbon of the aliphatic chain. Synthesis of LA and ALA is therefore not possible in mammals (Christie, 1982). Diets rich in seed oils such as soya beans, sunflower and safflower contain high amounts of LA (AbuGhazaleh et al., 2007) whereas ALA is found in oils from soya beans, rapeseed, oats and linseed (Shingfield et al., 2010). ALA can also occur in oil from sunflower seeds, albeit in small amounts.

1.5.5 Mechanisms of FAs metabolism in BAT

The synthesis, metabolism and storage of FAs are crucial in the activation of UCP 1 during thermogenesis (Divakaruni and Brand, 2011, Fedorenko et al., 2012). In order to obtain lipids in BAT, two mechanisms can take place. One involves the uptake of FAs through lipogenesis and lipoprotein carriers. The second is through de novo FA synthesis (Calderon-Dominguez et al., 2016). The lipoprotein lipase enzyme (LPL) provides the highest amount of FAs in BAT, which, when synthesised, binds the enzyme at the endothelium cell surface (ECS) (Bartelt et al., 2012).

Lipids gained from the diet are transported through lymphatic vessels into the circulation with the aid of very low-density proteins (VLDP) and chylomicrons (Calderon-Dominguez et al., 2016). Upon arrival of the triglyceride-rich lipoproteins in the bloodstream, they are hydrolysed into monoacylglycerol and FFAs by lipoprotein lipase (Bartelt et al., 2012; Bartelt et al., 2013). Exposing mice to a cold environment leads to an increase in FA uptake in the brown adipocytes rather than in skeletal muscle (Bartelt et al., 2011). The β3-adrenergic pathway promotes the expression and activity of LPL and, as a result, the FA flow increases in BAT. Raised LPL activity can also cause insulin resistance and promote adiposity in mice (Duivenvoorden et al., 2005) and can enhance the lipogenic gene expression (Bartelt et al., 2011). When hydrolysis is completed, FAs are absorbed into the cellular structure through receptors of the plasmatic membrane. The FA binding proteins (FABP) function to transport the absorbed FAs to sites where they are stored or used (Calderon-Dominguez et al., 2016).

The synthesis of FAs can arise through lipogenesis in the cytosol of the cell cytoplasm. The first stage is the conversion of acetyl-CoA into malonyl-CoA through the influence of acetyl-CoA carboxylase (Berg et al., 2011). Fatty acids synthetase (FAS) then serval reaction catalyses until the generation of palmitic acid (16:0) (Lodhi et al., 2011). The last phase in brown adipocytes consists of the elongation of stearoyl-CoA desaturase (SCD) 1 and of very long chain fatty acids (ELOVL) 3 (Calderon-Dominguez et al., 2016). Once the process of lipogenesis is complete, the synthesised FAs undergo esterification before they are oxidised and stored as TG in droplets of lipids (Calderon-Dominguez et al., 2016)

1.5.6 Fatty acids abound and UCP1 gene expression.

The type influences expression of UCP1 and the amount of the FA consumed. Exposure of mice to dietary intervention of PUFAS supplementation (4.3% compared with 1.6% within a conventional 9% proportion of fat) for a period of two weeks increased UCP1 protein by 41%, thereby indicating that the thermogenic potential of brown adipocytes may be boosted by a dietary regimen high in PUFAs (Sadurskis et al., 1995). Mice fed on a diet containing fish oil (rich in docosahexaenoic acid (DHA) and n-3 eicosapentaenoic acid (EPA)) were reported to have enhanced UCP1 expression in brown and beige adipocytes (Kim et al., 2015), which may be as a result of the effects of fish oil on SNS. This would induce β3-adrenergic receptor gene expression which then binds to NA, and in turn, UCP1 is activated (Lowell and Bachman, 2003; Kim et al., 2015; Kajimura and Saito, 2014). Conversely, when mice were fed on EPA and DHA supplements, no effect on UCP1 was reported (Janovska et al., 2013). In vitro treatment of human pre- and mature adipose cells with EPA up-regulates UCP1, whereas DHA had no effect (Fleckenstein-Elsen et al., 2016).

A diet high in MUFAs fed to adult rats stimulated UCP1 (Rodriguez et al., 2002). Lactating and expectant mothers fed on olive oil supplements were also reported to show lower weight gain while UCP1 gene expression in their progeny was boosted (Priego et al., 2013). In postmenopausal women, utilising olive oil to provide dietary fat was shown to initiate diet-induced thermogenesis (DIT) (Soares et al., 2004). Westerter (2004) described DIT as an increment in energy consumption beyond the basal fasting level as a proportion of the energy content of the consumed diet. Therefore, part of the total energy intake will be expended.

1.6 Lipolysis in the rumen

1.6.1 Lipid metabolism in the rumen

In non-ruminants, the digestion and absorption of lipids occur in the stomach and the small intestines. For ruminants, on the other hand, the rumen is of great significance during this process. Fermentation rates of the rumen depend on the type of FAs and therefore this influences the digestive process (Jenkins, 1993). Upon digestion of dietary fat, the amount transported to milk fat depends on rumen biohydrogenation, digestibility, absorption, and accumulation in the adipocytes (Palmquist et al., 1993; Wu et al., 1991). Numerous studies have used supplements of lipids and FAs in order to boost the FA content in milk (Chilliard et al., 2000, 2007; Givens and Shingfield, 2006) with the proposition that the source of the supplement and FA composition determines the outcome. Moreover, variations in the specific content of FAs will influence other FAs. For instance, additives that enhance Conjugated Linoleic Acid (CLA) and/or PUFAs content in milk whilst minimising SFAs have been shown to promote the quantity of (E)-11-octadecenoic acid (18:1) *trans* (Lock et al., 2005, Chilliard et al., 2007, Roy et al., 2007).

1.6.2 The process of lipolysis

Lipolysis is the result of hydrolysis of dietary lipids into glycerol and FFAs by bacterial lipases (Buccioni et al., 2012). Jenkins (1993) reported that minimal amounts of monoglycerides and diglycerides are produced. In turn, the glycerol undergoes fermentation to form volatile short chain fatty acids (SCFAs) (Doreau and Ferlay, 1994) that are then absorbed across the wall of the rumen for the de novo synthesis of SCFAs and medium chain fatty acids (MCFAs) (Mansbridge & Blake, 1997; Buccioni et al., 2012). Produced FAs undergo biohydrogenation and may be used in synthesising microbial lipids. The resultant short-chained FAs (produced due to lipolysis) undergo absorption and are transferred into the bloodstream (Doreau and Ferlay, 1994). The lipids that undergo esterification and are subjected to hydrolysis with influence from microbial lipases such as phospholipases, a process that results in the formation of free FAs (FFAs) (Jenkins, 1993).

1.7 The impact of maternal consumption of canola oil during lactation on milk fatty acid profile.

Previous research has established that modifying milk fatty acid content through FAs supplementation could be beneficial to human health (Chilliard et al., 2000, 2007; Dewhurst et al., 2006; Givens and Shingfield, 2006; Lock and Bauman, 2004; Shingfield et al., 2006); however, there are varying outcomes in different species.

Table 1-2 Summary of established studies on the impact of supplementing the maternal diet with canola oil on milk fatty acid profile

Study	Species	Supplement	Outcome
Mir et al. (1999)	Goats	4/6% canola	Total fat, C18:0, Total CLA MCFAs, C16:0
Okine et al. (2003)	Goats	4/6% canola	Total fat, MUFAs, C18:0, Total CLA SFAs, MCFAs, C14:0,C16:0, n-3,n-6
Welter et al. (2016)	Cows	6% canola	MUFAs, C18:0, n-3,n-6 Total fat, PUFAs, MCFAs, C14:0, C16:0

PUFAs = polyunsaturated fatty acids, MUFAs = monounsaturated fatty acids, SFAs = saturated fatty acids, MCFAs = medium chain fatty acids, CLA = conjugated linoleic acid. Blue indicates reduction, while red shows an increase in content compared with controls.

1.8 Maternal nutrition and birth outcomes

Human epidemiological studies report that maternal diet, including macro- and micronutrients, as well as weight, age and lifestyle could have significant effects on the outcomes of pregnancy (Abu-Saad and Fraser, 2010). For example, poor nutrition during pregnancy can negatively impact on infant development, which may increase the risk of the offspring developing adult cardiovascular disease (Stein et al., 1996).

1.8.1 Manipulation of the maternal diet in different gestational periods

Some studies have shown that the timing of the manipulation of maternal diet could have different outcomes, depending on the stage of gestation (Roseboom et al., 2000, Symonds et al., 2004). According to Bispham et al. (2003), manipulation of the maternal diet from early to mid-gestation impacts on the metabolism of certain maternal hormones including cortisol and leptin. These two maternal hormones impact directly and indirectly on foetal adipose tissue development and could elevate UCP1 abundance, and hence the amount of BAT at term (Mostyn et al., 2003, Mostyn et al., 2002). The respective adaptations are also crucial towards sustaining maternal blood plasma glucose that will affect the growth of the foetus. Maternal dietary manipulation, especially during late gestation, may affect size at birth, which correlates with food consumption, and may also reduce plasma glucose by ~30% if the diet is restricted (Roseboom et al., 2000, Sebert et al., 2009).

Enhancing maternal metabolism, by manipulating the diet or through exposure to cold, will lead to an increase in BAT development in the fetal perirenal region, at least in sheep (Clarke et al., 1997a, Budge et al., 2000). For example, one study in sheep found that allowing the mother to feed according to her appetite may increase birth weight while also decreasing white adipose tissue formation and promoting BAT (Budge et al., 2000). This will improve the ability of the body to adapt to later life and to prevent excess fat mass.

1.9 Importance of performing animal studies in different species

For examining the potential biological mechanisms that could control BAT it would be considered unethical to conduct invasive studies in humans that involve tissue sampling. This is also the case when studying the effect of nutritional interventions in early life and its potential impact on later life, for which animal modules play a vital role in identifying the mechanisms that could explain the development of several diseases, including obesity. However, in such cases, the developmental differences between large and small mammals should be considered, particularly in terms of the rate of maturation (Pearce et al., 2005) (Lindberg, 1970). Most studies on BAT location, type and function have been conducted in rodents (Timmons et al., 2007), in which hypothalamic maturity occurs after birth, in contrast with humans where it happens before birth (Symonds, 2007). Therefore, the size and type of mammals should be considered separately, depending on the research question and on the validity of other resources such as experience, equipment, funding and time.

Because no animal is directly comparable to humans, each module has its limitations, which must be considered when examining potential human outcomes (McGonigle and Ruggeri, 2014). Sheep are often the preferred module when investigating the manipulation of the maternal diet and its impact on the foetus (Barry and Anthony, 2008). This is because of standard features in terms of the maturation of the hypothalamus (Clarke et al., 1997b) and in terms of the complete develop organ system (Symonds, 2007). In addition, sheep have a birth weight (about 4.5 kg) and gestational period (140-150 days) that makes them closer to humans (270 days) than rats (21-22 days) (Barry and Anthony, 2008). However, the sheep module has some limitations as well as advantages when compared to human biology, as they have a complex digestive system that involves the rumen, and therefore the nutritional requirements and glucose metabolism are entirely different (Barry and Anthony, 2008). The main advantage of the sheep module, nonetheless, is its similarity to human perinatal BAT, which allows the regulation of body temperature through non-shivering thermogenesis to be studied (Clarke et al., 1997b).

1.10 Machine learning (ML)

In recent years, using genomic data, through open sources, has improved published bioinformatics data (Ross and Krumholz, 2013). However, analysis of such big datasets remains highly challenging, particularly when taking a development approach, where there is a set of linkages between organ and tissue systems which could impact on disease processes (Claussnitzer et al., 2015a). Adipose tissue due to its different anatomical location and function has recently become an endocrine organ of particular interest for research on obesity development (Cinti, 2011). Machine learning is an analytical technique for big data in order to classify the types of gene interactions by using different logarithms (Alpaydin, 2009). It allows investigating of the regulatory relationships between genes in a probabilistic environment while compensating for any missing data, that takes place through the use of training sets, which are used to generate a predictive module based on the observations within the data (Yeoh et al., 2002).

In general, machine learning algorithms can be classified into two main groups, supervised and unsupervised learning.

1.10.1 Supervised learning

The machine learning algorithm is trained using predefined data. For example, you have both input variables (x) and output variables (Y) and use an algorithm to develop mapping function from the (X) to the (Y). Supervised learning logarithm can be further divided into two categories:

- **Classification:** apply an aim to classify a specific number of output variables in group or category, such as age (i.e. 7 days or 28 days), and dietary group (i.e. control vs. supplemented) (Alpaydin, 2009).
- **Regression**: mainly used when the output variable is a real value, and the aim is to predict an unspecified number in a particular category. This could include a prediction module based on data such as the number of gene interactions, and connectivity (Alpaydin, 2009).

1.10.2 Unsupervised learning

In contrast to supervised learning, in this type of machine learning logarithms are use no predefined data. For example, you only have input data (X) and no corresponding output variables. The logarithm combines similar data into groups, and then the test sample is classified based on its proximity to these groups. For example , one of the most commonly used algorithms in this category is (K-means) (Alpaydin, 2009).

1.10.2.1 Clustering

Unsupervised learning logarithms are mainly used with the aim of the classification of big datasets such as microarrays, where you want to discover the characteristic groupings in the data, such as a group of genes expressed by a particular pattern (Alpaydin, 2009).

Algorithms can be combined to perform a specific task, such as using a clustering algorithm and then training a classification algorithm. For example, in one study genes were classified according to their similarities using unsupervised hierarchical clustering and principal component analysis expression clustering (Qu & Xu, 2004). In this thesis I have used supervised learning algorithms such as the random forest (RF) (Breiman, 2001) in combination with the positive sample-only learning (PSOL) algorithm with the aim of predicting optimal gene expression patterns for five adipose tissues depots with age at two time points (i.e. 7 days and 28 days of age) in each dietary group. Each group of gene clusters where aiming to investigate a specific function, such as a cell differential, response to a stimulus, or mitochondria biogenesis. More details can be found in section 2.2.6.1 to 2.2.6.9 of chapter 2 Materials and methods.

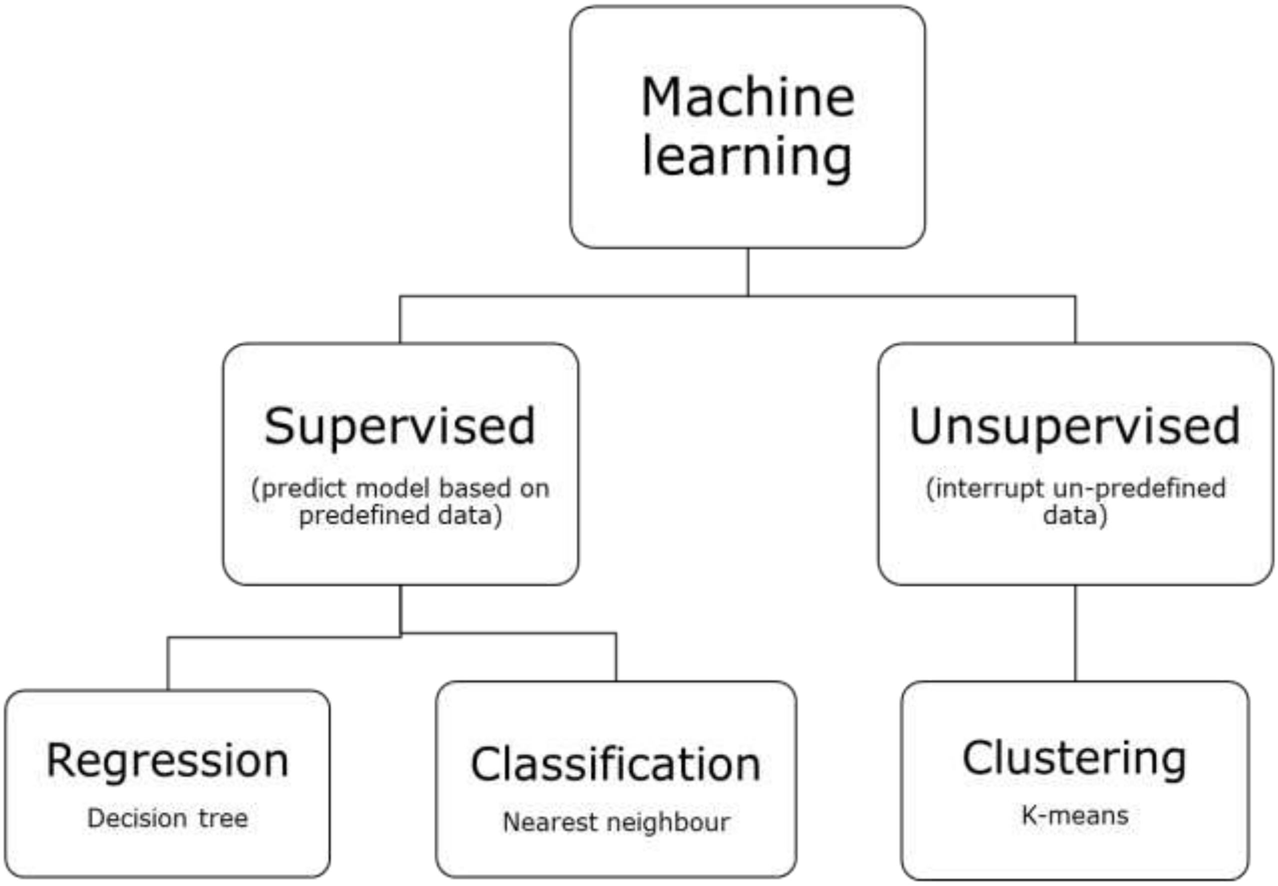

Figure 1-10 Summary of machine learning types
The diagram represents different logarithms that are used by machine learning techniques in an aim to classify (categorical) or predict (continuous) module in supervised learning or to use clustering function in unsupervised learning.

1.11 Aims and hypotheses

In this chapter, early life nutritional programming and the capacity of the brown adipose tissue to act as an anti-obesity target by increasing energy expenditure are reviewed. I was particularly interested in the impact of the high level of MUFAs in different anatomical locations of fat depots during the development in early life.

The aim of my thesis is to describe the changes in the lipid and gene expression profiles of adipose tissue in five different anatomical locations separately, in early life and to determine whether each fat depot develops and responds to stimuli differently, by supplementing the maternal diet with a high short fatty acid nutritional source (i.e. 3% of canola).

The main hypothesis of this study is that the gene expression of adipose tissue will be distinct for each depot with significant changes including the loss of mitochondria gene function in early life, mediated by anatomical localisation. In addition, I hypothesise that manipulation of the maternal diet through lactation by enhancing milk fatty acid content in early life delays the loss of mitochondrial gene expression in the offspring adipose tissue.

The following chapters were designed to test the hypotheses:

- Chapter 4 describes the dynamic transdifferentiation of the adipose tissue gene expression profile and function in different depots during the first month of young sheep life.

- Chapter 5 investigates the impact of anatomical location on adipose tissue development, by comparing the gene expression profile of five different depots at two time points (7 and 28 days).
- Chapter 6 identifies the change of lipid and gene expression profile and function in five different depots of young sheep raised to mothers whose diet has been supplemented with canola oil.

2 Materials and methods

2.1 Experimental designs

The experimental sheep study was carried out as part of a study designed to examine the impact on lambs of maternal food supplementation during lactation. The study was carried out in the Academic Department of Child Health, School of Medicine, University of Nottingham. Based on reduction principles in the utilisation of animals, guidelines in the 3Rs (NC3Rs, 2011) and to study new hypotheses emerging from new discoveries in the discipline, tissues obtained from the control animals (n=10) were further utilised in this investigation. All practices regarding the utilisation of animals in this investigation were carried out by Professor Michael E. Symonds, Dr Viv Perry and Mr Mark Birtwistle at the University of Nottingham, Sutton Bonington Campus from November 2014 to February 2015, with the consent of the UK Home Office and in compliance with UK animal law/scientific practices (1986). These trials received the required ethical approval from the University of Nottingham. All safety standards, risk assessments and chemical and laboratory activities complied with standards set forth by the UK's Health and Safety Executive's Control of Substances Hazardous to Health (COSHH, SI No. 1657, 1988). Chemicals used in this study met biology grading, and technicians wore lab coats and disposable nitrile gloves during all laboratory processes. Unless declared otherwise, Professors Michael Symonds and Helen Budge oversaw these procedures.

2.1.1 Summary of the sheep study design

Ten Blue-faced Leicester ewes were involved in this study, each of which had twin lambs (n = 20). Once they had given birth, each ewe was allocated to either a control (n = 10) or canola supplemented diet, i.e standard diet + 3% canola oil supplement (45 g in 1500 g of concentrate) (n = 10). All lambs were fed by the mothers until their tissues were sampled. Lambs which were born to the same mother were randomly chosen for sampling at either 7 ± 2 (7-day group) or 28 ± 3 days (28-day group). They were humanely euthanised using an excess dose of a drug known as barbiturate (i.e. 200 mg/kg pentobarbital sodium, Euthatal: RMB Animal Health, UK). Adipose tissue samples were frozen in liquid nitrogen and kept at -80°C until further analysed.

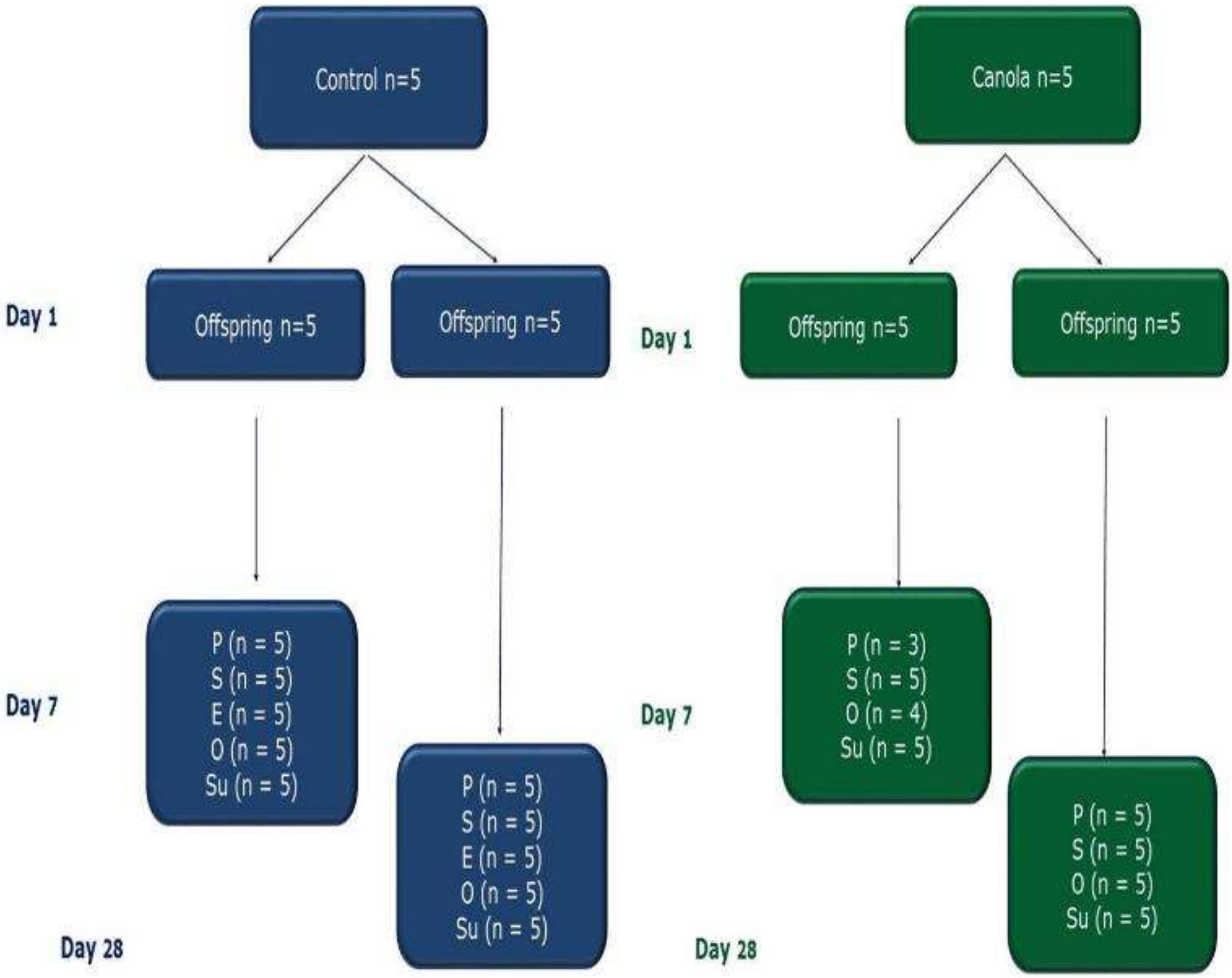

Figure 2-1: Representation of the study design

Ewes in the control group were fed a standard diet, ewes in the canola group were fed a standard diet + 3% canola oil, and offspring lambs were mother-fed from birth until the day of tissue sampling either at 7 or 28 days of age. The day numbers indicate age in days. Adipose tissues are (P) perirenal, (S) sternal, (E) epicardial, (O) omental, and (Su) subcutaneous.

2.1.2 Animals and environments

A Texel ram was used to mate with Blue-faced Leicester ewes during the same period in order to enable all offspring to be experimented on as one cohort. For the majority of the gestational period, all ewes were housed at a farm located in Skipton, Yorkshire. They were then moved to a barn at Melton Lane Complex of the Sutton Bonington campus of Nottingham University two weeks prior to birth. Here they were kept in groups until they delivered. After delivery, each ewe and its offspring were housed in a separate two by two metres pen for the rest of the study.

2.1.3 Sheep allocation into feeding groups

A standard diet was given to all ewes until natural parturition at 21 weeks. Five out of the 28 ewes gave birth to triplets while 23 bore twins, giving a total of 61 lambs, of which 26 were male and 35 female. Ten lactating ewes were categorised into the control group, nine into the canola group. The process of allocation ensured that the sex of the offspring was evenly distributed across the two dietary categories. There was a stillbirth of one female lamb and another died within 24 hours after birth, reducing the number of live lambs to 33. One male lamb was recorded to have a reduced growth rate and was ruled out of the experiment. The five triplet-bearing ewes were grouped as the control subjects. Tissues from one lamb chosen from each triplet batch were sampled at one day of age (1M, 4F). The five ewes were then left with two lambs to feed, reducing the total lamb count to 53 (23M, 29F).

2.1.4 Animal feeding and tissue sampling

2.1.4.1 Ewes

The standard diet during gestation was 1 kg of standard commercial concentrate (Ewe 18 Mix; Manor Farm Feeds, Oakham, Leicestershire, UK) and 2 kg of hay. The concentrate contained the necessary nutrients required to sustain expectant and lactating ewes in accordance with recommended dietary requirements (Alderman & Cottrill, 1993). After parturition, every ewe was grouped in one of two dietary categories: control group (2kg hay, 1kg of standard concentrate), canola group (2kg hay, 1kg of concentrate containing 3% canola oil supplement). The fat content in the canola group was twice that fed to the control subjects. Every group had unrestricted water access. Table 2-1 shows the composition of the concentrates.

Table 2-1: Concentration of the feed concentrates

Component	Canola Group (%)	Control Group (%)
Canola oil	3	0
Crude protein	18	18
Crude fibre	7	7
Crude Ash	6	6
Other crude oils and fats	3	3
Moisture	15	15

2.1.5 Quality and quantity of RNA isolated

All the ribonucleic acid (RNA) extraction procedure including isolation, quantification and quality control was performed by Dr Reham AlAgal and Dr Hernan Fainberg at the Department of Academic Child Health, University of Nottingham (unless otherwise stated).

For RNA isolation from each fat depot from five animals within each nutritional group, and approximately 250 mg or 1000 mg of sampled tissue (at 7 and 28 days of age respectively). These were mixed separately using tri-reagent (2 ml, Sigma-Aldrich). Total RNA was extracted using the RNeasy Plus kit (Qiagen), in accordance with the manufacturer's instructions, and RNA quantity was measured with the aid of a NanoDrop® ND-1000 Spectrophotometer (Thermo Scientific, DE, USA). Optical density ratios (260/280 nm) were > 1.9 for all samples. Total RNA quality was assayed using Agilent 6000 bio analyser Nano Kit (Agilent Technologies, USA) and the samples with a RIN (RNA Integrity Number) exceeding 7 were chosen to undergo microarray analyses(Fainberg, 2018) (see section 2.2.3-2.2.4 for more details).

2.1.6 Calculation of the Integrity, Purity and Concentration of RNA

Evaluation of the purity (260:230 nm, 260:280nm) and concentration (ng/µl) of RNA was performed a NanoDrop® ND-1000 Spectrophotometer (Thermo Scientific, DE, USA) using a 2.0 260:280 nm ratio, that is evidence of a superior RNA content (Manchester, 1996). RNA extracted from tissues aged 28 days was additionally examined in order to determine the integrity of the RNA using Agilent 2100 Bioanalyzer Eukaryote total RNA toolkit (Agilent Technologies, USA). During the analyses, RNA samples were partitioned using electrophoresis on a micro-fabricated chip. The RNA was examined using fluorescence detection with the aid of laser beams in the form of a clump and size standard during the electrophoresis run. A RNA ladder was used, that enabled evaluation of the size of each RNA band, and the 18S and 28S bands of ribosomes of RNA were used to determine integrity level of RNA. This was evaluated by the aid of the 2100 Expert Software version 2.6 (Agilent Technologies, USA). Those samples with a RIN (RNA Integrity Number) exceeding 7 were chosen to undergo microarray analyses (see figure 2.2 and appendix 9-2). This was performed by Dr Reham AlAgal , Dr Hernan Fainberg , Mr Mark Pope, Mrs Victoria Wilson and Dr Ian Bloor.at the Department of Academic Child Health, Obstetrics and Gynaecology University of Nottingham and the School of Veterinary Medicine, Sutton Bonington Campus between November 2013 and February 2018, under the supervision of Professor Michael Symonds and Professor Helen Budge.

Excessive freezing and thawing may degenerate RNA (Wilson & Walker, 2010) and to prevent this, 10 µl aliquots of every RNA sample was individually taken and diluted to µg/µl to standardize the samples and prepare a reverse transcriptase-polymerase chain reaction (RT-PCR). They were then kept in labelled tubes at -20 °C for a later examination. The residual RNA was then kept at -80 °C to be easily accessed, if necessary.

The quantity and the quality of messenger ribonucleic acid. (mRNA) could be varied among adipose tissue depots extracted at both time points (i.e. 7 and 28 days). This is dependent on the ability and abundance of the RNA amount extracted from different depots. For example, the small size of the epicardial adipose depot at early life (Barber et al., 2000) could impact on the availability of the sample number for RNA extraction, compared to other adipose tissue depots at both time points (Sons and Hoffmann, 1985, Sacks and Fain, 2007). However, microarray data analysis shows epicardial tissue was the site of the highest mRNA gene expression in the majority of the genes examined, so this reduction in quantity or quality of mRNA is unlikely to have skewed those results and conclusions.

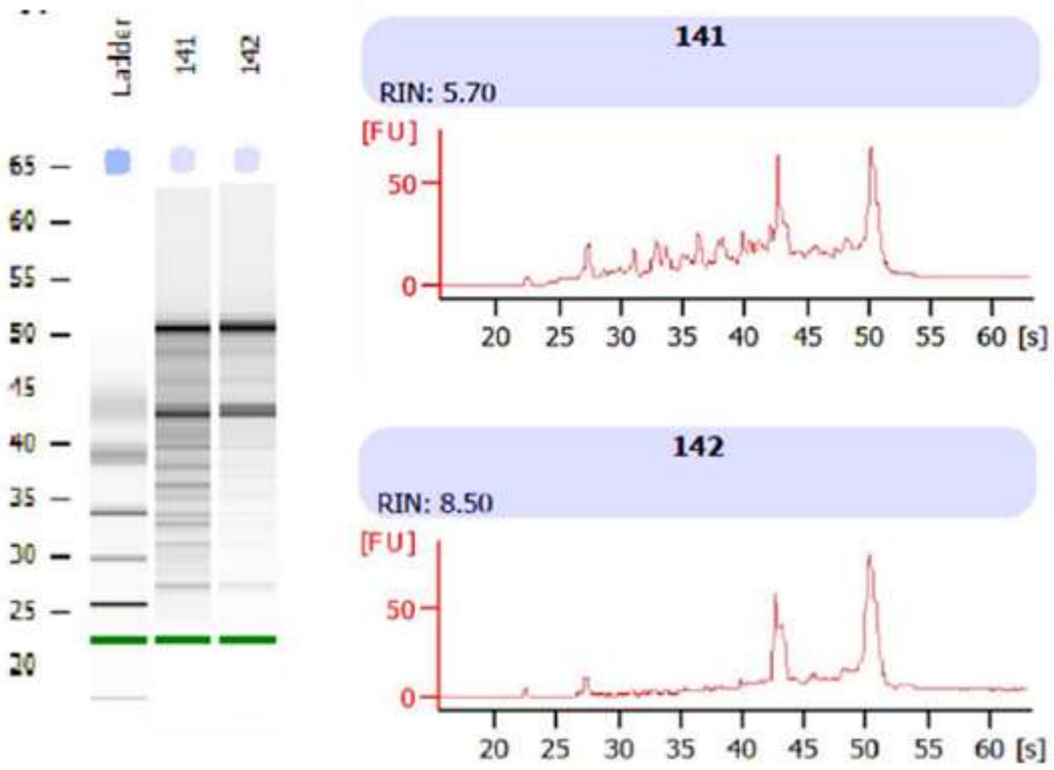

Figure 2-2 RNA integrity

Two RNA samples showing different degrees of integrity. Sample 141 is degraded (RIN = 5.70), as indicated by multiple peaks in the electropherogram, and an increase in the fluorescent signal indicates the destruction of dye intercalation sites. Sample 142 had an RNA integrity number (RIN) of 8.50, and the electropherogram is typical for high-quality RNA, showing a clearly visible 28/18S ribosomal RNA peak ratio.

2.2 Microarray analysis

2.2.1 Principle of the microarray

A microarray is a laboratory tool that detects and arranges expressions of multiple sequenced genes concurrently with the aid of a silicon sliver or a waterproof solid support glass. The tool analyses and identifies any homogeneities and disparities amongst sequences of expression in the target samples in order to widen the knowledge base on biological function. Every sequenced gene coincides with a complementary Deoxyribonucleic acid (cDNA), Genomic (gDNA), Polymerase chain reaction (PCR) by-product or oligonucleotides that have undergone chemical synthesis that typifies a single gene. The microarray then creates a comparative analysis of the gene expression patterns amongst a multitude of recorded and unrecorded gene functions. For example, the effect of the diet intervention theory could be evaluated by measuring the change in mRNA level and gene expression profile compared to the non-intervention group (see Figure 2-3 and Figure 2-4).

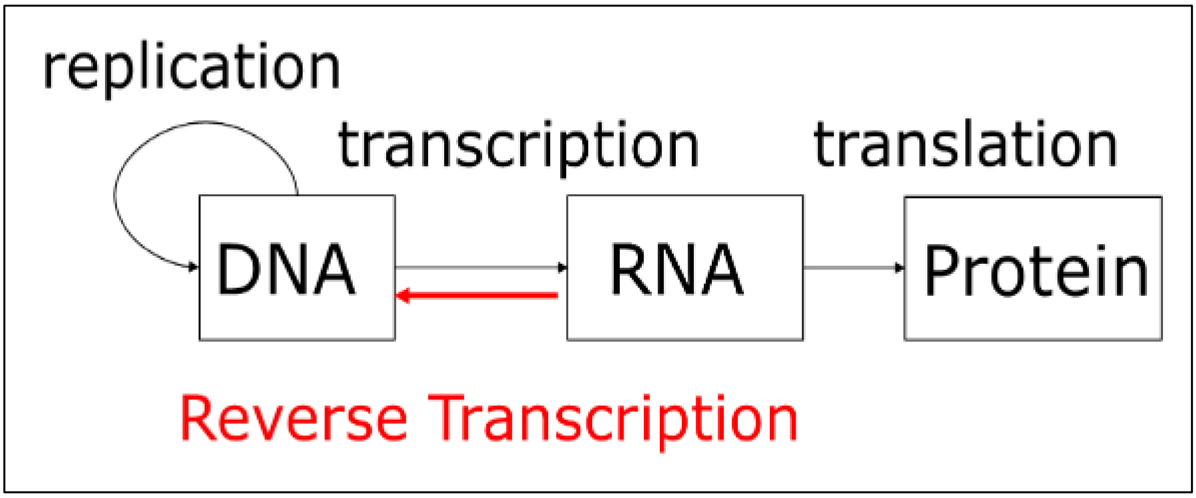

Figure 2-3: mRNA and reverse transcription

In the target adipose tissue gene is expressed by transcribing DNA into single-stranded mRNA, by reverse transcriptase, we convert RNA into complementary DNA (cDNA).

2.2.2 Microarrays Affymetrix GeneChips

All microarray analyses were carried out at Nottingham Arabidopsis Stock Centre (NASC) at the School of Biosciences in University of Nottingham. The integrity of the mRNA extricated from epicardial, perirenal, sternal, omental and subcutaneous adipose tissue samples was analysed using Agilent 6000 bioanalyser (Agilent Technologies, Santa Clara, USA), and successive activities on mRNA were carried out using GeneChip® 3' IVT Express kit (Affymetrix, High Wycombe, UK). Graham et al. (2011) reported the productivity of Affymetrix Human U133+2 chip in analysing gene array expression from sheep tissues (Graham et al., 2011). Every procedure adhered to the recommendations of the manufacturer. Every individual GeneChip® was inserted into Affymetrix® Genechip® Scanner 3000 7G (Affymetrix, High Wycombe, UK) in order to perform fluorescence tests. Partek (Partek Inc., St. Louis, USA) was used to ensure quality control in the appropriate tagging, hybridisation and evaluation of recorded data.

2.2.3 Microarrays quality control analysis

Measures of quality control (QC) are necessary in order to maintain an effective analysis of microarray datasets (Wilson and Miller, 2005). The accuracy of gene expression analysis can be enhanced by eliminating outlier arrays (Wilson and Miller, 2005). The integrity of all quantifications, elimination of noise and a minimum signal-to-noise ratio were as a result of correctional measures during profiling of expression patterns, which led to accurate experimental outputs (Chen at al., 2002). As a result, a higher number of genes could be identified and the amount that was statistically filtered also increased (Wilson et al., 2004). The resultant data was then recorded on a log file that enabled explanation of the significantly highly skewed data reported in some trial outcomes. Systematic variations in microarrays (expression of a similar gene or gene clusters in varying quantities across different microarrays) could also be eliminated.

Accession numbers. All original microarray data were deposited in the NCBI's Gene Expression Omnibus (accession GSE115799).

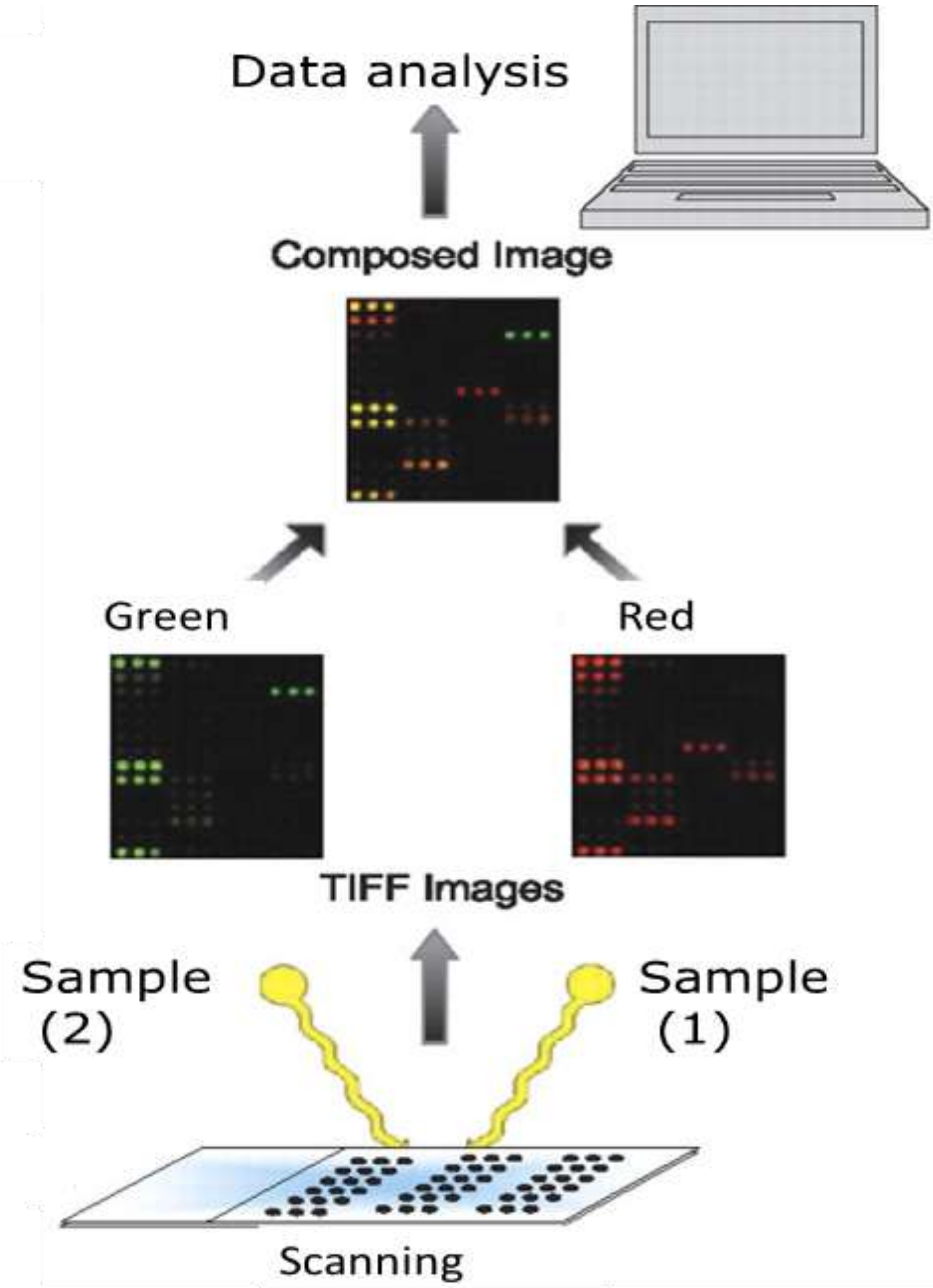

Figure 2-4: Microarray analysis procedure

The mRNAs of two different samples were labelled with two different colours, (green and red), and were combined in one picture which shows if a specific gene is differently expressed in sample 1 (red) compared to sample 2 (green), or the opposite, while the yellow shows that no difference has been found in the probes.

2.2.4 Microarrays bioinformatics analysis by using R programme

Using the power of advanced technology in biological sciences helps in deepening understanding, especially in the genesis and development of complex biologicals systems such as adipose tissue. By using a large dataset of gene expression profiles and showing the modality and mechanics of this system which could help in treat the target in an advance performance (Hansen and Jensen, 1985, Ghafoorunissa, 2008). In this research, I used the R programme, one of the free programmes that can deal with the size of large data to some extent, this mainly by establish supervised, and tested the data under one environment, specifically in the advanced stage of the analysis (Wene et al., 1975, Hansen and Jensen, 1985). On the other hand, it is not easy to deal with this type of software, since R programme is based on statistical computing languages for performing the commands and analysis functions, which require advanced skills, especially in dealing with a large dataset. This requires a complex course of procedures, including using different packets and commands in several stages of analysis in order to indicate the pathway of the gene that has been highly expressed in the discussed-microarrays including the computation and visualisation procedures in the same programme.

2.2.5 Summary of statistical analyses

Based on the recommendation of the manufacturer (Affymetrix) I utilised the Human Genome U133A plus 2 arrays in conducting this study. Free and open source packages could possibly be accessible through the R project in all the microarrays processing stages beginning from normalisation until the evaluation of the network (http://cran.r-project.org/). I was able to access the precise packages for the high-throughput genomic data assessment which were developed by the Bioconductor community for Affymetrix arrays (http://www.bioconductor.org/).The activities of this come under a similar platform, and with the R project's open source regulations. The function of Guanine Cytosine Robust Multi-Array Analysis 'gcrma' implanted in the 'affy' package was also utilised in the prior processing of the data stages, using methods to make background corrections as well as in the normalisation and verification of the probe match. I made use of the 'limma' library in conducting the gene expression statistical analyses. This made it possible for us to perform the empirical Bayesian statistical moduleling (Wettenhall and Smyth, 2004). It is the most suitable for the structure of my study, as it makes it possible for me to be flexible with regard to the presumptions made on prior distributions and the posterior inference found to exist among all groups (Smyth, 2004). The False Discovery Rate or FDR (Benjamini and Hochberg, 1995) approach was utilised in expressing genes as well as for analysing other statistics. The value result $q \leq 0.05$ derived is seen as significant. Both the fold change heat map and the volcano expression plots utilised the R-package graphical Plot 'gplots'. Finally, I utilised the public access online software BioinfoGP for the application of the Venn diagram graphs (http://bioinfogp.cnb.csic.es/). I carried out every part of the statistical analysis with the aid of Dr Hernan Fainberg of the Department of Academic Child Health at the University of Nottingham. Any auxiliary processes relating to statistical analysis will be described in their corresponding chapters.

2.2.5.1 Data pre-processing

The resulting images were used to produce a dataset once the microarrays had been hybridised. Prior to the analysis, this dataset is supposed to be 'pre-processed' and the result interpretation carried out. Pre-processing involves the process of extracting or developing significant data attributes including removing missing data and errors, as well as checking data quality and removing or correcting inappropriate data and setting up the dataset for analysis. The analyses were performed on the R programme.

2.2.5.2 Background correction

For non-specific hybridisation, the process devised to adjust is known as background corrections. This refers to the hybridisation of sample transcripts whose sequences fail to compare with the probe on the array completely.

2.2.5.3 Data transformations

First, the gene expression matrix needs to be saved as a comma-separated values (CSV) delimited text file before the microarrays data background corrected, and complete the log-transformed process. Log transformation facilitates the utilisation of classical parametric statistic testing and enhances the data distribution attributes.

2.2.5.4 Normalisation

Normalisation is a pre-processing phase that tries to correct for systematic variations between arrays or genes that are constantly lower or higher than the ones on the other arrays by using the median as a robust measure.

2.2.5.5 Primary visual examination

These are the most widely used techniques which are based on the principle that visual analysis can be used to examine the extent to which the distribution of sample values is consistent with a theoretical distribution (e.g. normal distribution) or with the distribution of other sample values using different charts (i.e. box plot and histograms).

2.2.5.6 Clustering analysis

Clustering approaches are a very useful technique to classify the differences and similarities across different samples, to specify the outliers, inadequately annotated samples, and to deal with other problems that might be present when examining large datasets of gene expression, based on the single gene expression patterns and function (Simpson, 2012). In my study, principal component analysis (PCA) and the K-means of unsupervised tree-shaped ‘hierarchy’ displayed on ‘Dendrograms’ were applied in order to classify and divide the adipose tissue microarrays data into clusters based on the similarity of individual gene expression and function across five different anatomical depot locations that been supplemented with canola oil in early life. In some cases, the gene expression patterns were not only either closely clustered or spread out but also significantly changed by -fold expression, suggesting gene expression changes in fat depots with age (down- or up-regulation), i.e. temporal regulation. The number of genes expressed was also different across replicates. Performing multiple analyses was therefore very useful in correcting for background noise to avoid type 1 or type 2 errors.

2.2.5.7 Heat Map and volcano plot analysis

The heatmap and volcano plot function can be utilised in R, after the clustering method. Both tests are mainly used to provide an overview and identify the changes in gene expression patterns. Volcano plots indicate those genes that experience significant changes in gene expression (up-/down-regulated) based on a q-value < 0.05 and a twofold change in standard error. The heat map in this study was used to classify the top 100 differentially expressed genes and lipids (down- or up-regulated) from the lipidomic and microarray analyses.

2.2.5.8 Selection of informative genes

An ML algorithm and weighted gene co-expression network analysis enabled identification of any alterations in the roles and functioning of genes throughout the five fat depots with respect to age (7 and 28 days). The optimal pattern of gene expression within every depot and each control and the dietary group was analysed through iterations and ML algorithms like the Random Forest (Breiman, 2001), so as to reduce the magnitude of the random error term. A PSOL algorithm generated from the Random Forest was also used within the R package of ml-DNA (Ma et al., 2014) since its estimation accuracy (c. 95-98%) in gene recognition is superior (Díaz-Uriarte and De Andres, 2006; Ma et al., 2014; Wang et al., 2006).

The machine learning algorithms successfully classified or estimated the first 100 genes that had been chosen on the basis of Bayesian analysis and moduleling from distinct adipocyte cells within every dietary category. Afterwards, the fivefold cross-validation method was carried out in order to determine the precision of obtained values by splitting the dataset into five different subsets. (Breiman, 2001). In this procedure, the dimensional scores of the x and y-axes of every chosen interaction pattern were analysed starting from the thresholds. The axes (x and y) indicate false and true positives correspondingly. The dimensional scores, also simply referred to as area under the curve (AUC), were determined using ROC analysis with a range of 0 to 1. The rate of precision is expected to increase as the AUC score tends to 1 in the RF module (see Appendix 9.3).

2.2.5.9 Network formation of gene co-expression

Datasets analysed in this study consisted of data from 50 samples, divided equally into two groups, (i.e. 25 samples in each age group; 7 and 28 days), which were acquired from experimental subjects in the control category, as well as an additional 20 samples acquired from experimental subjects in the canola group. The data were recorded on five types of fat depots; the epicardial, perirenal, sternal, omental, subcutaneous adipose tissues from five lambs in every dietary group. However, sampled tissues of the sternal fat depot numbered four from the group subjected to supplements of canola oil. Each dataset was separately formed through a standard workflow, in line with recommendations of the weighted analysis of correlation patterns; the weighted gene co-expressed network analysis (WGCNA) data-mining approach (Zhang & Horvath, 2005). These were then further remoduleled by the technique of Yao et al., 2005. Individual datasets were then referred to in the formation of an integrative signed correlation network. The non-informative genes in each group were excluded from the analysis of biological and molecular activity, and instead, the informative genes were designated for inclusion into the ML procedure of filtering (Ma et al., 2014). However, it is important to note that there exists no conclusive interpretation of what an 'informative' or 'non-informative' gene is (Dziuda, 2010). As a result, it is necessary to clarify the term 'informative gene' in the context of this study. In this review, the term is used to define all genes that are of significance to the anticipated pathways of module differentiation and functioning of the BAT.

The process of weighted gene co-expression analysis involves the formation and identification of sequences of gene expression amongst sampled tissues that occur as microarray datasets from every dietary group. A function referred to as 'module preservation' was embedded in the R package of weighted gene co-expression network analysis (Yao et al., 2005). The function was used to analyse relations between the established modules arising from the two age and dietary groups. It is also important in determining the correct expression of modules of the reference set. The algorithm evaluates statistical module preservation in terms of pairs of the relevant reference and test sets. In this study, the reference set is the control group (animals fed on a standard diet) while the test set is the canola group (animals fed on a standard diet and 3% canola oil supplements). In every reference-test pair, the 'module preservation' algorithm returns a Z-summary score. The score is used to determine a ratio/measure of how the generated modules of the control group are transferred and maintained within the group receiving supplements of canola oil with respect to similar genes that occur between the two sets (i.e. the reference set and the test set). A Z-summary value exceeding 10 is regarded to be an indicator of high levels of module preservation (i.e. the design of the found modules has not been altered). A value in the range of two to ten is regarded as an indicator of moderate preservation. On the other hand, a value lower than two indicates no preservation in the found modules. The Z-summary statistic may be computationally intensive since it is evaluated on the basis of a generation of 200 random permutations between two independent datasets, and may also be affected by the size of the module (Oldham et al., 2006).

2.2.5.10 Analysis of gene ontology (GO)

A utilitarian enrichment analysis test was carried out with the aim of identifying and explaining the genes existing within every module. The analyses were conducted with the use of Web Gestalt, a WEB-based GEne SeT Analyses Toolkit. GO labels having an FDR score below 0.05 and an enrichment value exceeding five in every grouping are illustrated (Wang et al., 2013) below in Figure 2-4.

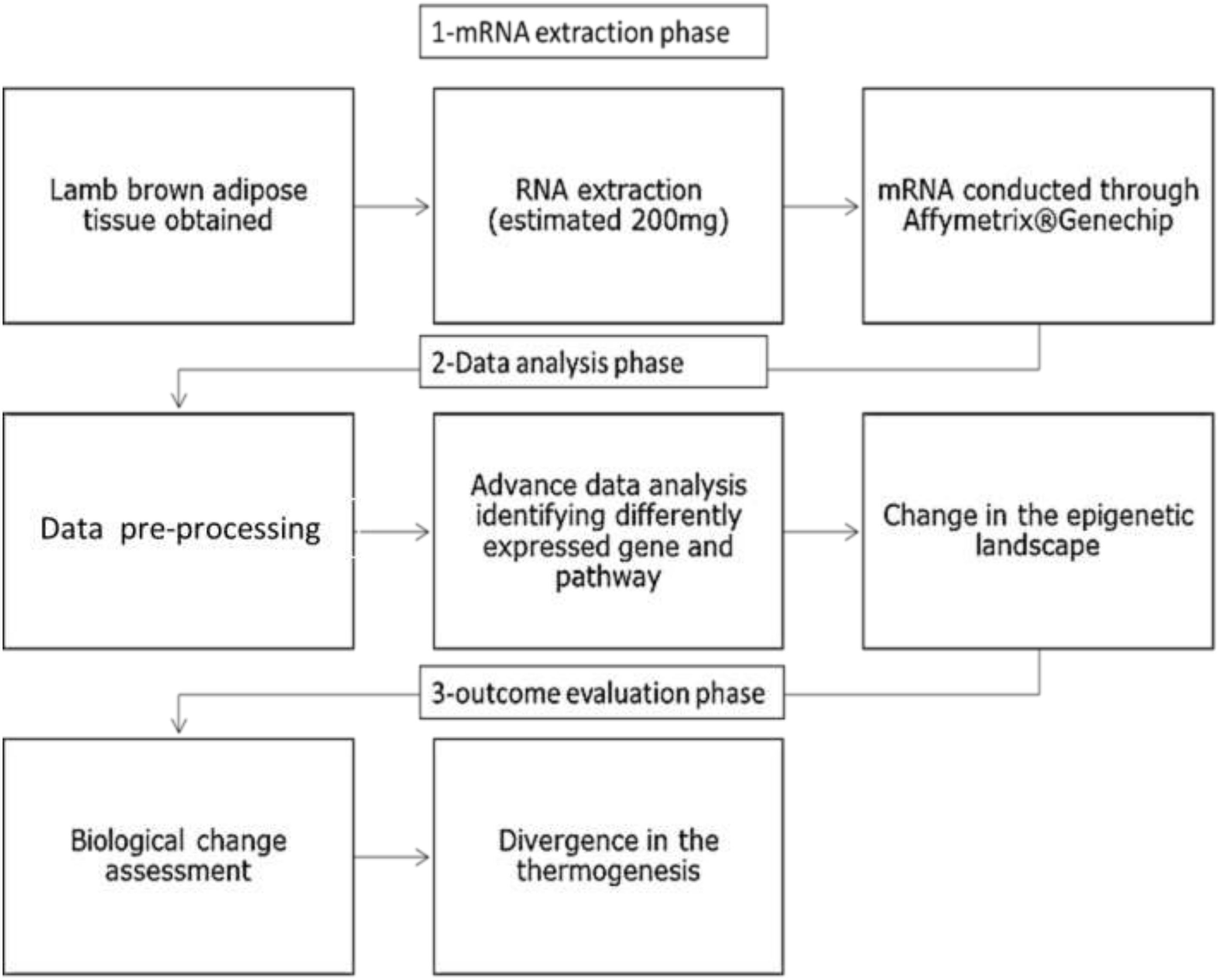

Figure 2-5: Overview of the microarray data study design from RNA extraction to data analysis process to data outcome

2.3 Determination of adipose tissue lipid composition

All the lipid preparation and procedures (excluding the lipid MS analysis) were done by Prof David Barrett and Dr Catharine Ortori.

The samples of adipose tissue (100 – 200 mg) were ground in Retsch ball mill for three minutes using six-millimetre stainless steel balls and then pre-chilled to −18°C. Chilled chloroform, that is, 2:1 methanol, was added (0.5 mL), and the mixture was stirred up for 20 minutes at room temperature, then centrifuged at 10,000 × g at 4°C for 10 minutes. The bottom layer was taken out and put into a centrifugal evaporator. The samples were re-formed to 100 μL chloroform, i.e. 1:2 methanol centrifuged, and transferred to amber glass LC vessels with inserts and kept at −80°C until LC-MS analysis. Lipidomic QC specimens were prepared by mixing up equal amounts of all specimen extracts. Five microlitres of the obtained lipids were put into a an Agilent Poroshell 50 × 2.1 mm at 45°C 120 SB-C18 Agilent Poroshell with 2.7 μm particle size, and washed with 0.1% aqueous ammonium acetate (A) to 0.1% aqueous ammonium isopropanol/acetonitrile/acetate gradient (8:1:1) (B) by means of gradient elution. The Hemel Hempstead, UK's Thermo Scientific Accela modular HPLC system was applied at 0.45 mL/min flow rate. The ThermoScientificHemel Hempstead, UK's Exactive series mass spectrometer was used for detections in the range *m/z* 100 to 1900 in electrospray method with +/−ve switching at 25000 resolution setting. Total ion account was normalised, pre-processed and transferred to Excel for further analysis with the help of Progenesis, Newcastle upon Tyne, UK's Progenesis QI software. Lipid MS Predict, a production prediction tool from Lipidmaps, was used to facilitate spectral understanding. The identities of the chosen isobaric lipid types were then revealed by preparing

MS/MS spectra (nominal mass) with the help of a particular LC method using a Thermo Scientific LTQ Velos ion trap mass spectrometer through the same electrospray basis and with an impact energy of 40 (Ravipati et al., 2015).

3 Method validation

3.1 Introduction

By using published data from a previous study (Svensson et al., 2011), this chapter evaluates the validity of my thesis methodology of using bioinformatics tools to analyse microarray data.

3.2 Methods

3.2.1 Statistical and function profiling analysis

A detailed description of the statistical methods and function profiling analysis used in my investigation can be found in Chapter 2.

3.2.2 Subjects and samples

Human microarray data profiles were obtained from parathyroid adipose tissue containing islets of brown adipose tissue (BAT) and paired subcutaneous adipose tissue (WAT) profiles from patients who were undergoing surgery in the thyroid area (GSE27657) (seven women and two men; aged 21–76 years) (see Table 3-1) (Svensson et al., 2011).

Table 3-1: Patient characteristics
Adapted from (Svensson et al., 2011)

Patient	Sex	Age (years)	BMI (kg/m^2)	Reason for surgery
1	Male	21	23.6	Hyperparathyroidism
2	Female	39	23.3	Non-toxic goiter
3	Male	23	20.2	Thyrotoxicosis
4	Female	60	20.3	Benign thyroid cyst
5	Female	59	21.6	Hyperparathyroidism
6	Female	71	26.4	Hyperparathyroidism
7	Female	50	23.1	Non-toxic goiter
8	Female	76	25.7	Non-toxic goiter
9	Female	32	23.8	Thyrotoxicosis

3.3 Results

3.3.1 Quality control of microarrays

In order to prepare microarray data (nine paired samples from parathyroid), previously published data were analysed by microarrays for gene expression analysis for non-specific hybridisation and background corrections. The data are usually log-transformed once background correction is completed. After this, the pre-processing phase takes place, which tries to correct the systematic variation between arrays or genes that are constantly lower or higher than those on the other arrays and thus removes the variance effect Figure 3-1. Then, by using K-means and depending on the similarity in gene expression pattern the data are divided into groups (clusters) in tree-shaped 'hierarchies' displayed on 'Dendrograms', dividing the data obtained into two unique groups (subcutaneous and parathyroid) (see Figure 3-2). However, the results indicate that one sample was regulated differently when comparing BAT to WAT. According to the data in Table 3-1, I found that there was only one patient who was diagnosed as 'Benign thyroid cyst', therefore I decided to remove that sample from the analysis.

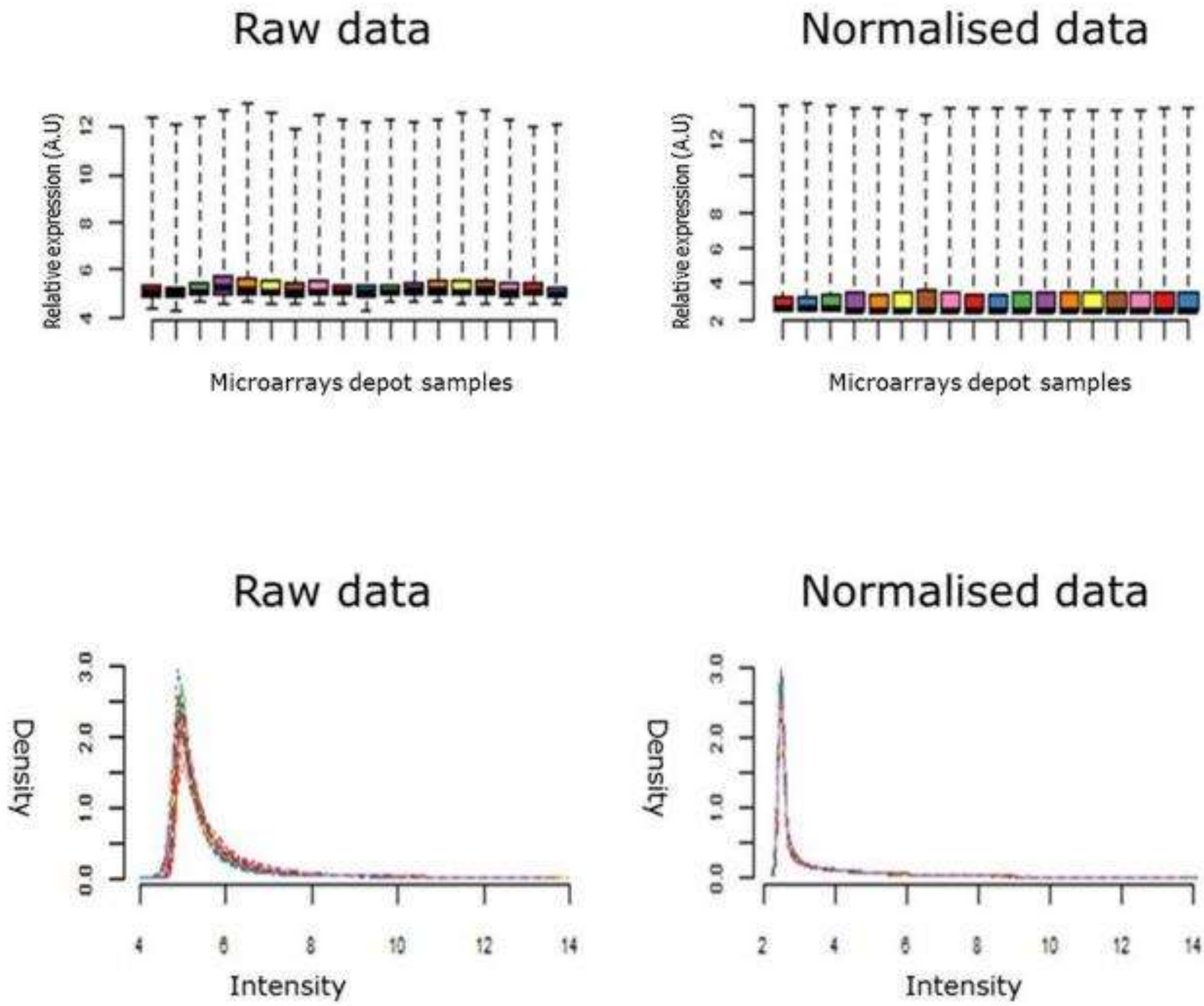

Figure 3-1: Microarray data normalisation process

The box plot shape of the data distribution by the mean, while the density plots using a signal distribution across the chip.

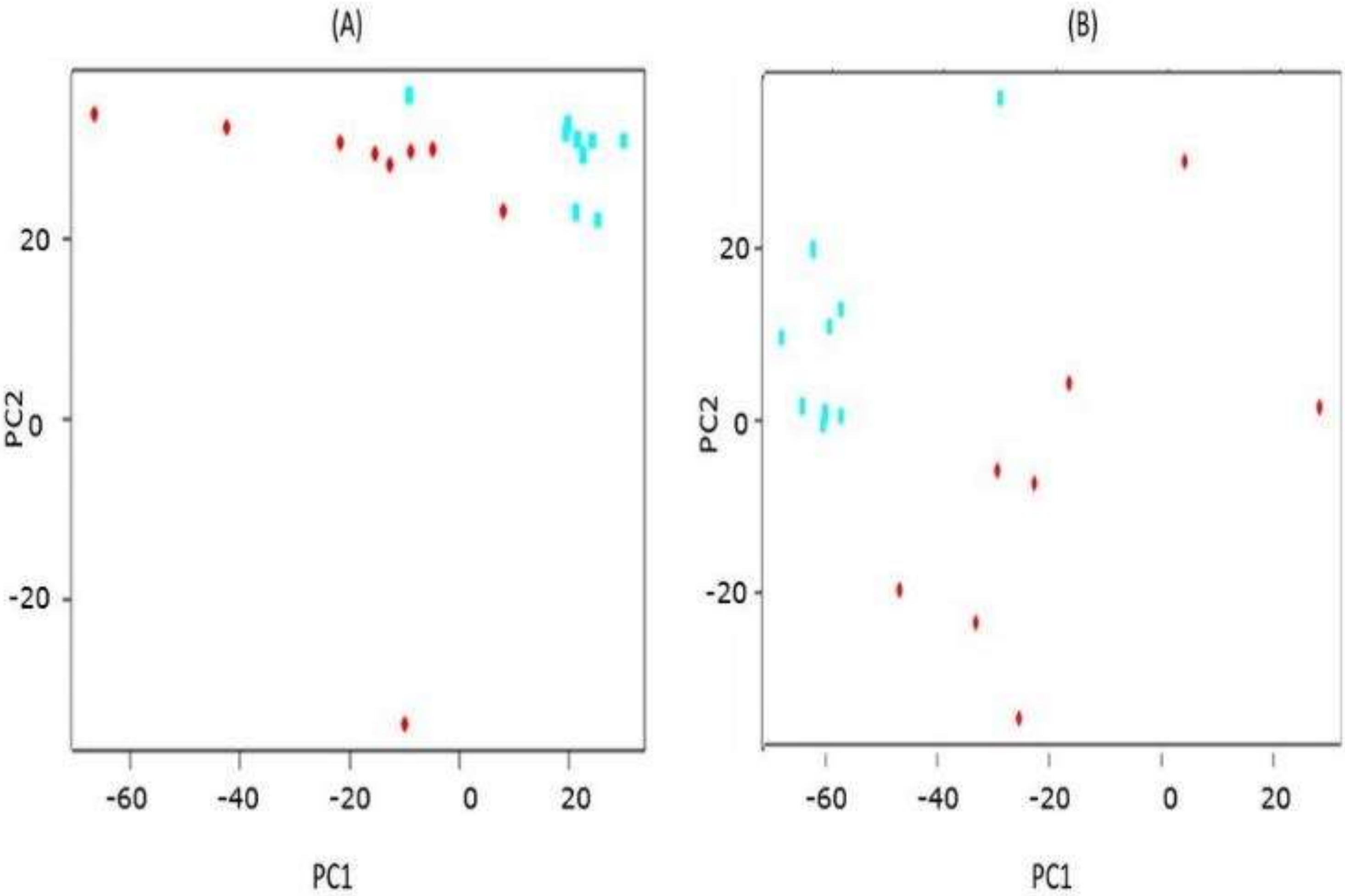

Figure 3-2: Principal component analysis and tree cluster analysis

(A) Principal component analysis (PCA) of gene expression data from two adipose tissue depots from each subject was performed using 1982 datasets that passed the variance test QC. Each sample is represented by colour-coding to indicate the depot to which it belongs: parathyroid - red (n = 9); subcutaneous – turquoise (n = 9). (B) The graph shows the difference in PCA after removing the outlier sample number (PT80) from the parathyroid cluster (represented by the red circle). PC1 axis is the first principal direction along which the samples show the largest variation. The PC2 axis is the second most important direction and it is orthogonal to the PC1 axis.

3.3.2 Identification of gene expression profiles

To identify genes that were differentially expressed in human BAT compared to WAT, nine paired samples from parathyroid (8) and subcutaneous (9) were analysed by microarray. The analysis from the microarray data obtained confirmed that 1982 genes from a total of 10077 genes were significantly expressed in BAT compared to WAT; 49 of those genes had at least a twofold higher expression. Further analysis of the expression profiles, using the criteria described above, it was confirmed that the UCP1 gene was overexpressed in the samples classified as BAT, as shown in Figure 3-4 and Table 3-4.

3.3.3 Gene expression pattern

In order to provide an overview and identify the change in gene expression patterns (up- and down-regulated) in the examined sample, the data were tested in a Volcano plot (Figure 3-4). My results indicate that there are 1982 genes (represented by a solid red circle) that were significantly changed (down- or up-regulated) according to the q-value < 0.05, and a twofold change. This result suggests that there is a significant change when comparing BAT to WAT in terms of gene expression profiling. However, it should be noted that not all the genes with a significant q-value have a change of twofold or more. The heat map in Figure 3-4 was used to classify the top 100 differentially expressed genes (down- or up-regulated) from the microarrays analysis by comparing BAT to WAT, and as expected it showed that UCP1 gene expression was significantly different between examined depots.

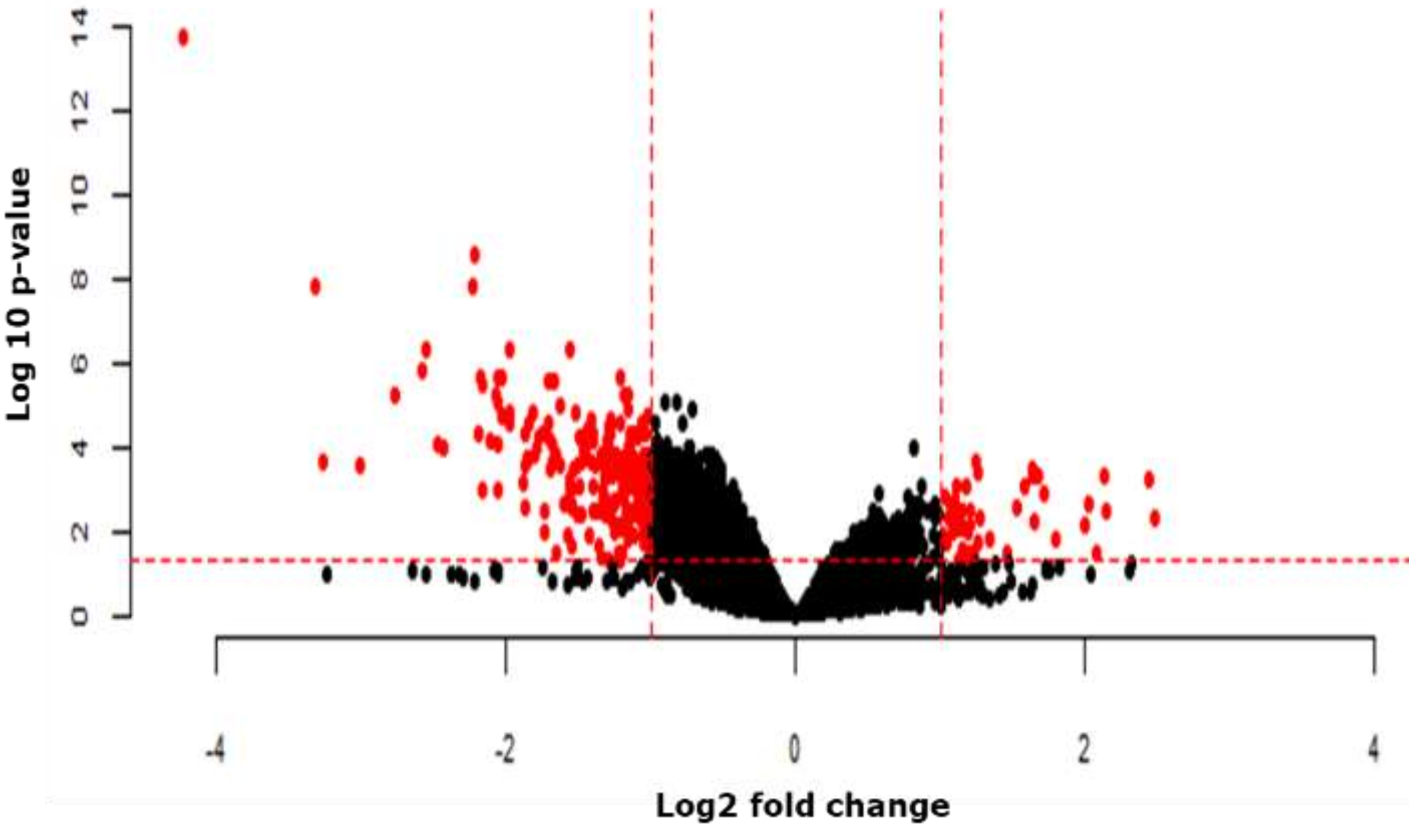

Figure 3-3: Volcano plots representing changes in gene expression of all transcripts when comparing BAT to WAT

Volcano plot was performed using 1982 datasets that passed the variance test QC. The log of the FDR-adjusted probability values (q-value) (y-axis) plotted against the log fold-changes (x-axis) between the parathyroid (n = 8) and subcutaneous (n = 9) adipose tissues. Those genes that were expressed significantly differently in the sample are represented by a solid red circle, and those that did have significant change are coloured black (q < 0.05 (FDR correction - Bayes moderated t-statistics).

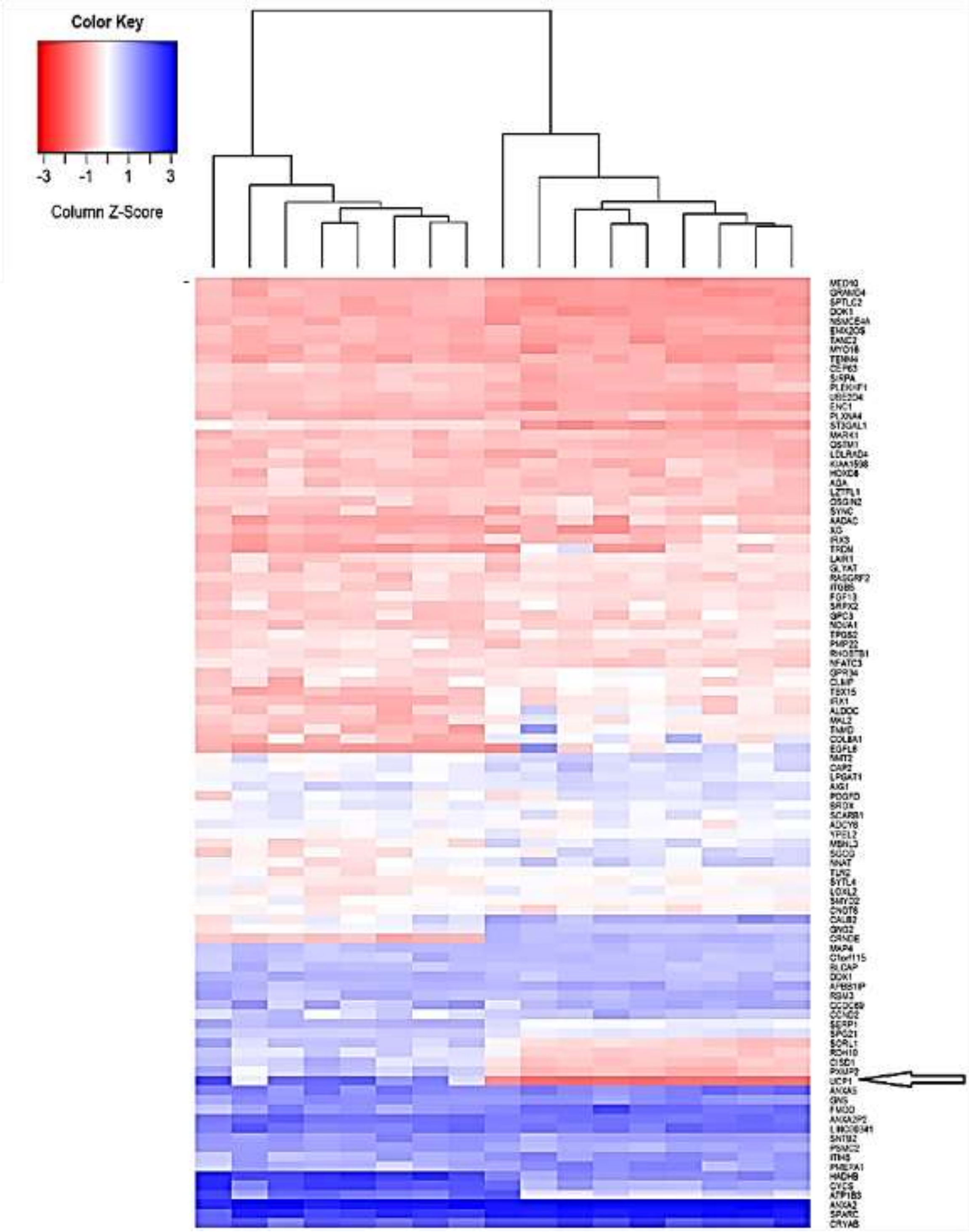

Figure 3-4: Heatmap of the top 100 genes

Dendrograms visualise the hierarchical clustering results of the top 100 differentially expressed genes identified from the microarray analysis in comparing BAT representing by Parathyroid (n = 8); to WAT representing by subcutaneous (n = 9), Gene expression using 1982 datasets that passed the variance test QC data were transformed to a Z-score, shown by a colour code, with blue representing an increase in gene expression and red showing the opposite.

3.3.4 Functional profiling

Gene ontology (GO) and Kyoto Encyclopedia of Genes and Genomes (KEGG) pathway were utilised in order to examine further the biological processes, including metabolic or regulatory pathways, in terms of the genes that were significantly down- and up-regulated expressed in the samples. In accordance with (GO) analysis using the AmiGO browser (http://amigo1.geneontology.org), 378 biological processes were enriched ($q < 0.05$). The diagram in Figure 3-5 shows the top four4 (coloured in pink) of a total of the top 12 biological processes that were differentially expressed when comparing BAT to WAT. The top 10 biological processes by Q-value are presented in Table 3-3. In order to identify and determine a specific biological pathway, in relation to the thermogenesis process, the data were analysed by using the KEGG pathway. The results show there are n KEGG pathways that were significant ($q < 0.05$) when comparing parathyroid and subcutaneous adipose tissues (see Table 3-3).

Practically the pathway in Figure 3-6 suggests that 13 genes from a total of 71 genes have significant changes (down- or up-regulated) according to the standard twofold of change. A majority of these genes have their main function in mitochondria (see Table 3-4). In addition, this pathway assumes that PPARG could impact significantly on UCP1. It is a nuclear hormone receptor, activated by fatty acids and their derivatives, that plays a role in promoting adipocyte differentiation to enhance blood glucose uptake (Jones et al., 2005; Nolte et al., 1998). It regulates the transcription of the UCP1 gene and has the ability to rapidly increase energy expenditure by increasing the oxidation of free fatty acids (FFA) and glucose uptake (Cinti, 2006), so thermogenesis is activated (Cannon and Nedergaard, 2004).

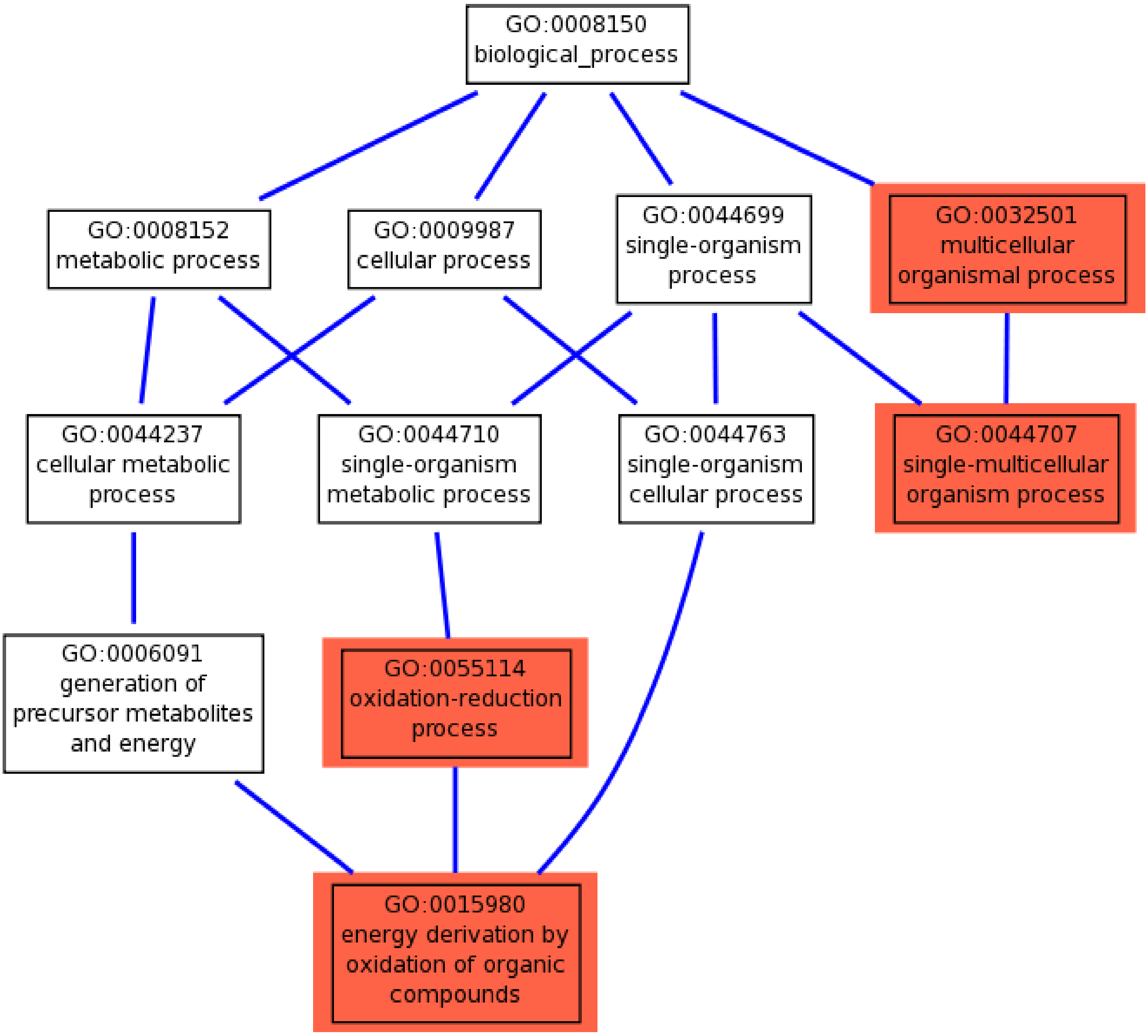

Figure 3-5: Gene ontology overview in comparing WAT to BAT

The top biological processes that were significantly different ($q < 0.05$), represented in pink squares) when comparing subcutaneous (WAT) to parathyroid (BAT).

Table 3-2: The top 10 enriched biological processes in the comparison between subcutaneous and parathyroid adipose tissue

Gene Ontology code	Biological process	Q-value
GO:0032501	multicellular organismal process	0.00
GO:0044707	single-multicellular organism process	0.00
GO:0015980	energy derivation by oxidation of organic compounds	0.00
GO:0055114	oxidation-reduction process	0.00
GO:0048731	system development	0.00
GO:0001667	ameboidal cell migration	0.00
GO:0035295	tube development	0.00
GO:0009719	response to endogenous stimulus	0.00
GO:0001568	blood vessel development	0.00
GO:0007275	multicellular organismal development	0.00

Table 3-3: The nine KEGG pathways that were significantly different between parathyroid and subcutaneous adipose tissue

Pathway	Genes reference
Protein digestion and absorption	4974
Citrate cycle (TCA cycle)	20
Cardiac muscle construction	4260
ECM-Receptor interaction	4512
Proximal tubule bicarbonate reclamation	4964
Bile secretion	4976
Pancreatic secretion	4972
Fatty acid degradation	5016
Huntington disease	71

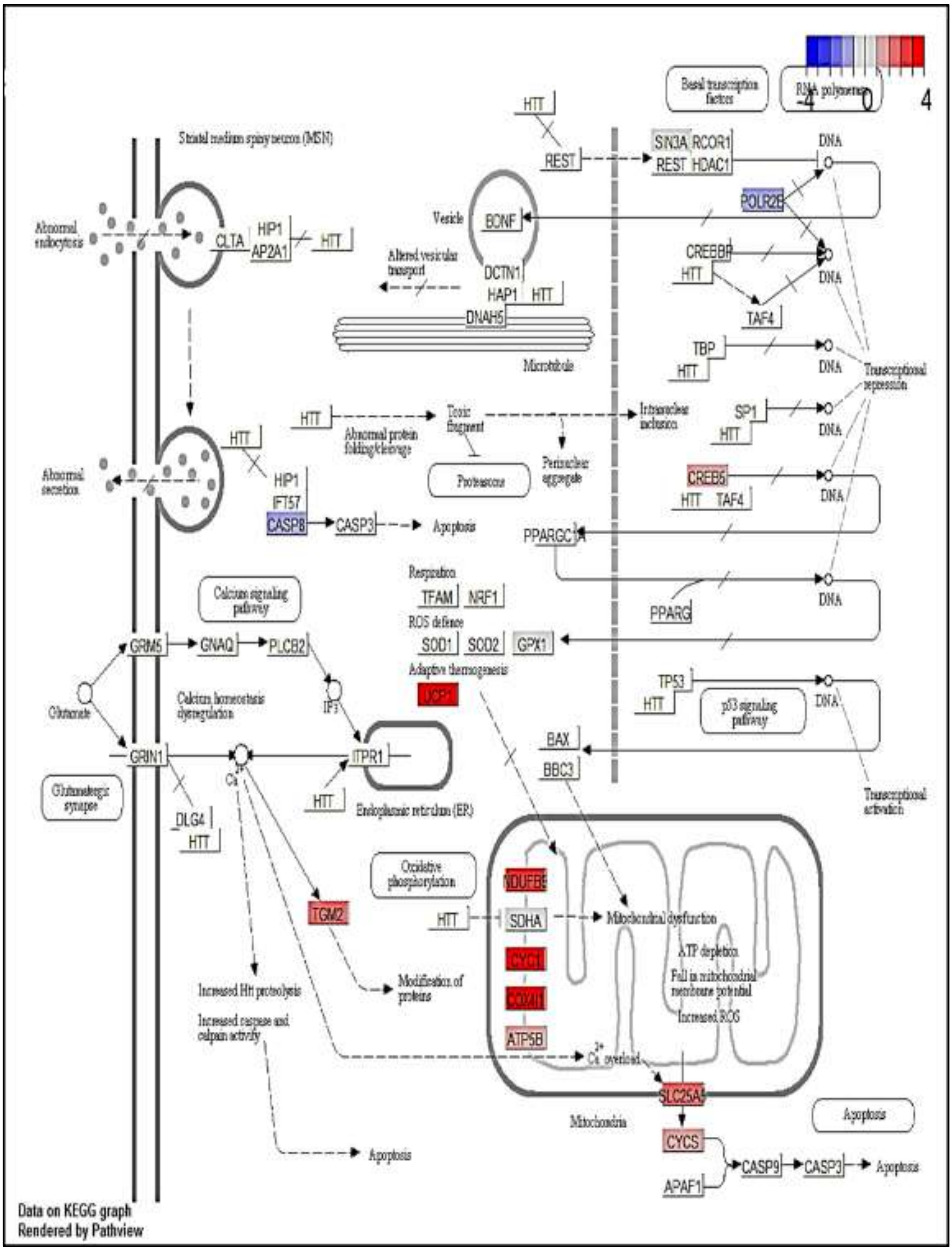

Figure 3-6: KEGG Pathway

Thirteen genes (including ucp1) involved in the above pathway were found to be significantly different when comparing subcutaneous (WAT) to parathyroid (BAT), shown by colour scale, with blue colour representing a decrease in gene expression and red showing the opposite.

Table 3-4: Top 10 genes expressed differently in the KEGG pathway when comparing WAT to BAT

Symbol	Gene name	Change fold
UCP1	Mitochondrial uncoupling proteins 1	4.29
COX4I1	Cytochrome C Oxidase Subunit IV Isoform 1	4.14
CYC1	Cytochrome C-1	3.40
NDUFB9	NADHDehydrogenase(Ubiquinone) 1 Beta Subcomplex, 9, 22kDa	2.43
TGM2	Transglutaminase 2	2.06
SLC25A5	Solute Carrier Family 25 (Mitochondrial Carrier; Adenine Nucleotide Translocator), Member 5	1.98
CYCS	Cytochrome C, Somatic	1.25
ATP5B	ATP Synthase, H+ Transporting, Mitochondrial F1 Complex, Beta Polypeptide	1.08
CREB5	CAMP Responsive Element Binding Protein 5	0.97
SDHA	**Succinate dehydrogenase complex, subunit A, flavoprotein variant**	0.68

3.4 Discussion

Using the bioinformatics data in combination with the R programme, which uses advanced statistical analysis tools, has become one of the innovative ways, in biological sciences, to deal with big datasets (i.e. microarrays). It is able to design a complex transcription which comprises various mathematical equations and algorithms with the aim of gaining an accurate assessment of the developmental mechanisms in certain metabolic diseases, including obesity (Ghafoorunissa, 2008).

However, developing such a long transcript, which comprises different stages of analysis and multiple commands and functions, should be primarily tested by using different methods to evaluate the accuracy of the whole procedure and the final outcome. Therefore, in this chapter, I have established an experiment to determine the validity of the method, by using human microarray data obtained from a previously published study in 2011, which was used with the aim of identifying the parathyroid, gene expression profile and function as BAT, in comparison with the subcutaneous WAT which was obtained from different anatomical locations (Svensson et al., 2011).

By performing a transcriptomic analysis to identify differences in gene expression profiles between the two examined depots (i.e. BAT and WAT), in different anatomical locations, my results partially matched those of the previous study. Although the PCA and tree cluster analysis results indicated that one of the investigation samples was regulated differently when comparing BAT to WAT, by reviewing the original data, I found that the patient was diagnosed and classified in a different stage of the disease (i.e. thyroid cyst), compared to other patients who were mostly diagnosed as either having hyperparathyroidism or a non-toxic goitre. This could have an impact on the biological function of the obtained tissue (Divakaruni and Brand, 2011, Westerterp and Goran, 1997).

In addition, the published study indicated that there was a significant difference between the two biopsied depots including parathyroid (BAT) and subcutaneous (WAT), in terms of the gene expression profile and mitochondrial genes, particularly ucp1, which has been found to be highly expressed in brown adipocytes. This was confirmed in my experiment, and further evaluated visually, by using the advanced tools of analysis (i.e. volcano, box plot and the heat map) which are based on robust statistical relationships (i.e. significant FDR < 0.05, and change of twofold or more) (Gentleman et al., 2004). These reflect the power of combining statistical and visual technical tools (i.e. plot, dendrogram, heat map) when evaluating such a big dataset.

GO enrichment and KEGG pathway were applied with the purpose of translating and transferring the significant differences in gene expression profiles between BAT and WAT. It identified the biological functional phase that could explain gene expression variations through specific pathways linked to mitochondrial function (i.e. thermogenesis) (Larson et al., 1996, Kanehisa et al., 2017). The mitochondrial oxidative phosphorylation pathway thus differed between BAT and WAT and was linked to the mitochondrial energy capacity, and to the ability of UCP1 in BAT to produce heat rather than ATP (Hill et al., 1992).

3.5 Conclusion

In conclusion, my results demonstrate that there are significant changes in gene expression profiling and function when comparing different depots in terms of anatomical locations in humans. The same method can now be used in the examination of adipose tissue from sheep whose diet has been supplemented with canola to examine a nutrition intervention in early life and its potential consequences for metabolic health in later life (Symonds et al., 2012). The data presented in this study suggest that the microarray gene expression in combination with advanced data analysis tools provide a robust and accurate approach for producing adipose depot-specific gene signatures. Moreover, this approach is also expected to enhance the ability to identify and manipulate specific characteristics of adipose tissue in different anatomical locations. However, it should be acknowledged that reactivating the thermogenesis process, particularly in a human, is more complicated than targeting single genes (UCP1).

4 Dynamic transition in the gene expression profile during postnatal development

4.1 Introduction

In humans, the functionality of brown adipocytes reduces with age (Nedergaard et al., 2007, Virtanen et al., 2009), and they are replaced with white adipose tissue (Symonds et al., 2015, Pope et al., 2014). In the present study, I addressed this hypothesis and further investigated how age influences the physiological functioning of BAT in sheep.

4.2 Hypothesis

For this study, based on previous research (discussed above) about the association between adipose tissue and age I hypothesised that:

-Adipose tissue transforms from energy consumption to an energy storage tissue coincident with the loss of the brown adipose tissue-specific uncoupling protein 1 in different degrees between depots during the first month of young sheep life.

4.3 Methods

Ten twin-bearing, non-identical Blue-faced Leicester cross Swaledale ewes were given a standard roughage diet after they gave birth (n = 10). Every twin was raised naturally with their mother until they reached the age of 28 days when they were then euthanised and samples of their tissues taken for analysis (see Figure 4-1).

I performed a transcriptomic comparison between five different depots (epicardial, sternal, perirenal, omental and subcutaneous) over the specific time of period from 7 to 28 days of age. I applied a machine learning (ML) algorithm and a weighted co-expression network analysis (Claussnitzer et al., 2015b, Frayling et al., 2007, Lotta et al., 2017, Rajakumari et al., 2013) to identify the dynamic transformation of the gene expression profiling with age in early life development on adipose tissue function and cellular plasticity.

A detailed description of the statistical methods and function profiling analysis used can be found in Chapter 2.

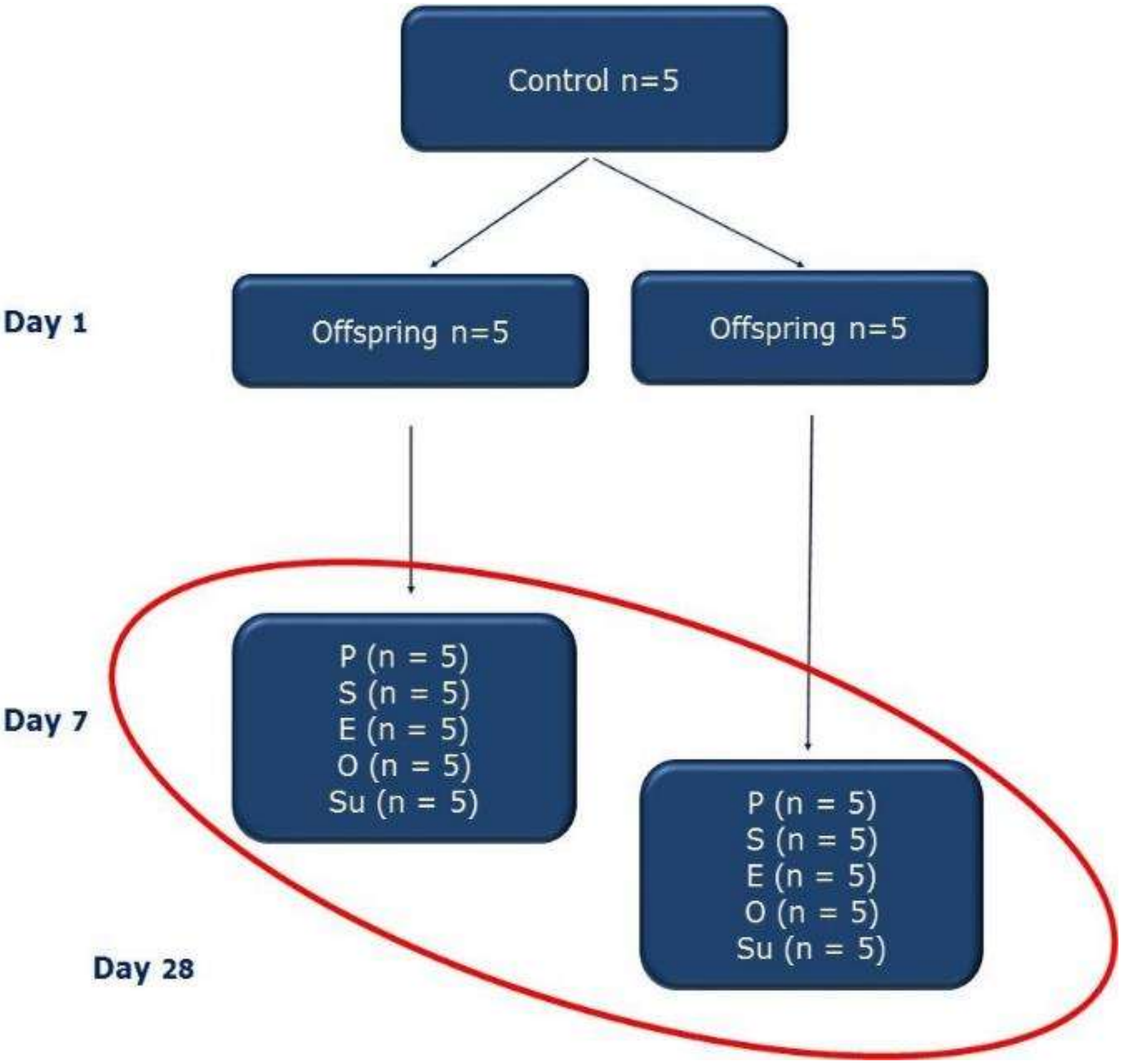

Figure 4-1: Summary of the study design

Datasets included data from 50 samples obtained from 10 lambs with the aim of characterising the gene expression profile difference within the same depot at two time points, either seven days or 28 days (n = 5 at each time point within each depot) for five different adipose tissues depots ((P) perirenal, (S) sternal, (E) epicardial, (O) omental, and (Su) subcutaneous). The day numbers indicate age.

4.4 Results

4.4.1 Principal component analysis and hierarchical clustering at 7 and 28 days of age

Principal component analysis (PCA), heatmap and unsupervised hierarchical clustering dendrograms were applied for each examined depot to show the level of variation in the gene expression pattern between all examined depots, as well as in each fat depot independently, during the development from 7 to 28 days of age. The results in Figure 4-3, Figure 4-2, Figure 4-4, Figure 4-5 ,and Figure 4-6 show that each of the fat tested depots has separated at this stage of physiological development (i.e. from 7 to 28 days), suggesting that the gene expression pattern (down- or up-regulation), has been significantly changed in each fat depot with age.

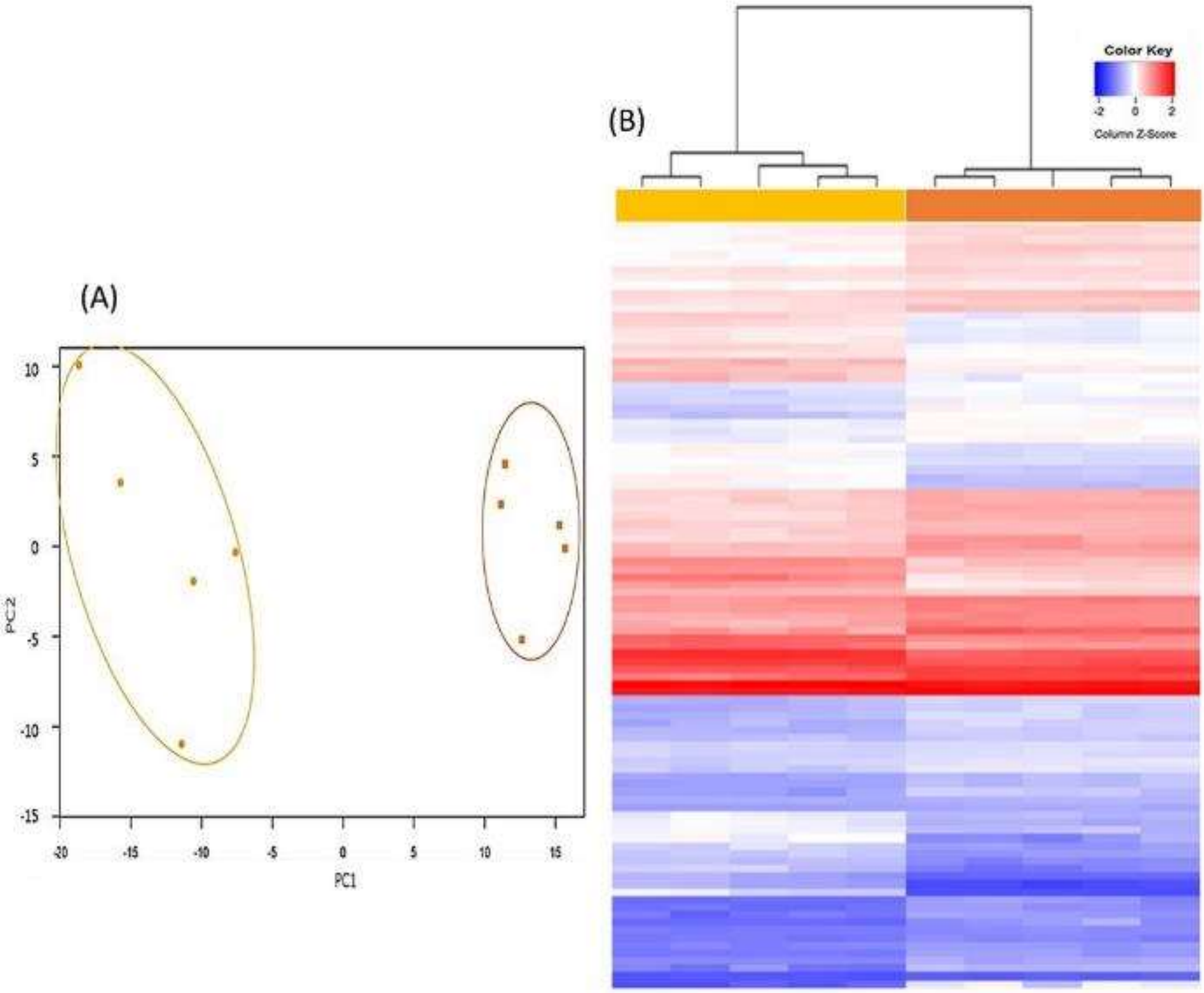

Figure 4-2: Cluster analysis of the perirenal fat depot

(A) Principal component analysis (PCA) of gene expression data from perirenal adipose tissue depot from each animal was performed using 1649 datasets that passed the variance test QC. Each sample is represented by colour-coding to indicate the age to which it belongs: seven days, light orange (n = 5); 28 days, dark orange (n = 5). PC1 axis is the first principal direction along which the samples show the largest variation. The PC2 axis is the second most important direction and it is orthogonal to the PC1 axis. (B) Heat map and unsupervised hierarchical clustering dendrograms for the top 100 deferentially-expressed genes identified by microarray analysis (average linkage, Euclidean distance metric) between 7 and 28 days as selected by eBayes moderated t-statistics (FDR < 0.05). Gene expression was transformed to a Z-score, and blue represents a decrease and red an increase in gene expression with age.

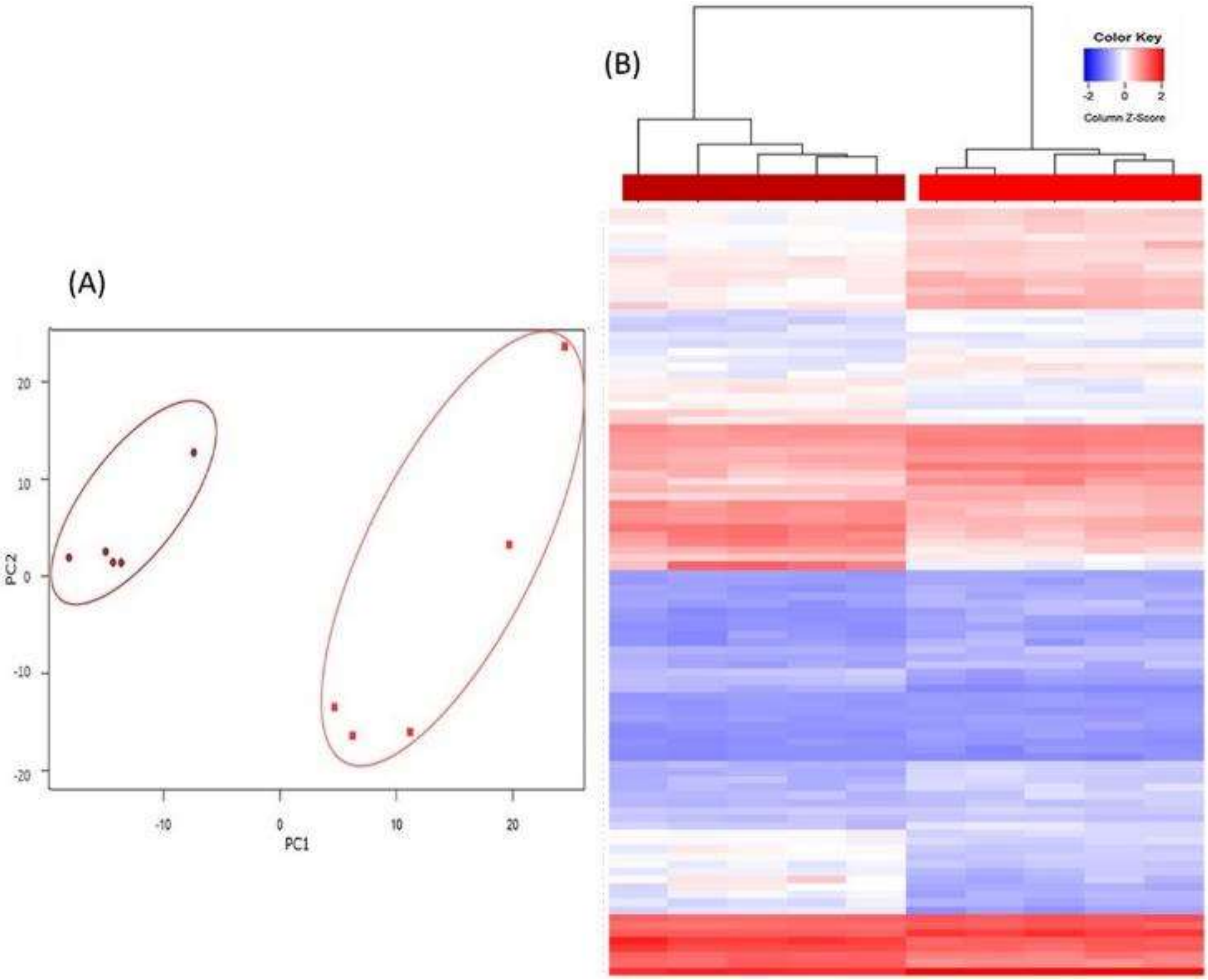

Figure 4-3: Cluster analysis of the sternal fat depot

(A) Principal component analysis (PCA) of gene expression data from sternal adipose tissue depot from each animal was performed using 820 datasets that passed the variance test QC. Each sample is represented by colour-coding to indicate the age which it belongs: seven days, light red (n = 5); 28 days, dark red (n = 5). PC1 axis is the first principal direction along which the samples show the largest variation. The PC2 axis is the second most important direction and it is orthogonal to the PC1 axis. (B) Heat map and unsupervised hierarchical clustering dendrograms for the top 100 deferentially-expressed genes identified by microarray analysis (average linkage, Euclidean distance metric) between 7 and 28 days as selected by eBayes moderated t-statistics (FDR < 0.05). Gene expression was transformed to a Z-score, and blue represents a decrease and red an increase in gene expression with age.

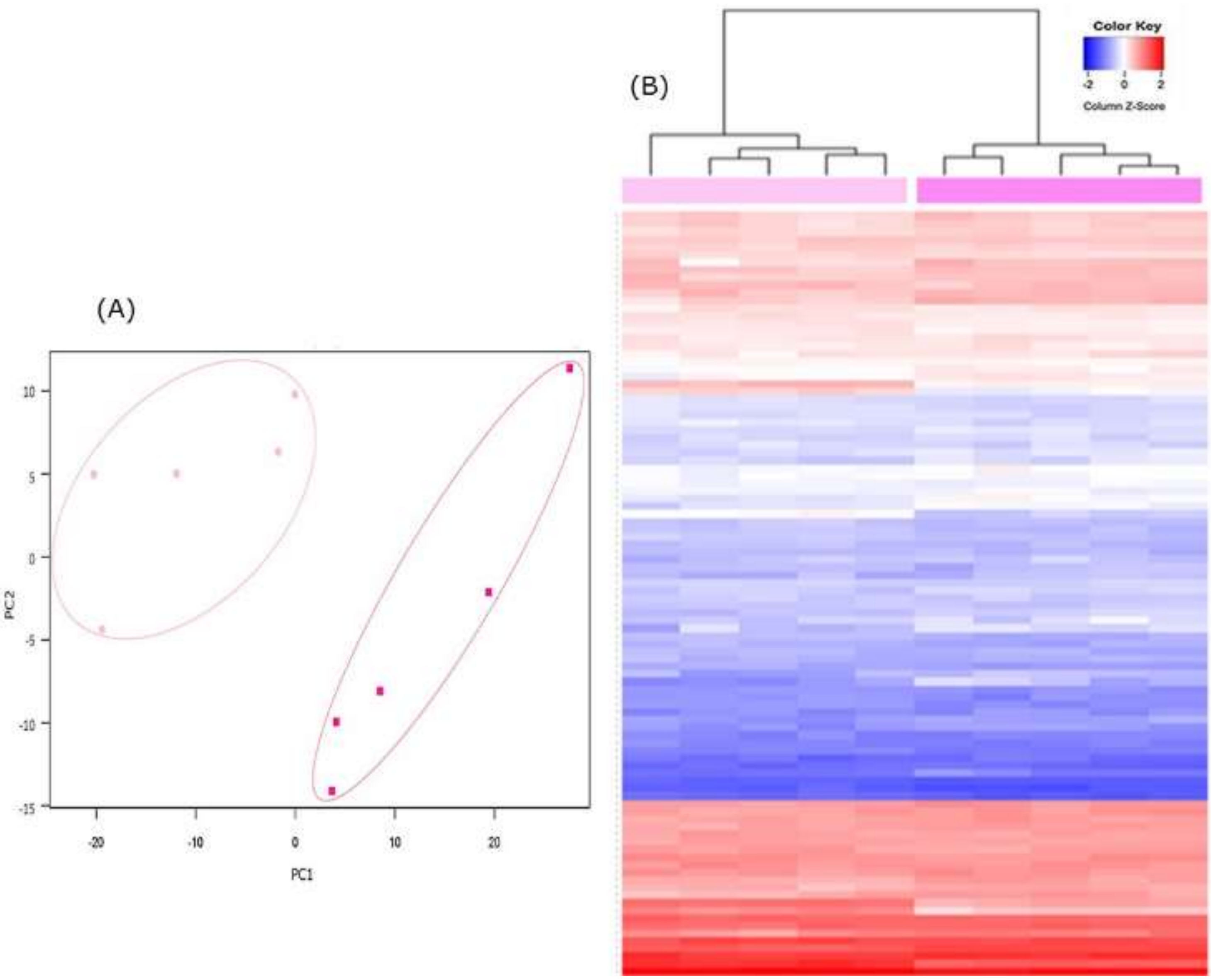

Figure 4-4: Cluster analysis of the epicardial fat depot

(A) Principal component analysis (PCA) of gene expression data from epicardial adipose tissue depot from each animal was performed using 693 datasets that passed the variance test QC. Each sample is represented by color-coded to indicate the age which it belongs: seven days, light pink (n = 5); 28 days, dark pink (n = 5). PC1 axis is the first principal direction along which the samples show the largest variation. The PC2 axis is the second most important direction and it is orthogonal to the PC1 axis. (B) Heat map and unsupervised hierarchical clustering dendrograms for the top 100 deferentially-expressed genes identified by microarray analysis (average linkage, Euclidean distance metric) between 7 and 28 days as selected by eBayes moderated t-statistics (FDR < 0.05). Gene expression was transformed to a Z-score, and blue represents a decrease and red an increase in gene expression with age.

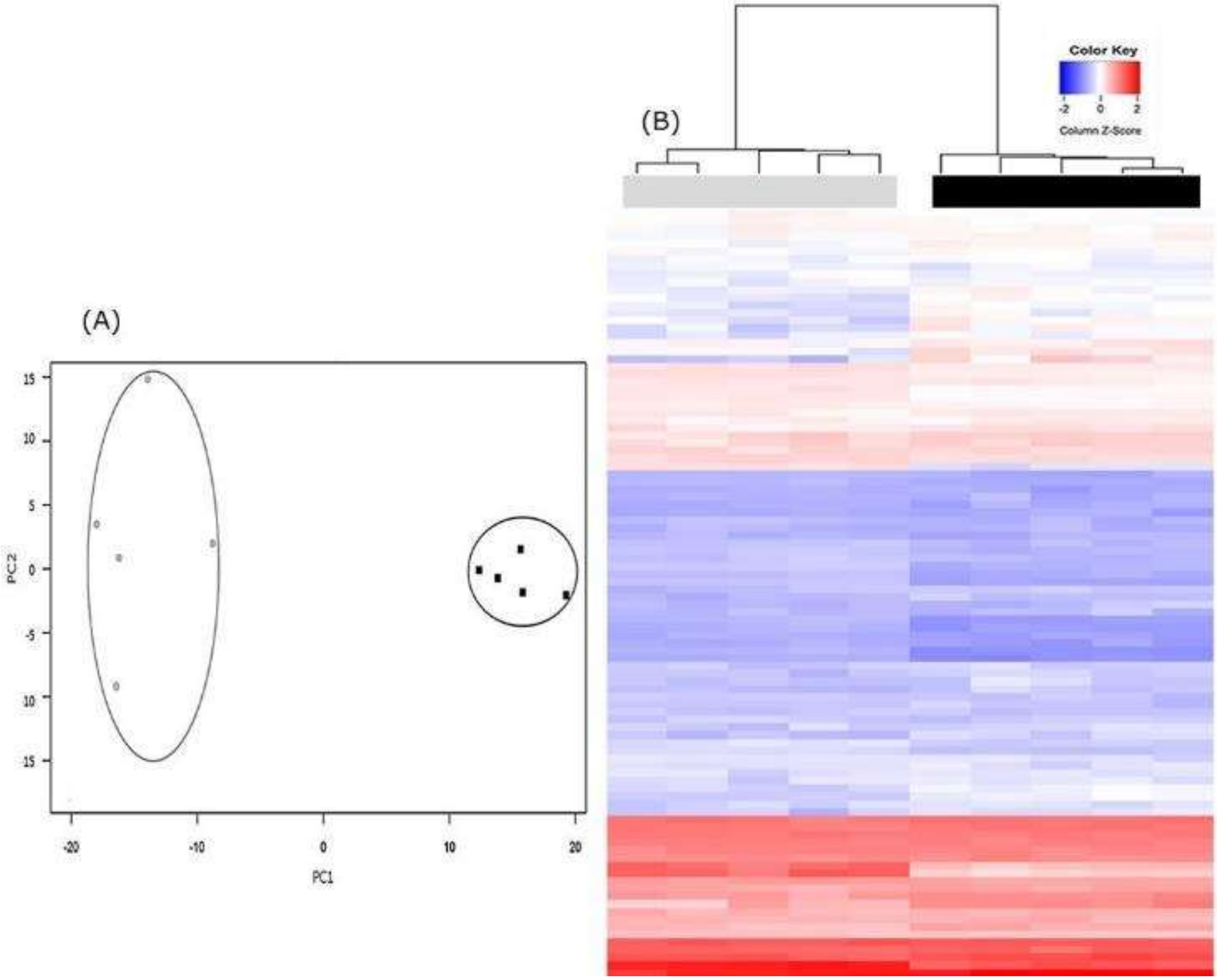

Figure 4-5: Cluster analysis of the omental fat depot

(A) Principal component analysis (PCA) of gene expression data from omental adipose tissue depot from each animal was performed using 2574 datasets that passed the variance test QC. Each sample is represented by color-coded to indicate the age which it belongs: seven days, grey (n = 5); 28 days black (n = 5). PC1 axis is the first principal direction along which the samples show the largest variation. The PC2 axis is the second most important direction and it is orthogonal to the PC1 axis. (B) Heat map and unsupervised hierarchical clustering dendrograms for the top 100 deferentially-expressed genes identified by microarray analysis (average linkage, Euclidean distance metric) between 7 and 28 days as selected by eBayes moderated t-statistics (FDR < 0.05). Gene expression was transformed to a Z-score, and blue represents a decrease and red an increase in gene expression with age.

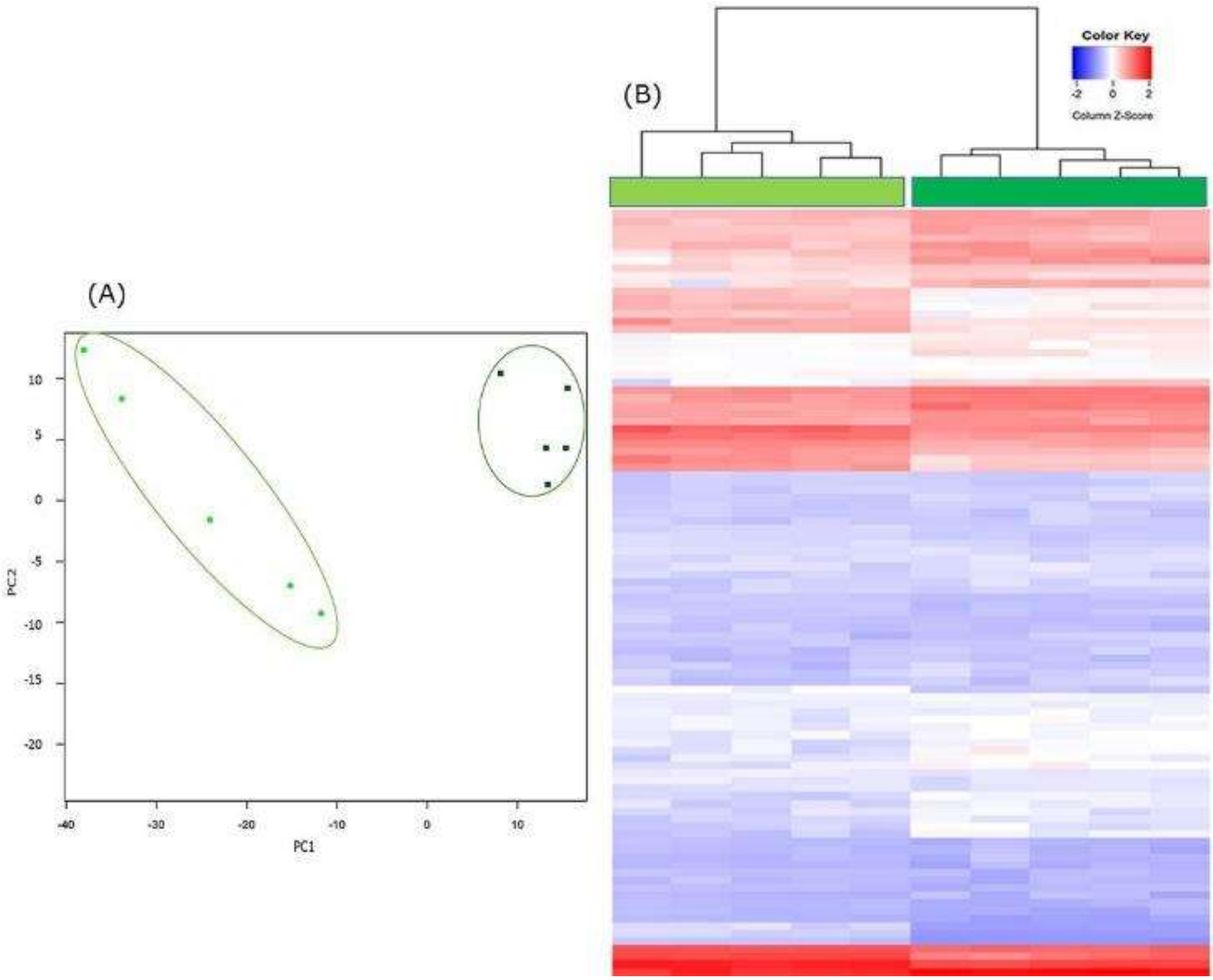

Figure 4-6: Cluster analysis of the subcutaneous fat depot

(A) Principal component analysis (PCA) of gene expression data from subcutounc adipose tissue depot from each animal was performed using 1938 datasets that passed the variance test QC. Each sample is represented by colour-coded to indicate the age which it belongs: seven days, light green (n = 5); 28 days green (n = 5). PC1 axis is the first principal direction along which the samples show the largest variation. The PC2 axis is the second most important direction and it is orthogonal to the PC1 axis. (B) Heat map and unsupervised hierarchical clustering dendrograms for the top 100 deferentially-expressed genes identified by microarray analysis (average linkage, Euclidean distance metric) between 7 and 28 days as selected by eBayes moderated t-statistics (FDR < 0.05). Gene expression was transformed to a Z-score, and blue represents a decrease and red an increase in gene expression with age.

4.4.2 Volcano plot and gene profile expression

To provide an overview and identify the changes in gene expression patterns the data were also tested using a volcano plot, indicating those genes (represented by solid red circles) that expressed significant changes in gene expression (up- or down-regulated) based on a q-value < 0.05 and a twofold difference in standard error between days 7 and 28. The comparison of age using the volcano plot shows that each depot has a different degree of transformation depending on the number as well as the patterns (up- or down-regulation) of significantly expressed genes between sampling ages. For example, the results indicate that the maximum change in genes occurred in omental adipose tissue while the minimum change occurred in the epicardial adipose tissue in development from age 7 to 28 days (i.e., omental: 2574 genes, perirenal: 1648 genes, epicardial: 639 genes, sternal: 820 genes and subcutaneous: 1938 genes) (see Figure 4-7).

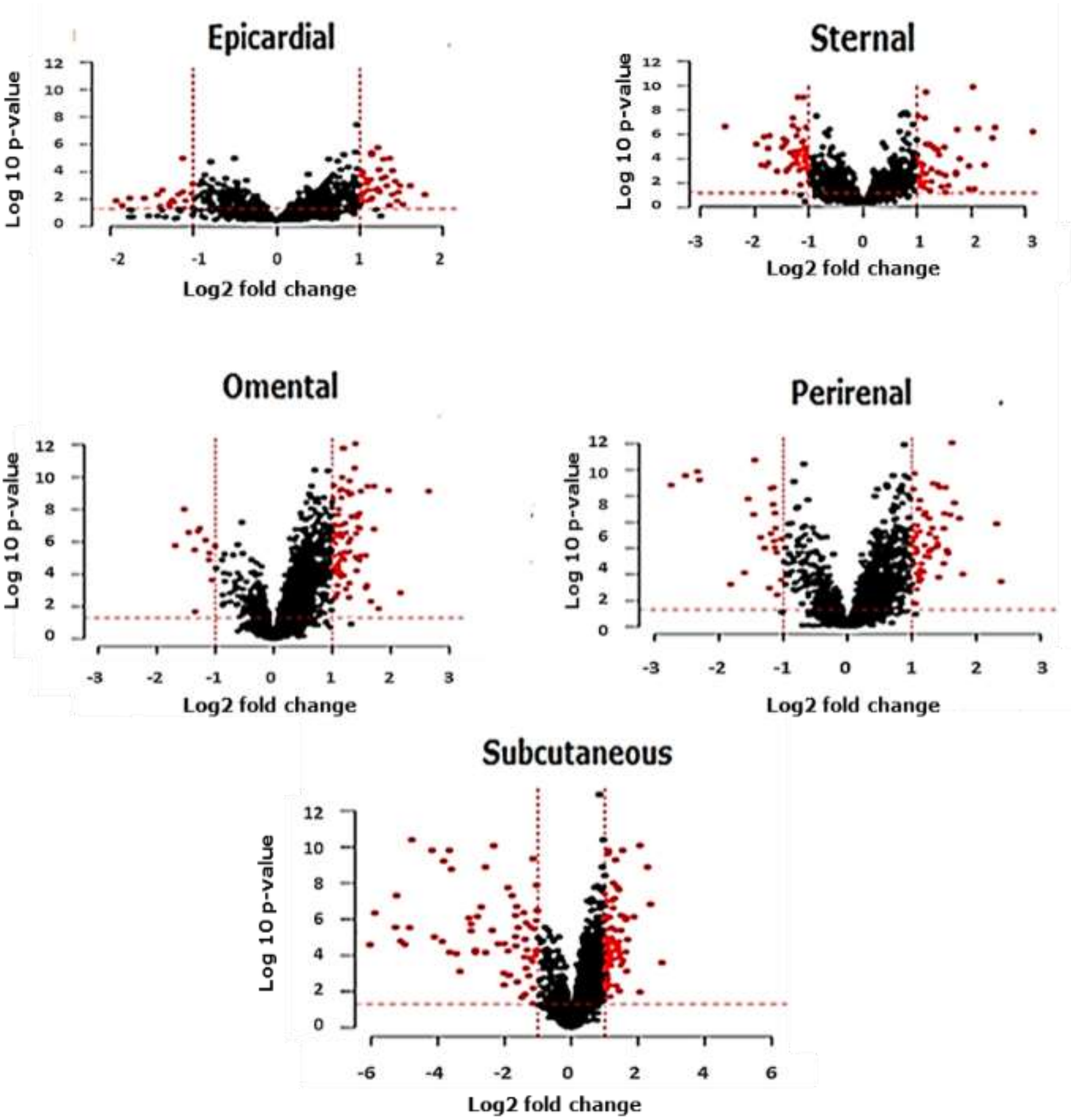

Figure 4-7: Volcano plots of the five depots gene transformation from seven to 28 days

The volcano plot representing the changes in sheep adipose tissue gene expression of all the transcripts from day seven to day 28, with the log of the FDR-adjusted probability values (q-value; y-axis) plotted against the log fold changes (x-axis) between the tested adipose tissues. The genes that were expressed significantly differently in the sample are represented by the solid red circle (epicardial: 639 genes, sternal: 820 genes, omental: 2574 genes, perirenal: 1648 genes, and subcutaneous: 1938 genes), and those that did not express significantly differently are coloured black.

4.4.3 Function profile in Venn diagrams and GO enrichment analysis

To uncover all possible logical relations regarding the gene sets of the five depots, I used a Venn diagram where each circle represents a gene set, and the unique genes (i.e. those only expressed in one specific depot) are located close to the sides of the circles. Shared genes (i.e., those found in one or more tissue depot) are located close to the centre of the loop or in the overlapping areas.

A large number of genes (4162) were significantly expressed across the five examined depots between 7 and 28 days. Each depot expressed a unique set of genes during development (omental: 1051 genes, perirenal: 463 genes, epicardial: 136 genes, sternal: 254 genes and subcutaneous: 592 genes). All depots also shared a small number of shared genes (60) and had the same pattern regarding being up- or down-regulated (see Figure 4-10).

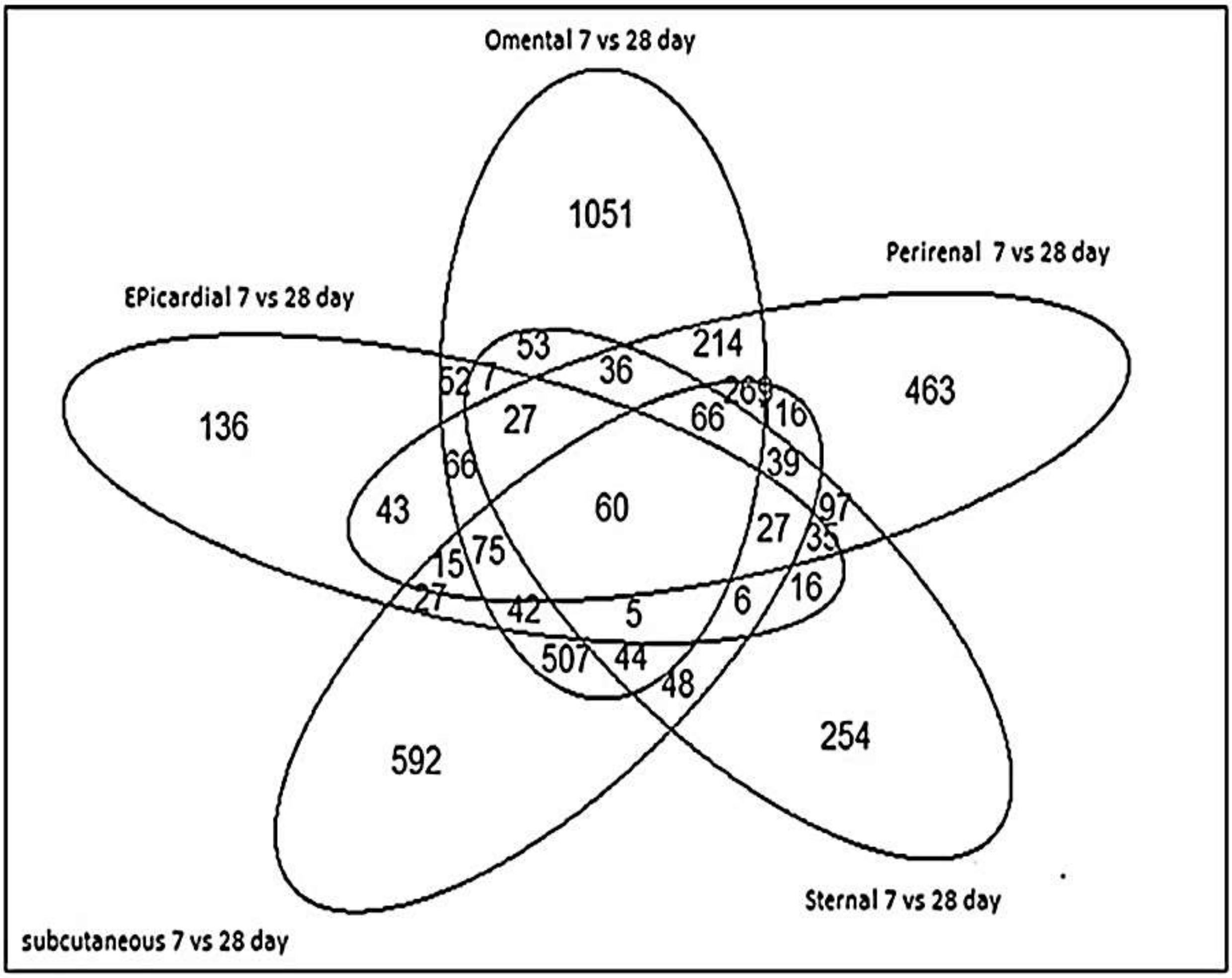

Figure 4-8: Five-way Venn diagram of significant gene expression among all examined depots

Venn diagram was generated representing the numbers of genes (4162) significantly expressed (adjusted p-value < 0.05) between two time points, 7 and 28 days, in five adipose tissue depots independently. Overlapping circles represent the number of gene sets significantly expressed, including unique genes sets which are located close to the sides of the circles in each depot, whereas common genes are located in the overlapping areas.

Genes that were significantly (FDR: $q \le 0.05$) up- or down-regulated were then analysed using the DAVID bioinformatics tool and the KEGG pathway database (http://www.genome.jp/kegg/) (Sherman and Lempicki, 2009).

GO Enrichment and KEGG analyses indicated that 87 biological processes and 45 pathways were significantly different ($q < 0.05$) in the comparison of all the five examined depots. The q-values highlight a very significant finding of the enrichment pathways of the five depots, all of which share identical biological pathways. For example, the GO enrichment analyses in Table 4-1 to 4-8 indicate that all five examined depots exhibited a similar down-regulation pattern in mitochondrial metabolic genes and function, including mitochondrial respiratory chain and ribosome pathways as a common enrichment pathway, both of which were down-regulated with age.

Further analysis in the KEGG pathway (Table 4-3) shows that some genes were involved in the oxidative phosphorylation pathways. I found that a total of 54 out of 122 genes were significantly expressed, and the majority were down-regulated with age (see Figure 4-9).

Table 4-1: Enriched biological processes between the five examined depots from day 7 to 28

Biological process	Q-value
Mitochondrial respiratory chain	1.40E-05
Energy derivation by oxidation of organic compounds	4.9E-22
ATP synthesis coupled electron transport	6.8E-22
Cellular lipid catabolic process	6.8E-22
Fatty acid biosynthetic process	1E-21
Ribosomal subunit	1.2E-21
Lipid modification	3.8E-20
System development	1.9E-18
Mitochondrial transport	7.7E-15
Cell differentiation	6.5E-12

Table 4-2: Enriched biological processes of the common genes (60) between the five adipose depots from days 7 to 28

Biological process	Q-value
Mitochondrial proton-transporting ATP synthase complex	7.06e-09
Electron transport chain	8.63e-05
NADH dehydrogenase activity	2.48e-05
Regulation of biosynthetic process	2.00E-03

Table 4-3: Top five enriched KEGG pathways in comparison to the five examined adipose depots from day 7 to 28

Pathway	Gene reference	Gene in the list	Q-value
Ribosome	82	48	1.33E-09
RNA degradation	69	36	3.80E-06
Oxidative phosphorylation	122	55	2.56E-06
Cell cycle	122	53	1.29E-05
Citrate cycle (TCA cycle)	29	14	0.013

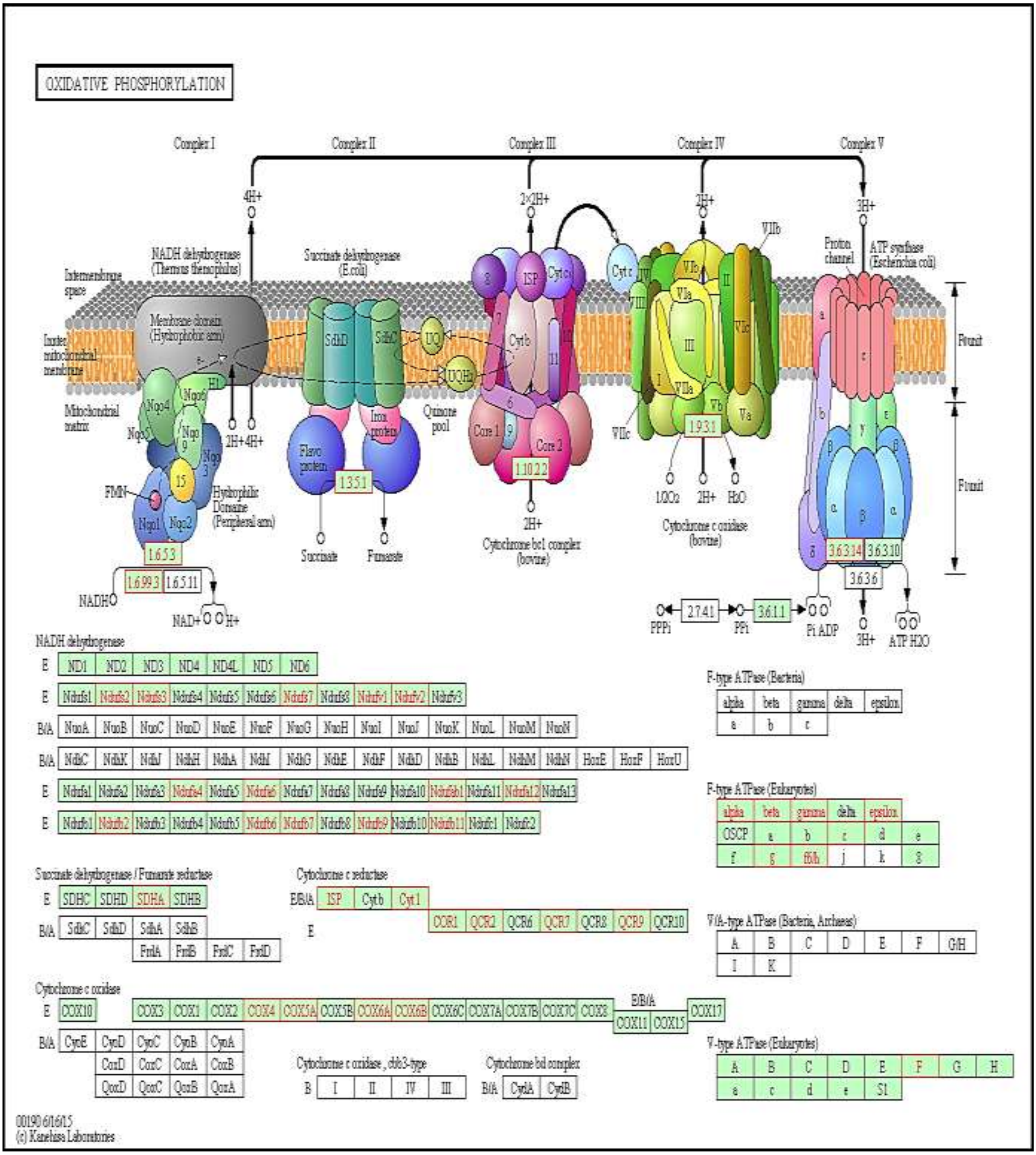

Figure 4-9: Oxidative phosphorylation pathway

Several genes involved in the above pathway; some of them were found to be significantly expressed (54 genes-represented by red colour) in comparison to five different adipose tissue depots at two time points from seven to 28 days of age.

4.4.4 Gene co-expression network and module identification

Datasets of the genes were used to generate WGCNA for each depot. These gene networks utilise data-reductive techniques that create modules (coded by colour) of pairwise correlations of the gene expression patterns in each sample, which enables the identification of hub genes (genes with the highest module membership) that could correlate with age in different clusters within and between depots, thereby facilitating the biological interpretation of transcriptional patterns.

I used the biological functions of each established module to identify the metabolic and physiological differences between depots during development from 7 to 28 days of age, specifically focusing on modules that are related to thermogenesis during the transition from BAT to WAT. Additionally, dendrogram analysis (Figures 4-12 to 4-16) was performed to study the gene co-expression networks of the five tested depots with 4162 genes significantly expressed between 7 and 28 days of age. I were able to identify a different number of modules in each depot separately (omental: 28 modules, perirenal: 30 modules, epicardial: 34 modules, sternal: 26 modules and subcutaneous: 35 modules), therefore identifying the different biological functions of the significant module (tables 4-11 to 4-15) including the top 30 hub genes in the substantial thermogenic cluster specifically.

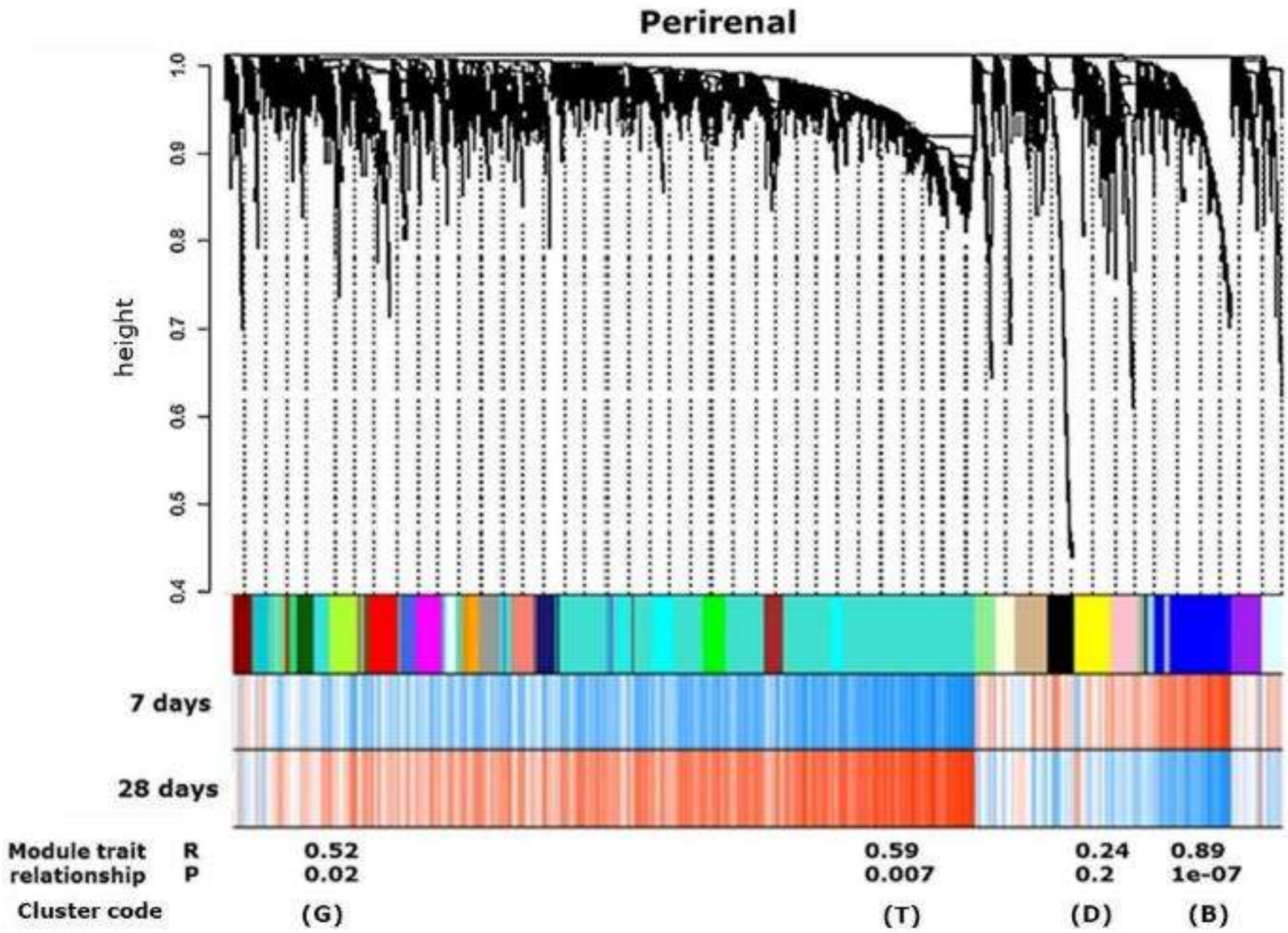

Figure 4-10: Co-expression dendrograms analysis for Perirenal depot sampled from seven to 28 days of age

The first row is subdivided into co-expressed modules founded in each age group. The other two rows (below) show the differential expression relationships between module genes and the adipose depot. The relationship of each gene with the assigned module is colour-coded from blue (negative co-expression) to red (positive co-expression). Module trait relationships represent the correlation R (and corresponding p-values) among co-expressed clusters which are coded by letters in the fat depot.

Table 4-4: Summary of the top four significant biological processes in the perirenal depot with the highest enrichment values within co-expressed gene modules from 7 to 28 days of age

Module	Number of genes	Biological process	Fold change	Q- Value
Turquoise (T)	1737	Cell differentiation	4.8	7.40E-06
Green (G)	148	Response to stimulus	2.5	1.43E-02
Blue (B)	328	ATP metabolic process	-5.1	3.10E-07
Dark grey (D)	78	Mitochondrial translational	-1.21	2.30E-03

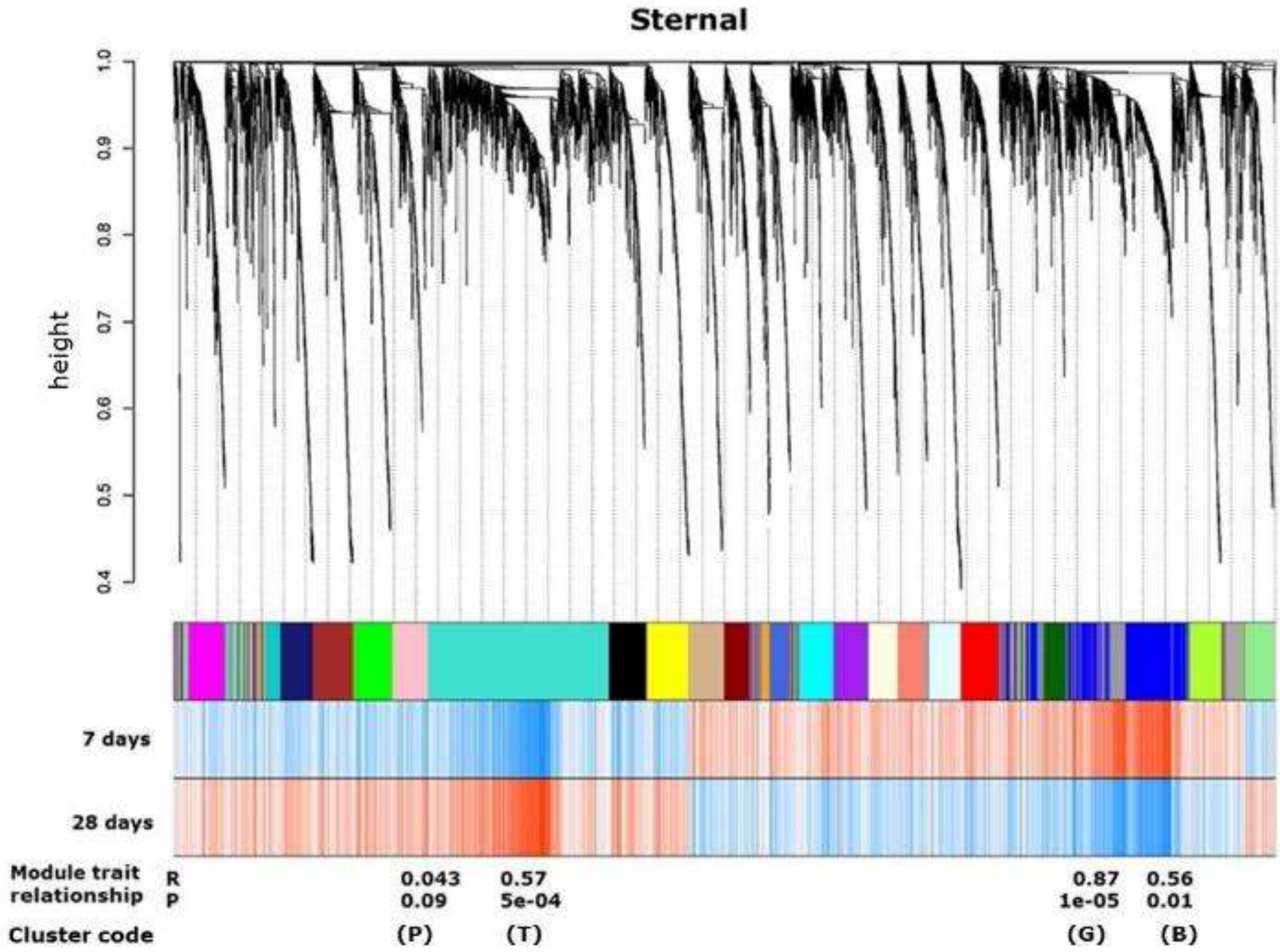

Figure 4-11: Co-expression dendrograms analysis for sternal depot sampled from seven to 28 days of age

The first row is subdivided into co-expressed modules founded in each age group. The other two rows (below) show the differential expression relationships between module genes and the adipose depot. The relationship of each gene with the assigned module is colour-coded from blue (negative co-expression) to red (positive co-expression). Module trait relationships represent the correlation R (and corresponding p-values) among co-expressed clusters which are coded by letters in the fat depot.

Table 4-5: Summary of the top four significant biological processes in the sternal depot with the highest enrichment values within co-expressed gene modules from 7 to 28 days of age

Module	Number of genes	Biological process	Fold change	Q- Value
Turquoise (T)	877	Response to stimulus	4.1	7.40E-06
Pink (P)	203	Cell differentiation	1.3	4.10E-02
Blue (B)	512	ATP metabolic process	-3.8	3.15E-04
Grey (G)	134	Mitochondrial translational	-3.7	7.28E-22

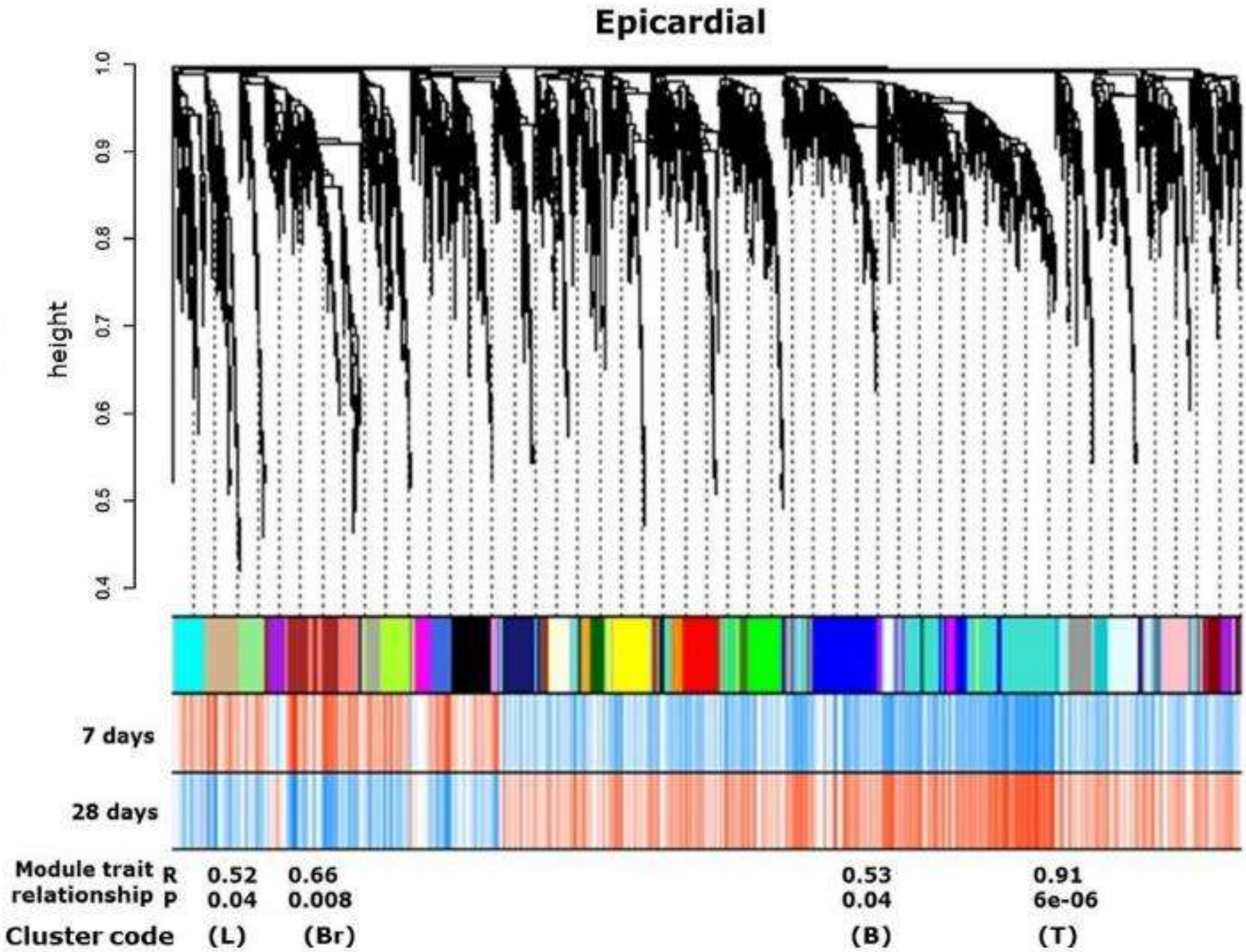

Figure 4-12: Co-expression dendrograms analysis for epicedial depot sampled from seven to 28 days of age

The first row is subdivided into co-expressed modules founded in each age group. The other two rows (below) show the differential expression relationships between module genes and the adipose depot. The relationship of each gene with the assigned module is colour-coded from blue (negative co-expression) to red (positive co-expression). Module trait relationships represent the correlation R (and corresponding p-values) among co-expressed clusters which are coded by letters in the fat depot.

Table 4-6: Summary of the top four significant biological processes in the epicardial depot with the four enrichment values within co-expressed gene module from 7 to 28 day of age

Module	Number of genes	Biological process	Fold change	Q- Value
Turquoise (T)	799	Cell differentiation	4.3	5.90E-06
Blue (B)	196	Response to stimulus	1.8	6.97E-02
Brown (Br)	225	ATP metabolic process	-3.6	2.90E-07
Light brown (L)	166	Mitochondrial translational	-1.83	2.60E-03

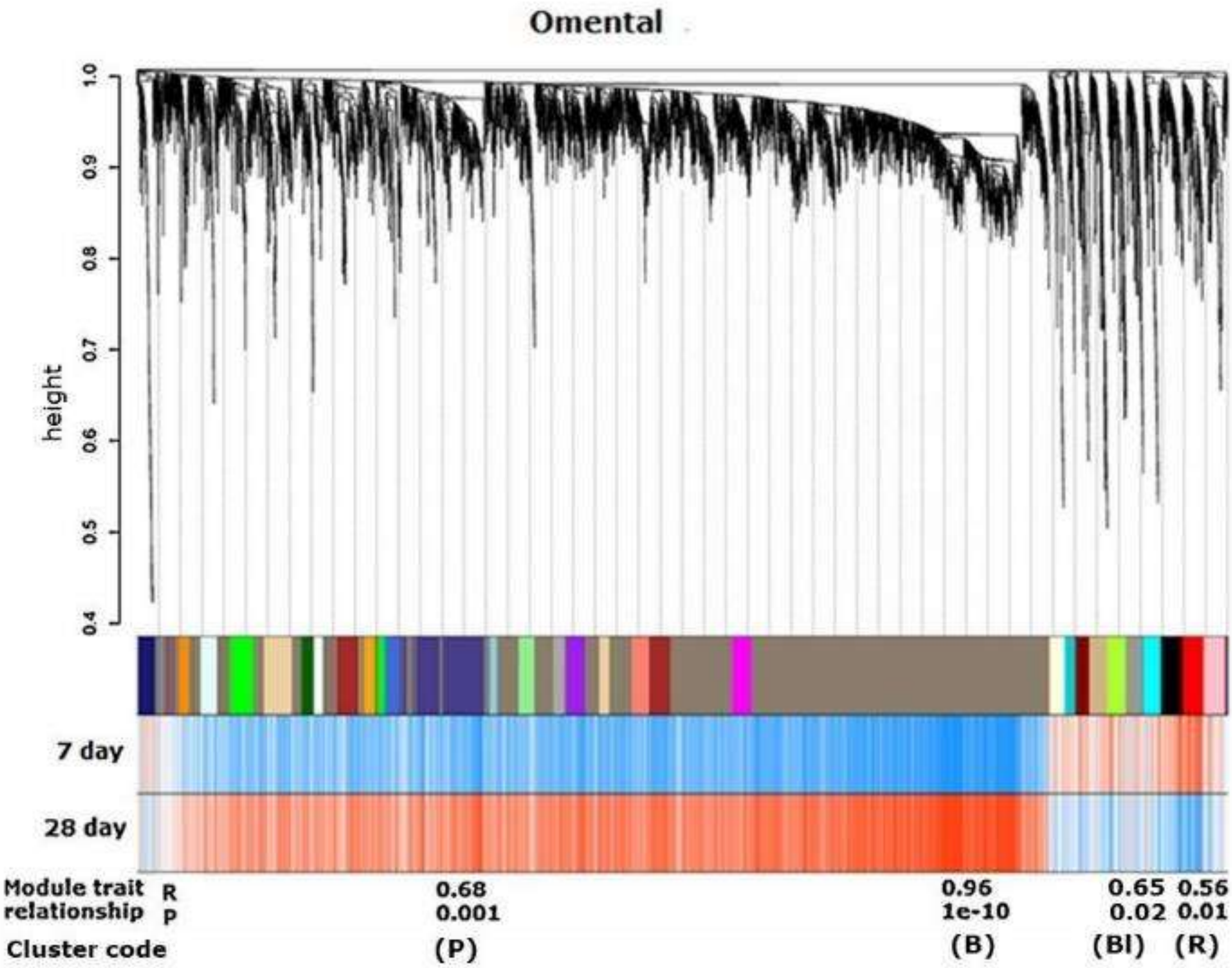

Figure 4-13: Co-expression dendrograms analysis for omental depot sampled from seven to 28 days of age

The first row is subdivided into co-expressed modules founded in each age group. The other two rows (below) show the differential expression relationships between module genes and the adipose depot. The relationship of each gene with the assigned module is colour-coded from blue (negative co-expression) to red (positive co-expression). Module trait relationships represent the correlation R (and corresponding p-values) among co-expressed clusters which are coded by letters in the fat depot.

Table 4-7: Summary of the top four significant biological processes in the omental depot with the highest enrichment values within co-expressed gene module from 7 to 28 day of age.

Module	Number of genes	Biological process	Fold change	Q- Value
Bisque (B)	1937	Cell differentiation	4.1	4.98E-06
Purple (P)	734	Response to stimulus	3.7	7.20E-05
Black (Bl)	97	ATP metabolic process	-1.6	2.80E-06
Red (R)	104	Mitochondrial translational	-1.83	2.60E-03

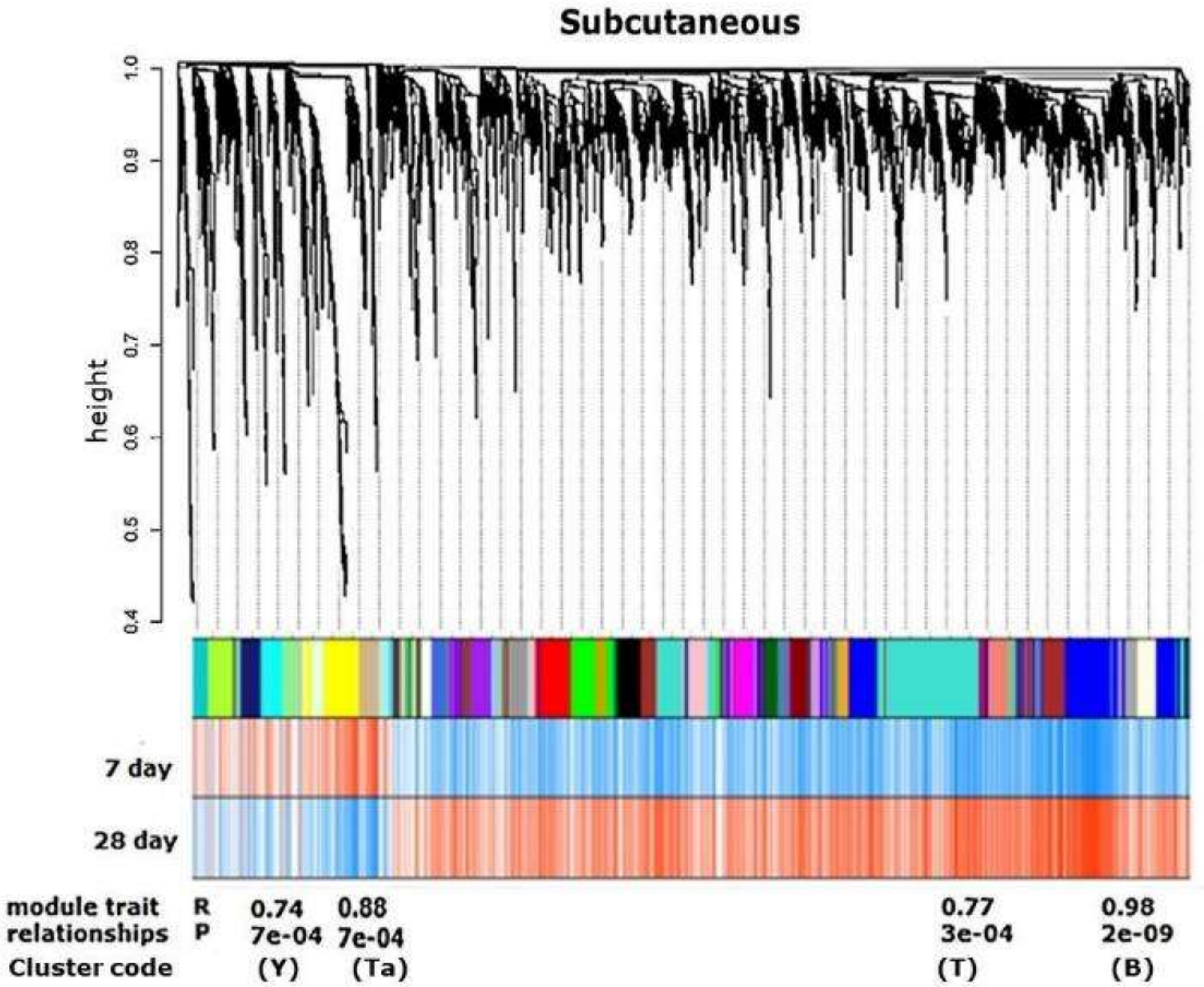

Figure 4-14: Co-expression dendrograms analysis for subcutaneous depot sampled from seven to 28 days of age

The first row is subdivided into co-expressed modules founded in each age group. The other two rows (below) show the differential expression relationships between module genes and the adipose depot. The relationship of each gene with the assigned module is colour-coded from blue (negative co-expression) to red (positive co-expression). Module trait relationships represent the correlation R (and corresponding p-values) among co-expressed clusters which are coded by letters in the fat depot.

Table 4-8: Summary of the top four significant biological processes in the subcutaneous depot with the four enrichment values within co-expressed gene module from 7 to 28 day of age.

Module	Number of genes	Biological process	Fold change	Q- Value
Turquoise (T)	814	Response to stimulus	4.1	5.80E-04
Blue (B)	734	Cell death	3.7	4.10E-03
Tan (Ta)	117	ATP metabolic process	-2.1	3.10E-05
Yalow (Y)	166	Muscle cell differentiation	-2.7	2.67E-02

The gene networks show that most of the examined depots were generally characterised by up-regulated gene expression, specifically in the regulation of biosynthetic and cell differentiation in the RNA metabolic process from weeks one to four. For example, some modules in the gene network (sternal - pink, perirenal - white, epicardial – blue) showed a significant increase in white adipocyte differentiation genes like Fibroblast Growth Factor family1 (FGFR1) – Myosin Heavy Chain 10 (MYH10)- Myosin Heavy Chain 14 (MYH14) which classify as non-selective markers of skeletal myogenic cells (Vicente-Manzanares et al., 2009, Adams et al., 2013). However the only depot that followed a different pattern was the subcutaneous module (in blue, turquoise, and yellow) which showed an increase in apoptosis genes; for example, associated agonist of cell death BCL2 Associated Agonist (BAD) and BCL2-associated X protein (BAX) (Levesley et al., 2011) as well as an inhibitor of muscle cell differentiation gene (i.e. Myosin Heavy Chain 1(MYH1)- Myosin Heavy Chain 2 (MYH2)) (Asp et al., 2011).

Moreover, all the tested depots (perirenal - green 184 genes, sternal - black 186 genes, epicardial - light blue 196 genes, omental – brown 104 genes and subcutaneous – turquoise 182 genes) had significantly increased responses to different stimuli. For example, the response to hormones rose dramatically in EphrinA5 and oestrogen-related receptor gamma (ESRRG) in epicardial adipose tissue, while other Hermon receptors (i.e. thyroid hormone receptor beta (THRB)) present in white adipose tissue including omental and subcutaneous as well as a brown populated depot (i.e. Perirenal). Additionally, those modules were different regarding the gene numbers, which may indicate that each depot responds to a different type and level when stimulated by cold exposure or by diet, which could support the idea that anatomical location plays a vital role in adipose tissue function and development.

4.4.5 UCP1 clustering comparison and identification of the hub gene in weighted gene co-expression network analysis

The results also indicate that ATP metabolic processes, including the mitochondrial respiratory chain, mitochondrial ATP synthesis and the tricarboxylic acid cycle, were significantly down-regulated in different modules and genes. For example, pro-thermogenic depots (i.e., blue perirenal: 328 genes, blue sternal: 512 genes, brown epicardial: 225 genes and cyan epicardial: 225 genes) expressed mitochondrial genes more than other depots (subcutaneous: 117 genes and omental: 80 genes). However, mitochondrial genes in depots primarily populated by white adipocytes (subcutaneous blue: 117 genes and omental black: 80 genes) had fewer genes involved in ATP related metabolic processes, which could reflect the lower capacity of these two depots to produce energy compared to pro-thermogenic depots. Further analysis showed that 30 genes were represented in these three depots (sternal, perirenal, epicardial), particularly in the ATP metabolic modules (e.g., ATPase H+ Transporting V1 Subunit F (ATP6V1F), ATP Synthase Peripheral Stalk Subunit D (ATP5H) , dehydrogenase ubiquinone iron-sulfur protein 7 (NDUFS7), NADH:Ubiquinone Oxidoreductase Subunit A12 (NDUFA12) and UCP1), that were not detected in the other two depots (subcutaneous, omental), therefore enabling thermogenesis during postnatal life.

UCP1 was selected as the essential gene for comparison between depots since down-regulation of UCP1 during development has already been reported (Schulz and Tseng, 2014). In addition to UCP1, other genes were also studied to determine whether other processes besides energy utilisation were also affected. UCP1 was detected in three of the five tested depots (sternal, perirenal and epicardial), all of which were primarily populated by brown adipocytes. These results indicate local differences in transcriptional regulation between fat depots during postnatal life. The gene expression and fold changes of these depots varied, with the perirenal depot having the highest down-regulation with respect to fold change and q-value, while the lowest was epicardial tissue (see Table 4-9).

Table 4-9: UCP1 expression in three of five depots between days 7 and 28

Depot name	Symbol	Gene name	FC	Q value
Perirenal	UCP1	Uncoupling protein 1 (mitochondrial, proton carrier)	-2.73	1.45E-11
Sternal	UCP1	Uncoupling protein 1 (mitochondrial, proton carrier)	-1.88	7.49E-06
Epicardial	UCP1	Uncoupling protein 1 (mitochondrial, proton carrier)	-1.11	0.046

4.4.6 Comparison of the UCP1 cluster between the brown depots

In the next step of the analysis, I created a Venn diagram to investigate the difference in the gene list of UCP1 clusters among pro-thermogenic depots (i.e. sternal, perirenal and epicardial) during development from 7 to 28 days (Figure 4-15). The Venn diagram shows that sternal and perirenal depots (blue) shared more common genes (68) compared with epicardial gene list (cyan) with sternal and perirenal blue respectively (nine and ten genes), including UCP1. Likewise, the results indicate that other clusters of genes in epicardial (brown) shared a large number of genes with sternal and perirenal (blue) respectively (44 and 21 gens). However, the epicardial (brown) list did not include UCP1, which may indicate the influence of anatomical location on adipose tissue gene expression specifically in the thermogenic process during development.

Additionally, the Venn diagram shows that the sternal depot has the most extensive ATP metabolic module (blue, 512 genes) compared with perirenal (blue, 328 genes) and epicardial (cyan, 150 genes). However, only eight genes (1%) were shared between the three targeted clusters on the examined depots (i.e. sternal, perirenal and epicardial), including UCP1. Some of these genes are related to mitochondrial function, such as Coenzyme Q6, Monooxygenase (COQ6) , ethylmalonic encephalopathy 1 (ETHE1) , endonuclease G (ENDOG), while others in this cluster were related to ribosomal biogenesis, such as mitochondrial ribosomal protein S31 (MRPS31) , forkhead box O6 (FOXO6), SDHA and eukaryotic translation initiation factor 4B (EIF4B) (see Table 4-10).

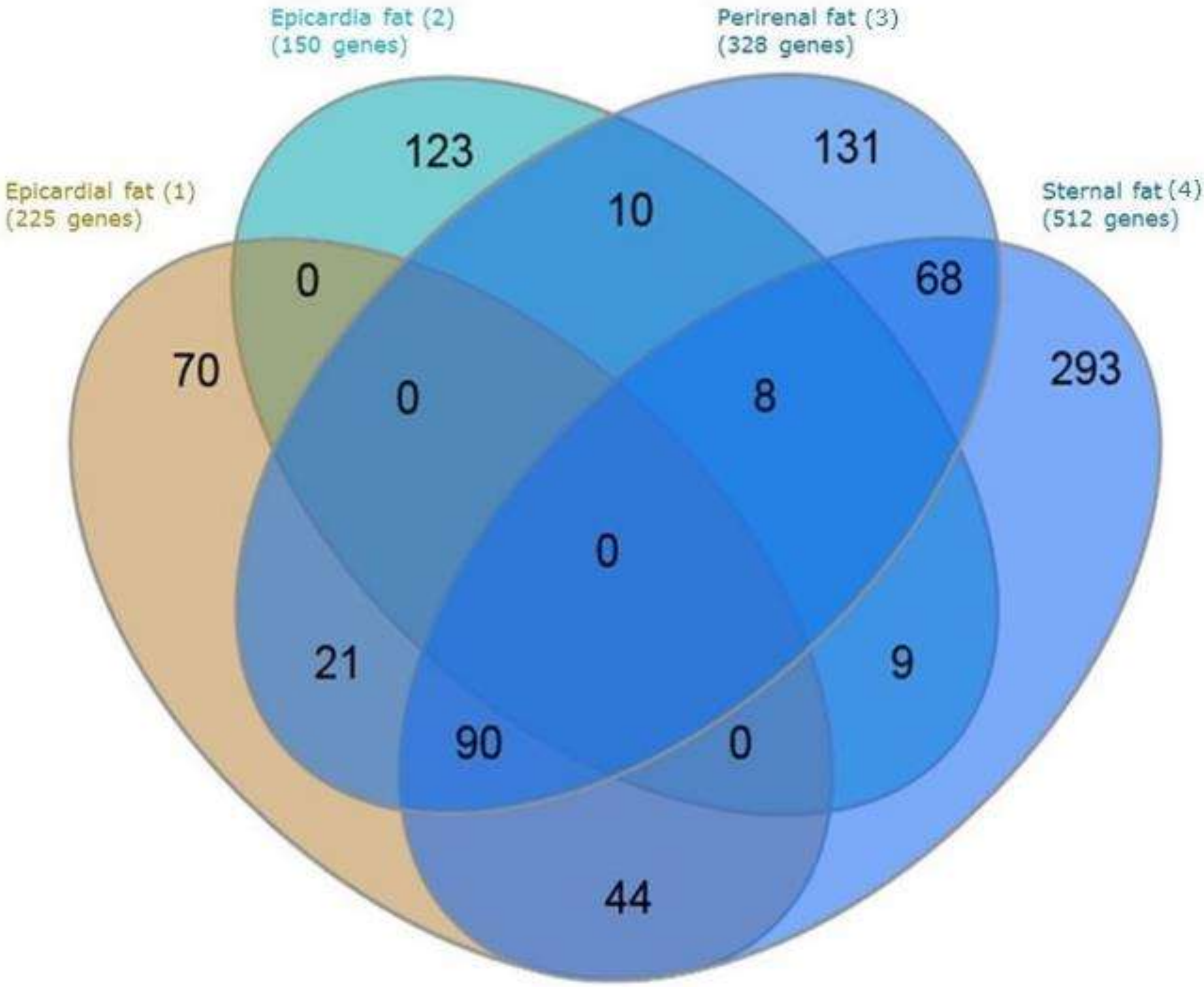

Figure 4-15: Venn diagram of UCP1 gene cluster in brown adipose depots

Venn diagram showing comparison of gene interaction between only the modules that include UCP1 by using a multi overlapping circle curve. Each circle represents the number of the gene set within a specific depot, with overlap the shared gene with another depot. Epicardial (1) is represented in brown, (2) epicardial (include ucp1) in cyan, (3) perirenal fat in blue, and (4) sternal fat in blue.

Table 4-10: Commonly expressed genes in a comparison of the UCP1 cluster in three depots; epicardial (E), perirenal (P) and sternal (S).

Symbol	Name	Average of expression	(E) kME*	(P) kME*	(S) kME*	Q-value
UCP1	uncoupling protein 1 (mitochondrial, proton carrier)	3.37	0.86	0.97	0.60	9.08E-14
SDHA	succinate dehydrogenase complex flavoprotein subunit A	6.02	0.71	0.91	0.80	1.14E-08
ENDOG	endonuclease G	3.28	0.64	0.79	0.58	1.53E-08
MRPS31	mitochondrial ribosomal protein S31	2.88	0.81	0.77	0.64	9.79E-08
ETHE1	ethylmalonic encephalopathy 1	5.11	0.86	0.83	0.70	7.32E-06
EIF4B	eukaryotic translation initiation factor 4B	6.52	0.66	0.86	0.66	9.63E-06
COQ6	coenzyme Q6 monooxygenase	3.50	0.78	0.67	0.72	2.82E-05
FOXO6	forkhead box O6	4.00	0.43	0.68	0.79	1.79E-02

*KME value: its expression values are highly correlated with that module's eigengene values across samples (eigengene-based connectivity) in range 0 to 1, where 1 indicated the highest connectivity and 0 the lowest.

4.4.7 Hub genes list identification in thermogenic clusters

in the classification of the difference regarding hub genes and UCP1 expression between the three pro-thermogenic depots (epicardial-sternal-perirenal).The results show that UCP1 was represented as a hub gene only in two depots (perineal [0.96] and epicardial [0.86]), whereas in the sternal cluster gene list it is not expressed as a hub gene (0.59), which may indicate that each depot may use different gene profiles, mechanisms, and levels of stimulus for UCP1 activation and thermogenesis, even between the pro-thermogenic depots (see Table 4-11 to 4-19). In addition, I noted that the hub genes list in the sternal and perirenal depots clusters were distinguished by specific transcriptional, like nuclear receptor subfamily 1, group H, member 3 (NR1H3); as well as other fatty genes like acyl-CoA dehydrogenase, very long chain (ACADVL), which are mainly involved in glycerol uptake and metabolism (Aoyama et al., 1995) and other BAT marker genes like members of the mitochondrial carrier subfamily of solute carrier protein genes (e.g., Solute Carrier Family 25 Member 4 (SLC25A4)) (Kuan and Saier, 1993, Gough, 2016). Overall, these findings suggest the importance of the association between mitochondrial energy capacity in the ageing of brown adipose tissue and thermogenesis.

Table 4-11: Top 10 perirenal hub (blue module) and UCP1 genes

Symbol	Name	Gene connectivity kME
ATP5L	ATP synthase, H+ transporting, mitochondrial Fo complex subunit G	0.97
HINT2	Histidine triad nucleotide-binding protein 2	0.96
UCP1	Uncoupling protein 1 (mitochondrial, proton carrier)	0.96
ATP5C1	ATP synthase, H+ transporting, mitochondrial F1 complex, gamma polypeptide 1	0.96
NDUFS2	NADH:ubiquinone oxidoreductase core subunit S2	0.95
TMEM120A	Transmembrane protein 120A	0.94
GK	Glycerol kinase	0.94
EIF3I	Eukaryotic translation initiation factor 3 subunit I	0.94
USP2	Ubiquitin specific peptidase 2	0.94
ATP5G2	ATP synthase, H+ transporting, mitochondrial Fo complex subunit C2 (subunit 9)	0.93

Table 4-12: Top 10 epicardial hub (cyne Module) and UCP1 genes

Symbol	Name	Gene connectivity kME
FAM96B	Family with sequence similarity 96, member B	0.98
MGAT3	Mannosyl (beta-1,4-)-glycoprotein beta-1,4-N-acetylglucosaminyltransferase	0.96
LOC284865	Uncharacterised LOC284865	0.95
DNAJC12	DnaJ heat shock protein family (Hsp40), member C12	0.95
AKR7A3	Aldo-keto reductase family 7, member A3 (aflatoxin aldehyde reductase)	0.95
EMX2	Empty spiracles homeobox 2	0.95
LRRC28	Leucine-rich repeat-containing 28	0.95
SPATA6L	Spermatogenesis associated 6-like	0.94
SLC27A5	Solute carrier family 27, member 5	0.92
MRS2	MRS2, magnesium transporter	0.92
UCP1	Uncoupling protein 1 (mitochondrial, proton carrier)	0.86

Table 4-13: Top 10 sternal hub (blue module) and UCP1 genes

Symbol	Name	Gene connectivity kME
QKI	QKI, KH domain containing, RNA binding	0.95
PSME3	Proteasome activator subunit 3	0.95
SMDT1	Single-pass membrane protein with aspartate-rich tail 1	0.94
PTP4A2	Protein tyrosine phosphatase type IVA, member 2	0.93
ATP5L	ATP synthase, H+ transporting, mitochondrial Fo complex subunit G	0.93
ATL2	Atlastin GTPase 2	0.93
HSPD1	Heat shock protein family D (Hsp60), member 1	0.93
HSD17B10	Hydroxysteroid (17-beta) dehydrogenase 10	0.92
LDHB	Lactate dehydrogenase B	0.92
MGST3	Microsomal glutathione S-transferase 3	0.92
UCP1	Uncoupling protein 1 (mitochondrial, proton carrier)	0.59

4.5 Discussion

Adipose tissue is an essential metabolic organ and regulates energy balance and lipid metabolism (Ali et al. 2013). I focused on early postnatal life when brown depots transform into white fat. Through the use of machine learning and methods, including weighted gene co-expression during a critical development phase, each of the major fat depots was found to utilise different mechanisms and genes. I compared five adipose depots in different anatomical regions (epicardial, perirenal, sternal, omental and subcutaneous) from 7 to 28 days of development, and focused on changes in gene expression patterns (i.e. up/down-regulation), as well as unique and shared genes and biological processes. As outlined in the results section, several shared and unique mechanisms were identified across the fat depots, which could explain changes in thermogenesis, mitochondrial gene expression/density and energy utilisation that occur in BAT over time.

4.5.1 The dynamics of biological transformation in adipose tissue development during early life

Early postnatal life (days 7–28) is highly critical in the regulation of the growth of fat depots, particularly their ability to maintain UCP1 (Symonds, 2013). The GO enrichment and KEGG pathway analyses revealed 587 biological processes and 63 pathways of the selected fat depots and the differences in the transdifferentiation of BAT into white adipose tissues. The KEGG pathway analysis confirmed that the oxidative phosphorylation pathway plays a crucial role in adipose tissue development, particularly in early life, through the generation of mitochondria ATP energy, necessary for all cellular processes (Schultz and Chan, 2001**;** Krauss et al., 2002). Previously published reports indicate that mitochondrial oxidative phosphorylation requires PPARG to enhance adipogenesis (Ryu et al., 2013), since PPARG is a nuclear hormone receptor which plays a role in the regulation and differentiation of adipocytes to facilitate the uptake of blood glucose (Jones et al., 2005; Nolte et al., 1998). Additionally, other studies have demonstrated the ability of PPARG agonists to stimulate both the production and thermogenic activity of brown adipose cells. For example, in one study PPARG agonists suppressed visceral white adipose genes while inducing the expression of brown adipose genes (including UCP1) in white adipocytes (Vernochet et al., 2009). Another study demonstrated the ability of the thiazolidinedione darglitazone (a PPARG agonist) to induce the proliferation of BAT in rats and monkeys (Aleo et al., 2003); this function, in particular, is highly pronounced in perirenal as it was observed with increased PPARG expression with age and expressed as well as height UCP1 abundance.

In addition, early adipocytes have been shown to have a myogenic signature, as evidenced by the increased expression of myogenic markers at early stages of development (Timmons et al., 2007), which could play a vital role in enhanced muscle cell differentiation and improved the mitochondriogenesis in early life (Rochard et al., 2000).

Several controllers of UCP1 gene expression exist, of which the majority belong to the mitochondrial pathway, suggesting that the pathway is complicated and does more than altering the expression of single genes.

4.5.2 Regulation of UCP1 cluster by transcriptional components

Studies of adipose tissue function during early postnatal life have mostly focused on explaining the loss of genes associated with cellular thermogenesis, especially UCP1 (Symonds et al., 2015). The analysis of the transcription traits of adipose tissue further revealed that the co-expression of UCP1 can help in the suppression of obesity-related changes along with the decrease in BAT mass (Clément and Spiegelman, 2010; Dube, 2010). Therefore, co-expressed clusters can be used to examine genetic functionality. WGCNA analysis has confirmed that a group of genes that are tightly co-expressed could be a single functional unit (Zhang and Horvath, 2005). Such clusters are useful in linking multi-gene association maps with traits. The clustering traits could also show the interaction among different genes under specific conditions. Overall, the gene network demonstrates the existence of varying gene expressions and biological processes (e.g., cell differentiation, ATP metabolism and stimuli response), which may reflect the effect of age on adipose tissue development.

UCP1 clustering in BAT was found to be prominent in specific fat depots (i.e. sternal, perirenal: blue; and epicardial: cyan). The balance between transcription and mRNA degradation is regulated by the gene expression level (up- or down-regulation) of mRNA (Haimovich et al., 2013). For instance, it is found that the transcriptional factors EIF4B, Eukaryotic Translation Initiation Factor 4 Gamma 3 (EIF4G3), Eukaryotic Translation Initiation Factor 3 Subunit D (EIF3D), and Eukaryotic Translation Initiation Factor 3 Subunit G (EIF3G) down-regulate the transcription of mRNA in UCP1, and this occurs in response to raised temperature (van Breukelen et al., 2004, Symonds, 2013). A large number of ribosomal proteins co-expressed with UCP1 are similarly regulated, including RPS5 and RPS9 (Maier et al., 2013). These are made up of part of the original mitochondrial protein assembly machinery. UCP1 clusters also show significant representing of cytochrome c oxidase group of the genes (COX) particularly in sternal and perirenal depots (blue module), for example, Cytochrome C Oxidase Subunit 5A (COX5A) which is mainly involved in the mitochondrial respiratory chain process (Fontanesi et al., 2008, Scarpulla, 2008).

Other common genes were found in the UCP1 clusters gene list (sternal-blue, perirenal-blue, epicardial-cyan), which belonged to the mitochondrial carrier adenine nucleotide and ubiquinone; for example Solute Carrier Family 35 Member B1 (SLC35B1), Solute Carrier Family 16 Member 1 (SLC16A1) and Solute Carrier Family 25 Member 5 (SLC25A5) which play a role similar to that of UCP1 as the leading suppliers of adenosine diphosphate (ADP) to the mitochondria and ATP to the cytoplasm (Palmieri et al., 2011), where UCP1 uses different glycolytic metabolisms as well as the H+ transport mechanism to produce heat instead of ATP (Fedorenko et al., 2012, Palmieri, 2013). This suggests that those depots, including sternal, perirenal, and epicardial depots, may have common transcription factors, and therefore similar mechanisms to activate UCP1 and thermogenesis (Basse et al., 2015). Other mitochondrial-nuclear genes found in UCP1 modules were linked to cell cycles like Muscleblind-like protein 2 (MBNL2) and ENDOG, which suggest adipocyte differentiation has an impact on thermogenesis (Pardo et al., 2016, Ho et al., 2004).

4.5.3 Cell differentiation gene expression in offspring adipose tissue

From my analysis, a significant change in adipose tissue plasticity can be expected to occur between 7 and 28 days due to cell differentiation. Past literature has shown that adipose tissue differs with age regarding cell differentiation and energy metabolism (Ojha et al., 2016). Increased adipocyte differentiation was found to be the primary cause of the variances in the ratio of brown fat transdifferentiation to white among different depots during development in early life (Rosen et al., 2009, Harms and Seale, 2013).

Some genes identified in the present study were noted to play a role in cellular growth, proliferation and cycle control, and cell differentiation. For example, myosin heavy chain specific genes (MYH1 and MYH2) which are linked to muscle cell differentiation (Stern-Straeter et al., 2011), were found to be down-regulated with age in subcutaneous fat, suggesting that functions are ongoing and change during the developmental phases of adipose tissue.

Each depot is also characterised by differences in apoptotic patterns during development. As the present study identified, several genes show increased expression related to cell cycle and apoptotic function especially in subcutaneous fat; for example, the BCL2 family members (BAX), PPARG and mitogen-activated protein kinase 10 (MAPK10) genes (Levesley et al., 2011, Rogers et al., 2012). There are also several key factors (e.g., TNF) that have been shown to play a role by acting as modulators of apoptosis (Zhang et al., 2016, Porras et al., 1997) which could be correlated with the extent of active thermogenesis in a depot (Inagaki et al., 2016), and could contribute to insulin sensitivity and fat mass (Tinahones et al., 2012).

4.5.4 Differential response to stimulus (endocrine and external) between anatomical locations

Numerous studies have investigated the role of endocrine and external stimulus in affecting negative, positive responses to energy expenditure and homeostasis in different anatomical locations of brown fat (van Marken Lichtenbelt et al., 2009; Inagaki et al., 2016). Other studies have noted that UCP1 in the presence of external factors (e.g. cold exposure, diet manipulation) could increase fatty acid oxidation and thermogenesis specifically in brown adipocytes (Symonds, 2013, Rosell et al., 2014); this could be through enhancing FGF21 gene expression, which has been shown to improve glucose uptake and fatty acid oxidation in skeletal muscle of mice after cold exposure.(Morrow et al., 2017; Badman et al., 2007). Furthermore, the gene expression patterns in the current study were noted to be stimulated by nearby endocrine organs such as the adrenals on the perirenal or thyroid in the sternal adipose tissue, which determines changes in the metabolic/phenotypic characteristics of existing fat cells (Symonds, 2013). This sort of endocrine influence was not observed in epicardial fat and therefore may not exhibit an adipogenic profile and would, thus, exhibit little capacity for plasticity.

These findings further suggest the appropriate application of a potential stimulatory mechanism that could be used to delay the loss of mitochondrial respiratory capacity genes, mainly UCP1. The use of a stimulatory mechanism could ultimately assist BAT phenotypes to maintain normal body weight.

4.6 Conclusion

Overall, this study was able to address critical questions about gene expression patterns across different BAT depots in early life and correlate them with biological processes and pathways that ultimately affect thermogenesis and adipogenesis. The data showed that the age factor plays a substantial role during the development of adipose tissues, particularly in regard to loss of brown adipose tissue function in early life, with note that there is a variation in the effect of this factor when testing it in different locations, which may indicate that there are other factors (e.g., anatomical location, external stimuli and internal factors) which may interfere in this process (Herzig, 2016; Wu, 2016).

.

5 Anatomical localisation, gene expression profiling and functional characterisation of young sheep adipose tissue

5.1 Introduction

Most studies done on the development of adipose tissue are specific to the isolated tissue (Gesta et al., 2007), and therefore the effect adjacent organs may have on it or its deposits (Lotta et al., 2017, Gesta et al., 2007, Symonds, 2013, Symonds et al., 2015). In sheep, brown adipose tissue shows its characteristics most dominantly at 7 days of age and is scarce at 28 days. I employed the use of a machine learning algorithm and weighted co-expression network analysis to detect biologically significant relations in microarray datasets of the five major fat depots in sheep (for 7- and 28 day-old sheep).

5.2 Hypothesis

For this study, based on my first chapter results in comparison to different depot development with age, I hypothesised that:

- Each anatomical location maintained unique gene expression and transcription transformation independently during the whitening of brown adipose tissue.

5.3 Methods

All methods used in this phase have been thoroughly expounded on in Chapter 2. In the same chapter, operating procedures for gene expression have been described. The experimental module used in this chapter is summarised in Figure 5-1.

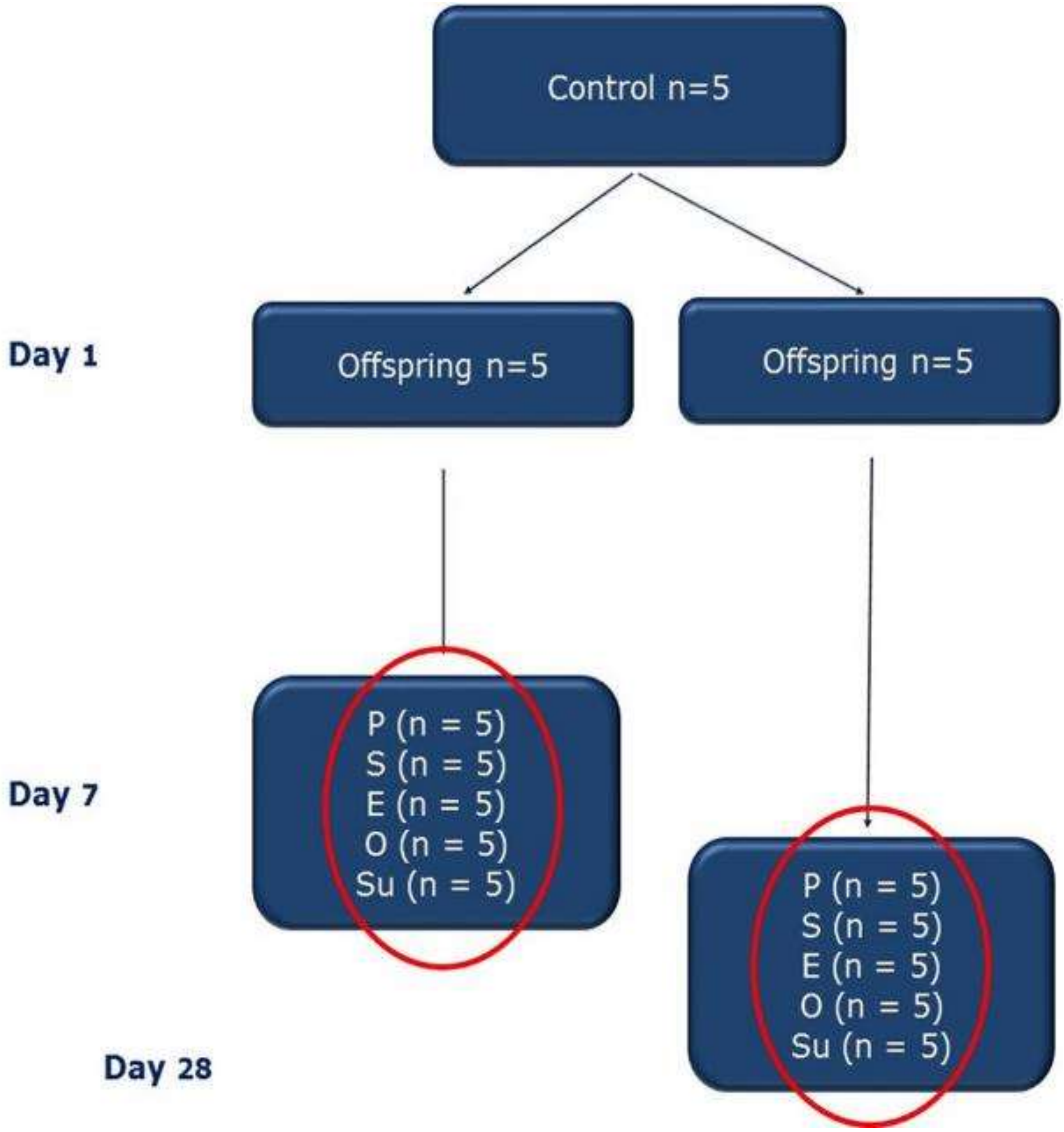

Figure 5-1: Experimental summary design

The study was carried out on 50 samples extracted from lambs (n = 10) adipose tissue in five different location at two time points, either at seven days (n = 25), or 28 days (n = 25) of age, from lambs (n = 10), that were suckling from their mother that had been fed a control diet (n = 5), ((P) perirenal, (S) sternal, (E) epicardial, (O) omental, and (Su) subcutaneous). Numbers indicate age by days.

5.4 Results

5.4.1 Changes in the cellular structure of the brown and white adipose tissue within the first 28 days of postnatal life

I studied the transcription makeup and identified differences among the five fat depots and any changes in gene regulation with age and observed 839 genes (false discovery rate [FDR] ≤ 0.05) that had been highly expressed among the five depots at 7 days. The most significant disparity in terms of the expression of genes that I observed was between the omental and epicardial fat depots (429 significant genes, FDR ≤ 0.05, Figure 5-6A and C). In addition, thermogenic genes, including UCP1, were constantly up-regulated in perirenal adipose tissue, as opposed to the other depots including the pro-thermogenic depot epicardial (q-value =1.00E-02). However, the sternal was the only depot that showed similar UCP1 expression to perirenal at this time point (q-value = 0.09). From the above observations, it is necessary to remember that variability occurs in transcriptional regulation amongst fat depots throughout the postnatal period. This is consistent with the development of their disparate growth and functions between the examined depots, as the brown populated depot mainly appears in late gestation (Henry et al., 2017) while the other two depots (omental and subcutaneous) appear after birth (Saroha et al., 2018).

Transcriptomic data observed in the seven-day-old lambs were then analysed through hierarchical clustering (unsupervised) and principal component analysis (PCA). The two methods exhibited a well-defined cluster formation by each fat depot, as illustrated in Figure 5-2A. Most of the variance within the dataset was attributed to the two initial components, implying a substantial correlation between the computational module and the presence of congenital disparity in gene expression across the five fat depots. Moreover, the PCA revealed a conglomeration of the subcutaneous, omental, sternal and the pro-thermogenic perirenal fat depots while the adipose tissue of the epicardial depot separated from other examined depots (Figure 5-2C).

At 28 days, I performed the same statistical methods with the aim of determining critical changes in gene expression. In this phase, I identified 2059 genes that were expressed differently between the fat depots (FDR $\leq$ 0.05), with a note of the significant increase in pre-adipocyte differentiation gene (i.e. Homeobox protein Hox-B6 (HOXB6), Homeobox protein Hox-B3 (HOXB3)) across all examined depots. During this period, a down-regulation of the sternal adipose tissue was more prominent in comparison to the other fat depots.

UCP1 expressed was observed to be somehow constant in pro-thermogenic depot (i.e. Perirenal, sternal and epicardial) or not detectable in white adipocyte (i.e. omental and subcutaneous) at this time of age, as the results indicate that there is no significant difference between the brown examined depot at this time of age (FDR q-value = 0.09) .

The adipose tissue samples profiled into three stable clusters whereas the variability observed when gene expression between the five fat depots was analysed is explainable by the two initial elements of the PCA, as shown in Figure 5-2 D.

In effect, the anatomical location in the adipose tissue was observed to influence the transcriptomic alterations redefined by age when examined through clustering analysis. A higher transcriptomic restructuring was evident in the perirenal and sternal fat depots, thereby demonstrating the various variations in their biological and metabolic functions based on age (Ojha et al., 2016, Rockstroh et al., 2015).

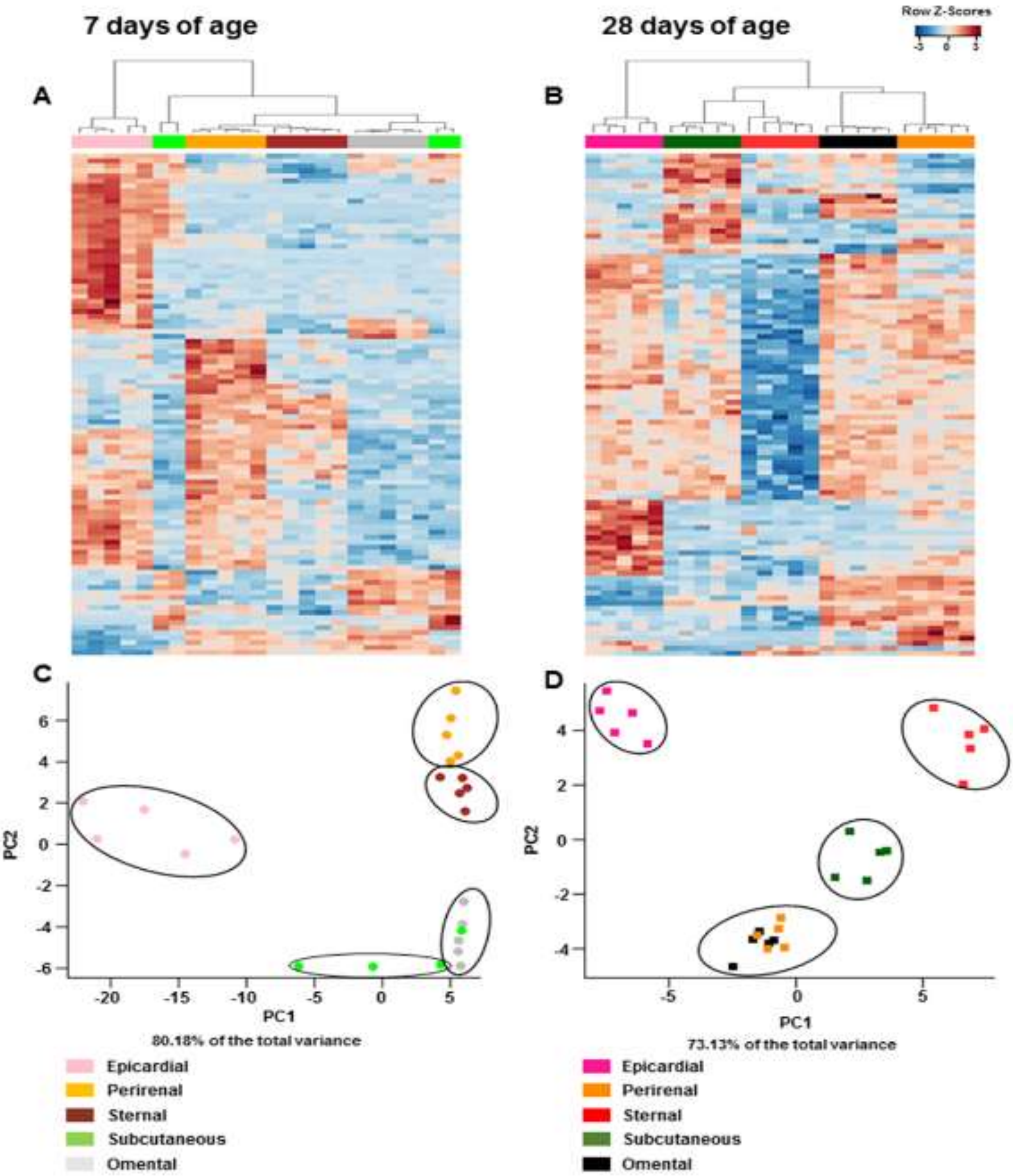

Figure 5-2: Gene expression in five fat depots, A at 7 days and B at 28 days.

Heat map and unsupervised hierarchical clustering dendrograms for the top 100 genes that were expressed divergent to the others are illustrated. The analyses were performed through microarray analysis (average linkage, Euclidean distance metric). The selection was made through eBayes t-statistic (FDR < 0.05). The expression of genes was modified into a Z-score. Blue and red denote decrease and increase of gene expression respectively. 10055 datasets were used for PCA and subjected to variance test QC at C (7) and D (28) days of age. Each sample is illustrated by a sphere for 7 days and rectangle at 28 days. The colour code defines the age and tissue to which it belongs.

5.4.2 Use of machine learning and gene network analysis to determine the transcriptional changes between adipose tissue depots with age

I observed a variation with age in the number of informative genes identified in each fat depot. 2274 informative genes were present in 7-day-old lambs, while there were 3339 of the same at 28 days of age. This variation in number illustrated different responses in gene patterns. The next step I applied was the generation of two weighted co-expressed modules in each of the ages. These networks were generated from the datasets of the informative genes and were independent of each other. The generated patterns are based on the pairwise correlation of gene expression within each sample, enabling comprehension of their transcriptional sequence (Zhang and Horvath, 2005). At 7 days, I was able to identify 11 modules (designated as C1.1-11; Figure 5-3A) whereas 14 modules were identified at the 28 day period (designated as C2.1-14; Figure 5-3B).

I conducted an in-depth analysis of the two weighted co-expressed genes patterns and observed that the gene modules for each fat depot primarily correlated with the metabolic and transcriptional roles of the depot. The vigour of these modules in the adipose tissue depots was also observed to differ based on age.

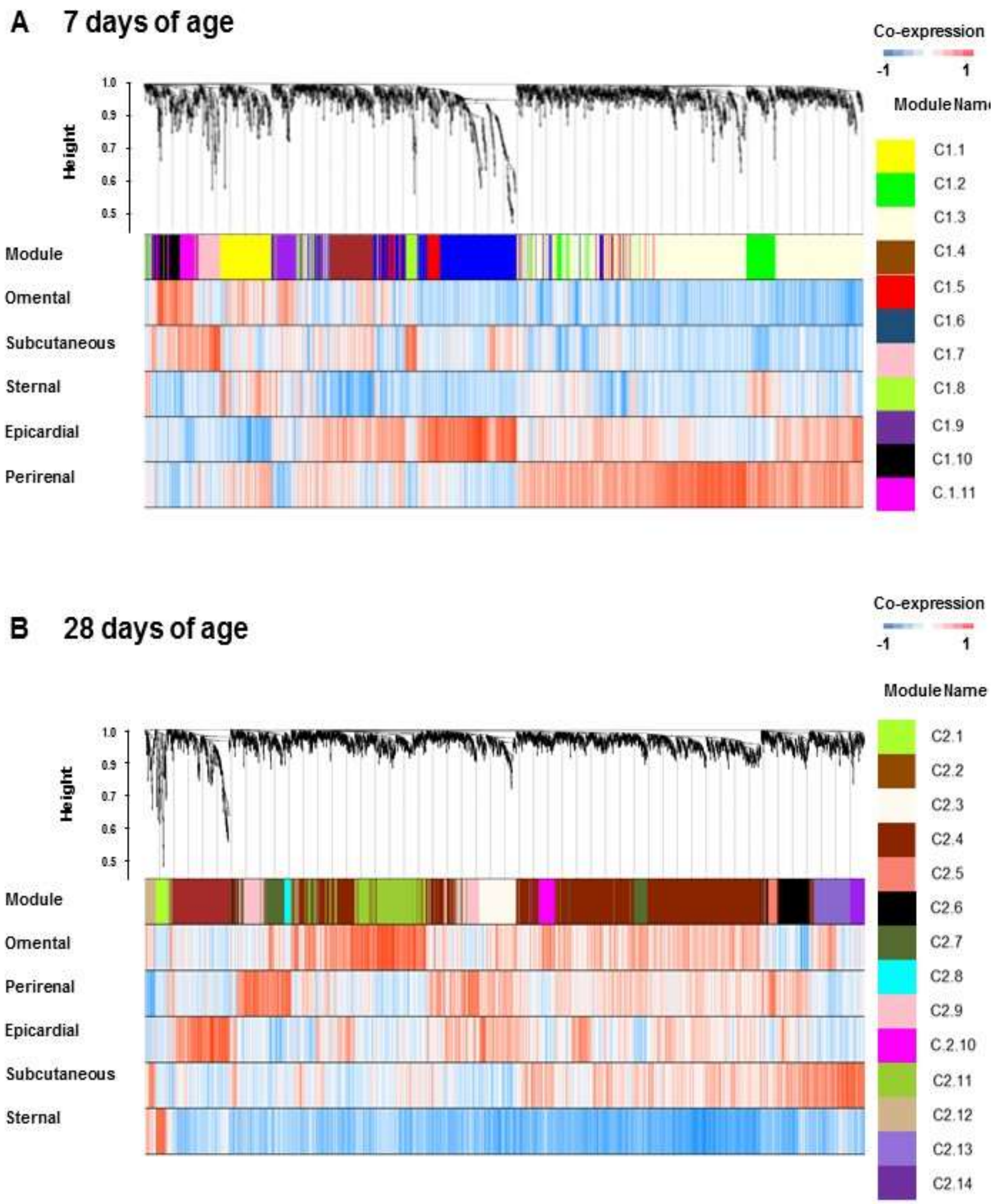

Figure 5-3: Demonstration of co-expression analysis for fat depots at 7 (A) or 28 (B)

Rows two to six indicate differential expression association. Blue colour indicates negative co-expression whereas red indicates positive co-expression.

5.4.3 Functional enrichment of gene clusters at seven days of age

The gene network indicated a similar utility in transcription within the sternal and perirenal depots (Figure 5-4A, and B). The functionality was more evident in adipose tissue of the perirenal fat depot. Most of the modules identified in figure 5-9 (i.e. C1.1, C1.2 and C1.3) consisted of genes that are necessary for the regulation of mitochondria biogenesis and for aerobic respiration, including mitochondrial ATP production gene. For example, ATP synthase, H+ transporting, mitochondrial F1 complex, delta subunit (ATP5D) as well as Eukaryotic initiation factors (eIFs) group of the expressed gene . A significant number of genes, associated with oxidation-reduction in the C1.3 module, and mitochondrial regulation of mRNA translation in the C1.2 module have undergone gene ontology, including around 13 genes significantly expressed from 16 genes in oxidation-reduction pathway (FDR q–value = 1.45E-03), (i.e. NADH dehydrogenase [ubiquinone] 1 beta subcomplex subunit 2, mitochondrial (NDUFB2)).

The separation between these co-expressed modules, however, suggested the possibility of different transcriptional loops regulating genes of the mitochondria (Claussnitzer et al., 2015b, Kajimura et al., 2009, Rajakumari et al., 2013). These separations favour the regulation of mitochondrial gene expression by the brown adipocytes without necessarily needing the influence of the uncoupling protein 1 (Lidell et al., 2013).

A significant number of gene modules, oriented with the epicardial adipose tissue, corresponded with distinct phases of the cell differentiation process of the transcriptome cardiomyocyte (Yamada et al., 2006). For instance, the C1.4 module displayed evidence of DNA and mRNA activity related to the sustenance of pluripotency of the stem cell (i.e. RNA-binding protein 42 (RBM42) or (MBNL2)) (Yamada et al., 2006).

The C1.6 module also displayed several changes. There was advanced cell differentiation in the C1.6 module, associated with the presence of a substantial transcriptional imprint, which is common in mature cardiomyocyte cells (i.e. myosin, light chain 2, regulatory, cardiac, slow [MYL2]), and myosin heavy chain 6, cardiac muscle, alpha (MYH6) (Boheler et al., 2002).

All the results I obtained in my discourse conformed to the pluripotency of adipose tissue-derived stem cells towards differentiation into cardiac myocyte-like cells or brown adipocytes (Yamada et al., 2006). Modules C1.7 and C1.8 illustrate the various transcriptional changes that happen in subcutaneous adipose tissue and consist of gene processes associated with myocyte precursors (i.e. myosin, heavy chain 2, skeletal muscle, adult [MYH2] and actin, alpha 1, skeletal muscle [ACTA1]) (Yamada et al., 2006). The above property facilitates the growth of brown adipocytes and a category of white adipocytes that are dominantly present in subcutaneous fat depots. At the final stage, I reported three modules (C1.9, C1.10 and C1.11). The modules were observed in omental fat and were enhanced with genes associated with metabolism of carbohydrates (i.e. malate dehydrogenase, cytoplasmic [MDH1] and malate dehydrogenase, mitochondrial (MDH2)] (Mazo et al., 1990, Hung et al., 2004), structuring of the cytoskeleton and restructuring of body tissues through promotion of the immune response, including CD6 Molecule gene (CD6) (Hassan et al., 2006) and immunoglobulin heavy constant mu (IGHM) (Linton and Dorshkind, 2004, Gesta et al., 2007, Lu et al., 2010).

.

5.4.4 Functional enrichment of gene clusters at 28 days of age

I derived the second network of gene co-expression at 28 days of age and used it to determine if any phenotypical results had been achieved due to the observed disparities in transcriptome regulation within the five fat depots in seven-day-old lambs. The most substantial marked change in expression of genes through principal component analysis was in the perirenal depot where four co-expression modules with discriminatory enhancement were identified (Figure 5-4C and D). The C2.7 module was also observed to have omental fat enrichment. The similarity so observed stipulated a shift in metabolism, due to a modification of perirenal adipose tissue in its transdifferentiation from heat production in the brown adipocytes to its lipid storage in white fat depots (Claussnitzer et al., 2015b; Rockstroh et al., 2015; Symonds et al., 2015; Virtanen et al., 2009). Multiple genes involved in the metabolism of fatty acids and which regulate differentiation of adipocyte cells (such as 1-acylglycerol-3-phosphate O-acyltransferase (ABHD5), 2,4-Dienoyl-CoA Reductase 1 (DECR1), PPARG and growth hormone receptor (GHR)) were also identified as present in module C2.7 (Lu et al., 2010, Rajakumari et al., 2013, Claussnitzer et al., 2015b). Pre-adipocyte precursor genes (HOXB6, Homeobox B8 (HOXB8), and homeobox protein Hox-B5 (HOXB5) (Cantile et al., 2003; Park et al., 2013), angiogenic genes (HOXA5, Hypoxia Inducible Factor 1 Subunit Alpha (HIF1A)) and genes related to the growth of white adipose tissue were co-expressed within the module. The C2.5 module contained genes enhanced in perirenal fat, and transcripts involved in promotion of inflammatory responses. Endoplasmic reticulum was also present in the C2.5 module, including gene function in apoptosis (i.e. apoptosis-inducing factor, mitochondrion-associated, 2 [AIFM2]) (Ohiro et al., 2002) and inflammation Janus kinase 3 (JAK3) (Kim et al., 2011), pointing out cellular stress (Sharkey et al., 2009; Hotamisligil, 2005). The C2.9 and C2.8 modules had significant imprints of mRNA transcriptional regulation and cell division, indicating cellular differentiation or diversification increment (Lee et al., 2017; Macotela et al., 2012; Spalding et al., 2008). On the other hand, the cellular events observed in perirenal depots were suppressed sternal fat depots (Figure 5-4D). All clusters were also negatively aligned apart from the C2.1 module, which was enhanced with genes associated with hormonal response and tissue angiogenesis (i.e. insulin-like growth factor 1 [somatomedin C] [IGF1]) (Park et al., 2013; Sharkey et al., 2009). At seven days of age, the epicardial adipose tissue was also observed to contain modules enhanced with genes that are involved in cardiomyocyte cell differentiation, such as C2.2 (Yamada et al., 2006).

There was considerable correspondence of omental adipose tissue in the C2.1O and C2.11 modules (Figure 5-4C and D) (Macotela et al., 2012). Transcripts associated with maintaining equilibrium between anabolic and catabolic processes in adult adipocytes were also heavily present in the two modules (Pietilainen et al., 2011). Most of the genes in subcutaneous adipose tissue were aligned to modules C2.12, C2.13 and C2.14 and were involved cell restructuring, growth and differentiation (Lee et al., 2013; Lotta et al., 2017; Park et al., 2013).

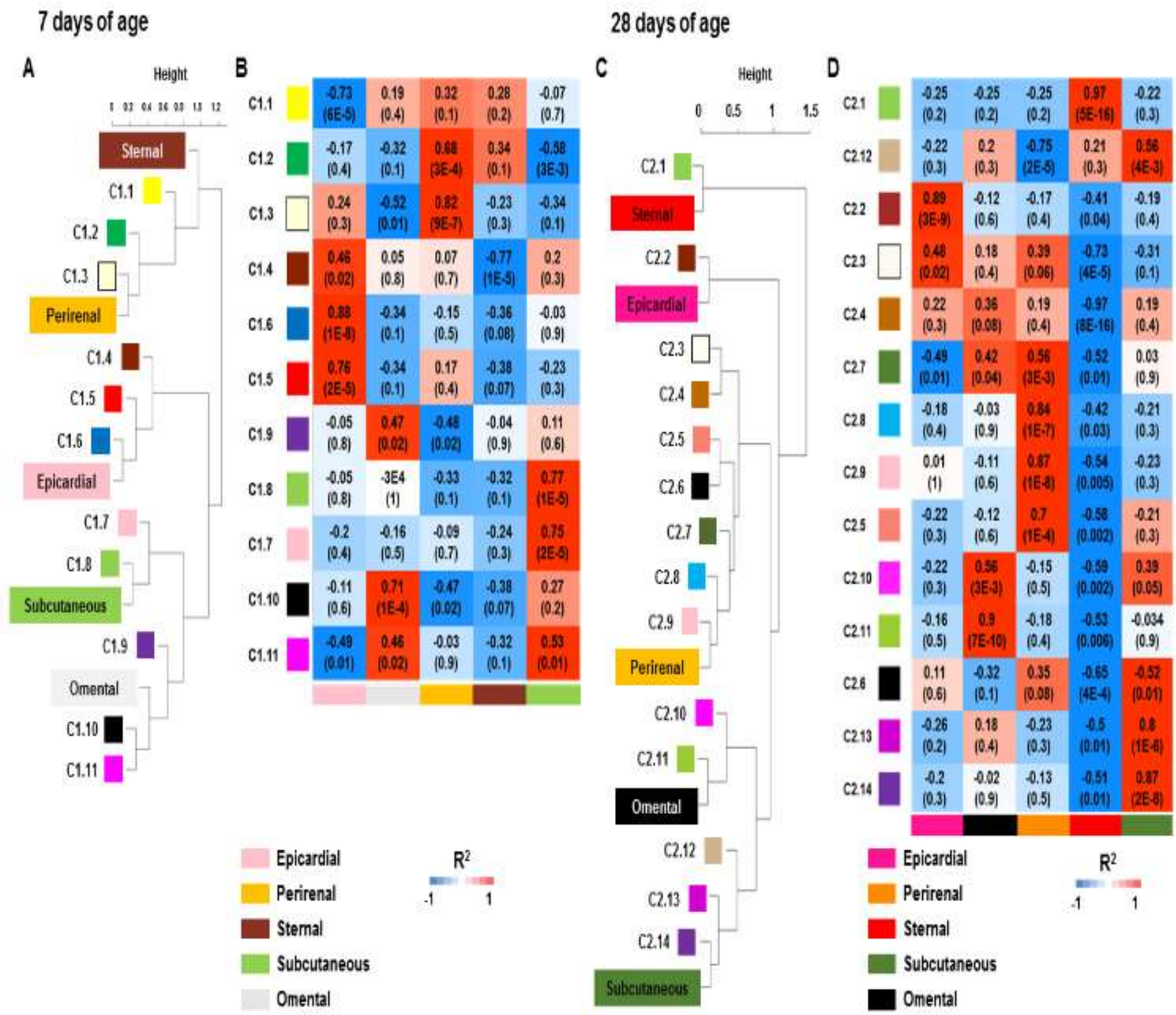

Figure 5-4: Illustration of functional modules depending on age and adipocyte type

They had an initial relation based on the ME (module eigengene) property. Co-expression and positive alignment of genes is shown in each dendrogram at an age of (A) 7 and (C) 28 days. The horizontal axis represents the level of correlation on a Euclidean scale. The heat maps show the concurrence and respective p-values amongst co-expressed modules in each depot at an age of (B)7 and (D)28 days. Blue indicates low correlation; red indicates high. The columns indicate the modules with a high correlation in each fat depot.

A 7 days of age

Term	Gene Count	Fold Enrichment
C1.1		
SRP-dependent cotranslational protein targeting to membrane	22	17.93
rRNA binding	5	15.22
cytosolic small ribosomal subunit	9	24.64
C1.2		
translational initiation	11	8.4
translation initiation factor activity	5	12.03
mitochondrial part	20	3.42
C1.3		
respiratory electron transport chain	32	5.61
NADH dehydrogenase (ubiquinone) activity	13	5.85
mitochondrial inner membrane	65	3.87
C1.4		
mRNA splicing, via spliceosome	17	7.70
RNA binding	36	4.03
nuclear lumen	53	2.03
C1.5		
regulation of cellular component organization	19	2.69
chromatin binding	9	5.33
nuclear part	33	1.99
C1.6		
myofibril assembly	12	14.60
structural constituent of muscle	13	12.78
Z disc	16	10.98
C1.7		
nucleolus	17	2.61
C1.8		
actin filament-based process	8	6.45
cytoskeletal protein binding	7	4.53
myofibril	5	13.68
C1.9		
regulation of macromolecule metabolic process	36	2.01
structure-specific DNA binding	5	6.12
nuclear body	10	9.57
C.1.10		
extracellular matrix organization	11	10.74
extracellular matrix structural constituent	6	17.29
basement membrane	6	15.54
C1.11		
positive regulation of ligase activity	5	12.70
protein binding	49	1.52
nuclear outer membrane-endoplasmic reticulum membrane	14	4.32

Figure 5-5: Summary of significant biological, molecular and cellular functions that are highly enhanced in every module exhibiting gene co-expression at seven days old

Hypergeometric enrichment analysis was carried out via the Web Gestalt approach on every distinct module. The figure also shows the normalised enhancement rating and the estimated proportion impacted on.

B 28 days of age

Term	Gene Count	Fold Enrichment
C2.1		
angiogenesis	7	7.55
C2.2		
muscle filament sliding	10	16.03
actinin binding	5	15.42
intercalated disc	9	19.22
C2.3		
RNA splicing	34	7.71
mRNA binding	8	6.72
nuclear speck	19	10.38
C2.4		
nuclear-transcribed mRNA catabolic process	52	3.76
structural constituent of ribosome	36	2.99
intracellular organelle lumen	390	1.63
C2.5		
antigen processing and presentation of exogenous peptide antigen	5	11.77
chromatin binding	5	5.64
coated vesicle	5	7.99
C.2.6		
negative regulation of nucleobase-containing compound metabolic process	29	3.17
transcription factor binding	14	3.54
nucleoplasm	43	3.33
C2.7		
embryonic skeletal system morphogenesis	9	9.45
threonine-type peptidase activity	5	21.79
proteasome core complex	5	23.42
C2.8		
intracellular organelle lumen	16	2.44
C2.9		
organic cyclic compound biosynthetic process	60	1.81
nucleic acid binding transcription factor activity	26	2.93
nucleoplasm	27	2.13
C2.10		
protein binding	52	1.43
endoplasmic reticulum membrane	12	3.49
C2.11		
GTP catabolic process	25	3.43
transmembrane receptor protein kinase activity	9	5.18
endosomal part	23	3.45
C2.12		
cellular response to amino acid stimulus	5	41.85
extracellular matrix structural constituent	8	32.66
basement membrane	6	23.95
C2.13		
outflow tract morphogenesis	5	10.66
transcription factor binding	12	2.97
synapse	12	2.63
C2.14		
cytoskeleton organization	10	3.28
binding	59	1.22
cytoplasmic vesicle part	7	4.51

Figure 5-6: Summary of major biological, molecular and cellular functions that are highly enhanced in every module exhibiting gene co-expression at 28 days old

Hypergeometric enrichment analysis was carried out via the Web Gestalt approach on every distinct module. The figure also shows the normalised enhancement rating and the estimated proportion impacted on.

5.4.5 Changes in gene networks represent functional adaptations of different adipose depots during development

I used a statistical technique to identify the biological functioning and effect of each module through random permutations between datasets. I was able to identify which network topology contrasted to or showed correspondence at 7 and 28 days of age. I observed a prolonged interaction of most of the genes at both ages (Figure 5-7A and B). A proportion of 86.4% of all of the genes had been assigned to a reserved module at seven days of age, including the C1.2 module which was enhanced with mitochondrial such as uncoupling protein 1 (Figure 5-7A). Evaluation of gene ontology for the four non-reserved modules indicated related functionality attributed to initial phases of cell differentiation and restructuring of the adipose tissue (Lee et al., 2013). At 28 days of age, 71.4% of all genes were assigned to a reserved module within the network. I performed a broader evaluation of the enhancement of gene ontogeny on these reserved modules and was able to identify transcriptomic and metabolic activity related to metabolism of lipids, restructuring of tissues and immune responses, which are all processes of a mature adipocyte cell (Figure 5-7B).

A 7 days of age

Module	Size	Z summary	Tissue		Preservation	Summary of biological process
C1.6	389	10.9			High	Cardiac myocyte cell differentiation
C1.1	182	6.2			Moderated	transcription of protein targeting to membrane
C1.3	910	5.4				Mitochondrial respiration
C1.11	73	4.6				Cellular cytoskeletal remodelling
C1.4	176	3.4				mRNA splicing regulation
C1.2	142	2.9				Regulation of translation
C1.9	70	2.4				Changes in chromatin conformation
Total genes	1942					

Module	Size	Z summary	Tissue		Preservation	Summary of biological process
C1.10	76	1.9			No preservation	Tissue remodelling
C1.5	104	0.9				Cell differentiation
C1.8	43	0.7				Cellular cytoskeletal remodelling
C1.7	84	-1.6				NA
Total genes	307					

Epicardial
Perirenal
Sternal
Subcutaneous
Omental

Z (Scores) summary
-1 0 15

Module size
40 1000

B 28 days of age

Module	Size	Z summary	Tissue		Preservation	Summary of biological process
C2.2	270	15.6			High	Cardiac myocyte cell differentiation
C2.4	1000	12.2				mRNA regulation
C2.7	190	7.7			Moderated	Tissue remodelling
C2.12	50	6.7				Tissue remodelling regulation
C2.3	236	3.4				mRNA splicing regulation
C2.6	166	2.8				Regulation of gene expression and changes in chromatin conformation
C2.14	174	2.1				Cytoskeleton organization
Total genes	2086					

Module	Size	Z summary	Tissue		Preservation	Summary of biological process
C2.10	83	1.8			No preservation	NA
C2.9	160	1.6				DNA transcription
C2.5	45	0.7				Immune responses, cellular stress
C2.8	40	-0.1				NA
C2.14	73	-0.2				Cellular metabolism
C2.11	376	-0.9				GTP catabolic process
C2.1	58	-0.9				Angiogenesis
Total genes	835					

Epicardial
Perirenal
Sternal
Subcutaneous
Omental

Z (Scores) summary
-1 0 15

Module size
40 1000

Figure 5-7: Illustration of preservation of cross-adipocyte depots module depending on age

Gene connectivity at (A) 7 and (B) 28 days was evaluated using the Z-score approach. The rows denote modules whereas columns denote distinct properties of the module. A Z-score greater than two indicates moderate preservation whereas a score higher than ten shows a highly preserved module.

5.5 Discussion

I have demonstrated the postnatal changes that occur in profiles of gene expression of the principal fat depots in sheep, occurring at the same time as the transdifferentiation of brown fat depot into the white depot (Symonds et al., 2015, Pope et al., 2014). In spite of the depots harbouring almost identical macroscopic morphology, developmental alterations over age were identified for each depot. For instance, each fat depot had a different gene expression profile at 28 days of age even though sheep fat is essentially white during this period (Henry et al., 2017; Pope et al., 2014). Very little is known of the different functions and changes the adipose tissue causes between the five major fat depots in the postnatal period. Our new findings substantiate that adipose tissue performs its metabolic role as several well-defined organs that all have particular functions as opposed to the widely known notion that it functions as one metabolic organ (Macotela et al., 2012).

Through the application of a computer-assisted supervised learning algorithm I was able to determine that during postnatal maturation, distinct gene clusters form as a result of transcriptomic activity within fat depots (Barabasi and Oltvai, 2004). With time, networks of these gene clusters may restructure themselves either through a loss or assimilation of new novel constituents (Ojha et al., 2016; Zhang and Horvath, 2005). Natural factors prompt an ontogenic plasticity response, whereas an increased response to an extraneous influence can help an organism to survive in harsh and constantly-changing environments (Symonds et al., 2015). However, an erroneous or maladaptive trait in plasticity response may result in an over-accumulation of fat and therefore may lead to obesity. Obesity has been identified as a risk factor for many serious medical conditions and is, therefore, a threat to human life (Gregg and Shaw, 2017)**.**

In order to create control measures against obesity, it is critical to comprehend the early life factors that influence the usage and storage of energy in tissue cells. Through an in-depth gene-network analysis of adipose tissue development in postnatal life, I have formulated novel biological explanations (Barabasi and Oltvai, 2004; Zhang and Horvath, 2005) targeting individual fat depots whenever the initiation of nutritional, physiological or environmental responses in large mammals is required (Symonds et al., 2015)**,** through reviewing the critical gene regulation dynamic adaptations that call for these responses (Barabasi and Oltvai, 2004, Zhang and Horvath, 2005). Genes have different regulatory functions, a property that enables an equally distinct cell differentiation and adaptation from the fat depots to regulate metabolic homeostasis (Lee et al., 2017, Macotela et al., 2012). Little is known about the effect of genetics on the endocrine organ, or about the effect of environmental factors on growth of fat despite the large amount of published research on the transcriptome and cellular structure of fat depots (Cypess et al., 2013, Lee et al., 2017, Lidell et al., 2013, Macotela et al., 2012, Rockstroh et al., 2015). Our discourse was able to bring into light patterns of co-expression modules that are specific to particular depots and are enhanced to execute specific functions.

Previous discourses on adipose tissue during postnatal development have mostly been centred on identifying the causes of gene loss during thermogenesis, particularly UCP1 (Symonds et al., 2015). Various inter-connected systems within brown adipose tissue are involved in the balance of mitochondrial activity, which is supported by this study when comparing the three fat depots (i.e. sternal, perirenal, and epicardial) (Claussnitzer et al., 2015b; Rajakumari et al., 2013). The C1.2 module is particularly crucial in controlling UCP1, thereby sustaining a balance between mRNA degradation and transcription and enabling an efficient mRNA expression (Takahashi et al., 2015).

I was able to identify transcriptional characteristics that promote myoblastic precursor transition to brown fat cells, including C/EBPβ and EP300 (Kajimura et al., 2009; Vargas et al., 2016). The C1.2 module also consisted of EIF4B, EIF4G3, EIF3D and EIF3G, which down-regulate mRNA transcription of UCP1 when exposed to a temperature increase (van Breukelen et al., 2004). I also identified RPS5, RPS9 and several other down-regulated ribosomal proteins co-expressed with the uncoupling protein which is in the original mitochondrial protein assembly (Maier et al., 2013). UCP1 is also controlled by AU-rich elements (AREs), which are mRNA binding proteins (Takahashi et al., 2015) in nature. mRNA binding proteins such as ZFP36 Ring Finger Protein Like 1, (ZFP36L1) and DEAH-Box Helicase 32 (DHX32) co-expressed with UCP1 could potentially degrade AREs since it only controls about 8% of the human genes (Adachi et al., 2014; Fallmann et al., 2016; Takahashi et al., 2015). ZFP36L1 destabilises mRNA by binding at its 3′-UTR mRNA site and recruiting the Cnot7-Tob-BRF1 axis (Adachi et al., 2014, Takahashi et al., 2015). Several transcripts associated with fat metabolism and mRNA transcription in C1.1 and C1.3 modules are co-regulated together with the genes in the perirenal fat from the time of birth up to 28 days of age. I also made a novel discovery about the correlation of epicardial adipose tissue to genes involved in cell differentiation of cardiomyocytes (Liu et al., 2014).

Cardiomyocyte cells in prenatal life differentiate and increase in number at a high rate, but their activity ends soon after birth, leading to a high risk of fatalities in case of any injuries to the heart muscle (Yamada et al., 2006). Most fat depots have storage mediums for multipotent stem cells which are capable of in vitro differentiation to brown adipocytes and, as recently discerned, into cardiomyocytes (Boheler et al., 2002). As displayed in Figure 5-7, cardiac myocytes in epicardial fat cells had the highest number of gene expression in module C1.6 at 7 days and module C2.2 at 28 days. Chronic adrenergic stress is a potential biological pathway to cell differentiation in brown adipocytes. This property was identified in rodents after prolonged subjection to a cold environment (van Breukelen et al., 2004) and in patients who had suffered severe skin burns (Sidossis et al., 2015). Recently, a study has identified a considerable number of brown adipocyte cells in the epicardial fat depot of children suffering from a congenital heart defect (Ojha et al., 2016). Distinct growth factors associated with disease response and physiological development could, therefore, have the potential to affect the functioning and differentiation of multipotent stem cells (Ojha et al., 2016, Yamada et al., 2006).

5.6 Conclusion

There is a substantial variation in gene expression, cell differentiation, cellular composition and stimuli response in adipocytes from different fat depots (Seidell et al., 1990; Sidossis et al., 2015). The perirenal adipocyte is more inclined to cell differentiation and external stimuli response, while sternal and epicardial adipocytes have minimal plasticity ability since they lack an adipogenic profile. From my findings, the application of advanced data analysis in microarray gene expression is an efficient method for generating depot-specific gene expression signatures of adipocytes. This method should also increase my precision in the identification and exploitation of distinct properties of adipocytes in different anatomical environments.

6 The influence of maternal diet supplementation on offspring gene expression and lipid profiling

6.1 Introduction

This study was conducted to evaluate the feasibility of a nutritional intervention in lactating ewes concerning modulating fat composition in sheep offspring. Four adipose tissue depots from different anatomical locations were sampled and then analysed for their lipidomic profile and UCP1 gene expression. I also examined genes that are firmly related to thermogenesis processes including those associated with brown and white adipose tissue.

6.2 Hypothesis

The findings of Chapter 6 form the basis for my primary hypothesis: gene expression within each adipose tissue depot responds differently in response to nutritional intervention. Furthermore, built on the previous study discussed above I hypothesised that ewes subjected to supplements of canola oil would have increased MUFAs and UCP1 expression in offspring as well as a reduced level of the polyunsaturated fatty acids content.

6.3 Methods

All methods used in this study have been described in Chapter 2. Figure 6-1 illustrates the experimental module that has been applied in this chapter.

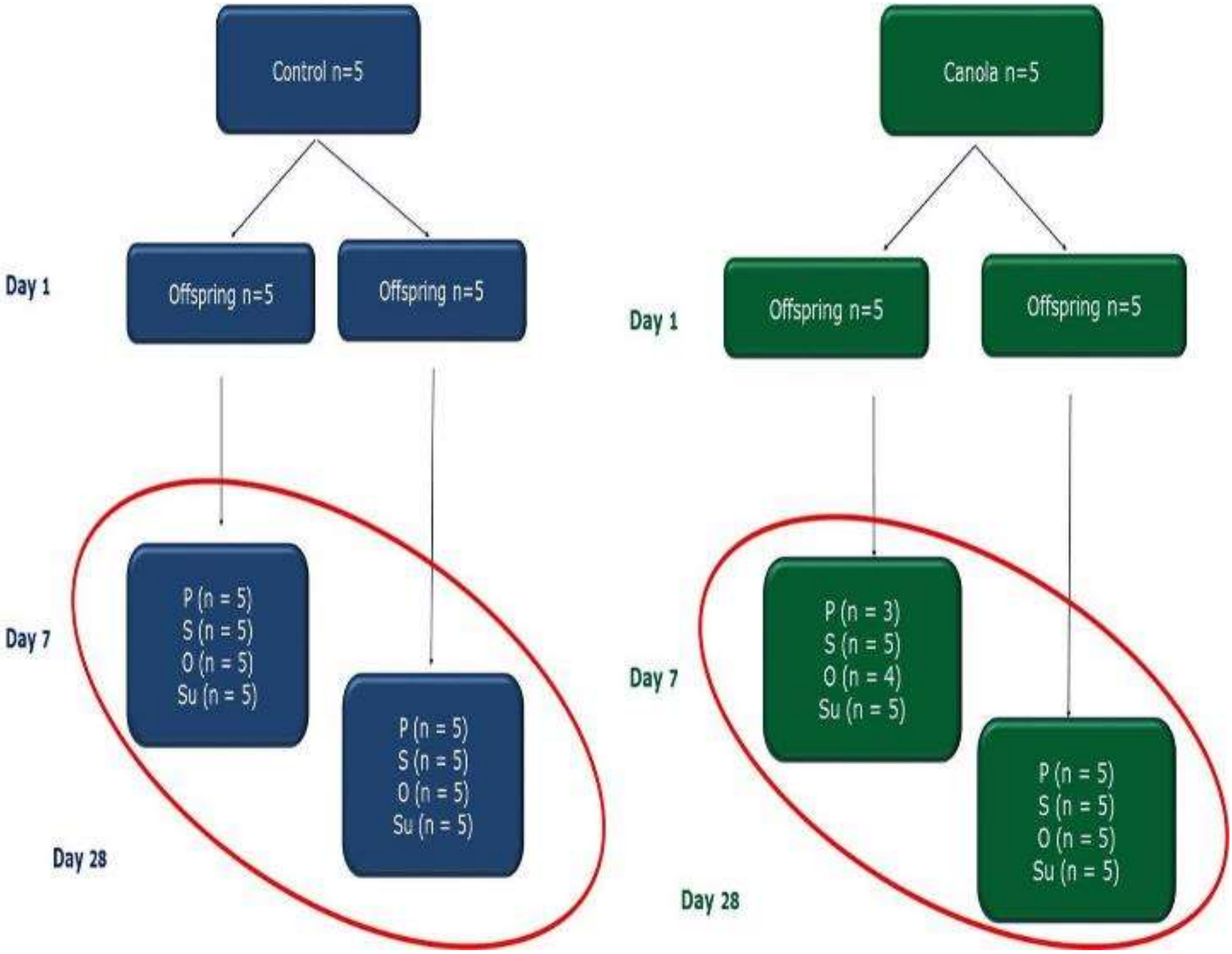

Figure 6-1: Summary of experimental design

Datasets included data from 40 samples obtained from the control group at two time points either at seven days (n = 20), or 28 days (n = 20), in comparison with 37 samples obtained from the canola oil-supplemented group at the same time points, seven days (n = 17) and 28 days (n= 20) from four different adipose tissues depots (i.e. sternal (S), perirenal (P), omental (O), and subcutaneous (Su)) from five animals in each dietary group.

6.4 Results

6.4.1 Principal component analysis (PCA) and hierarchical clustering in the diet intervention groups from 7 to 28 days of age

Figures 6-2 to 6-5 summarises the PCA, separating the data of each fat depot and showing the general level of variation in microarrays between each age and group to further examine the effect of the maternal dietary intervention. The results of the clustering analysis suggest that dietary intervention contributes to transcriptomic differences in metabolic order, which are then modified with age. Furthermore, the dietary group exhibits a slightly different clustering when compared with the control group within the same depot and age, which reflects the changes in their biological/metabolic functions with diet through age (Ojha et al., 2016; Rockstroh et al., 2015).

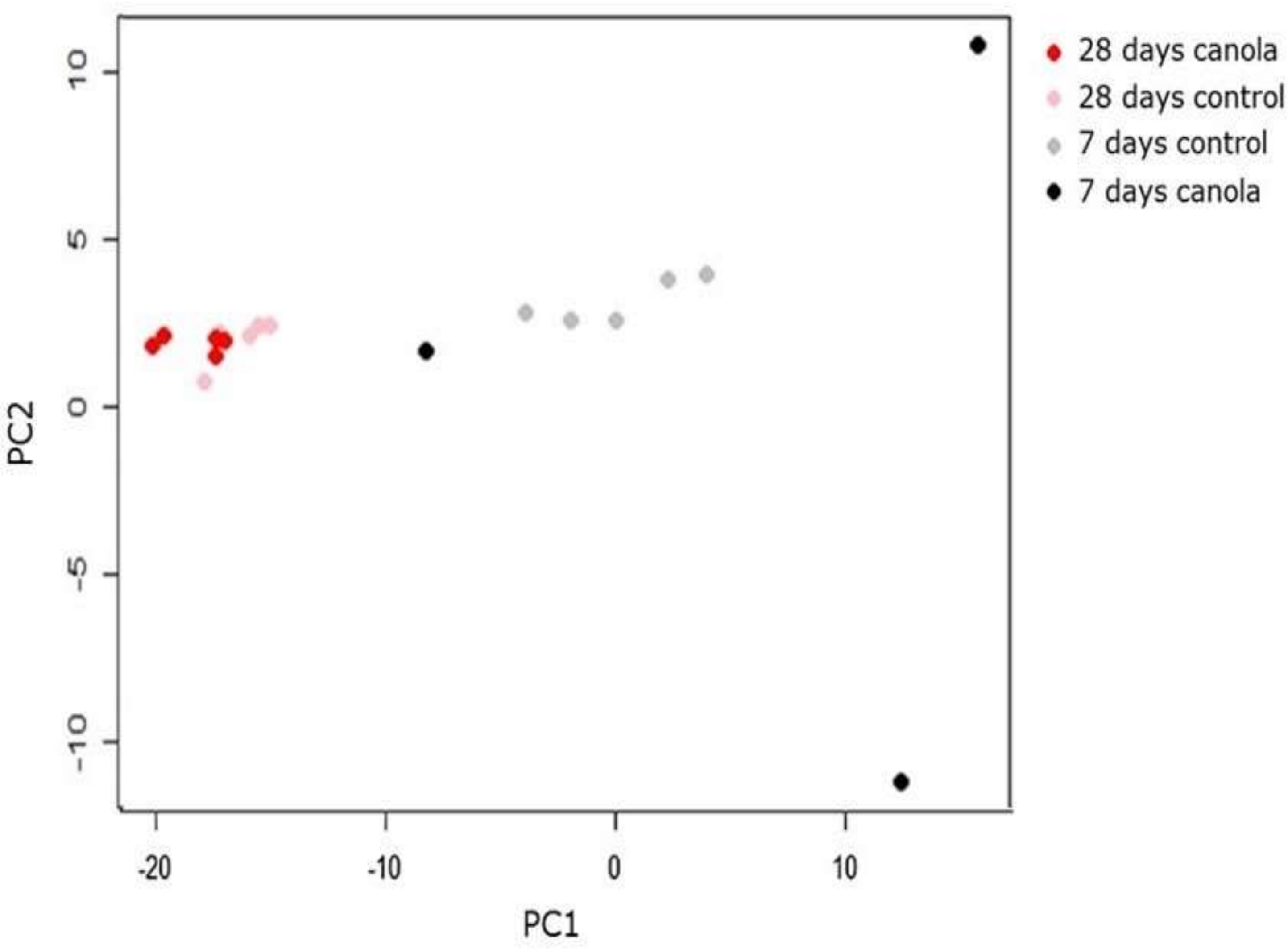

Figure 6-2: Perirenal adipose tissue PCA

Principal component analysis (PCA) of gene expression data from perirenal adipose tissue depot from each animal was performed using 1649 and 401 datasets in control and supplemented group respectively, which passed the variance test QC. Each sample is represented by colour-coding to indicate the age and the dietary group to which it belongs: control group (seven days, grey [n = 5]; 28 days, pink [n = 5]), supplemented group (seven days, black [n = 3]; 28 days, red (n=5]). PC1 axis is the first principal direction along which the samples show the largest variation. The PC2 axis is the second most important direction and it is orthogonal to the PC1 axis.

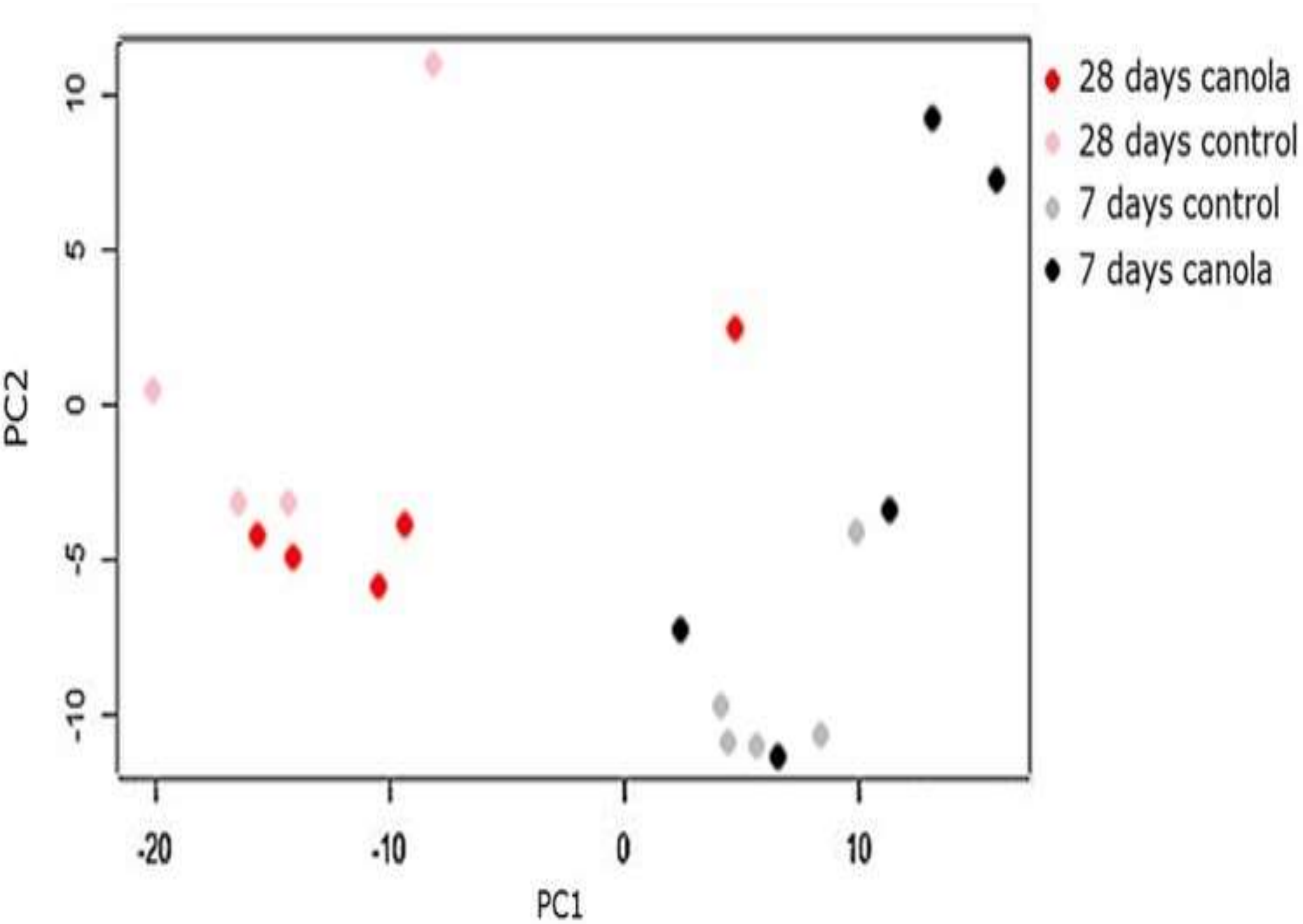

Figure 6-3: Sternal adipose tissue PCA

Principal component analysis (PCA) of gene expression data from sternal adipose tissue depot from each animal was performed using 521 and 158 datasets in control and supplemented group respectively, which passed the variance test QC. Each sample is represented by colour-coding to indicate the age and the dietary group to which it belongs: control group (seven days, grey [n = 5]; 28 days, pink [n = 5]), supplemented group (seven days, black [n = 5]; 28 days red [n = 4]). PC1 axis is the first principal direction along which the samples show the largest variation. The PC2 axis is the second most important direction and it is orthogonal to the PC1 axis.

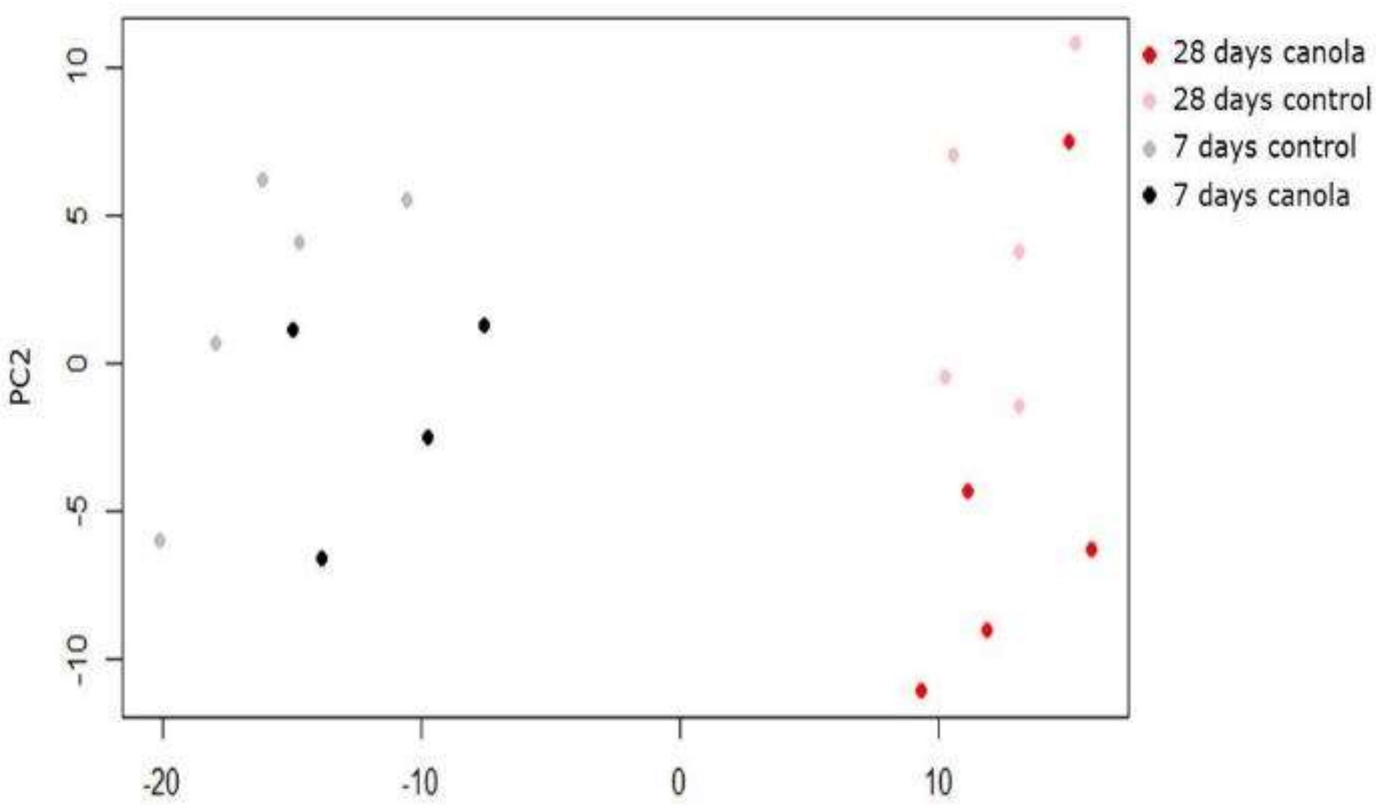

Figure 6-4: Omental adipose tissue PCA

Principal component analysis (PCA) of gene expression data from omental adipose tissue depot from each animal was performed using 1379 and 749 datasets in control and supplemented group respectively, which passed the variance test QC. Each sample is represented by color-coding to indicate the age and the dietary group to which it belongs: control group (seven days, grey [n = 5]; 28 days, pink [n = 5], supplemented group (seven days, black [n= 5]); 28 days, red [n = 5]). PC1 axis is the first principal direction along which the samples show the largest variation. The PC2 axis is the second most important direction and it is orthogonal to the PC1 axis.

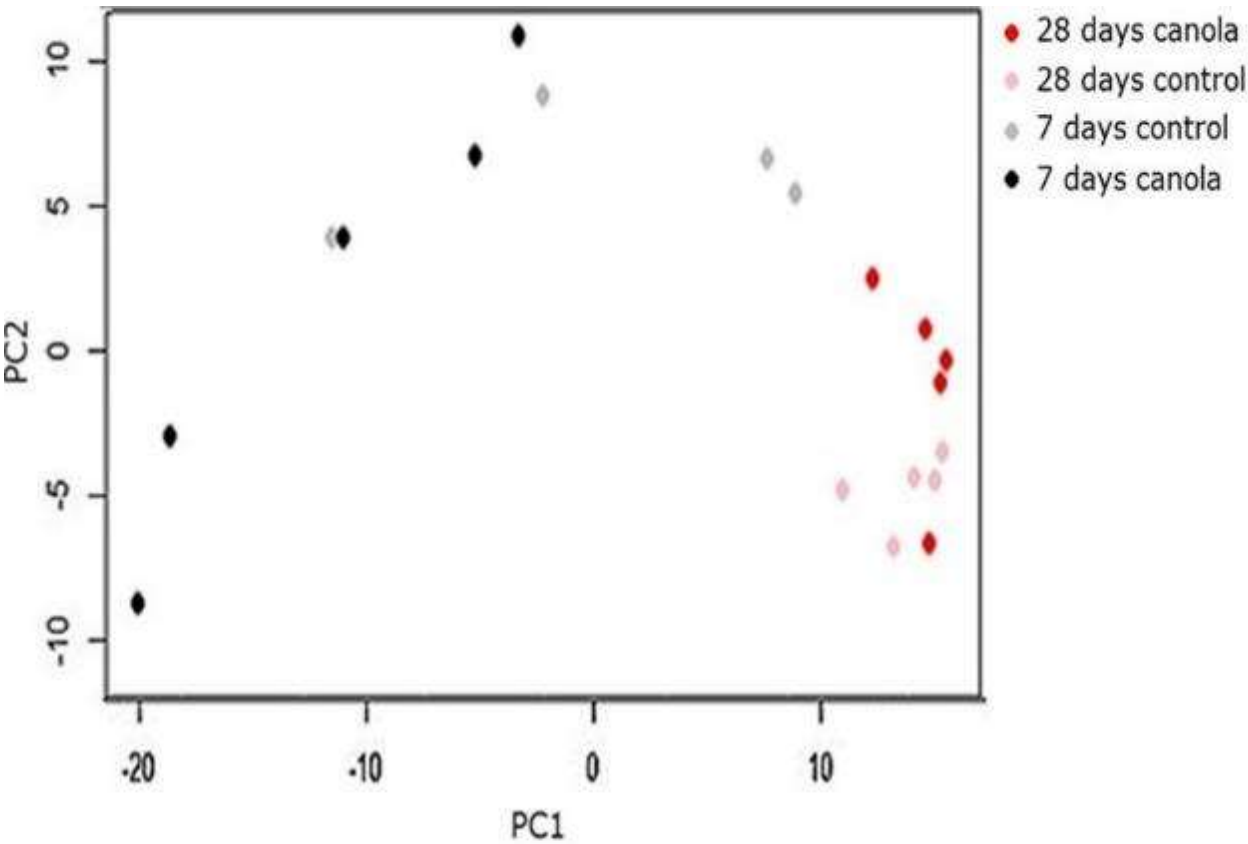

Figure 6-5: Subcutaneous adipose tissue PCA

Principal component analysis (PCA) of gene expression data from subcutaneous adipose tissue depot from each animal was performed using 1341 and 1654 datasets in control and supplemented group respectively, which passed the variance test QC. Each sample is represented by colour-coding to indicate the age and the dietary group to which it belongs: control group (seven days, grey [n = 5]; 28 days pink, [n = 5]), supplemented group (seven days, black [n = 5]; 28 days, red [n = 5]). PC1 axis is the first principal direction along which the samples show the largest variation. The PC2 axis is the second most important direction and it is orthogonal to the PC1 axis.

6.4.2 Description of different transcriptions in the diet intervention gene expression profile

I performed a transcriptomic comparison between all four depots (false discovery rate (FDR) ≤ 0.05) to characterise the differences in the gene sets between the dietary intervention and control groups.

The Venn diagram shows a larger number of genes (i4148) were significantly expressed in the control group when compared with the canola group (2961), across the four examined depots between 7 and 28 days. Furthermore, the Venn diagram graph illustrates that all tested depots in each group shared a different number of genes (control: 34 genes; canola: 12 genes) (see Figure 6-6). However, further analysis shows that the list of shared genes in both groups (canola: 12 genes; control: 34 genes) had only two genes in common (UBE2Q1 and FTH1).

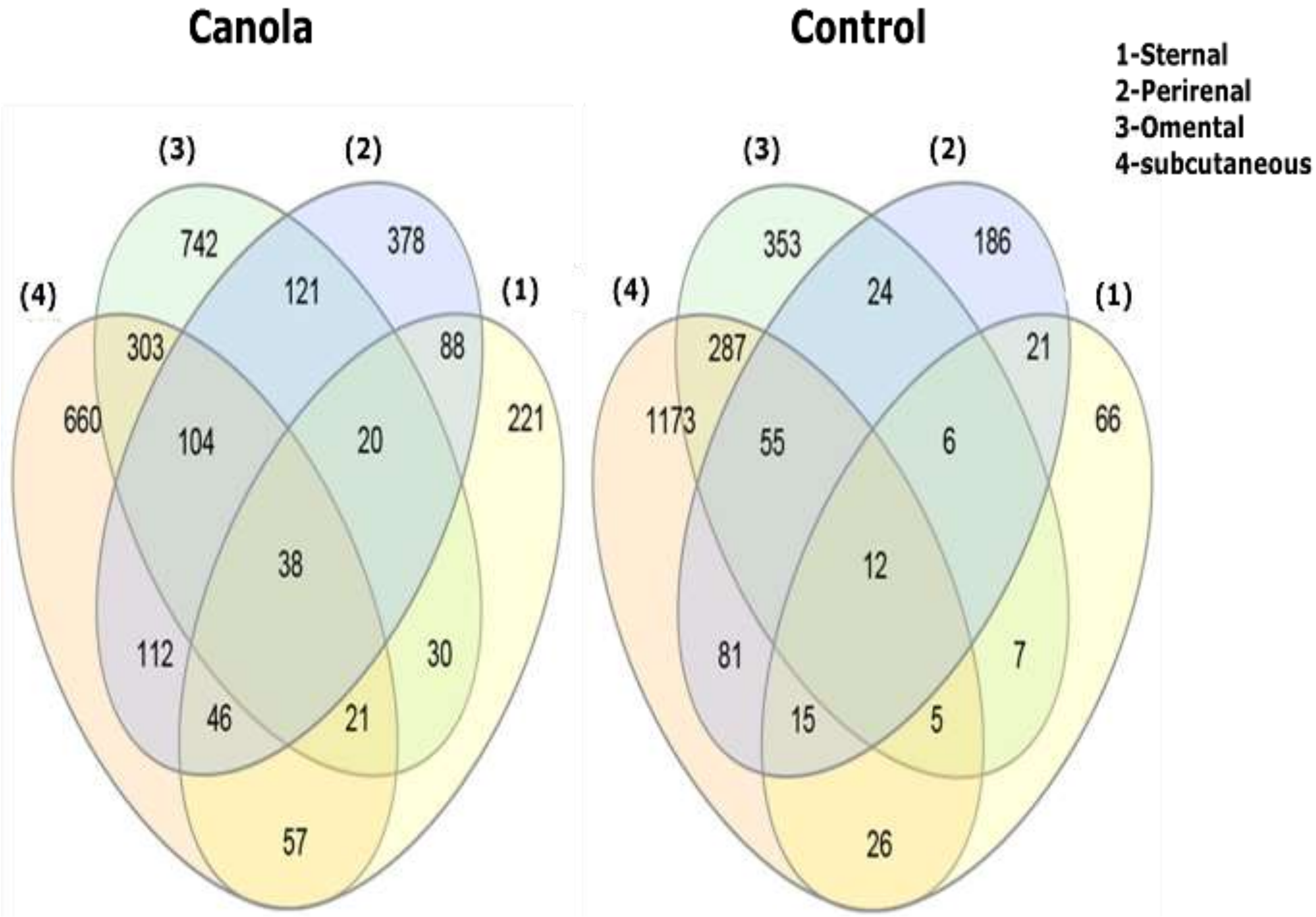

Figure 6-6: Four-way Venn diagram showing comparison of canola and control significant genes expressed amongst all examined depots

Venn diagram was generated for four adipose tissue depots extracted from lambs at seven and 28 days with overlapping circles, each of which represents a gene set significantly expressed (adjusted p-value < 0.05) within the same depot in the two dietary groups; control (4148 genes) or canola (2961 genes). The number of genes expressed uniquely in one set is located close to the sides of the circles whereas the numbers of genes expressed commonly among sets are located in the overlapping areas.

As a further comparison, the Venn diagram shows that the dietary intervention resulted in a different degree of gene expression transformation when independently compared with the control group. For example, the results indicate that the 7 to 28-day-old diet group (canola) had a reduction in the expression profile compared with the control group in three tested depots respectively (sternal 158-521; perineal 401-907; omental 740-1,379). On the other hand, subcutaneous fat was the only tissue that increased the number of significant genes in the canola group (1,654 genes) when compared with the control (1,341 genes). In addition, the results indicate that sternal depot was highly shifted in the gene expression profile after canola treatment, as it retained the minimum number of the common genes between the dietary intervention and control groups when compared with other tested depots independently; for example, sternal (78 genes), perirenal (196 genes), omental (368 genes) and subcutaneous (693 genes) (see Figure 6-7).

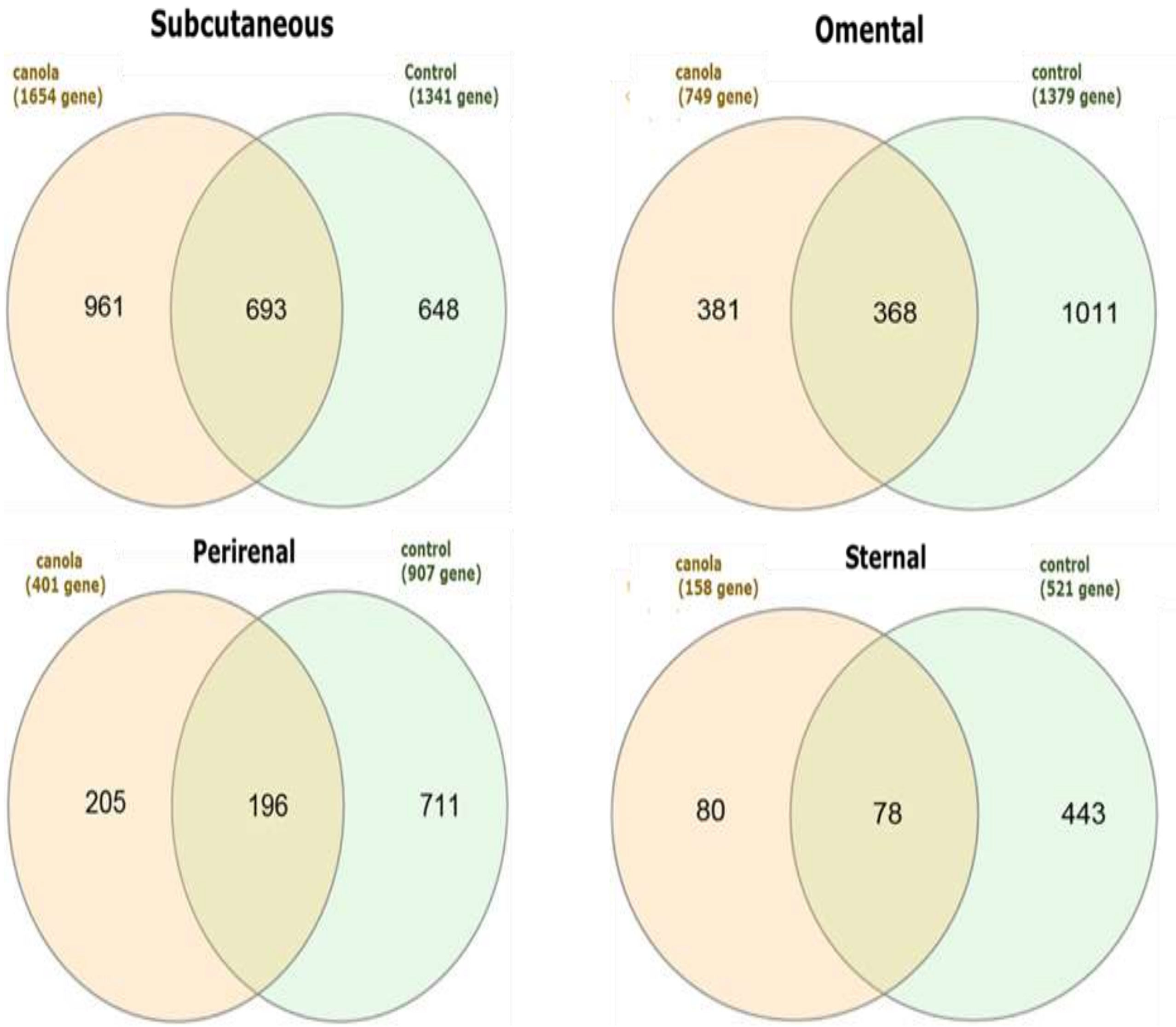

Figure 6-7: Venn diagram summary of the difference in the number of significant gene expressions between the canola and control groups in each tested depot

Venn diagram was generated for four adipose tissue depots extracted from lambs at 7 and 28 day with overlapping circles, each of which represents a gene set significantly expressed (adjusted p-value < 0.05), within the same depot in two dietary groups. The number of genes expressed uniquely in one set is located close to the sides of the circles whereas the numbers of genes expressed commonly among sets are located in the overlapping areas.

6.4.3 Transformation in offspring adipose tissue function after maternal dietary treatment with canola oil

Overall, the GO enrichment analysis indicated that 87 biological processes were significantly different ($q < 0.05$) in the control group between the depots with age, compared to 55 biological processes in the canola group. The main finding was that fat from the control group exhibited more mitochondrial, functional genes (down-regulated) that were related to the ATP process, when compared with the canola, including mitochondrial respiratory chain complex I assembly, mitochondrial ATP synthesis and tricarboxylic acid cycle (see Table 6-1).For instance, the mitochondrial ATP synthesis coupled with proton transport biological processes showed that 10 genes were expressed by canola compared with 12 in controls(see Tables 6-4 and 6-5). Furthermore, the KEEG Pathway results in Figure 6-9 confirmed that a different number of genes were involved in oxidative phosphorylation pathways (28 genes) in the canola group, while in the controls 42 genes were significantly expressed.

Table 6-1: Difference in gene expression of ATP metabolic process in all examined depots between canola diet and control group from 7 to 28 days of age

Biological Process	Gene Ref	Number of Genes in Control	Number of Genes in Canola	Q-value
mitochondrial ATP synthesis coupled proton transport	21	12	10	1.57E-07
tricarboxylic acid cycle	31	13	8	1.78E-03
mitochondrial electron transport, NADH to ubiquinone	49	15	9	5.41E-03
ATP hydrolysis coupled cation transmembrane transport	58	10	9	5.18E-03
mitochondrial respiratory chain complex I assembly	65	17	10	2.04E-02
ATP metabolic process	204	40	24	2.04E-02

Table 6-2: Genes significantly expressed in the mitochondrial ATP synthesis process from the control depots group

Rank	Gene symbol	Gene name
1	ATP5A1	ATP synthase subunit alpha, mitochondrial
2	ATP5G1	ATP synthase F(0) complex subunit C1, mitochondrial
3	COX5B	Cytochrome c oxidase subunit 5B, mitochondrial
4	ATP5C1	ATP synthase subunit gamma, mitochondrial
5	ATP5H	ATP synthase subunit d, mitochondrial
6	ATP5G2	ATP synthase F(0) complex subunit C2, mitochondrial
7	STOML2	Stomatin-like protein 2, mitochondrial
8	ATP5L	ATP synthase subunit g, mitochondrial
9	ATP5G3	ATP synthase F(0) complex subunit C3, mitochondrial
10	ATP5B	ATP synthase subunit beta, mitochondrial
11	ATP5E	ATP synthase subunit epsilon, mitochondrial
12	CYC1	Cytochrome c1, heme protein, mitochondrial

Table 6-3: Genes significantly expressed in the mitochondrial ATP synthesis process in the canola group

Rank	Gene symbol	Gene name
1	ATP5A1	ATP synthase subunit alpha, mitochondrial
2	ATP5G1	ATP synthase F(0) complex subunit C1, mitochondrial
3	COX5B	Cytochrome c oxidase subunit 5B, mitochondrial
4	ATP5C1	ATP synthase subunit gamma, mitochondrial
5	ATP5G2	ATP synthase F(0) complex subunit C2, mitochondrial
6	STOML2	Stomatin-like protein 2, mitochondrial
7	ATP5L	ATP synthase subunit g, mitochondrial
8	ATP5G3	ATP synthase F(0) complex subunit C3, mitochondrial
9	ATP5B	ATP synthase subunit beta, mitochondrial
10	CYC1	Cytochrome c1, heme protein, mitochondrial

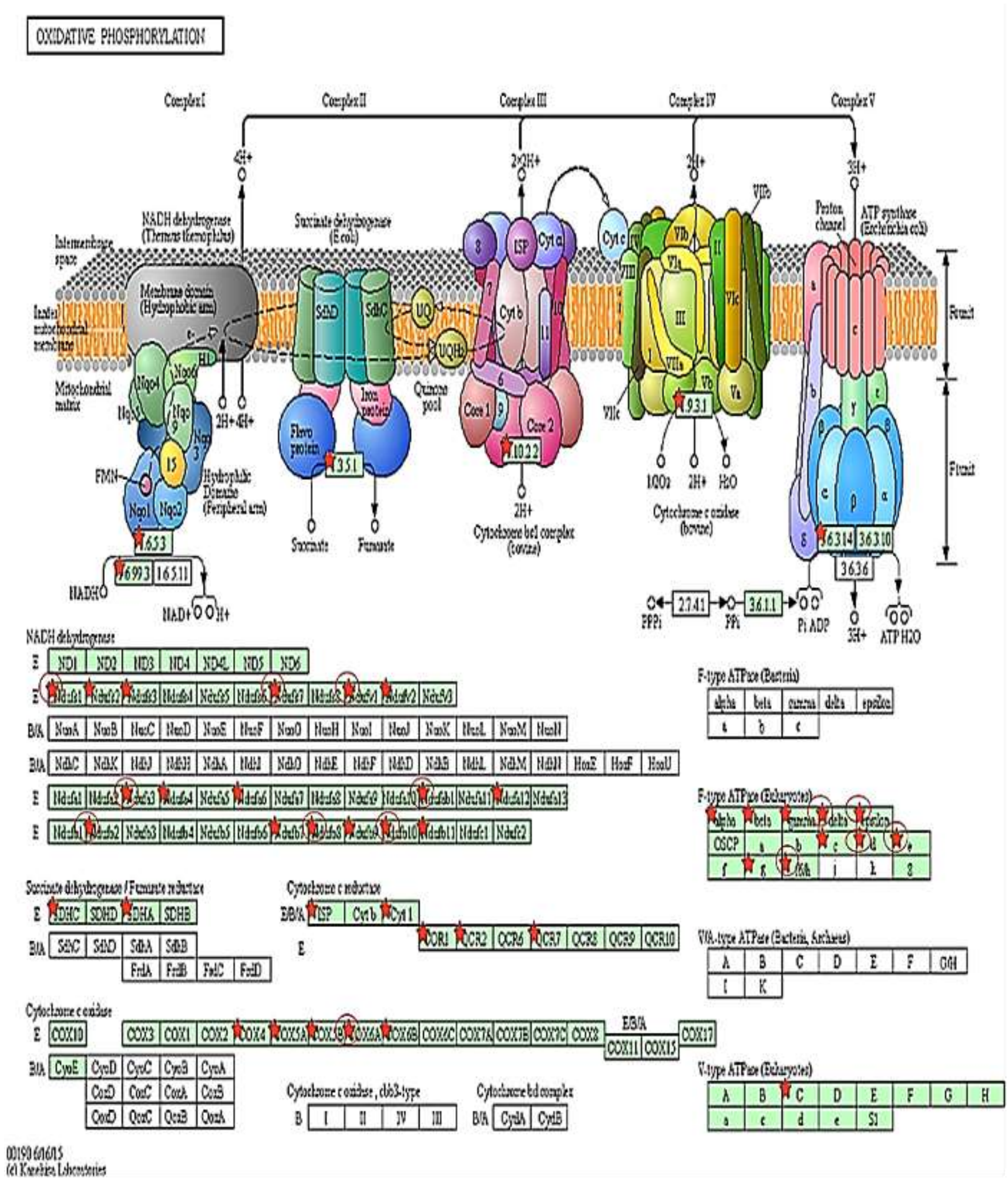

Figure 6-8: Summary of the genes involved in the oxidative phosphorylation pathway

Genes that are significantly expressed are indicted by a red star symbol (42 genes), while the red star with circle indicates those genes that have not changed after adding canola to the diet (29 genes).

6.4.4 Use of machine learning and gene network analysis in young sheep adipose tissues with maternal diet intervention

The results of the gene pattern and enrichment analysis indicate that all four examined depots in the canola group exhibited a different function and level of down-regulation in the mitochondrial metabolic genes when compared with controls. Therefore, the aim was to characterise the different metabolic functions, including ATP metabolic gene expressions, in each examined depot independently by using gene networks to compare the effect of dietary intervention on gene network in comparison with controls (see Chapter 2 for more details about the methods).

To translate the gene terms and define the biological functions of each module the different module numbers of each depot were identified (perirenal: 18 modules; sternal: 27 modules; omental: 18 modules; and subcutaneous: 16 modules)

The gene networks show that most of the examined depots were generally characterised by up-regulated gene expression, which are specified in the regulation of cell differentiation metabolic processes from 7-28 days: for instance, perirenal light steel blue: 505 genes,;sternal dark orange: 43 genes; omental light pink: 285 genes; subcutaneous brown: 657 genes; as well as in response to potential stimuli such as endocrine: perirenal blue: 596 genes; sternal turquoise: 330 genes; omental light cyan: 1,300 genes; subcutaneous white: 1,053 genes. On the other hand, ATP metabolic process modules were down-regulated with age: for example, perirenal back: 177 genes; sternal dark turquoise: 82 genes; omental tan: 97 genes; subcutaneous light steal blue: 276 genes.

The main finding was that the canola diet decreased the number of expressed gene lists in different biological function modules across three depots; perirenal, sternal and omental when compared with the control group. For example, in the control group, cell differentiation biological function (perirenal green 530 genes; sternal pink: 203 genes; omental bisque: 734 genes) in response to the stimulus (perirenal turquoise: 814 genes; sternal turquoise: 877 genes; omental purple: 1,937 genes) as well as the ATP module (perirenal blue: 328 genes; sternal blue: 512 genes; omental black: 80 genes). However, the only depot that followed a different pattern was subcutaneous as the canola diet increased the number of genes expressed in cell differentiation in response to the stimulus and the ATP metabolic respectively (blue module: 550 genes; turquoise: 814 genes; light steal blue: 117 genes) (see figures 6-10 to 6-18 and tables 6-6 to 6-13).

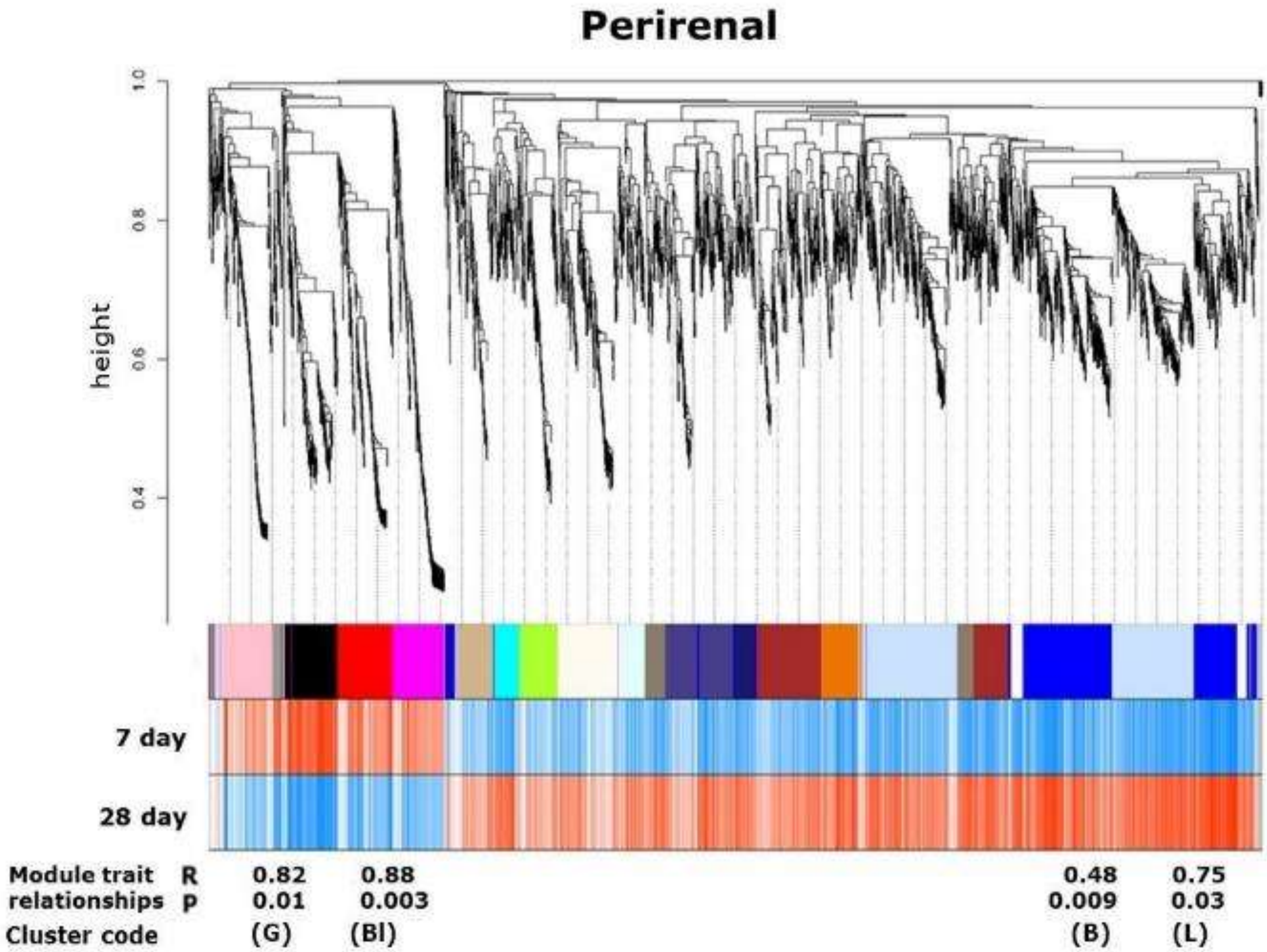

Figure 6-9: Co-expression dendrogram analysis for perirenal fat depot sampled from young sheep whose mothers' diet was supplemented with canola at seven and 28 days of age

The first row is subdivided into co-expressed modules founded in each age group. The other two rows (below) show the differential expression relationships between module genes and the adipose depot. The relationship of each gene with the assigned module is colour-coded from blue (negative co-expression) to red (positive co-expression). Module trait relationships represent the correlation R (and corresponding p-values) among co-expressed clusters which are coded by letters in the fat depot.

Table 6-4: Summary of the top four significant biological enrichment processes in the perirenal depot supplemented with canola oil within co-expressed gene modules from 7 to 28 days of age

Module	Number of genes	Biological process	Q-Value
Lightstealblue (L)	505	Cell differentiation	6.73E-03
Blue (B)	596	Response to stimulus	3.28E-03
Black (Bl)	177	ATP metabolic process	9.42E-04
Grey (G)	30	Ribosome mitochondrial translational	7.45E-02

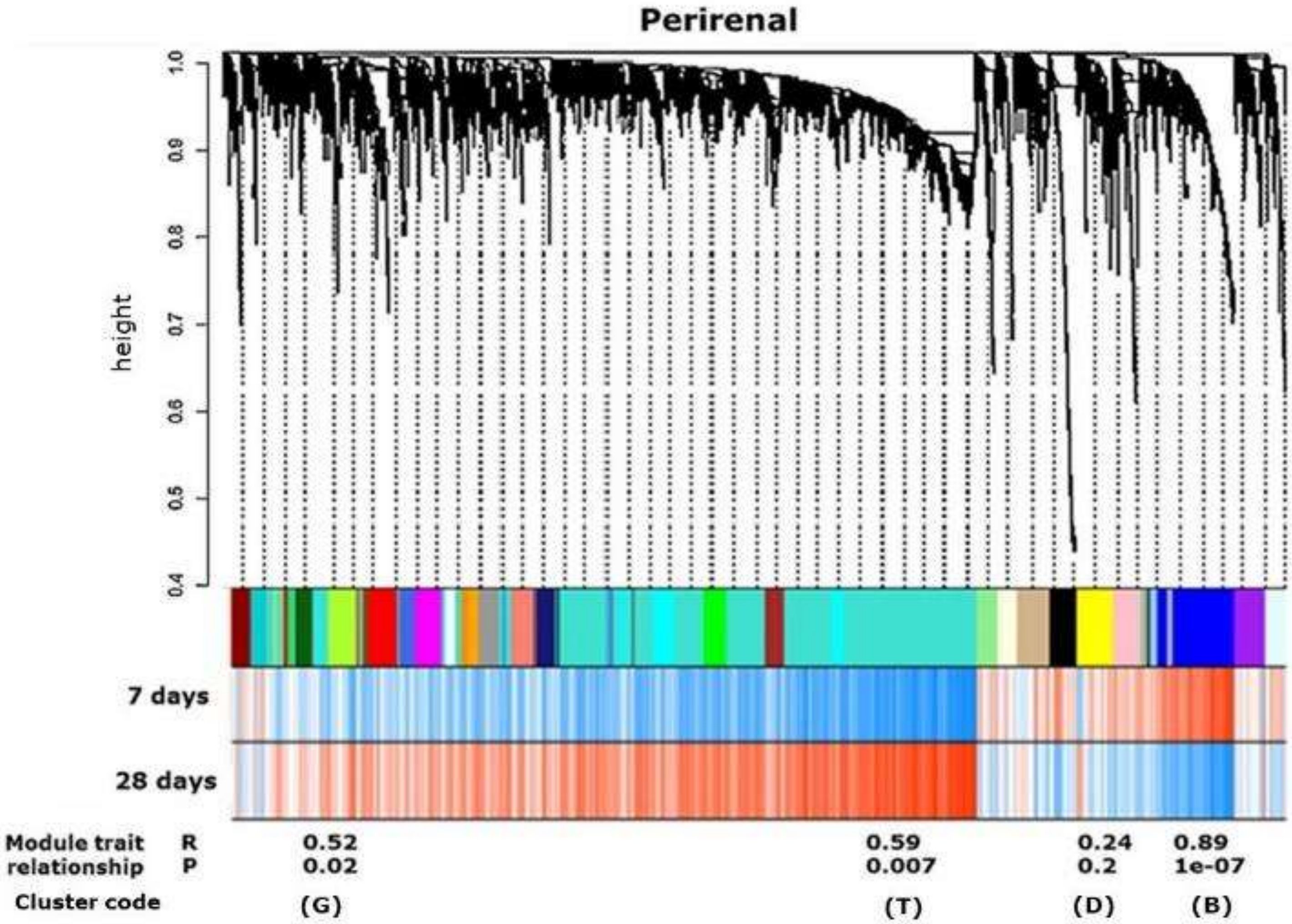

Figure 6-10: Co-expression dendrogram analysis for perirenal fat depot sampled at seven and 28 days of age

The first row is subdivided into co-expressed modules founded in each age group. The other two rows (below) show the differential expression relationships between module genes and the adipose depot. The relationship of each gene with the assigned module is colour-coded from blue (negative co-expression) to red (positive co-expression). Module trait relationships represent the correlation R (and corresponding p-values) among co-expressed clusters which are coded by letters in the fat depot.

Table 6-5: Summary of the top four significant biological enrichment processes in the perirenal depot within co-expressed gene modules at 7 and 28 days of age

Module	Number of genes	Biological process	Q-Value
Green (G)	530	Cell differentiation	1.43E-02
Turquoise (T)	814	Response to stimulus	7.40E-06
Blue (B)	328	ATP metabolic process	3.10E-07
Dark grey (D)	78	Ribosome mitochondrial translational	2.30E-03

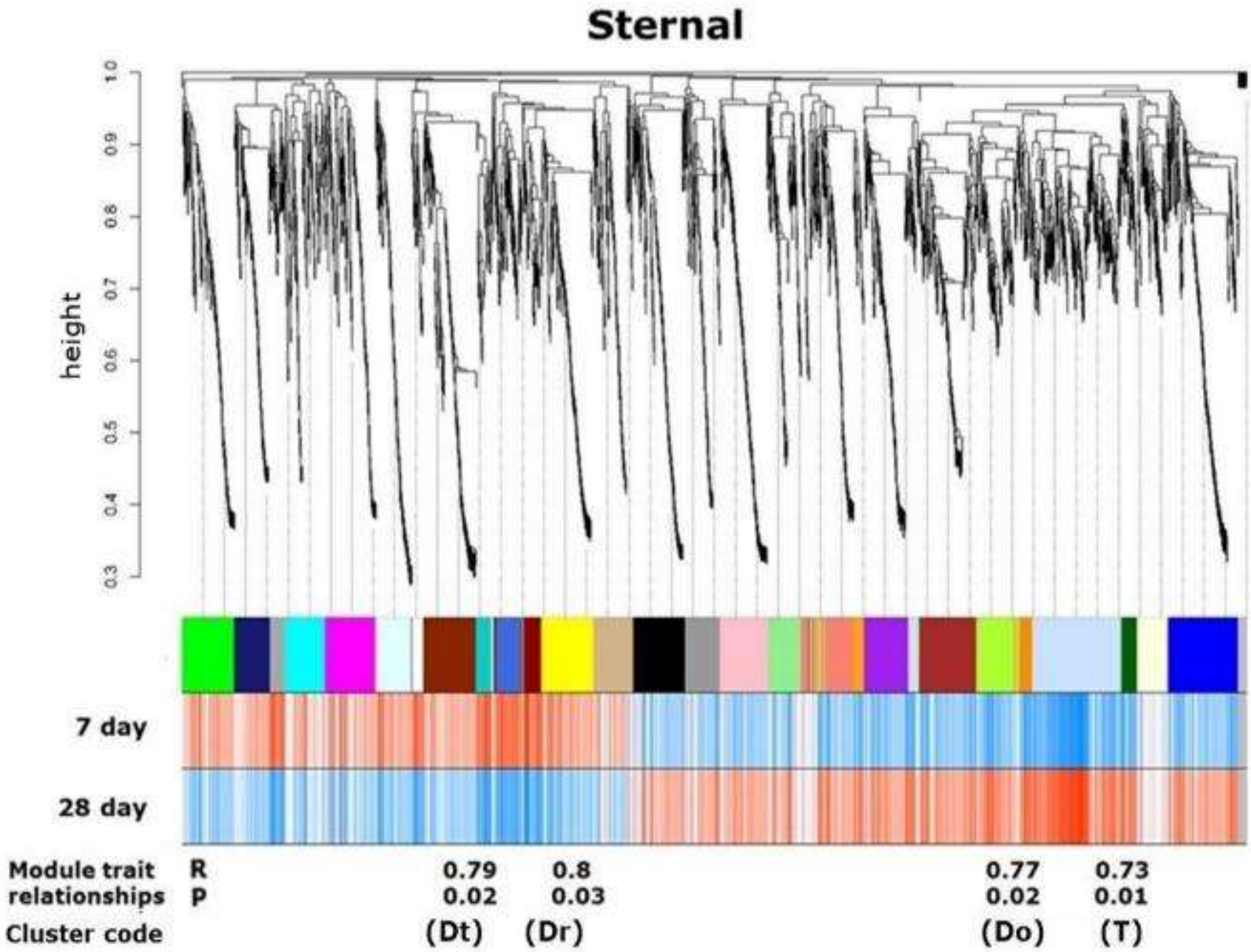

Figure 6-11: Co-expression dendrogram analysis for sternal fat depot supplemented with canola at seven and 28 days of age

The first row is subdivided into co-expressed modules founded in each age group. The other two rows (below) show the differential expression relationships between module genes and the adipose depot. The relationship of each gene with the assigned module is colour-coded from blue (negative co-expression) to red (positive co-expression). Module trait relationships represent the correlation R (and corresponding p-values) among co-expressed clusters which are coded by letters in the fat depot.

Table 6-6: Summary of the top four significant biological enrichment processes in the sternal depot supplemented with canola oil within the co-expressed gene modules at 7 and 28 days of age

Module	Number of genes	Biological process	Q- Value
Dark orange (Do)	43	Cell differentiation	7.30E-08
Turquoise (T)	330	Response to stimulus	1.27E-03
Dark turquoise (Dt)	49	ATP metabolic process	7.94E-03
Dark red (Dr)	65	Ribosome mitochondrial translational	1.09E-04

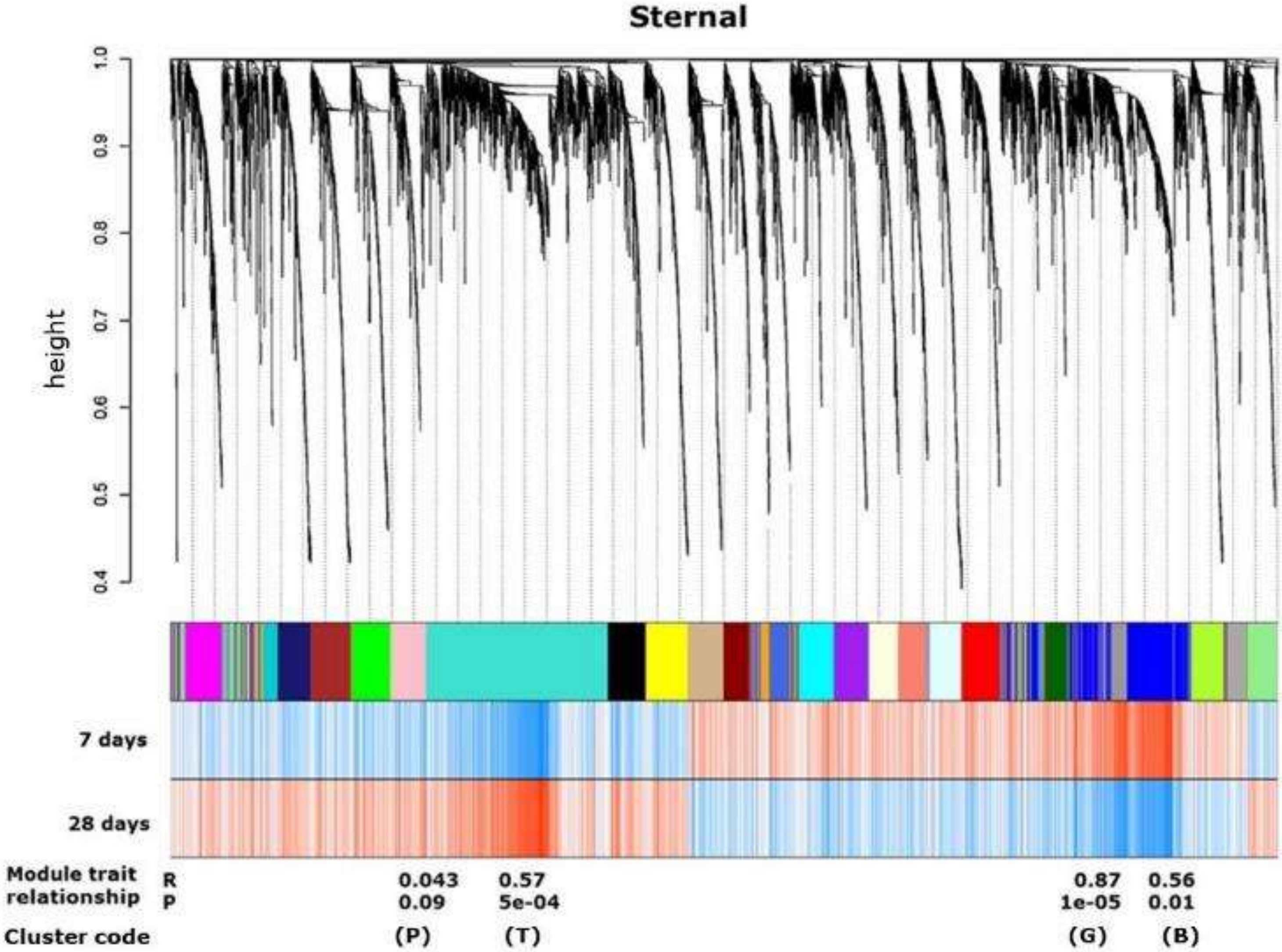

Figure 6-12: Co-expression dendrogram analysis for sternal fat depot sampled at seven and 28 days of age

The first row is subdivided into co-expressed modules founded in each age group. The other two rows (below) show the differential expression relationships between module genes and the adipose depot. The relationship of each gene with the assigned module is colour-coded from blue (negative co-expression) to red (positive co-expression). Module trait relationships represent the correlation R (and corresponding p-values) among co-expressed clusters which are coded by letters in the fat depot.

Table 6-7: Summary of the top four significant biological enrichment processes in the sternal depot within the co-expressed gene modules at 7 and 28 days of age

Module	Number of genes	Biological process	Q-Value
Pink (P)	203	Cell differentiation	4.10E-02
Turquoise (T)	877	Response to stimulus	7.40E-06
Blue (B)	512	ATP metabolic process	3.15E-04
Grey (G)	134	Ribosome mitochondrial translational	7.28E-22

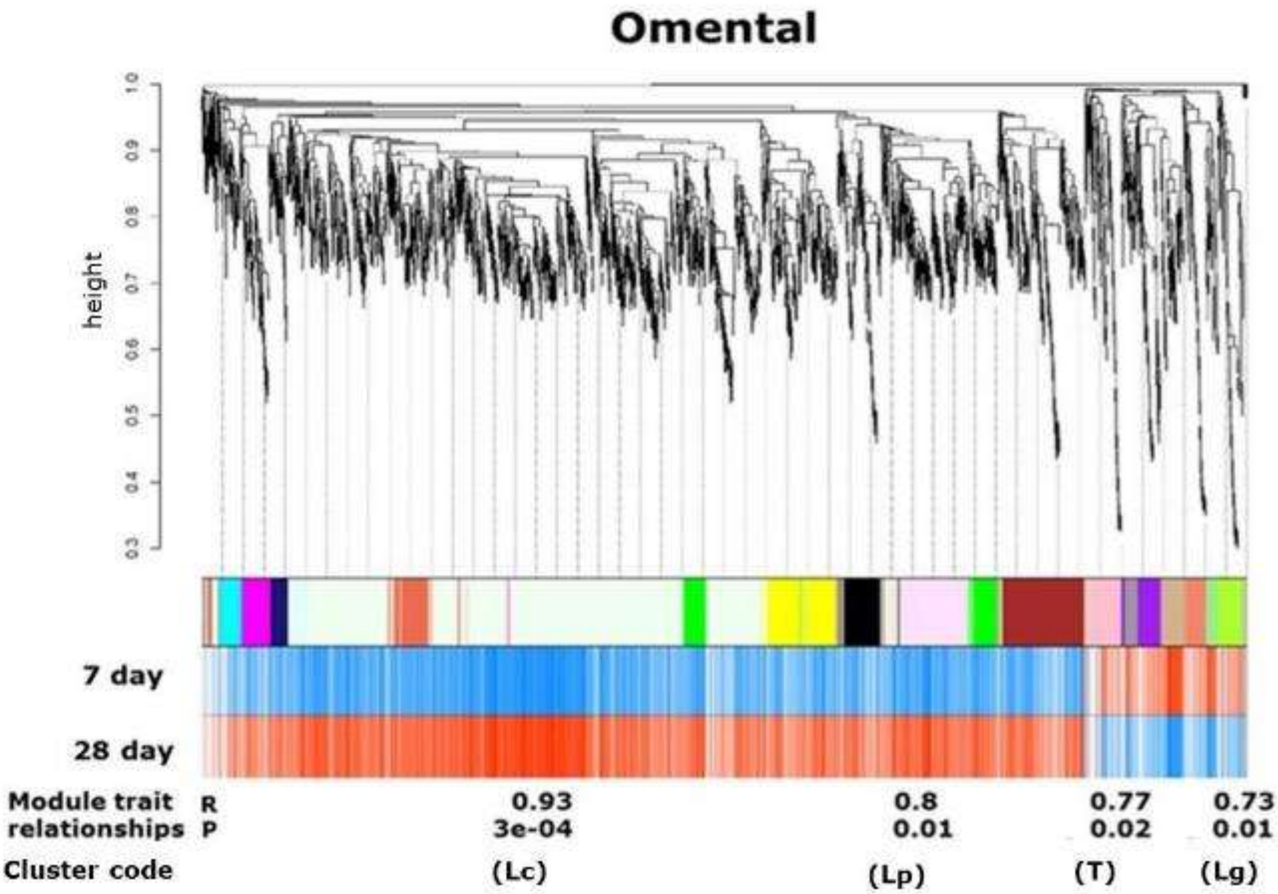

Figure 6-13: Co-expression dendrogram analysis for omental fat depot supplemented with canola at seven and 28 days of age

The first row is subdivided into co-expressed modules founded in each age group. The other two rows (below) show the differential expression relationships between module genes and the adipose depot. The relationship of each gene with the assigned module is colour-coded from blue (negative co-expression) to red (positive co-expression). Module trait relationships represent the correlation R (and corresponding p-values) among co-expressed clusters which are coded by letters in the fat depot.

Table 6-8: Summary of the top four significant biological enrichment processes in the omental depot supplemented with canola oil within co-expressed gene modules at 7 and 28 days of age

Module	Number of genes	Biological process	Q- Value
Light pink (Lp)	285	Cell differentiation	1.15E-02
Light cyan (Lc)	1,300	Response to stimulus	8.65E-03
Tan (T)	97	ATP metabolic	4.45E-03
Light green (Lg)	42	Ribosome mitochondrial translational	2.1 E-03

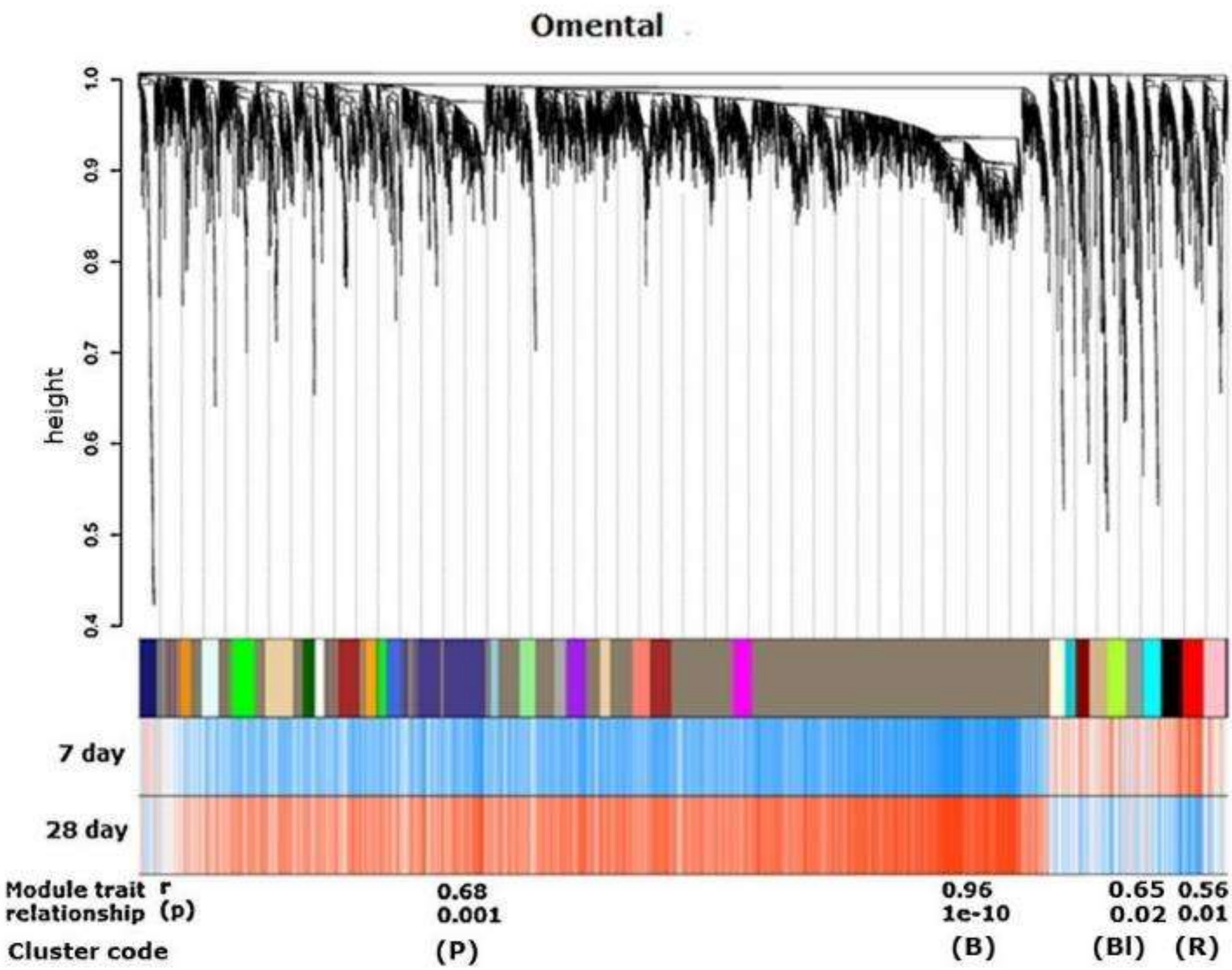

Figure 6-14: Co-expression dendrogram analysis for omental fat depot sampled at seven and 28 days of age

The first row is subdivided into co-expressed modules founded in each age group. The other two rows (below) show the differential expression relationships between module genes and the adipose depot. The relationship of each gene with the assigned module is colour-coded from blue (negative co-expression) to red (positive co-expression). Module trait relationships represent the correlation R (and corresponding p-values) among co-expressed clusters which are coded by letters in the fat depot.

Table 6-9: Summary of the top four significant biological enrichment processes in the omental depot within the co-expressed gene module at 7 and 28 days of age

Module	Number of genes	Biological process	Q-Value
Purple (P)	734	Cell differentiation	4.98E-06
Bisque (B)	1937	Response to stimulus	7.20E-05
Black (Bl)	80	ATP metabolic process	2.80E-06
Red (R)	104	Ribosome mitochondrial translational	2.60E-03

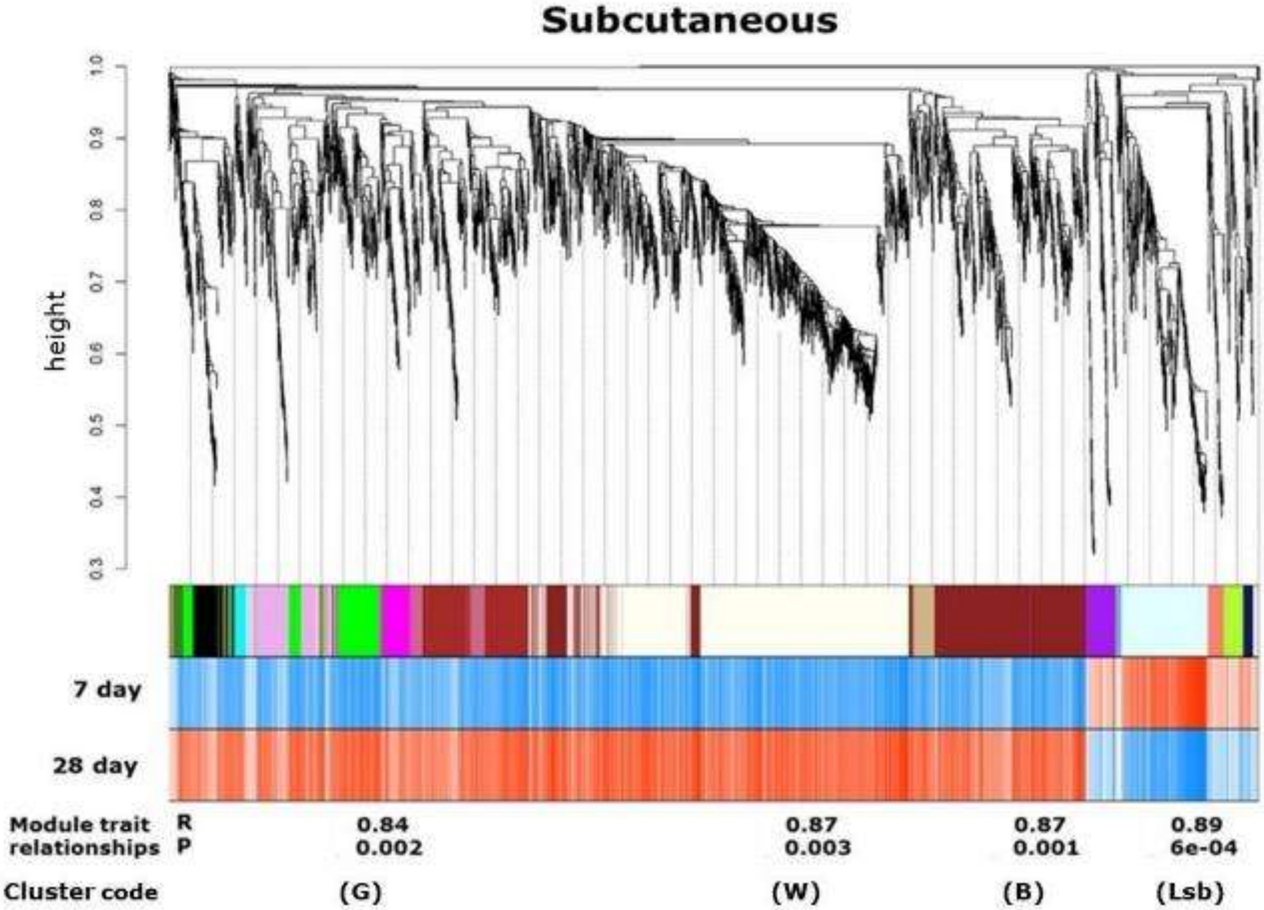

Figure 6-15: Co-expression dendrogram analysis for subcutaneous fat depot supplemented with canola at seven and 28 days of age

The first row is subdivided into co-expressed modules founded in each age group. The other two rows (below) show the differential expression relationships between module genes and the adipose depot. The relationship of each gene with the assigned module is colour-coded from blue (negative co-expression) to red (positive co-expression). Module trait relationships represent the correlation R (and corresponding p-values) among co-expressed clusters which are coded by letters in the fat depot.

Table 6-10: Summary of the top four significant biological enrichment processes in the subcutaneous depot supplemented with canola oil within co-expressed gene modules at 7 and 28 days of age

Module	Number of genes	Biological process	Q- Value
Brown (B)	657	Cell differentiation	1.90E-02
White (W)	1053	Response to stimulus	5.82E-06
Green (G)	237	Cell cycle	3.93E-06
Light steel blue (Lsb)	276	ATP metabolic and Muscle cell differentiation	3.66E-04

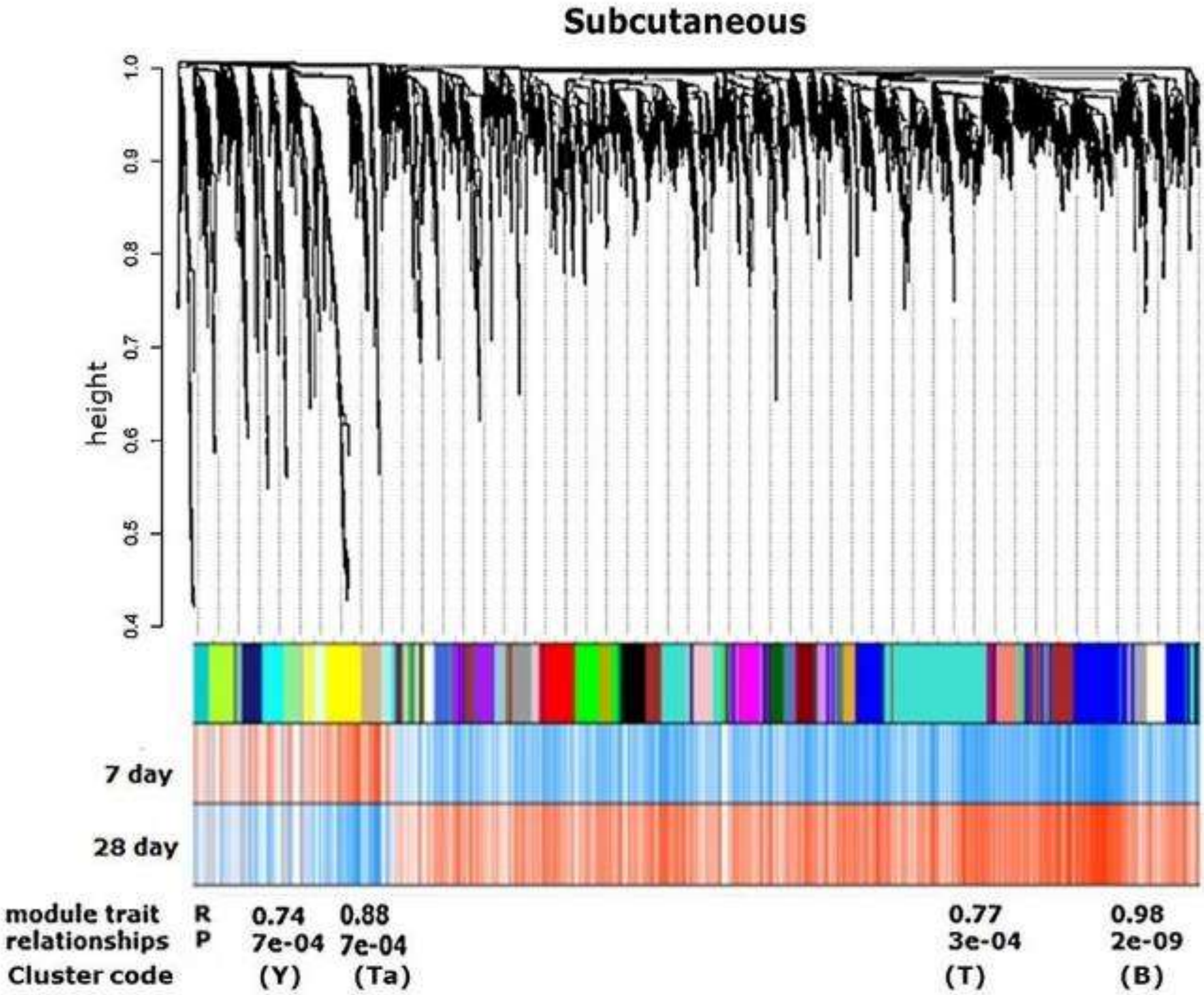

Figure 6-16: Co-expression dendrogram analysis for subcutaneous fat depot sampled at seven and 28 days of age

The first row is subdivided into co-expressed modules founded in each age group. The other two rows (below) show the differential expression relationships between module genes and the adipose depot. The relationship of each gene with the assigned module is colour-coded from blue (negative co-expression) to red (positive co-expression). Module trait relationships represent the correlation R (and corresponding p-values) among co-expressed clusters which are coded by letters in the fat depot.

Table 6-11: Summary of the top four significant biological enrichment processes in the subcutaneous depot within co-expressed genes modules at 7 and 28 days of age

Module	Number of genes	Biological process	Q- Value
Blue (B)	550	Cell cycle and differentiation	4.10E-03
Turquoise (T)	814	Response to stimulus	5.80E-04
Tan (Ta)	117	ATP metabolic process	3.10E-05
Yellow (Y)	166	Muscle cell differentiation	2.67E-02

6.4.5 UCP1 clustering comparison in weighted gene co-expression network analysis

In the next step of the study, the focus was on mitochondrial function genes, particularly UCP1, which was selected as the critical gene for comparison between depots since a down-regulation of UCP1 during development has already been reported (Henry et al., 2017; Pope et al., 2014; Symonds et al., 2012). In addition to UCP1, other genes were also studied to determine whether additional processes, besides energy utilisation, were affected. UCP1 was detected in two of the four tested depots (sternal and perirenal), which are primarily populated by brown adipocytes (Table 6-12). Therefore, a Venn diagram was created to show the different UCP1 modules and the gene list of pro-thermogenic depots between the diet intervention and control group from 7 to 28 days. The Venn diagram in Figure 6-17A shows the presence of bigger mitochondria genes clusters in the control group (blue perirenal: 328 genes; blue sternal: 512 genes) when compared with the canola group (black perirenal: 177 genes; dark turquoise sternal: 49 genes). In addition, the Venn diagrams in Figure 6-17B and C show that each cluster expressed a different set of genes in the canola and control groups during development within the same depots respectively (black perirenal canola: 61 genes; blue perirenal control: 328 genes), as well as sternal (dark turquoise sternal canola: 32 genes; blue sternal control: 495 genes). However, the analysis demonstrates that few genes were shared among the two depot groups (canola/control) regarding the ATP module depots (nine genes), including UCP1 (see table 6-12).

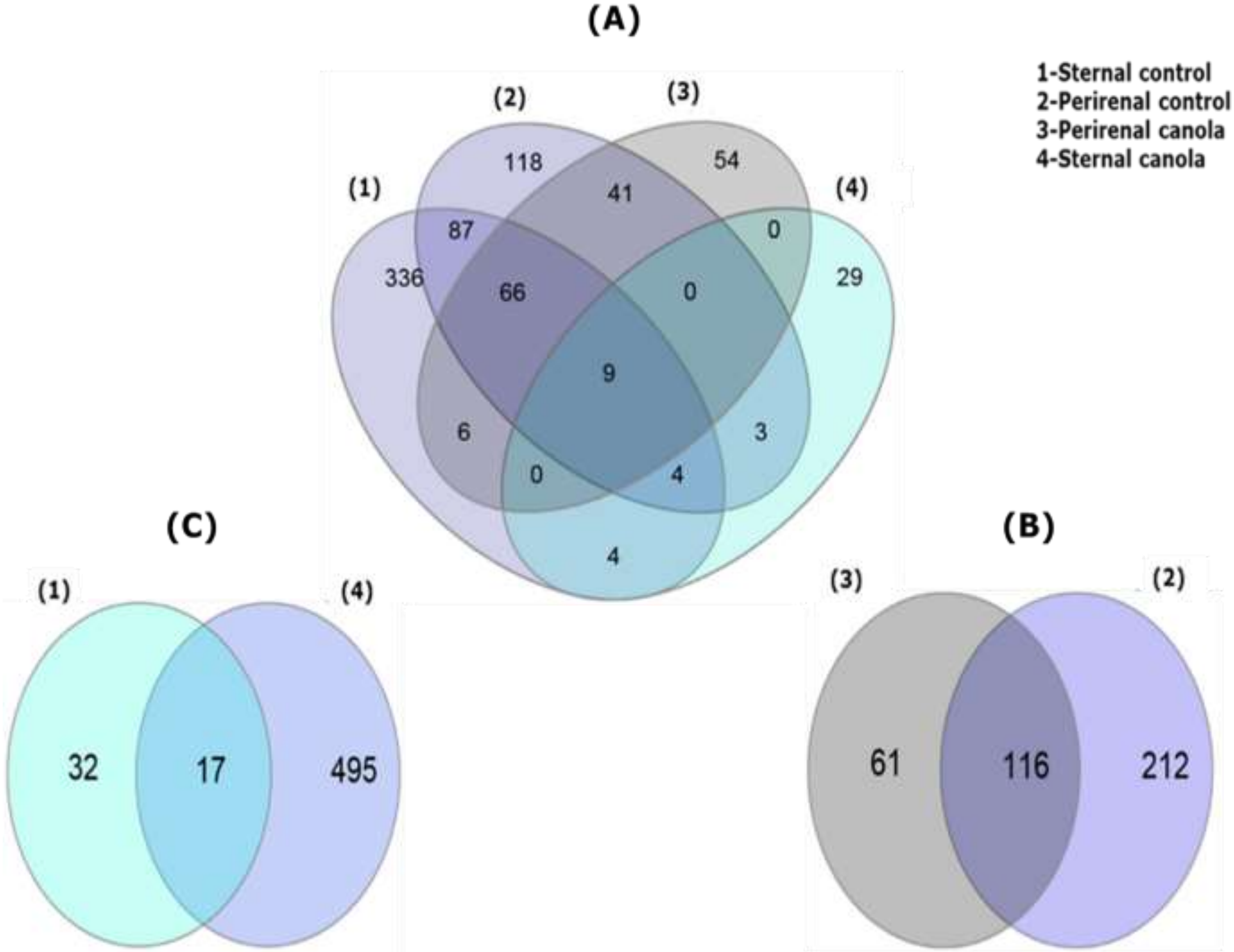

Figure 6-17: Venn diagram showing a comparison of the UCP1 module interaction between the canola and control groups

(A) UCP1 module interaction between the two depots (sternal and perirenal) comparing the two dietary groups (control and canola) at two time points (seven and 28 days of age).
(B) represents the UCP1 module interaction between canola and control groups of perirenal depot.
(C) represents the UCP1 module interaction in sternal depot between canola and control groups. Each circle represents the number of genes set within specific depots, with an overlap of the sharing gene with other depots. Control group: (1) sternal blue and (2) perirenal blue; canola group (3) perirenal black and (4) sternal turquoise.

Table 6-12: Commonly expressed genes in comparison of the UCP1 cluster in two supplemented depots; perirenal (P) and sternal (S)

Symbol	Gene name	Average expression in supplemented samples	Average expression in control samples	Q-value
CDC27	cell division cycle 27	5.61	5.36	2.76E-05
USP2	ubiquitin specific peptidase 2	3.90	5.06	3.63E-05
UCP1	uncoupling protein 1 (mitochondrial, proton carrier)	3.10	4.79	1.82E-04
CSRP2	cysteine and glycine rich protein 2	4.88	7.70	3.05E-04
TMEM126A	transmembrane protein 126A	4.23	5.69	4.01E-04
EIF3I	eukaryotic translation initiation factor 3 subunit I	8.10	6.77	4.77E-04
PSME3	proteasome activator subunit 3	7.13	4.06	1.55E-03
CISD1	CDGSH iron sulphur domain 1	5.55	3.35	2.55E-03
PGP	phosphoglycolate phosphatase	6.26	3.22	4.22E-03

6.4.6 Effects of maternal canola oil supplementation in sheep on offspring lipid profile in the first month of lactation

At 7 days and 28 days of age, I undertook a lipidomic evaluation of perirenal and sternal fat depots in the progeny of mothers fed with the 3% canola oil additive. The analysis as carried out to identify the effect of different transcription transformation between the fat depots. At 7 days of age, there was no effect of the anatomical location or the diet intervention on the lipid profile of the sternal and perirenal depots (Figure 6-18 and Figure 6-19A). However, a significant impact of the anatomical location was found at 28 days of age between sternal and perirenal (28 lipids) (Figure 6-18B). In addition, perirenal fat undergoes a detectable localised change at 28 days of age after maternal diet supplemented with canola oil (31 lipids) (Figure 6-20B). From those lipids that were significantly modified, I were able to identify 10 lipids that were different between the two tested depots (sternal and perirenal) at 28 days of age (Table 6-15) and 11 lipids in the perirenal depot after maternal diet supplemented with canola oil (Table 6-16) based on the accurate mass determination by the Lipid Maps databases (Pollard et al., 2017; Ortori et al., 2014) (see section 2.3).

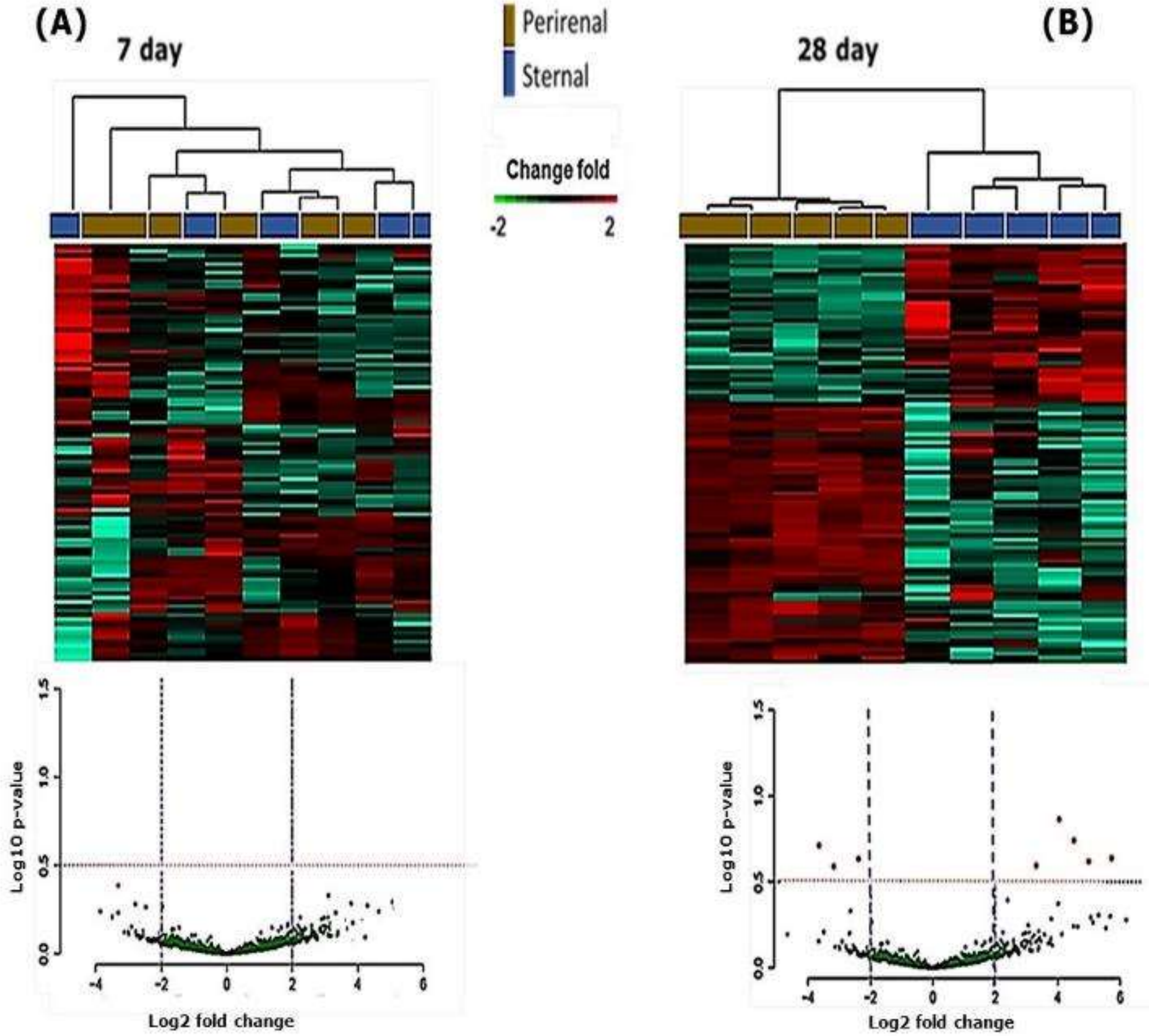

Figure 6-18: Lipid profile comparison of two fat depots, sternal and perirenal, at seven days (A) and 28 days (B)

The heat map and unsupervised hierarchical clustering dendograms for the top 100 lipids that were divergent to the others are illustrated. The analysis was performed by average linkage, Euclidean distance metric analysis. Selection was done through eBayes t-statistic (FDR < 0.05). Green and red denote decrease and increase of lipid expression respectively. The colour code defines the tissue to which it belongs. Volcano plots under the heat map representing the changes in sheep adipose tissue lipids profile at the same time point, with the log of the FDR-adjusted probability values (q-value; y-axis) plotted against the log fold changes (x-axis) between the tested adipose tissues. The lipids that were expressed significantly differently in the sample are represented by the solid red circle, and those that did not express significantly differently are coloured green.

Table 6-13: Variation of lipid content between sternal and perirenal depots at 28 days of age

Lipid symbol	Formula	Fold change	Q-value
TG(48:3)	C53H95O8	6.21	4.60E-04
TG(50:3)	C55H99O8	3.77	1.79E-03
PC(O-40:4)	C48H94N2O7P	3.76	2.54E-03
TG(47:6)	C50H85O6	4.02	1.33E-02
PA (O-45:0)	C48H97O7PNa	6.96	1.51E-02
PA(49:0)	C52H102O8P	5.48	1.51E-02
TG(50:6)	C55H93O8	4.34	1.56E-02
Cer (d40:0)	C42H84NO5	5.11	1.56E-02
FA(18:0(OH3,Ke2,Ep2,cyclo)	C18H27O9	-1.82	1.66E-02
Cer (t42:0)	C44H88NO6	3.44	1.66E-02

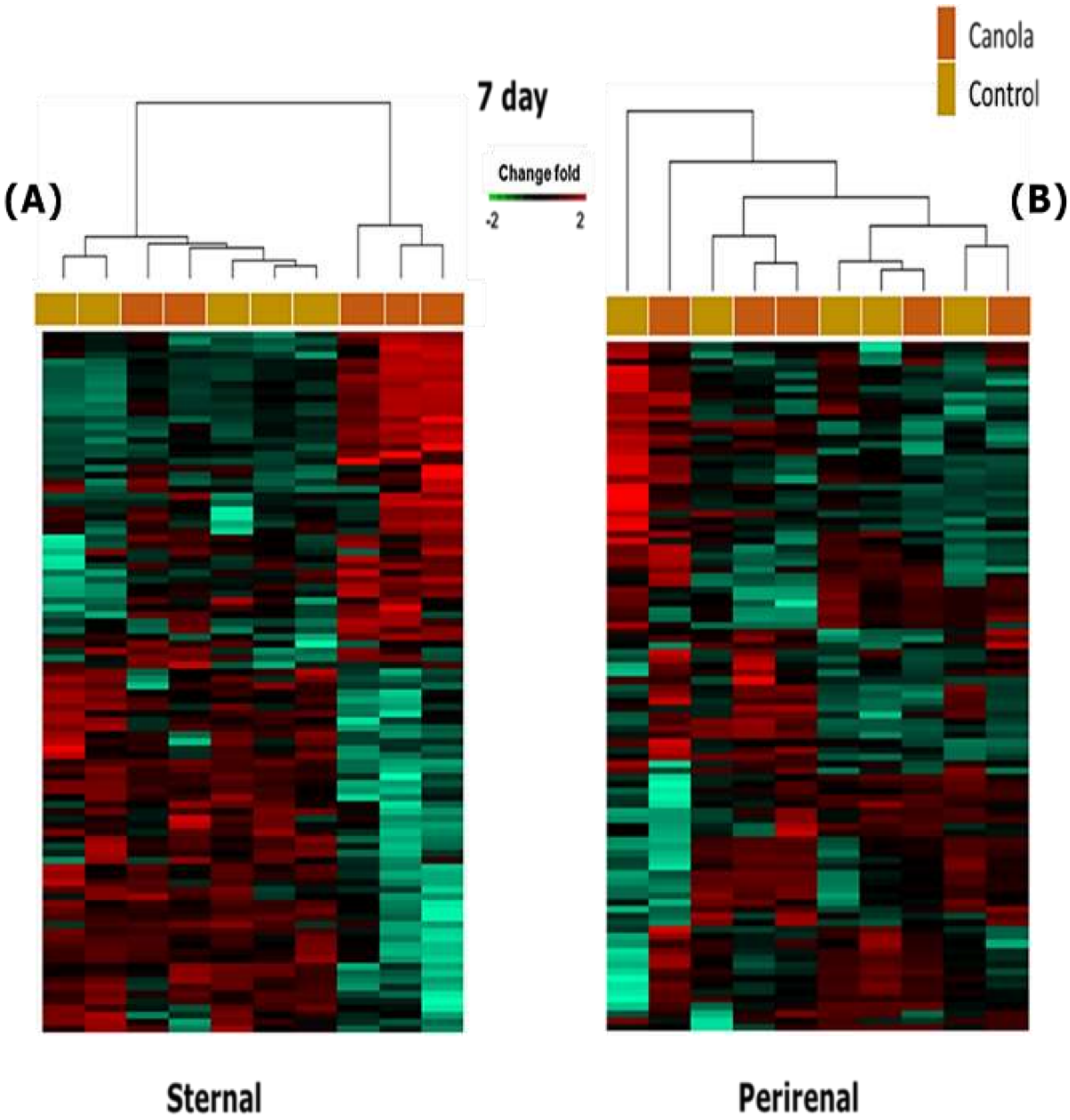

Figure 6-19: Between-group lipid profile comparison of samples in diet intervention group (orange), and control group (gold), in two fat depots (A) Sternal, (B) Perirenal at seven days of age

Heat map and unsupervised hierarchical clustering dendrograms for the top 100 lipids that were divergent to the others are illustrated. The analysis was performed by average linkage, Euclidean distance metric analysis. Selection was done through eBayes t-statistic (FDR < 0.05). Green and red denote decrease and increase of lipid expression respectively. The colour code defines the tissue to which it belongs.

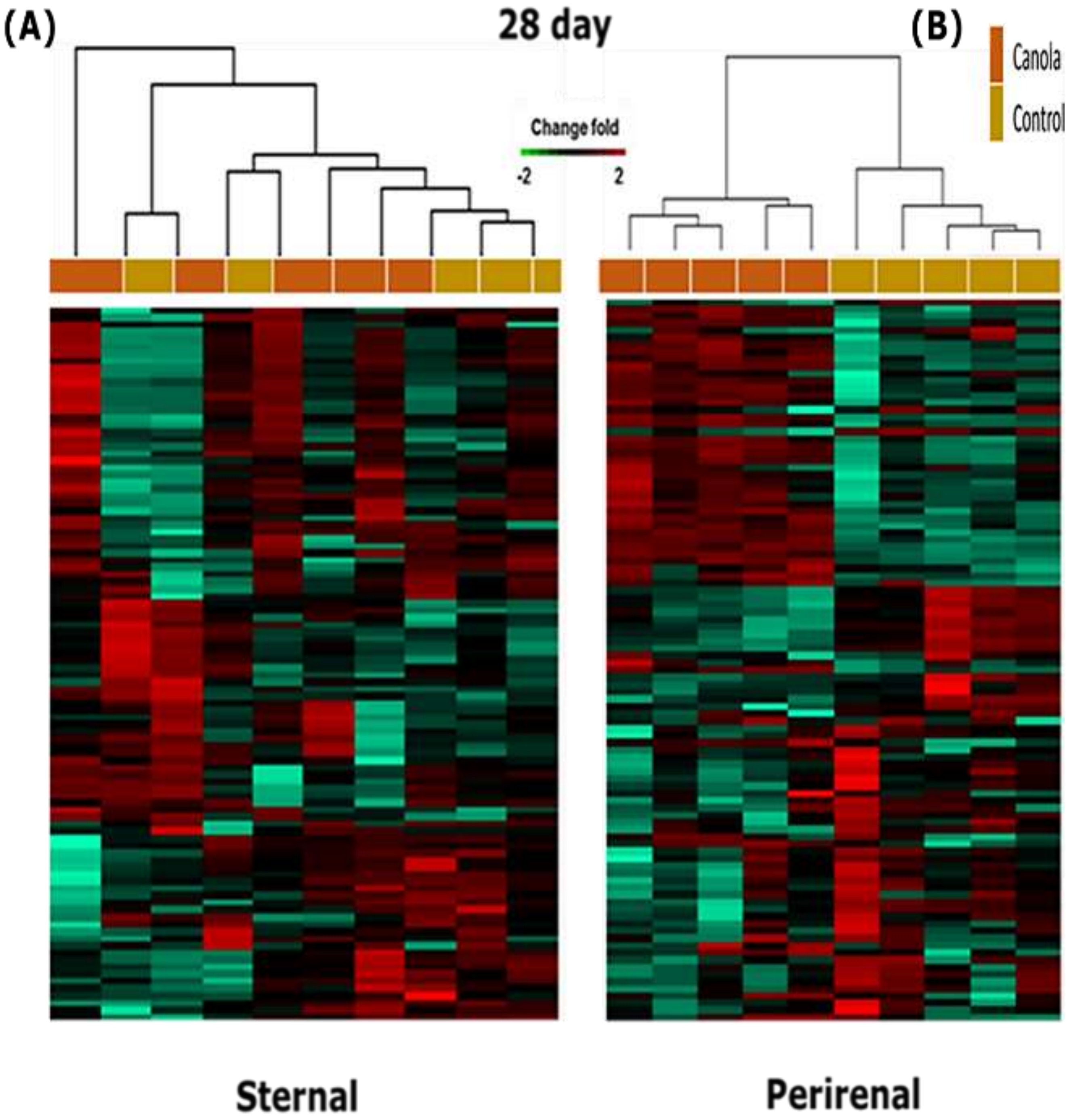

Figure 6-20: Between-group lipid profile comparison of samples in diet intervention group (orange), and control group (gold), of two fat depots (A) Sternal, (B) Perirenal at 28 days of age

Heat map and unsupervised hierarchical clustering dendrograms for the top 100 lipids that were divergent to the others are illustrated. The analysis was performed by average linkage, Euclidean distance metric analysis. Selection was done through eBayes t-statistic (FDR < 0.05). Green and red denote decrease and increase of lipid expression respectively. The colour code defines the tissue to which it belongs.

Table 6-14: Change in lipid composition of perirenal depot between control and diet intervention at 28 days of age

Symbol	Common name	Q-value
LysoSM (d18:0)	Lysosphingomyelins a	0.00
FA(22:3)	docosatrienoic acid	0.01
PS(35:0)	1-octadecanoyl-2-hexadecanoyl-sn-glycerol	0.01
FA(18:0(Ep2))	octadecenoic acid	0.01
DG(34:0)	Diradylglycerols	0.01
FA(17:0(Ep,cyclo))	heptadecadienoic acid	0.01
DG(59:6)	Diradylglycerols	0.02
FA(22:4)	Adrenic Acid	0.04
Cer(d28:1)	N-hexacosanoylglycine	0.04
LPG(28:0)	Phosphtatidylglycerols	0.04
MGDG(64:12)	Monogalactosyldiacylgylcerols	0.04

The nutritional intervention resulted in substantial alterations in the lipid content of the perirenal adipose tissue. There was a reduction in the quantity of fatty acid content including polyunsaturated fatty acids; for example, omega-6 Adrenic acid FA (22:4) and omega-3 docosatetraenoic acid FA (22:3), which are considerably lower than the non-intervention ratios (see Figure 6-21). The sternal adipose tissue, however, showed no change in lipid composition following the nutritional intervention. Generally, the results I obtained from microarray analysis and lipid profiling demonstrated that dietary intervention only initiated a response in the perirenal fat depot. It is important to note that when assessing the genes that were most significantly affected, there was an accentuation of the influence of the glucocorticoid receptor, Nuclear Receptor Subfamily 3 Group C Member 1 (NR3C1) gene, which is directly involved in cellular differentiation, proliferation and promotion of inflammatory response (Lu et al., 2006). Based on these results, it can be concluded that the perirenal fat depot responds to maternal nutritional intervention and undergoes remodelling in the cellular structure.

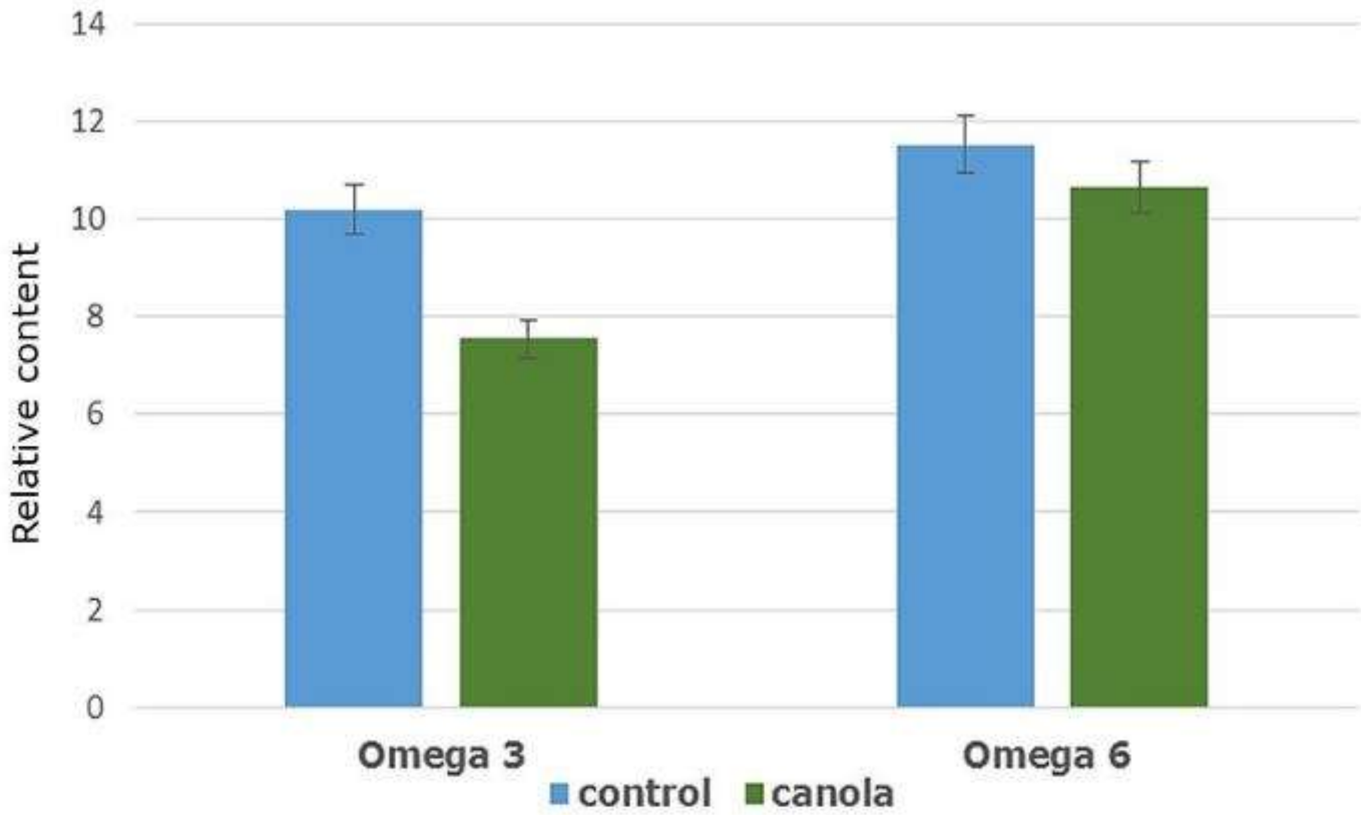

Figure 6-21: Polyunsaturated fatty acid (PUFA) omega 3 and omega 6 content at 28 days in control and diet intervention perirenal depot

6.5 Discussion

Adipose tissue is an essential metabolic structure responsible for maintaining the homeostatic milieu of the body (Cypess and Kahn, 2010), regulating both energy balance and lipid metabolism (Ali et al., 2013; Coelho, et al., 2013). The present study evaluated the effect of a maternal canola dietary intervention on adipose tissue development in early life, since there is existing evidence of brown to white adipose tissue transdifferentiation (Montanari et al., 2017). Four different fat depots — perirenal, sternal, omental and subcutaneous — were included in the study, and the effect of canola intervention was assessed from 7 to 28 days of development. The focus of this investigation was to identify changes in gene expression patterns (i.e. up- or down-regulation) of unique and shared genes, and the related biological processes, by using machine learning methods, including weighted gene co-expression, during a critical development phase. Each of the major fat depots was found to utilise different mechanisms and genes. As outlined in the results section, several conventional and unique mechanisms were identified across the fat depots, which could explain diet intervention changes in thermogenesis and mitochondria energy utilisation that occur in adipose tissue over time.

6.5.1 Differences in biological function after canola oil treatment from 7 to 28 days

The current study highlights critical differences and similarities between the different fat depots studied; such investigations have also been conducted in different species including in humans (Virtanen et al., 2009; Vergnes et al., 2016)**.** in particular, **c**Changes in the gene expression and subsequent biological processes at different stages and phases of development (specifically 7 and 28 days) have been documented in sheep (Fainberg et al., 2018; Basse et al., 2015, Henry et al., 2017). There are also reports in the existing literature where dietary intervention, such as increasing total fat intake in female mice, resulted in substantial differences in gene expression in BAT; specifically, an increase in the Oxidative phosphorylation (OXPHOS) mitochondrial genes (Lettieri Barbato et al., 2015). However, in the current study, overall gene expression was found to be different between 7 and 28 days for both the control and canola treatment groups; differences were also observed between the fat depots independently. For example, a minor degree of transformation in the expression of the gene profile was observed in the treatment group when compared with the controls from the same period (7 to 28 days) in perirenal, omental and sternal tissues, while the opposite effect was observed in subcutaneous depots. The difference in gene expression after fatty acid dietary interventions has also been investigated and reported in the published literature (Fainberg et al., 2018; Welter et al., 2016), which further validates the findings reported in this study.

Another important observation of this study was that at both 7 days and at 28 days, the number of genes that were common between the control and canola treatment groups was low, with a high number of unique genes featuring individually in each group, suggesting that biological function, including energy utilisation and metabolism, shifts in different directions with and without dietary fatty acid intervention, as observed in the published literature (Lim et al., 2013; Welter et al., 2016).

In further investigations regarding the differences in the unique gene expression and biological functions of the control groups, I noted those genes involved in multiple functions including ATP synthesis, mitochondrial respiratory chains, the citric acid cycle, transcriptional, hormonal regulation, and skeletal muscle function. Conversely, the unique genes of the canola treatment groups were observed as necessary for the modulation maintenance of the extracellular matrix and pre-mRNA processing, as well as in transport and cell cycle regulation.

The unique sets of gene expression between the control and canola treatment groups further support the activation of different processes. Modular analysis of gene expression in the various fat depots studied also indicated a different thermogenic transition pattern associated with energy utilisation amongst the depots, with only the sternal fat depot behaving as an outlier since it was relatively stable when compared with other depots. It can be inferred that, in addition to changes caused by dietary fat intervention, there is also a temporal change associated with different anatomical locations and age.

6.5.2 Impact of dietary intervention on the ATP metabolic process in adipose tissue

Although studies that have examined gene expression differences across all brown fat depots across the body in the same study are limited, individual investigations have been conducted for separate fat depots (Gesta et al., 2007; Symonds, 2013). An analysis of gene expression patterns between different adipose tissue fat depots, with and without treatment with canola oil, has not been previously reported, and indicates not only the unique nature of the current study, but the fact that dietary intervention with fatty acids, particularly canola oil, could result in gene expression differences in a depot-specific manner.

Previous studies have reported that mitochondrial ATP production is dependent on the electron transport chain (ETC) (Bratic and Trifunovic, 2010). The down-regulation in mitochondrial ATP is linked with the ageing process of cells (Bratic and Trifunovic, 2010), and past authors have focused on age-related changes in mitochondrial functionality (Bratic and Trifunovic, 2010). The findings of the current study show that the genes associated with ATP synthesis enzymes (e.g., Citrate cycle enzymes (TCA), ETC enzymes etc.) were more down-regulated in the control group when compared to the canola treatment group between 7 to 28 days. For example, two ATP genes variants (ATP5H and ATP5E) were noted as being down-expressed in the control group only, thus indicating metabolic energy differences in the presence or absence of dietary fats. The lower expression of genes regulating energy metabolism (Dahlman et al., 2005) suggests a definite link between rearrangements that are associated with mitochondria and the activation of the BAT (Gao and Houtkooper, 2014). It is this that probably accounts for the difference between control and canola treatment groups. However, when fatty acids are supplemented externally, this obviates the need for de novo lipogenesis and, therefore, also explains the reason for the observed difference between groups (Pénicaud et al., 2000). KEGG pathway analysis also confirms differences between control and canola treatment groups, as noted by differences in the number of expressed genes for oxidative phosphorylation genes; these are higher in the control group than in the canola treatment group. The inclusion of unsaturated dietary fats such as polyunsaturated fatty acids (PUFAs) (Sampath and Ntambi, 2005) and MUFAs (Lim et al., 2013) has resulted in a shift in gene expression (Welter et al., 2016; Sparks et al., 2005). In the present study, changes were noted in genes associated with ATP synthesis, genes involved in NADH to ubiquinone step, TCA cycle enzymes, genes involved in respiratory chain complex I assembly and genes involved in ATP metabolism.

6.5.3 Impact of canola diet intervention on UCP1 gene clustering in weighted gene co-expression network analysis

Early postnatal life (days 7–28) is highly critical in the regulation of the growth of fat depots, particularly their ability to maintain UCP1 (Symonds, 2013). UCP1 expression in perirenal and sternal brown fat depots displays a unique thermogenic pattern (Henry et al., 2017; Symonds et al., 2015). A high concentration of brown adipocytes in these tissues and such tissue-specific expression has been documented by investigators in other mammals (Restelli et al., 2015; Soppela et al., 1991). The importance of UCP1 in brown fat depots is vital for the maintenance of body temperature in newborn infants since protons shunt short-circuits in the ETC and an enhanced thermogenic capacity (Cannon et al., 1981, Cannon and Nedergaard, 2004).

It has been found that supplementing lactating and pregnant rats with a rich MUFAs diet such as canola oil could increase UCP1 in BAT in offspring and decrease weight gain (Lim et al., 2013). Additionally, the inclusion of canola oil in dairy ruminants' feed has been reported to reduce the omega 3 and omega 6 fatty acid ratio in milk, both of which are properties that have been found to up-regulate UCP1 gene in adipose tissue (Welter et al., 2016)

My WGCNA analysis indicates the presence of other thermogenic genes besides UCP1, thus showing changes and a complex interaction in pathways after adding canola to the maternal diet. All the additional genes identified were noted as crucial for mitochondrial function, adding support to similar published findings concerned with dietary fat intervention (Inokuma et al., 2005). The existence of multiple interactions between UCP1 and other genes is suggestive of a complex pathway of thermogenic responses that are mounted during infancy (Gilsanz et al., 2013).

Also in this module, and particularly in perirenal adipose tissue, up-regulation of PPARG gene expression was observed, which is critical for adipocyte differentiation and the facilitation of glucose uptake (Jones et al., 2005; Nolte et al., 1998). In addition, after canola oil supplementation I noted a reduction in white adipocyte differentiation genes; for example, HOX group gene, including homeobox B8 HOXB6, (HOXB8) and homeobox B6 (HOXB6) (Rivellese et al., 2002), which indicates that adding canola oil decreases white adipocyte differentiation, at least in the perirenal depot.

On other hand, my data demonstrate that adding canola oil could prevent the decline of PPARG 1 beta (PPARGC1B) expression in one of the tested depots (i.e. sternal), which could stimulate PPARGC1A (Ryan et al., 2000) and initiates a shifting in the oxidative fatty acid and BAT thermogenic functionality (Lim et al., 2013) since this is a crucial pathway for thermogenesis (Cannon and Nedergaard, 2004), and could further enhance lipid metabolism and utilisation (Tierney and Roche, 2007).

6.5.4 Impact of maternal canola dietary supplementation on transcriptional regulatory and biological responses within adipose tissue

Numerous studies have investigated the role of external stimuli in affecting negative, positive responses in different anatomical locations of brown fat (Kajimura et al., 2016). It is well established that heat, cold, and endocrine stimuli can affect brown fat (van Marken Lichtenbelt et al., 2009). Some of these stimuli include hypolipidemic agents to reduce fat depot size by directly increasing mitochondrial function (Bjorndal et al., 2011), endocrine stimulation of thermogenesis, including hypothalamic influences (Labbe et al., 2015) and the effect of cold stress on thermogenesis (Rosell et al., 2014).

In both brown and white fat depots studied, it was observed that adding canola oil to perineal, sternal and omental depots displayed a decrease in gene functional responses to stimuli such as endocrine and external stimulus. Even within these fat depots, the decrease was highest in the sternal depot, followed by omental and prerenal depots. However, the reverse response was observed in subcutaneous fat. This difference in response between each tested depot could be due to the additional factors outlined in the section above, such as tissue-specific location, which could be affected by the nutritional environment (Symonds et al., 2015) or nearby endocrine organs such as the adrenals (Fainberg et al., 2017) or thyroid (Vergnes et al., 2016).

The decrease in the gene expression and function of response to an external and internal stimulus, such as cold temperature (Symonds, 2013) or hormone stimulation (Maslov and Vychuzhanova, 2016), could impair fatty acid oxidation and thermogenesis specifically in brown adipocytes. Moreover, several ATP-related genes which also have an immune function, such as Voltage-dependent anion-selective channel (VDAC1), Eukaryotic translation initiation factor 1 (EIF1) and Solute Carrier Family 12 Member 4 (SLC12A4) (Kiecolt-Glaser, 2010), were not found to be significantly expressed in the canola group, which supports published findings on dietary fat affecting genes modulating during stress (Das et al., 2017; Renaud et al., 2014). Furthermore, other studies found that different types of response to a stimulus such as prolonged cold exposure in rodents (Welter et al., 2016) and severe burn injuries in humans (Cannon et al., 1981), could play a role in brown adipocyte differentiation.

Another finding is that adding canola oil could contribute to improved glucose homeostasis and insulin sensitivity, as specific genes were enriched only in the canola group including up-regulation of the beta-arrestin-1 (ARRB1) gene in perirenal (Ravier et al., 2014, Dalle et al., 2011), hypoxia-inducible factor 1-alpha (HIF1A) in omental (Pope et al., 2014), and dynein light chain 1, cytoplasmic (DLC1) in subcutaneous fat (Hong et al., 2018). Overall, this suggests that these functions are ongoing and that they change during the intervention phases of adipose tissue, and could lead to an increase in adipocyte size and development (Symonds et al., 2012).

6.5.5 Canola oil induces insulin sensitivity in white adipose tissue

In the adipose tissue of sheep, it has been identified that manipulating the diet in lactating ewes results in a significant change in glucose and insulin metabolic processes in the progeny (Sebert et al., 2009; Symonds et al., 2012). For example, a similar finding has been observed in human beings, in which a high MUFAs nutritional intervention diet intensifies sensitivity of insulin (Rivellese et al., 2002; Tierney and Roche, 2007). Numerous studies have been conducted to assess the effect of high oleic acid diet such as canola oil on insulin resistance (Ryan et al., 2000). Rigorous and extensive research is also being carried out to determine the interactions between gene expression, insulin sensitivity and fat content. Nuclear receptors associated with binds in fatty acids established a distinct function in gene and fatty acid regulation (Göttlicher et al., 1992; Sampath and Ntambi, 2005; Georgiadi and Kersten, 2012). More particularly, the omega 6 and omega 3 fatty acids have been identified to initiate the response and activity of PPAR nuclear receptor proteins (Clarke, 2001, Rodriguez et al., 1994), which play a vital role in cell differentiation and glucose uptake, as discussed in section 6.5.3 (Jones et al., 2005; Nolte et al., 1998).

In this study, I identified the enrichment of the insulin sensitivity pathway in the WAT of progeny subjected to ~3% of canola oil nutritional intervention in the maternal diet. I also determined that some genes that were in involved in the insulin signalling and energy homeostasis are up-regulated, including PPARG, also called the NR1C3 receptor (Soriguer et al., 2006), AKT Serine/Threonine Kinase 2 (AKT2) (George et al., 2004, Cho et al., 2001), natriuretic peptide receptor 1 (NPR1) (Wu et al., 2017) all of which are involved in enhancing sensitivity to insulin in white adipose tissue in mice.

Adipocytes with UCP1 deficiency (or lack of) have been observed to use glycolytic pathways rather than lipolysis in the production of ATP and the promotion of uncoupled respiratory response (Himms-Hagen, 1990; Ma and Foster, 1986; Grimpo et al., 2014). However, PPAR treatment of the multipotent mesenchymal stem cells resulted in the activation of white adipose tissue cells (Mezentseva et al., 2008). I achieved a parallel result whereby glucose uptake and energy use of the progeny's WAT were enhanced by canola oil nutritional intervention in maternal milk.

6.5.6 Impact of adding canola oil to the maternal diet on cell differentiation (adipogenesis) gene expression in adipose tissue

From my analysis, a significant change in adipose tissue plasticity can be expected to occur between 7 and 28 days due to cell differentiation. Past literature has shown that adipose tissue differs with age regarding cell differentiation and energy metabolism (Ojha et al., 2016). Increased adipocyte differentiation was found to be the primary cause of the differences in the level of brown fat transdifferentiation to white in all depots (Rosen et al., 2009). Reduction in the expression of cell differentiation-related genes is corroborated by reports of dietary fat interventions affecting fat depot micro-environments, which in turn affects cell differentiation (Jeffery et al., 2016).

Like the observation in the previous section, canola oil impacted adversely on cell differentiation genes, as they were found to be higher in the control group for sternal, omental and perirenal fat depots respectively. On the other hand, subcutaneous fat showed the opposite response. For example, in omental and subcutaneous depots I noted a comparative decrease in the expression of crucial muscle chain proteins, such as myosin light chain 2 (MYL2), myosin light chain

1 (MYL1), myosin, heavy chain 4, skeletal muscle (MYH4), and myosin, heavy chain 8, skeletal muscle (MYH8) (Vicente-Manzanares et al., 2009, Adams et al., 2013, Asp et al., 2011). Unlike the other two depots, i.e. sternal and perirenal, which are classified as brown depots, that developed from muscle precursor cells (Sharma et al., 2014), and distinguish with the capability of enhancing lipid metabolism and energy expenditure capacity (Gesta et al., 2007). This difference in loss of muscle-related genes and cell differentiation between the adipocytes after adding canola oil indicates that anatomical location and fat lineage play a vital role in response to external stimulus such as diet intervention.

6.5.7 Lipid profile and composition is defined by the anatomical location in adipose tissue of young sheep

My study suggests that in comparison to the others, perirenal and sternal depots develop divergently (Henry et al., 2017). Of the two depots, however, the perirenal depot shows more white adipocytes development activity (Hakim-Weber et al., 2011; Macotela et al., 2012; Pietilainen et al., 2011; Symonds et al., 2015), as indicated by changes in cellular lipidome of the perirenal tissue in offspring subjected to nutritional intervention. Generally, any changes in the metabolic or phenotypic functioning of existing fat cells can be influenced by the endocrine microenvironment tissue it is exposed to, such as the adrenal gland (Seidell et al., 1990).

6.6 Conclusion

Overall, this study has addressed the central questions related to the impact of the maternal canola diet intervention on BAT gene expression in early life. There was a reduction in the down-regulation of thermogenic gene expression including UCP1 clustering in weighted gene co-expression, and in response to a stimulus, as well as in cell differentiation. Dietary intervention implication with age-related factors was identified as necessary in making such differentiation. Moreover, biological mechanisms and co-expressed anatomical locations of genes were identified as being crucial in shaping the response of adipose tissue depots. External stimulus and internal factors were also recognised as significant in defining the thermogenesis. Such a differential response indicates that reducing dietary fat alone is not helpful in altering fat utilisation and the likelihood of obesity (Swift et al., 2014), but a sophisticated multifactorial approach is needed to ensure the intended effect (Andrianova et al., 2015).

7 Conclusion

7.1 General aims

The studies detailed in my thesis aimed to determine whether age and anatomical location regulate a fat depot's response to changes in maternal diet during postnatal development. This was achieved by analysing large numbers of differentially expressed genes and function from microarray data, including mitochondrial biogenesis, thermogenesis (i.e. UCP1), cell differentiation, and the ability to respond to local stimulus in offspring adipose tissue. The availability of abundant transcriptomic data and the modification of computational approach systems, coupled with the latest increments in computational power enabled the development of predictive modules quantitatively, based on the gene expression relationships. Such modules were developed through identification of similar co-expression regulation clustered genes that were engaged in interdependent or associated biological functions. Differences within the transcriptome between similar tissues sampled from the offspring of mothers given a fatty acid supplement might reflect the variations in the cellular composition, transcriptional programme, function, and type of adipocyte. This enabled differential network analyses to be interpreted by capitalising on the outcomes with an enhanced knowledge for adipose tissue development.

This chapter summarises the key findings and the main limitations of these studies and investigations.

7.2 Methods

Ewes raising twin lambs were supplemented with 3% canola or fed a standard diet from day one after delivery throughout lactation in an aim to modify the fatty acid profile of their milk. The data of the mRNA extracted from five different anatomical locations of lamb adipose tissue were transferred to GeneChips. The microarray gene expression datasets were subjected to multi-region bioinformatics analysis to obtain biologically meaningful information about the examined adipose tissues depots, including the mitochondrial genes that are associated with thermogenesis (i.e. UCP1).

7.3 Summary of findings

7.3.1 Adipose tissue gene expression and function modulated by age and anatomical location in early life

In order to understand the developmental origins of the molecular changes within fat depots of different anatomical sites in early life, multi-region bioinformatics analyses were conducted on microarray data generated from the five fat depots sampled from lambs at age 7 days and 28 days. Based on the analysis, it was found that all depots were unique in their gene expression profiles and all had negligible quantities of distinct co-expressed gene modules, linked to unique biological processes. The differences between depots of adipose tissues within their responses to local stimulants, differentiation ability, and gene expression profiles have previously been identified in 5-6-week-old mice (Lee et al., 2017).

7.3.2 Maternal canola oil supplementation delays the loss of mitochondrial gene expression but not UCP1 in offspring adipose tissue

A set of genes associated with mitochondrial biogenesis (i.e. ATP metabolic process, mitochondrial respiratory chain, and TCA cycle) were studied to gain a more comprehensive insight into the effect of maternal supplementation with fatty acids during the early life of sheep. The groups receiving the supplement had slightly more variation in gene expression profiles between adipose tissue depots compared with depots in controls. This included a reduction in the decline of the mitochondrial gene expression and functions, particularly in the ability to produce energy during early life development. Specifically, in BAT depots (i.e. perirenal and sternal), there was a higher expression of mitochondrial genes compared to WAT (i.e. omental, subcutaneous), which indicates that age and anatomical locations influence that response. However, these results are not consistent with non-shivering thermogenesis in BAT which showed no effect of dietary supplements on UCP1 gene expression (i.e. perirenal and sternal).

7.3.3 Perirenal adipose tissue exhibited a higher propensity of responding to maternal diet intervention

In lamb adipose tissue, the abundance of UCP1 peaked on day one and, as expected, decreased with age (Clarke et al., 1997). According to my findings, age and anatomical location modulate the adipose tissue response. Perirenal adipose tissue was most responsive to the nutritional intervention compared to other tested depots (i.e. sternal, omental and subcutaneous), as it retained the highest amount of UCP1 gene expression in early life, which could enhance the depot's ability to respond to the maternal dietary supplementation with canola oil. That was confirmed by further investigation in the offsprings' lipid profile which showed a significant reduction in omega 6 adrenic acid FA (22:4) and omega-3 docosatetraenoic acid FA (22:3) in perirenal adipose tissue after 28 days of maternal diet supplementation, which was in line with that found in an earlier study with regard to the change in milk fatty acid profiles after canola oil supplementation (Okine et al., 2003). This could also be beneficial in reducing the inflammatory response in the offsprings' adipose tissue (Yashodhara et al., 2009).

7.4 Study limitations

7.4.1 Sheep as a module for early life development in humans

Despite sheep emerging as one large animal model for examining human development as explained in chapter 1, they have certain limitations for nutrition studies. As ruminants and herbivores, their dietary requirements, digestive system and certain aspects of metabolic energy are entirely different from that of humans. In this regard, applying the results of the thesis directly to humans is not fully feasible. For instance, the intervention employed in the study cannot be applied directly to supplementing the diets of lactating women with 3% of canola oil with a similar impact as was seen in the milk of ewes. However, the development of rumen within newborn lambs is incomplete until they reach six to eight weeks, when they start eating solid food (Lane et al., 2000). Additionally, the process of suckling is initiated through direct transitioning of milk from the oesophagus towards the abomasum, the last stomach chamber, thus implying that the rumen has been bypassed (Ørskov, 1972). Hence, because the lambs investigated in the study depended entirely on the mother for a month, such a limitation does not constitute a significant issue when examining nutrition in young lambs.

While the number of offspring within sheep (triplets at the maximum) is more similar to that of humans compared to the quantity of mice offspring (big litters), human mothers normally have one offspring, thus creating another limitation in the current study. In sheep, the number of foetuses has been found to determine the birth weight of the offspring (Gardner et al., 2007) and its fat mass (Hancocks et al., 2012). As explained in chapter 2, if ewes had triplets, one lamb was removed immediately. Thus each ewe only raised two lambs up to one week (the initial point of sampling); therefore, the multiple numbers of foetuses was partially altered following birth. After this stage (from weeks one to four) each ewe nurtured only a single lamb.

7.5 Technical limitations

7.5.1 Gene expression

Another limitation is that an even distribution of offspring by sex could not be attained and there was, unfortunately, an imbalance between the number of males and females. As there was no significant difference in the outcomes between males and females within groups in gene expression analyses, the results from both sexes were combined. However, it would have been advantageous to have a greater number of animals in each group to examine potential differences between sexes.

7.5.2 Consequences of high fat intake on adipose tissue

In supplemented groups, ewes received an extra 3% of calories from canola oil that the control group did not. Therefore, the alteration seen in the gene expression profile could be attributed to the modest increase in fat, and thus increased energy intake. Although ewes in the supplemented groups were receiving more kilocalories per day than those in the control group, the percentage of this increase of total dietary intake on a kg/kg ewe body weight basis is tiny (metabolisable energy = 215 kcal/day). In addition, the result relating to milk fatty acid composition on suckling lambs revealed that this increase in fat intake altered the milk fatty acid content rather than the total fat (Alagal, 2018).

7.5.3 Bioinformatics tool and microarrays data analysis

Using microarray technology in bioinformatics has become a powerful tool to analyse the gene expression of tens of thousands of genes simultaneously. Microarray-based gene expression profiles are available to help us achieve a comprehensive understanding of complex system mechanisms such as adipose tissue. However, microarray studies are characterised by providing large datasets found to be primarily influenced by several factors, such as the quality and the design of the arrays (Russo et al., 2003). In addition to those factors mentioned earlier, I found that the statistical procedure, which used a different type of analysis in investigating the data, also has a significant impact on the study outcome. This includes the level of power used to normalise and log transform the data or whether additional correction (i.e. false discovery rate [FDR]) needs to be used to minimise multiple comparison errors (i.e. type 1, type 2) (Gentleman et al., 2006).

In addition, this type of examination has been found to be highly sensitive to the number and sex of the samples involved in the analysis (Langfelder and Horvath, 2008). As discussed in chapter 2, the effect of sex was minimised by recruiting mainly female lambs in this study, while regarding the number of samples in this study, the perirenal was found to be the only depot that could be impacted by this factor, particularly in the diet intervention group at 7 days of age (i.e. n = 3). However, the conclusions of this study are not based on one depot, as there were four more depots tested (sternal, epicardial, omental, subcutaneous) which all had an adequate number of samples that confirm my results (five in each age group). Furthermore, the outcome of the perirenal lipid profiles analysis, which has the same number of samples (n = 5 in each group), supports other results which have been published recently (Fainberg et al., 2018).

7.5.4 mRNA gene expression and protein level

Microarray data analysis and the results of this study were based on mRNA gene expression. However, it is well established that mRNA level does not always reflect protein abundance, as there are many other factors that could impact on the protein level, including translation, transcription and degradation (Vogel and Marcotte, 2012). Therefore, the microarray result should be tested by using another appropriate method (i.e. immunohistochemically and histology), which was partially done by testing a specific gene (UCP1) in three depots (i.e. perirenal, sternal, epicardial); the results of this test were found to match the microarrays result (Alagal, 2018).

7.6 Future work

7.6.1 Effects beyond one month of age

The maternal canola oil supplement significantly altered the rate of decline of mitochondrial gene expression in all fat depots examined (i.e. perirenal, sternal, omental, subcutaneous); it would be imperative to examine this for a prolonged duration, for instance, until the lamb reaches weaning (i.e. 12-14 weeks). This would reveal if the supplementation prevents or delays the mitochondrial gene expression loss of the offspring. Moreover, it would be important to determine the expression of various mitochondrial genes following the end of supplementation, to determine if the changes in gene expression are permanent. If the mitochondrial protein abundance were similar to controls, the supplementation would be considered redundant.

7.6.2 Direct supplementations using fatty acids

As cited earlier, it is impossible to attribute effects that an offspring exhibits, especially abundant UCP1, following supplementation with maternal fatty acids to one fatty acid. In order to examine this, it would be necessary to provide lambs and ewes with supplements directly with particular fatty acids such as LC-PUFA ω-3 and ω-6, or single SFAs, to determine the role they play in inhibiting or enhancing mitochondrial gene expression (i.e. UCP1) and capacity. Provision of the supplements directly alongside fatty acids might be an ideal method of enriching adipose tissues compared to providing the supplements indirectly with precursors of fatty acids such as canola oil. For example, data from one study revealed that precursor conversion into PUFA ω-3 fatty acids in humans was inefficient and limited (Anderson and Ma, 2009).

7.6.3 Further investigation in adipose tissue modality and function

This study, by using bioinformatics tools to analyse microarray gene expression data, provided a rich and vital source of the description of the dynamic transformations in lipid composition, gene expression, and biological pathways of adipose tissue from different anatomical locations in early life. Therefore, it would be useful to do a more in-depth investigation into the modality of adipose tissue development and its reflection on another specific list of gene functions that are involved in the particular biological pathway that may be linked to obesity (i.e. inflammation, hormone secretion) or another metabolic disease.

7.6.4 MicroRNAs identification within adipose tissues

Notably, an important source for uncovering miRNAs that underlie early life thermogenesis involves the integration of mRNA and miRNA expression profiling (Zhou et al., 2017) and how dietary supplements would affect these. This might be attained by analysing the miRNAs' functional characterisation and expression profile over the entire adipose tissue growth of sheep, with more focus on gene targets of associated miRNAs, which might feature in fat deposition and thermogenesis regulation. Moreover, future studies could examine the relationship between important miRNAs alongside their targeted genes in vitro as well as functional effects that miRNAs serve in the development of adipose tissues. This would offer novel understandings concerning the design of dietary intervention methods to enhance BAT development.

7.7 Concluding remarks

This study shows how depots of adipose tissues vary in terms of response to maternal diet changes, gene expression profiles, and characteristics. It has also shown that manipulation of the fatty acid profiles of milk ingested by a newborn might prevent or delay the loss of mitochondrial genes during early life, particularly within BAT. The findings from this study add to existing knowledge about adipose tissue development as it relates to anatomical location as well as explaining the differences in its response to dietary interventions. Therefore, this study might be beneficial to attempts aimed towards designing and testing dietary interventions for obesity treatment and prevention.

8 References

ABU-SAAD, K. & FRASER, D. 2010. Maternal nutrition and birth outcomes. *Epidemiologic reviews,* 32, 5-25.

ABUGHAZALEH, A., FELTON, D. & IBRAHIM, S. A. 2007. Milk conjugated linoleic acid response to fish oil and sunflower oil supplementation to dairy cows managed under two feeding systems. *Journal of Dairy Science,* 90, 4763-4769.

ADACHI, S., HOMOTO, M., TANAKA, R., HIOKI, Y., MURAKAMI, H., SUGA, H., MATSUMOTO, M., NAKAYAMA, K. I., HATTA, T., IEMURA, S. & NATSUME, T. 2014. ZFP36L1 and ZFP36L2 control LDLR mRNA stability via the ERK-RSK pathway. *Nucleic Acids Res,* 42, 10037-49.

ADAMS, A. C., YANG, C., COSKUN, T., CHENG, C. C., GIMENO, R. E., LUO, Y. & KHARITONENKOV, A. 2013. The breadth of FGF21's metabolic actions are governed by FGFR1 in adipose tissue. *Molecular metabolism,* 2, 31-37.

AKABAS, S., LEDERMAN, S. A. & MOORE, B. J. 2012. *Textbook of Obesity: Biological, Psychological and Cultural Influences*, John Wiley & Sons.

ALAGAL, R. 2018. *Nutritional Programming of Brown Adipose Tissue.* PhD, University of Nottingham.

ALDISS, P., BETTS, J., SALE, C., POPE, M. & SYMONDS, M. E. 2017. Exercise-induced 'browning'of adipose tissues. *Metabolism*.

ALEXANDER, G. 1978. Quantitative development of adipose tissue in foetal sheep. *Australian journal of biological sciences,* 31, 489-504.

ALEXANDER, G. & BELL, W. 1975. Quantity and calculated oxygen consumption during summit metabolism of brown adipose tissue in new-born lambs. *Neonatology,* 26, 214-220.

ALPAYDIN, E. 2009. *Introduction to machine learning*, MIT press.

AOYAMA, T., SOURI, M., USHIKUBO, S., KAMIJO, T., YAMAGUCHI, S., KELLEY, R. I., RHEAD, W. J., UETAKE, K., TANAKA, K. & HASHIMOTO, T. 1995. Purification of human very-long-chain acyl-coenzyme A dehydrogenase and characterization of its deficiency in seven patients. *The Journal of clinical investigation,* 95, 2465-2473.

ASP, P., BLUM, R., VETHANTHAM, V., PARISI, F., MICSINAI, M., CHENG, J., BOWMAN, C., KLUGER, Y. & DYNLACHT, B. D. 2011. Genome-wide remoduleing of the epigenetic landscape during myogenic differentiation. *Proceedings of the National Academy of Sciences,* 108, E149-E158.

ATIT, R., SGAIER, S. K., MOHAMED, O. A., TAKETO, M. M., DUFORT, D., JOYNER, A. L., NISWANDER, L. & CONLON, R. A. 2006. β-catenin activation is necessary and sufficient to specify the dorsal dermal fate in the mouse. *Developmental biology,* 296, 164-176.

AU-YONG, I. T., THORN, N., GANATRA, R., PERKINS, A. C. & SYMONDS, M. E. 2009. Brown adipose tissue and seasonal variation in humans. *Diabetes,* 58, 2583-2587.

AUCHTUNG, T., RIUS, A., KENDALL, P., MCFADDEN, T. & DAHL, G. 2005. Effects of photoperiod during the dry period on prolactin, prolactin receptor, and milk production of dairy cows. *Journal of dairy science,* 88, 121-127.

BARABASI, A. L. & OLTVAI, Z. N. 2004. Network biology: understanding the cell's functional organization. *Nat Rev Genet,* 5, 101-13.

BARBER, M., WARD, R., RICHARDS, S., SALTER, A., BUTTERY, P., VERNON, R. & TRAVERS, M. 2000. Ovine adipose tissue monounsaturated fat content

is correlated to depot-specific expression of the stearoyl-CoA desaturase gene. *J Anim Sci,* 78, 62-68.
BARLOW, S. E. & DIETZ, W. H. 1998. Obesity evaluation and treatment: expert committee recommendations. *Pediatrics,* 102, e29-e29.
BARRY, J. S. & ANTHONY, R. V. 2008. The pregnant sheep as a module for human pregnancy. *Theriogenology,* 69, 55-67.
BARTELT, A., BRUNS, O. T., REIMER, R., HOHENBERG, H., ITTRICH, H., PELDSCHUS, K., KAUL, M. G., TROMSDORF, U. I., WELLER, H. & WAURISCH, C. 2011. Brown adipose tissue activity controls triglyceride clearance. *Nature medicine,* 17, 200.
BARTELT, A., MERKEL, M. & HEEREN, J. 2012. A new, powerful player in lipoprotein metabolism: brown adipose tissue. *Journal of molecular medicine,* 90, 887-893.
BARTELT, A., WEIGELT, C., CHERRADI, M. L., NIEMEIER, A., TÖDTER, K., HEEREN, J. & SCHEJA, L. 2013. Effects of adipocyte lipoprotein lipase on de novo lipogenesis and white adipose tissue browning. *Biochimica Et Biophysica Acta (BBA)-Molecular and Cell Biology of Lipids,* 1831, 934-942.
BASSE, A. L., DIXEN, K., YADAV, R., TYGESEN, M. P., QVORTRUP, K., KRISTIANSEN, K., QUISTORFF, B., GUPTA, R., WANG, J. & HANSEN, J. B. 2015. Global gene expression profiling of brown to white adipose tissue transformation in sheep reveals novel transcriptional components linked to adipose remoduleing. *BMC genomics,* 16, 215.
BASSETT, J., BOMFORD, J. & MOTT, J. 1988. Photoperiod: an important regulator of plasma prolactin concentration in fetal lambs during late gestation. *Quarterly journal of experimental physiology,* 73, 241-244.
BENJAMINI, Y. & HOCHBERG, Y. 1995. Controlling the false discovery rate: a practical and powerful approach to multiple testing. *Journal of the royal statistical society. Series B (Methodological)*, 289-300.
BERG, J. M., DEIS, F., TYMOCZKO, J., STRYER, L., GERBER, N., GUMPORT, R. & KOEPPE, R. 2011. Biochemistry student companion. WH Freeman: New York.
BISPHAM, J., GOPALAKRISHNAN, G., DANDREA, J., WILSON, V., BUDGE, H., KEISLER, D., BROUGHTON PIPKIN, F., STEPHENSON, T. & SYMONDS, M. 2003. Maternal endocrine adaptation throughout pregnancy to nutritional manipulation: consequences for maternal plasma leptin and cortisol and the programming of fetal adipose tissue development. *Endocrinology,* 144, 3575-3585.
BOHELER, K. R., CZYZ, J., TWEEDIE, D., YANG, H. T., ANISIMOV, S. V. & WOBUS, A. M. 2002. Differentiation of pluripotent embryonic stem cells into cardiomyocytes. *Circ Res,* 91, 189-201.
BOLTON-SMITH, C., WOODWARD, M., FENTON, S. & BROWN, C. 1996. Does dietary trans fatty acid intake relate to the prevalence of coronary heart disease in Scotland? *European heart journal,* 17, 837-845.
BOUCHARD, C. 2007. The biological predisposition to obesity: beyond the thrifty genotype scenario. *Int J Obes (Lond),* 31, 1337-1339.
BRINE, T. 2006. *A Thermographic Study of Brown Adipose Tissue Activation in Infant Mice*, Indiana University.
BUCCIONI, A., DECANDIA, M., MINIERI, S., MOLLE, G. & CABIDDU, A. 2012. Lipid metabolism in the rumen: New insights on lipolysis and

biohydrogenation with an emphasis on the role of endogenous plant factors. *Animal Feed Science and Technology,* 174, 1-25.

BUDGE, H., BISPHAM, J., DANDREA, J., EVANS, E., HEASMAN, L., INGLETON, P. M., SULLIVAN, C., WILSON, V., STEPHENSON, T. & SYMONDS, M. E. 2000. Effect of maternal nutrition on brown adipose tissue and its prolactin receptor status in the fetal lamb. *Pediatric research,* 47, 781-786.

BUDGE, H., SEBERT, S., SHARKEY, D. & SYMONDS, M. 2009. Session on 'Obesity'Adipose tissue development, nutrition in early life and its impact on later obesity. *Proceedings of the Nutrition Society,* 68, 321-326.

CALDERON-DOMINGUEZ, M., MIR, J. F., FUCHO, R., WEBER, M., SERRA, D. & HERRERO, L. 2016. Fatty acid metabolism and the basis of brown adipose tissue function. *Adipocyte,* 5, 98-118.

CANNON, B. & NEDERGAARD, J. 2004. Brown adipose tissue: function and physiological significance. *Physiological reviews,* 84, 277-359.

CANNON, B., NEDERGAARD, J. & SUNDIN, U. 1981. Thermogenesis, brown fat and thermogenin. *Survival in the Cold*, 99-120.

CANTILE, M., PROCINO, A., D'ARMIENTO, M., CINDOLO, L. & CILLO, C. 2003. HOX gene network is involved in the transcriptional regulation of in vivo human adipogenesis. *J Cell Physiol,* 194, 225-36.

CAO, L., CHOI, E. Y., LIU, X., MARTIN, A., WANG, C., XU, X. & DURING, M. J. 2011. White to brown fat phenotypic switch induced by genetic and environmental activation of a hypothalamic-adipocyte axis. *Cell metabolism,* 14, 324-338.

CHILLIARD, Y., GLASSER, F., FERLAY, A., BERNARD, L., ROUEL, J. & DOREAU, M. 2007. Diet, rumen biohydrogenation and nutritional quality of cow and goat milk fat. *European Journal of Lipid Science and Technology,* 109, 828-855.

CHRISTIE, W. W. 1982. A simple procedure for rapid transmethylation of glycerolipids and cholesteryl esters. *Journal of Lipid Research,* 23, 1072-1075.

CINTI, S. 2006. The role of brown adipose tissue in human obesity. *Nutrition, metabolism and cardiovascular diseases,* 16, 569-574.

CINTI, S. 2011. Between brown and white: novel aspects of adipocyte differentiation. *Annals of medicine,* 43, 104-115.

CINTI, S., FREDERICH, R. C., ZINGARETTI, M. C., DE MATTEIS, R., FLIER, J. S. & LOWELL, B. B. 1997. Immunohistochemical Localization of Leptin and Uncoupling Protein in White and Brown Adipose Tissue 1. *Endocrinology,* 138, 797-804.

CLARKE, J. R., BRGLEVSKA, S., LAU, E. W., RAMDAVE, S. & HICKS, R. J. 2007. Atypical brown fat distribution in young males demonstrated on PET/CT. *Clinical nuclear medicine,* 32, 679-682.

CLARKE, L., BRYANT, M. J., LOMAX, M. A. & SYMONDS, M. E. 1997a. Maternal manipulation of brown adipose tissue and liver development in the ovine fetus during late gestation. *British Journal of Nutrition,* 77, 871-883.

CLARKE, L., BUSS, D., JUNIPER, D., LOMAX, M. & SYMONDS, M. 1997b. Adipose tissue development during early postnatal life in ewe-reared lambs. *Experimental Physiology,* 82, 1015-1027.

CLAUSSNITZER, M., DANKEL, S. N., KIM, K.-H., QUON, G., MEULEMAN, W., HAUGEN, C., GLUNK, V., SOUSA, I. S., BEAUDRY, J. L. & PUVIINDRAN,

V. 2015a. FTO obesity variant circuitry and adipocyte browning in humans. *New England Journal of Medicine,* 373, 895-907.
CLAUSSNITZER, M., DANKEL, S. N., KIM, K. H., QUON, G., MEULEMAN, W., HAUGEN, C., GLUNK, V., SOUSA, I. S., BEAUDRY, J. L., PUVIINDRAN, V., ABDENNUR, N. A., LIU, J., SVENSSON, P. A., HSU, Y. H., DRUCKER, D. J., MELLGREN, G., HUI, C. C., HAUNER, H. & KELLIS, M. 2015b. FTO Obesity Variant Circuitry and Adipocyte Browning in Humans. *N Engl J Med,* 373, 895-907.
CORRADI, D., MAESTRI, R., CALLEGARI, S., PASTORI, P., GOLDONI, M., LUONG, T. V. & BORDI, C. 2004. The ventricular epicardial fat is related to the myocardial mass in normal, ischemic and hypertrophic hearts. *Cardiovascular Pathology,* 13, 313-316.
COUSIN, B., CINTI, S., MORRONI, M., RAIMBAULT, S., RICQUIER, D., PENICAUD, L. & CASTEILLA, L. 1992. Occurrence of brown adipocytes in rat white adipose tissue: molecular and morphological characterization. *Journal of cell science,* 103, 931-942.
COUSIN, B., MUNOZ, O., ANDRÉ, M., FONTANILLES, A., DANI, C., COUSIN, J., LAHARRAGUE, P., CASTEILLA, L. & ENICAUD, L. 1999. A role for preadipocytes as macrophage-like cells. *The FASEB Journal,* 13, 305-312.
CYPESS, A. M., WHITE, A. P., VERNOCHET, C., SCHULZ, T. J., XUE, R., SASS, C. A., HUANG, T. L., ROBERTS-TOLER, C., WEINER, L. S., SZE, C., CHACKO, A. T., DESCHAMPS, L. N., HERDER, L. M., TRUCHAN, N., GLASGOW, A. L., HOLMAN, A. R., GAVRILA, A., HASSELGREN, P. O., MORI, M. A., MOLLA, M. & TSENG, Y. H. 2013. Anatomical localization, gene expression profiling and functional characterization of adult human neck brown fat. *Nat Med,* 19, 635-9.
DALLE, S., RAVIER, M. A. & BERTRAND, G. 2011. Emerging roles for β-arrestin-1 in the control of the pancreatic β-cell function and mass: new therapeutic strategies and consequences for drug screening. *Cellular signalling,* 23, 522-528.
DAS, U. N. 2006. Essential fatty acids: biochemistry, physiology and pathology. *Biotechnology journal,* 1, 420-439.
DIVAKARUNI, A. S. & BRAND, M. D. 2011. The regulation and physiology of mitochondrial proton leak. *Physiology,* 26, 192-205.
DOREAU, M. & FERLAY, A. 1994. Digestion and utilisation of fatty acids by ruminants. *Animal Feed Science and Technology,* 45, 379-396.
DRUBACH, L. A., PALMER, E. L., 3RD, CONNOLLY, L. P., BAKER, A., ZURAKOWSKI, D. & CYPESS, A. M. 2011. Pediatric brown adipose tissue: detection, epidemiology, and differences from adults. *J Pediatr,* 159, 939-44.
DUIVENVOORDEN, I., TEUSINK, B., RENSEN, P. C., ROMIJN, J. A., HAVEKES, L. M. & VOSHOL, P. J. 2005. Apolipoprotein C3 deficiency results in diet-induced obesity and aggravated insulin resistance in mice. *Diabetes,* 54, 664-671.
ENERBÄCK, S. 2010. Human brown adipose tissue. *Cell metabolism,* 11, 248-252.
FAINBERG, H., ALHADDAD, A., ALAGAL, R., BIRTWISTLE, M., DAVIES, G., CASTELLANOS, M., MAY, S., SACKS, H., BUDGE, H. & SYMONDS, M. 2017. Transcriptional landscape of the major adipose depots during early life reveals unique pathways during development. *The FASEB Journal,* 31, 886.10-886.10.

FAINBERG, H. P., BIRTWISTLE, M., ALAGAL, R., ALHADDAD, A., POPE, M., DAVIES, G., WOODS, R., CASTELLANOS, M., MAY, S. T. & ORTORI, C. A. 2018. Transcriptional analysis of adipose tissue during development reveals depot-specific responsiveness to maternal dietary supplementation. *Scientific Reports (Nature Publisher Group),* 8, 1-11.

FALLMANN, J., SEDLYAROV, V., TANZER, A., KOVARIK, P. & HOFACKER, I. L. 2016. AREsite2: an enhanced database for the comprehensive investigation of AU/GU/U-rich elements. *Nucleic Acids Res,* 44, D90-5.

FEDORENKO, A., LISHKO, P. V. & KIRICHOK, Y. 2012. Mechanism of Fatty-Acid-Dependent UCP1 Uncoupling in Brown Fat Mitochondria. *Cell,* 151, 400-413.

FONTANESI, F., SOTO, I. C. & BARRIENTOS, A. 2008. Cytochrome c oxidase biogenesis: new levels of regulation. *IUBMB life,* 60, 557-568.

FRAYLING, T. M., TIMPSON, N. J., WEEDON, M. N., ZEGGINI, E., FREATHY, R. M., LINDGREN, C. M., PERRY, J. R., ELLIOTT, K. S., LANGO, H., RAYNER, N. W., SHIELDS, B., HARRIES, L. W., BARRETT, J. C., ELLARD, S., GROVES, C. J., KNIGHT, B., PATCH, A. M., NESS, A. R., EBRAHIM, S., LAWLOR, D. A., RING, S. M., BEN-SHLOMO, Y., JARVELIN, M. R., SOVIO, U., BENNETT, A. J., MELZER, D., FERRUCCI, L., LOOS, R. J., BARROSO, I., WAREHAM, N. J., KARPE, F., OWEN, K. R., CARDON, L. R., WALKER, M., HITMAN, G. A., PALMER, C. N., DONEY, A. S., MORRIS, A. D., SMITH, G. D., HATTERSLEY, A. T. & MCCARTHY, M. I. 2007. A common variant in the FTO gene is associated with body mass index and predisposes to childhood and adult obesity. *Science,* 316, 889-94.

FREEMARK, M. S. 2010. *Pediatric Obesity*, Springer.

FRÜHBECK, G., BECERRIL, S., SÁINZ, N., GARRASTACHU, P. & GARCÍA-VELLOSO, M. J. 2009. BAT: a new target for human obesity? *Trends in pharmacological sciences,* 30, 387-396.

FU, L., JOHN, L. M., ADAMS, S. H., YU, X. X., TOMLINSON, E., RENZ, M., WILLIAMS, P. M., SORIANO, R., CORPUZ, R. & MOFFAT, B. 2004. Fibroblast growth factor 19 increases metabolic rate and reverses dietary and leptin-deficient diabetes. *Endocrinology,* 145, 2594-2603.

GAHAGAN, S. 2005. Haslam DW, James WP. Obesity. *The lancet,* 366, 1197-1209.

GAO, A. W. & HOUTKOOPER, R. H. 2014. Mitochondrial fission: firing up mitochondria in brown adipose tissue. EMBO Press.

GENTLEMAN, R., CAREY, V., HUBER, W., IRIZARRY, R. & DUDOIT, S. 2006. *Bioinformatics and computational biology solutions using R and Bioconductor*, Springer Science & Business Media.

GENTLEMAN, R. C., CAREY, V. J., BATES, D. M., BOLSTAD, B., DETTLING, M., DUDOIT, S., ELLIS, B., GAUTIER, L., GE, Y. & GENTRY, J. 2004. Bioconductor: open software development for computational biology and bioinformatics. *Genome biology,* 5, R80.

GEORGIADI, A. & KERSTEN, S. 2012. Mechanisms of gene regulation by fatty acids. *Advances in nutrition,* 3, 127-134.

GESTA, S., TSENG, Y. H. & KAHN, C. R. 2007. Developmental origin of fat: tracking obesity to its source. *Cell,* 131, 242-56.

GHAFOORUNISSA, G. 2008. Role of trans fatty acids in health and challenges to their reduction in Indian foods. *Asia Pacific journal of clinical nutrition,* 17, 212-215.

GILSANZ, V., SMITH, M. L., GOODARZIAN, F., KIM, M., WREN, T. A. & HU, H. H. 2012. Changes in brown adipose tissue in boys and girls during childhood and puberty. *The Journal of pediatrics,* 160, 604-609. e1.

GÖTTLICHER, M., WIDMARK, E., LI, Q. & GUSTAFSSON, J.-A. 1992. Fatty acids activate a chimera of the clofibric acid-activated receptor and the glucocorticoid receptor. *Proceedings of the National Academy of Sciences,* 89, 4653-4657.

GOUGH, N. R. 2016. Boosting energy expenditure. *Sci. Signal.,* 9, ec170-ec170.

GRAHAM, N., MAY, S., DANIEL, Z., EMMERSON, Z., BRAMELD, J. & PARR, T. 2011. Use of the Affymetrix Human GeneChip array and genomic DNA hybridisation probe selection to study ovine transcriptomes. *Animal,* 5, 861-866.

GREGG, E. W. & SHAW, J. E. 2017. Global Health Effects of Overweight and Obesity. *N Engl J Med*.

HAKIM-WEBER, R., KROGSDAM, A. M., JORGENSEN, C., FISCHER, M., PROKESCH, A., BOGNER-STRAUSS, J. G., BORNSTEIN, S. R., HANSEN, J. B., MADSEN, L., KRISTIANSEN, K., TRAJANOSKI, Z. & HACKL, H. 2011. Transcriptional regulatory program in wild-type and retinoblastoma gene-deficient mouse embryonic fibroblasts during adipocyte differentiation. *BMC Res Notes,* 4, 157.

HAMANN, A., FLIER, J. S. & LOWELL, B. B. 1996. Decreased brown fat markedly enhances susceptibility to diet-induced obesity, diabetes, and hyperlipidemia. *Endocrinology,* 137, 21-9.

HANSEN, H. S. & JENSEN, B. 1985. Essential function of linoleic acid esterified in acylglucosylceramide and acylceramide in maintaining the epidermal water permeability barrier. Evidence from feeding studies with oleate, linoleate, arachidonate, columbinate and α-linolenate. *Biochimica et Biophysica Acta (BBA)-Lipids and Lipid Metabolism,* 834, 357-363.

HARMS, M. & SEALE, P. 2013. Brown and beige fat: development, function and therapeutic potential. *Nature medicine,* 19, 1252-1263.

HASSAN, N. J., SIMMONDS, S. J., CLARKSON, N. G., HANRAHAN, S., PUKLAVEC, M. J., BOMB, M., BARCLAY, A. N. & BROWN, M. H. 2006. CD6 regulates T-cell responses through activation-dependent recruitment of the positive regulator SLP-76. *Molecular and cellular biology,* 26, 6727-6738.

HENRY, B. A., POPE, M., BIRTWISTLE, M., LOUGHNAN, R., ALAGAL, R., FULLER-JACKSON, J. P., PERRY, V., BUDGE, H., CLARKE, I. J. & SYMONDS, M. E. 2017. Ontogeny and Thermogenic Role for Sternal Fat in Female Sheep. *Endocrinology,* 158, 2212-2225.

HILL, J. O., LIN, D., YAKUBU, F. & PETERS, J. 1992. Development of dietary obesity in rats: influence of amount and composition of dietary fat. *International journal of obesity and related metabolic disorders: journal of the International Association for the Study of Obesity,* 16, 321-333.

HIMMS-HAGEN, J., MELNYK, A., ZINGARETTI, M., CERESI, E., BARBATELLI, G. & CINTI, S. 2000. Multilocular fat cells in WAT of CL-316243-treated rats derive directly from white adipocytes. *American Journal of Physiology-Cell Physiology,* 279, C670-C681.

HINOI, E., NAKAMURA, Y., TAKADA, S., FUJITA, H., IEZAKI, T., HASHIZUME, S., TAKAHASHI, S., ODAKA, Y., WATANABE, T. & YONEDA, Y. 2013. Growth differentiation factor-5 promotes brown adipogenesis in systemic energy expenditure. *Diabetes*, DB_130808.

HO, T. H., CHARLET-B, N., POULOS, M. G., SINGH, G., SWANSON, M. S. & COOPER, T. A. 2004. Muscleblind proteins regulate alternative splicing. *The EMBO journal,* 23, 3103-3112.
HONG, K.-W., KIM, S. H., ZHANG, X. & PARK, S. 2018. Interactions among the variants of insulin-related genes and nutrients increase the risk of type 2 diabetes. *Nutrition Research*.
HOTAMISLIGIL, G. S. 2005. Role of endoplasmic reticulum stress and c-Jun NH2-terminal kinase pathways in inflammation and origin of obesity and diabetes. *Diabetes,* 54, S73-S78.
HSCIC. 2014. *obesity* [Online]. Available: http://www.hscic.gov.uk/article/2021/Website-Search?productid=17440&q=obesity&sort=Relevance&size=10&page=1&area=both#top [Accessed 25/06 2015].
HUNG, G.-C., BROWN, C. R., WOLFE, A. B., LIU, J. & CHIANG, H.-L. 2004. Degradation of the gluconeogenic enzymes fructose-1, 6-bisphosphatase and malate dehydrogenase is mediated by distinct proteolytic pathways and signaling events. *Journal of Biological Chemistry,* 279, 49138-49150.
IACOBELLIS, G., CORRADI, D. & SHARMA, A. M. 2005. Epicardial adipose tissue: anatomic, biomolecular and clinical relationships with the heart. *Nature clinical practice Cardiovascular medicine,* 2, 536-543.
INAGAKI, T., SAKAI, J. & KAJIMURA, S. 2016. Transcriptional and epigenetic control of brown and beige adipose cell fate and function. *Nature reviews. Molecular cell biology,* 17, 480.
IQBAL, M. P. 2014. Trans fatty acids–A risk factor for cardiovascular disease. *Pakistan journal of medical sciences,* 30, 194.
ISHIBASHI, J. & SEALE, P. 2010. Beige can be slimming. *Science (New York, NY),* 328, 1113.
JANOVSKA, P., FLACHS, P., KAZDOVA, L. & KOPECKÝ, J. 2013. Anti-obesity effect of n-3 polyunsaturated fatty acids in mice fed high-fat diet is independent of cold-induced thermogenesis. *Physiological research,* 62, 153.
JENKINS, T. 1993. Lipid metabolism in the rumen. *Journal of Dairy Science,* 76, 3851-3863.
JIMENEZ, M., BARBATELLI, G., ALLEVI, R., CINTI, S., SEYDOUX, J., GIACOBINO, J. P., MUZZIN, P. & PREITNER, F. 2003. β3-Adrenoceptor knockout in C57BL/6J mice depresses the occurrence of brown adipocytes in white fat. *European Journal of Biochemistry,* 270, 699-705.
JONES, J. R., BARRICK, C., KIM, K.-A., LINDNER, J., BLONDEAU, B., FUJIMOTO, Y., SHIOTA, M., KESTERSON, R. A., KAHN, B. B. & MAGNUSON, M. A. 2005. Deletion of PPARγ in adipose tissues of mice protects against high fat diet-induced obesity and insulin resistance. *Proceedings of the National Academy of Sciences,* 102, 6207-6212.
KAJIMURA, S. & SAITO, M. 2014. A new era in brown adipose tissue biology: molecular control of brown fat development and energy homeostasis. *Annual review of physiology,* 76, 225-249.
KAJIMURA, S., SEALE, P. & BM., S. 2010. Transcriptional control of brown fat development. *Cell Metab,* 11, 257-262.
KAJIMURA, S., SEALE, P., KUBOTA, K., LUNSFORD, E., FRANGIONI, J. V., GYGI, S. P. & SPIEGELMAN, B. M. 2009. Initiation of myoblast to brown fat switch by a PRDM16-C/EBP-beta transcriptional complex. *Nature,* 460, 1154-8.

KANEHISA, M., FURUMICHI, M., TANABE, M., SATO, Y. & MORISHIMA, K. 2017. KEGG: new perspectives on genomes, pathways, diseases and drugs. *Nucleic acids research,* 45, D353-D361.

KATAN, M. B., ZOCK, P. L. & MENSINK, R. P. 1995. Trans fatty acids and their effects on lipoproteins in humans. *Annual review of nutrition,* 15, 473-493.

KELLY, T., YANG, W., CHEN, C.-S., REYNOLDS, K. & HE, J. 2008. Global burden of obesity in 2005 and projections to 2030. *International journal of obesity,* 32, 1431-1437.

KIEFER, F. W., VERNOCHET, C., O'BRIEN, P., SPOERL, S., BROWN, J. D., NALLAMSHETTY, S., ZEYDA, M., STULNIG, T. M., COHEN, D. E. & KAHN, C. R. 2012. Retinaldehyde dehydrogenase 1 regulates a thermogenic program in white adipose tissue. *Nature medicine,* 18, 918-925.

KIM, B. H., KIM, M., YIN, C. H., JEE, J. G., SANDOVAL, C., LEE, H., BACH, E. A., HAHM, D. H. & BAEG, G. H. 2011. Inhibition of the signalling kinase JAK3 alleviates inflammation in monoarthritic rats. *British journal of pharmacology,* 164, 106-118.

KIM, M., GOTO, T., YU, R., UCHIDA, K., TOMINAGA, M., KANO, Y., TAKAHASHI, N. & KAWADA, T. 2015. Fish oil intake induces UCP1 up-regulation in brown and white adipose tissue via the sympathetic nervous system. *Scientific Reports,* 5, 18013.

KLAUS, S., ELY, M., ENCKE, D. & HELDMAIER, G. 1995. Functional assessment of white and brown adipocyte development and energy metabolism in cell culture. Dissociation of terminal differentiation and thermogenesis in brown adipocytes. *Journal of cell science,* 108, 3171-3180.

KLEINER, S., DOURIS, N., FOX, E. C., MEPANI, R. J., VERDEGUER, F., WU, J., KHARITONENKOV, A., FLIER, J. S., MARATOS-FLIER, E. & SPIEGELMAN, B. M. 2012. FGF21 regulates PGC-1α and browning of white adipose tissues in adaptive thermogenesis. *Genes & development,* 26, 271-281.

KOZAK, L. P. 2011. The genetics of brown adipocyte induction in white fat depots. *Biology and therapeutic potential of brown adipose tissue*, 27.

KOZAK, L. P. & KOZA, R. A. 2009. The genetics of brown adipose tissue. *Progress in molecular biology and translational science,* 94, 75-123.

KUAN, J. & SAIER, M. H. 1993. The mitochondrial carrier family of transport proteins: structural, functional, and evolutionary relationships. *Critical reviews in biochemistry and molecular biology,* 28, 209-233.

LANGFELDER, P. & HORVATH, S. 2008. WGCNA: an R package for weighted correlation network analysis. *BMC bioinformatics,* 9, 559.

LARSON, D. E., HUNTER, G. R., WILLIAMS, M. J., KEKES-SZABO, T., NYIKOS, I. & GORAN, M. I. 1996. Dietary fat in relation to body fat and intraabdominal adipose tissue: a cross-sectional analysis. *The American journal of clinical nutrition,* 64, 677-684.

LAURITZEN, L. A., HANSEN, H. S., JØRGENSEN, M. H. & MICHAELSEN, K. F. 2001. The essentiality of long chain n-3 fatty acids in relation to development and function of the brain and retina. *Progress in lipid research,* 40, 1-94.

LE, H. D., MEISEL, J. A., DE MEIJER, V. E., GURA, K. M. & PUDER, M. 2009. The essentiality of arachidonic acid and docosahexaenoic acid. *Prostaglandins, Leukotrienes and Essential Fatty Acids,* 81, 165-170.

LEAN, M., HAN, T. & SEIDELL, J. 1998. Impairment of health and quality of life in people with large waist circumference. *The Lancet,* 351, 853-856.

LEAN, M. E. J. 1989. Brown adipose tissue in humans. *Proceedings of the Nutrition Society,* 48, 243-257.
LEE, P., LINDERMAN, J. D., SMITH, S., BRYCHTA, R. J., WANG, J., IDELSON, C., PERRON, R. M., WERNER, C. D., PHAN, G. Q. & KAMMULA, U. S. 2014. Irisin and FGF21 are cold-induced endocrine activators of brown fat function in humans. *Cell metabolism,* 19, 302-309.
LEE, Y. H., KIM, S. N., KWON, H. J. & GRANNEMAN, J. G. 2017. Metabolic heterogeneity of activated beige/brite adipocytes in inguinal adipose tissue. *Sci Rep,* 7, 39794.
LEE, Y. H., PETKOVA, A. P. & GRANNEMAN, J. G. 2013. Identification of an adipogenic niche for adipose tissue remoduleing and restoration. *Cell Metab,* 18, 355-67.
LEFF, T. & GRANNEMAN, J. G. 2010. *Adipose Tissue in Health and Disease*, John Wiley & Sons.
LETTIERI BARBATO, D., TATULLI, G., VEGLIANTE, R., CANNATA, S. M., BERNARDINI, S., CIRIOLO, M. R. & AQUILANO, K. 2015. Dietary fat overload reprograms brown fat mitochondria. *Frontiers in physiology,* 6, 272.
LEVESLEY, J., LUSHER, M. E., LINDSEY, J. C., CLIFFORD, S. C., GRUNDY, R. & COYLE, B. 2011. RASSF1A and the BH3-only mimetic ABT-737 promote apoptosis in pediatric medulloblastoma cell lines. *Neuro-Oncology,* 13, 1265-1276.
LIDELL, M. E., BETZ, M. J., DAHLQVIST LEINHARD, O., HEGLIND, M., ELANDER, L., SLAWIK, M., MUSSACK, T., NILSSON, D., ROMU, T., NUUTILA, P., VIRTANEN, K. A., BEUSCHLEIN, F., PERSSON, A., BORGA, M. & ENERBACK, S. 2013. Evidence for two types of brown adipose tissue in humans. *Nat Med,* 19, 631-4.
LIM, J.-H., GERHART-HINES, Z., DOMINY, J. E., LEE, Y., KIM, S., TABATA, M., XIANG, Y. K. & PUIGSERVER, P. 2013. Oleic acid stimulates complete oxidation of fatty acids through protein kinase A-dependent activation of SIRT1-PGC1α complex. *Journal of Biological Chemistry,* 288, 7117-7126.
LINDBERG, O. 1970. *Brown adipose tissue*, American Elsevier Publishing Company, Inc., New York.
LINTON, P. J. & DORSHKIND, K. 2004. Age-related changes in lymphocyte development and function. *Nature immunology,* 5, 133.
LIU, Q., HUANG, X., OH, J. H., LIN, R. Z., DUAN, S., YU, Y., YANG, R., QIU, J., MELERO-MARTIN, J. M., PU, W. T. & ZHOU, B. 2014. Epicardium-to-fat transition in injured heart. *Cell Res,* 24, 1367-9.
LOBB, K. & CHOW, C. K. 2007. Fatty acid classification and nomenclature. *Fatty Acids in Foods and Their Health Implications; Chow, CK, Ed*, 1-15.
LOCK, A. L., HORNE, C. A., BAUMAN, D. E. & SALTER, A. M. 2005. Butter naturally enriched in conjugated linoleic acid and vaccenic acid alters tissue fatty acids and improves the plasma lipoprotein profile in cholesterol-fed hamsters. *The Journal of nutrition,* 135, 1934-1939.
LODHI, I. J., WEI, X. & SEMENKOVICH, C. F. 2011. Lipoexpediency: de novo lipogenesis as a metabolic signal transmitter. *Trends in Endocrinology & Metabolism,* 22, 1-8.
LONG, J. Z., SVENSSON, K. J., TSAI, L., ZENG, X., ROH, H. C., KONG, X., RAO, R. R., LOU, J., LOKURKAR, I. & BAUR, W. 2014. A smooth muscle-like origin for beige adipocytes. *Cell metabolism,* 19, 810-820.

LOTTA, L. A., GULATI, P., DAY, F. R., PAYNE, F., ONGEN, H., VAN DE BUNT, M., GAULTON, K. J., EICHER, J. D., SHARP, S. J., LUAN, J., DE LUCIA ROLFE, E., STEWART, I. D., WHEELER, E., WILLEMS, S. M., ADAMS, C., YAGHOOTKAR, H., CONSORTIUM, E. P.-I., CAMBRIDGE, F. C., FOROUHI, N. G., KHAW, K. T., JOHNSON, A. D., SEMPLE, R. K., FRAYLING, T., PERRY, J. R., DERMITZAKIS, E., MCCARTHY, M. I., BARROSO, I., WAREHAM, N. J., SAVAGE, D. B., LANGENBERG, C., O'RAHILLY, S. & SCOTT, R. A. 2017. Integrative genomic analysis implicates limited peripheral adipose storage capacity in the pathogenesis of human insulin resistance. *Nat Genet,* 49, 17-26.

LOWELL, B. B. & BACHMAN, E. S. 2003. β-Adrenergic receptors, diet-induced thermogenesis, and obesity. *Journal of Biological Chemistry,* 278, 29385-29388.

LU, C., KUMAR, P. A., FAN, Y., SPERLING, M. A. & MENON, R. K. 2010. A novel effect of growth hormone on macrophage modulates macrophage-dependent adipocyte differentiation. *Endocrinology,* 151, 2189-99.

MACOTELA, Y., EMANUELLI, B., MORI, M. A., GESTA, S., SCHULZ, T. J., TSENG, Y. H. & KAHN, C. R. 2012. Intrinsic differences in adipocyte precursor cells from different white fat depots. *Diabetes,* 61, 1691-9.

MAIER, U.-G., ZAUNER, S., WOEHLE, C., BOLTE, K., HEMPEL, F., ALLEN, J. F. & MARTIN, W. F. 2013. Massively convergent evolution for ribosomal protein gene content in plastid and mitochondrial genomes. *Genome biology and evolution,* 5, 2318-2329.

MAZO, A., FORNER, A., DOMÈNECH, C., BUSQUETS, M., GELPÍ, J. & CORTÉS, A. 1990. Comparative Analysis of the Reduction of Oxaloacetate by Human Hepatoma and Normal Liver Extracts. *Tumor Biology,* 11, 120-128.

MCGONIGLE, P. & RUGGERI, B. 2014. Animal modules of human disease: challenges in enabling translation. *Biochemical pharmacology,* 87, 162-171.

MERKLIN, R. J. 1974. Growth and distribution of human fetal brown fat. *The Anatomical Record,* 178, 637-645.

MOSTYN, A., BISPHAM, J., PEARCE, S., EVENS, Y., RAVER, N., KEISLER, D. H., WEBB, R., STEPHENSON, T. & SYMONDS, M. E. 2002. Differential effects of leptin on thermoregulation and uncoupling protein abundance in the neonatal lamb. *FASEB JOURNAL,* 16, 1438-1440.

MOSTYN, A., PEARCE, S., BUDGE, H., ELMES, M., FORHEAD, A., FOWDEN, A., STEPHENSON, T. & SYMONDS, M. 2003. Influence of cortisol on adipose tissue development in the fetal sheep during late gestation. *Journal of Endocrinology,* 176, 23-30.

MURANO, I., ZINGARETTI, C. & CINTI, S. 2005. The adipose organ of Sv129 mice contains a prevalence of brown adipocytes and shows plasticity after cold exposure. *Adipocytes,* 1, 121-30.

NAGAI, N., SAKANE, N., TSUZAKI, K. & MORITANI, T. 2011. UCP1 genetic polymorphism (−3826 A/G) diminishes resting energy expenditure and thermoregulatory sympathetic nervous system activity in young females. *International Journal of Obesity,* 35, 1050-1055.

NATIONAL AUDIT OFFICE. 2011. *obesity* [Online]. Available: http://www.nao.org.uk/press-releases/tackling-obesity-in-england-2/ [Accessed 25/06/2015 2015].

NEDERGAARD, J., BENGTSSON, T. & CANNON, B. 2007. Unexpected evidence for active brown adipose tissue in adult humans. *American Journal of Physiology-Endocrinology and Metabolism,* 293, E444-E452.

NEE, P. W. 2013. *Key Facts on Brazil: Essential Information on Brazil*, The Internationalist.

NICE, C. F. P. H. E. A. & CARE, N. C. C. F. P. 2006. Obesity: the prevention, identification, assessment and management of overweight and obesity in adults and children.

NOLTE, R. T., WISELY, G. B., WESTIN, S., COBB, J. E., LAMBERT, M. H., KUROKAWA, R., ROSENFELD, M. G., WILLSON, T. M., GLASS, C. K. & MILBURN, M. V. 1998. Ligand binding and co-activator assembly of the peroxisome proliferator-activated receptor-γ. *Nature,* 395, 137-143.

OHIRO, Y., GARKAVTSEV, I., KOBAYASHI, S., SREEKUMAR, K. R., NANTZ, R., HIGASHIKUBO, B. T., DUFFY, S. L., HIGASHIKUBO, R., USHEVA, A. & GIUS, D. 2002. A novel p53-inducible apoptogenic gene, PRG3, encodes a homologue of the apoptosis-inducing factor (AIF). *FEBS letters,* 524, 163-171.

OHNO, H., SHINODA, K., OHYAMA, K., SHARP, L. Z. & KAJIMURA, S. 2013. EHMT1 controls brown adipose cell fate and thermogenesis through the PRDM16 complex. *Nature,* 504, 163-167.

OHNO, H., SHINODA, K., SPIEGELMAN, B. M. & KAJIMURA, S. 2012. PPARγ agonists induce a white-to-brown fat conversion through stabilization of PRDM16 protein. *Cell metabolism,* 15, 395-404.

OJHA, S., FAINBERG, H. P., WILSON, V., PELELLA, G., CASTELLANOS, M., MAY, S. T., LOTTO, A. A., SACKS, H., SYMONDS, M. E. & BUDGE, H. 2016. Gene pathway development in human epicardial adipose tissue during early life. *JCI Insight,* 1, e87460.

OKAMATSU-OGURA, Y., FUKANO, K., TSUBOTA, A., UOZUMI, A., TERAO, A., KIMURA, K. & SAITO, M. 2013. Thermogenic ability of uncoupling protein 1 in beige adipocytes in mice. *PloS one,* 8, e84229.

OKINE, E., GOONEWARDENE, L., MIR, Z., MIR, P., WANG, Z. & CHANMUGAM, P. 2003. Influence of canola oil on the fatty acid profile in goats' milk. *Canadian journal of animal science,* 83, 323-325.

ORTORI, C. A., HALLIDAY, N., CÁMARA, M., WILLIAMS, P. & BARRETT, D. A. 2014. LC-MS/MS quantitative analysis of quorum sensing signal molecules. *Pseudomonas Methods and Protocols.* Springer.

OUELLET, V., LABBE, S. M. & D. P.BLONDIN, E. A. 2012. Brown adipose tissue oxidative metabolism contributes to energy expenditure during acute cold exposure in humans. *The Journal of Clinical Investigation,* 122, 545-552.

PALMIERI, F. 2013. The mitochondrial transporter family SLC25: identification, properties and physiopathology. *Molecular aspects of medicine,* 34, 465-484.

PALMIERI, F., PIERRI, C. L., DE GRASSI, A., NUNES-NESI, A. & FERNIE, A. R. 2011. Evolution, structure and function of mitochondrial carriers: a review with new insights. *The Plant Journal,* 66, 161-181.

PARDO, R., BLASCO, N., VILÀ, M., BEIROA, D., NOGUEIRAS, R., CAÑAS, X., SIMÓ, R., SANCHIS, D. & VILLENA, J. A. 2016. EndoG knockout mice show increased brown adipocyte recruitment in white adipose tissue and improved glucose homeostasis. *Endocrinology,* 157, 3873-3887.

PARK, Y. K., PARK, B., LEE, S., CHOI, K., MOON, Y. & PARK, H. 2013. Hypoxia-inducible factor-2alpha-dependent hypoxic induction of Wnt10b expression in adipogenic cells. *J Biol Chem,* 288, 26311-22.

PEARCE, S., BUDGE, H., MOSTYN, A., GENEVER, E., WEBB, R., INGLETON, P., WALKER, A., SYMONDS, M. & STEPHENSON, T. 2005. Prolactin, the prolactin receptor and uncoupling protein abundance and function in adipose tissue during development in young sheep. *Journal of endocrinology,* 184, 351-359.

PEIRCE, V., CAROBBIO, S. & VIDAL-PUIG, A. 2014. The different shades of fat. *Nature,* 510, 76-83.

PETROVIC, N., WALDEN, T. B., SHABALINA, I. G., TIMMONS, J. A., CANNON, B. & NEDERGAARD, J. 2010. Chronic peroxisome proliferator-activated receptor γ (PPARγ) activation of epididymally derived white adipocyte cultures reveals a population of thermogenically competent, UCP1-containing adipocytes molecularly distinct from classic brown adipocytes. *Journal of Biological Chemistry,* 285, 7153-7164.

PIETILAINEN, K. H., ROG, T., SEPPANEN-LAAKSO, T., VIRTUE, S., GOPALACHARYULU, P., TANG, J., RODRIGUEZ-CUENCA, S., MACIEJEWSKI, A., NAUKKARINEN, J., RUSKEEPAA, A. L., NIEMELA, P. S., YETUKURI, L., TAN, C. Y., VELAGAPUDI, V., CASTILLO, S., NYGREN, H., HYOTYLAINEN, T., RISSANEN, A., KAPRIO, J., YKI-JARVINEN, H., VATTULAINEN, I., VIDAL-PUIG, A. & ORESIC, M. 2011. Association of lipidome remoduleing in the adipocyte membrane with acquired obesity in humans. *PLoS Biol,* 9, e1000623.

POLLARD, A. K., ORTORI, C. A., STÖGER, R., BARRETT, D. A. & CHAKRABARTI, L. 2017. Mouse mitochondrial lipid composition is defined by age in brain and muscle. *Aging (Albany NY),* 9, 986.

POPE, M., BUDGE, H. & SYMONDS, M. E. 2014. The developmental transition of ovine adipose tissue through early life. *Acta Physiologica Scandinavia,* 210, 20-30.

PORRAS, A., ÁLVAREZ, A. M., VALLADARES, A. & BENITO, M. 1997. TNF-α induces apoptosis in rat fetal brown adipocytes in primary culture. *FEBS letters,* 416, 324-328.

PUIGSERVER, P., WU, Z., PARK, C. W., GRAVES, R., WRIGHT, M. & SPIEGELMAN, B. M. 1998. A cold-inducible coactivator of nuclear receptors linked to adaptive thermogenesis. *Cell,* 92, 829-839.

RABKIN, S. 2007. Epicardial fat: properties, function and relationship to obesity. *Obesity reviews,* 8, 253-261.

RAJAKUMARI, S., WU, J., ISHIBASHI, J., LIM, H. W., GIANG, A. H., WON, K. J., REED, R. R. & SEALE, P. 2013. EBF2 determines and maintains brown adipocyte identity. *Cell Metab,* 17, 562-74.

RAVIER, M. A., LEDUC, M., RICHARD, J., LINCK, N., VARRAULT, A., PIROT, N., ROUSSEL, M. M., BOCKAERT, J., DALLE, S. & BERTRAND, G. 2014. β-Arrestin2 plays a key role in the modulation of the pancreatic beta cell mass in mice. *Diabetologia,* 57, 532-541.

RAVIPATI, S., BALDWIN, D. R., BARR, H. L., FOGARTY, A. W. & BARRETT, D. A. 2015. Plasma lipid biomarker signatures in squamous carcinoma and adenocarcinoma lung cancer patients. *Metabolomics,* 11, 1600-1611.

RIVELLESE, A. A., NATALE, C. & LILLI, S. 2002. Type of dietary fat and insulin resistance. *Annals of the New York Academy of Sciences,* 967, 329-335.

ROBINSON, L., OJHA, S., SYMONDS, M. E. & BUDGE, H. 2014. Body mass index as a determinant of brown adipose tissue function in healthy children. *The Journal of pediatrics,* 164, 318-322. e1.
ROCHARD, P., RODIER, A., CASAS, F., CASSAR-MALEK, I., MARCHAL-VICTORION, S., DAURY, L., WRUTNIAK, C. & CABELLO, G. 2000. Mitochondrial activity is involved in the regulation of myoblast differentiation through myogenin expression and activity of myogenic factors. *Journal of Biological Chemistry,* 275, 2733-2744.
ROCKSTROH, D., LANDGRAF, K., WAGNER, I. V., GESING, J., TAUSCHER, R., LAKOWA, N., KIESS, W., BUHLIGEN, U., WOJAN, M., TILL, H., BLUHER, M. & KORNER, A. 2015. Direct evidence of brown adipocytes in different fat depots in children. *PLoS One,* 10, e0117841.
ROGERS, H. A., KILDAY, J.-P., MAYNE, C., WARD, J., ADAMOWICZ-BRICE, M., SCHWALBE, E. C., CLIFFORD, S. C., COYLE, B. & GRUNDY, R. G. 2012. Supratentorial and spinal pediatric ependymomas display a hypermethylated phenotype which includes the loss of tumor suppressor genes involved in the control of cell growth and death. *Acta neuropathologica,* 123, 711-725.
ROSEBOOM, T. J., VAN DER MEULEN, J. H., OSMOND, C., BARKER, D. J., RAVELLI, A. C., SCHROEDER-TANKA, J. M., VAN MONTFRANS, G. A., MICHELS, R. P. & BLEKER, O. P. 2000. Coronary heart disease after prenatal exposure to the Dutch famine, 1944–45. *Heart,* 84, 595-598.
ROSELL, M., KAFOROU, M., FRONTINI, A., OKOLO, A., CHAN, Y.-W., NIKOLOPOULOU, E., MILLERSHIP, S., FENECH, M. E., MACINTYRE, D. & TURNER, J. O. 2014. Brown and white adipose tissues: intrinsic differences in gene expression and response to cold exposure in mice. *American Journal of Physiology-Endocrinology and Metabolism,* 306, E945-E964.
ROSS, J. S. & KRUMHOLZ, H. M. 2013. Ushering in a new era of open science through data sharing: the wall must come down. *Jama,* 309, 1355-1356.
ROY, A., CHARDIGNY, J.-M., BAUCHART, D., FERLAY, A., LORENZ, S., DURAND, D., GRUFFAT, D., FAULCONNIER, Y., SÉBÉDIO, J. & CHILLIARD, Y. 2007. Butters rich either in trans-10-C18: 1 or in trans-11-C18: 1 plus cis-9, trans-11 CLA differentially affect plasma lipids and aortic fatty streak in experimental atherosclerosis in rabbits. *Animal,* 1, 467-476.
RUSSO, G., ZEGAR, C. & GIORDANO, A. 2003. Advantages and limitations of microarray technology in human cancer. *Oncogene,* 22, 6497.
RYAN, M., MCINERNEY, D., OWENS, D., COLLINS, P., JOHNSON, A. & TOMKIN, G. 2000. Diabetes and the Mediterranean diet: a beneficial effect of oleic acid on insulin sensitivity, adipocyte glucose transport and endothelium-dependent vasoreactivity. *Qjm,* 93, 85-91.
RYU, M. J., KIM, S. J., CHOI, M. J., KIM, Y. K., LEE, M. H., LEE, S. E., CHUNG, H. K., JUNG, S. B., KIM, H.-J. & KIM, K. S. 2013. Mitochondrial oxidative phosphorylation reserve is required for hormone-and PPARγ agonist-induced adipogenesis. *Molecules and cells,* 35, 134-141.
SACKS, H. & SYMONDS, M. E. 2013. Anatomical Locations of Human Brown Adipose Tissue: Functional Relevance and Implications in Obesity and Type 2 Diabetes. *Diabetes,* 62, 1783-1790.
SACKS, H. S. & FAIN, J. N. 2007. Human epicardial adipose tissue: a review. *American heart journal,* 153, 907-917.

SACKS, H. S., FAIN, J. N., BAHOUTH, S. W., OJHA, S., FRONTINI, A., BUDGE, H., CINTI, S. & SYMONDS, M. E. 2013. Adult epicardial fat exhibits beige features. *The Journal of Clinical Endocrinology & Metabolism,* 98, E1448-E1455.

SADURSKIS, A., DICKER, A., CANNON, B. & NEDERGAARD, J. 1995. Polyunsaturated fatty acids recruit brown adipose tissue: increased UCP content and NST capacity. *American Journal of Physiology-Endocrinology And Metabolism,* 269, E351-E360.

SAELY, C., GEIGER, K. & DREXEL, H. 2012. Brown versus white adipose tissue: a mini-review. *Gerontology,* 58, 15-23.

SAITO, M. 2013. Brown adipose tissue as a therapeutic target for human obesity. *Obesity research & clinical practice,* 7, e432-e438.

SAITO, M., OKAMATSU-OGURA, Y., MATSUSHITA, M., WATANABE, K., YONESHIRO, T., NIO-KOBAYASHI, J., IWANAGA, T., MIYAGAWA, M., KAMEYA, T. & NAKADA, K. 2009. High incidence of metabolically active brown adipose tissue in healthy adult humans effects of cold exposure and adiposity. *Diabetes,* 58, 1526-1531.

SAMPATH, H. & NTAMBI, J. M. 2005. Polyunsaturated fatty acid regulation of genes of lipid metabolism. *Annu. Rev. Nutr.,* 25, 317-340.

SAROHA, V., DELLSCHAFT, N. S., KEISLER, D. H., GARDNER, D. S., BUDGE, H., SEBERT, S. P. & SYMONDS, M. E. 2018. Tissue cell stress response to obesity and its interaction with late gestation diet. *Reproduction, Fertility and Development,* 30, 430-441.

SCARPULLA, R. C. 2008. Transcriptional paradigms in mammalian mitochondrial biogenesis and function. *Physiological reviews,* 88, 611-638.

SCHULTZ, B. E. & CHAN, S. I. 2001. Structures and proton-pumping strategies of mitochondrial respiratory enzymes. *Annual review of biophysics and biomolecular structure,* 30, 23-65.

SCOTNEY, H., SYMONDS, M. E., LAW, J., BUDGE, H., SHARKEY, D. & MANOLOPOULOS, K. N. 2017. Glucocorticoids modulate human brown adipose tissue thermogenesis in vivo. *Metabolism,* 70, 125-132.

SEALE, P., CONROE, H. M., ESTALL, J., KAJIMURA, S., FRONTINI, A., ISHIBASHI, J., COHEN, P., CINTI, S. & SPIEGELMAN, B. M. 2011. Prdm16 determines the thermogenic program of subcutaneous white adipose tissue in mice. *The Journal of clinical investigation,* 121, 96.

SEALE, P., KAJIMURA, S., YANG, W., CHIN, S., ROHAS, L. M., ULDRY, M., TAVERNIER, G., LANGIN, D. & SPIEGELMAN, B. M. 2007. Transcriptional control of brown fat determination by PRDM16. *Cell metabolism,* 6, 38-54.

SEBERT, S., HYATT, M., CHAN, L., PATEL, N., BELL, R., KEISLER, D., STEPHENSON, T., BUDGE, H., SYMONDS, M. & GARDNER, D. 2009. Maternal nutrient restriction between early and midgestation and its impact upon appetite regulation after juvenile obesity. *Endocrinology,* 150, 634-641.

SEIDELL, J. C., BJORNTORP, P., SJOSTROM, L., KVIST, H. & SANNERSTEDT, R. 1990. Visceral fat accumulation in men is positively associated with insulin, glucose, and C-peptide levels, but negatively with testosterone levels. *Metabolism,* 39, 897-901.

SHARKEY, D., FAINBERG, H. P., WILSON, V., HARVEY, E., GARDNER, D. S., SYMONDS, M. E. & BUDGE, H. 2009. Impact of early onset obesity and

hypertension on the unfolded protein response in renal tissues of juvenile sheep. *Hypertension,* 53, 925-31.
SHARMA, A., GRUMMER-STRAWN, L., DALENIUS, K., GALUSKA, D., ANANDAPPA, M., BORLAND, E., MACKINTOSH, H. & SMITH, R. 2009. Obesity prevalence among low-income, preschool-aged children-United States, 1998-2008. *Morbidity and Mortality Weekly Report,* 58, 769-773.
SHERMAN, B. & LEMPICKI, R. 2009. Systematic and integrative analysis of large gene lists using DAVID bioinformatics resources. *Nat Protoc,* 4, 44-57.
SHIMOMURA, I., HAMMER, R. E., RICHARDSON, J. A., IKEMOTO, S., BASHMAKOV, Y., GOLDSTEIN, J. L. & BROWN, M. S. 1998. Insulin resistance and diabetes mellitus in transgenic mice expressing nuclear SREBP-1c in adipose tissue: module for congenital generalised lipodystrophy. *Genes & development,* 12, 3182-3194.
SHINGFIELD, K., LEE, M., HUMPHRIES, D. J., SCOLLAN, N., TOIVONEN, V., REYNOLDS, C. K. & BEEVER, D. 2010. Effect of incremental amounts of fish oil in the diet on ruminal lipid metabolism in growing steers. *British journal of nutrition,* 104, 56-66.
SHIRANI, J., BEREZOWSKI, K. & ROBERTS, W. C. 1995. Quantitative measurement of normal and excessive (cor adiposum) subepicardial adipose tissue, its clinical significance, and its effect on electrocardiographic QRS voltage. *The American journal of cardiology,* 76, 414-418.
SIDOSSIS, L. & KAJIMURA, S. 2015. Brown and beige fat in humans: thermogenic adipocytes that control energy and glucose homeostasis. *The Journal of Clinical Investigation,* 125, 478-486.
SIDOSSIS, L. S., PORTER, C., SARAF, M. K., BORSHEIM, E., RADHAKRISHNAN, R. S., CHAO, T., ALI, A., CHONDRONIKOLA, M., MLCAK, R., FINNERTY, C. C., HAWKINS, H. K., TOLIVER-KINSKY, T. & HERNDON, D. N. 2015. Browning of Subcutaneous White Adipose Tissue in Humans after Severe Adrenergic Stress. *Cell Metab,* 22, 219-27.
SMYTH, G. K. 2004. Linear modules and empirical bayes methods for assessing differential expression in microarray experiments. *Statistical applications in genetics and molecular biology,* 3, 1-25.
SNITKER, S., FUJISHIMA, Y., SHEN, H., OTT, S., PI-SUNYER, X., FURUHATA, Y., SATO, H. & TAKAHASHI, M. 2009. Effects of novel capsinoid treatment on fatness and energy metabolism in humans: possible pharmacogenetic implications. *The American journal of clinical nutrition,* 89, 45-50.
SONS, H. & HOFFMANN, V. 1985. Epicardial fat cell size, fat distribution and fat infiltration of the right and left ventricle of the heart. *Anatomischer Anzeiger,* 161, 355-373.
SPALDING, K. L., ARNER, E., WESTERMARK, P. O., BERNARD, S., BUCHHOLZ, B. A., BERGMANN, O., BLOMQVIST, L., HOFFSTEDT, J., NASLUND, E., BRITTON, T., CONCHA, H., HASSAN, M., RYDEN, M., FRISEN, J. & ARNER, P. 2008. Dynamics of fat cell turnover in humans. *Nature,* 453, 783-7.
STEGER, R., DEPAOLO, L., ASCH, R. & SILVERMAN, A. 1983. Interactions of Δ9-tetrahydrocannabinol (THC) with hypothalamic neurotransmitters controlling luteinisang hormone and prolactin release. *Neuroendocrinology,* 37, 361-370.
STEIN, C., FALL, C., KUMARAN, K., OSMOND, C., BARKER, D. & COX, V. 1996. Fetal growth and coronary heart disease in South India. *The Lancet,* 348, 1269-1273.

STERN-STRAETER, J., BONATERRA, G. A., KASSNER, S. S., ZÜGEL, S., HÖRMANN, K., KINSCHERF, R. & GOESSLER, U. R. 2011. Characterization of human myoblast differentiation for tissue-engineering purposes by quantitative gene expression analysis. *Journal of tissue engineering and regenerative medicine,* 5.

SVENSSON, P.-A., JERNÅS, M., SJÖHOLM, K., HOFFMANN, J. M., NILSSON, B. E., HANSSON, M. & CARLSSON, L. 2011. Gene expression in human brown adipose tissue. *International journal of molecular medicine,* 27, 227-232.

SYMONDS, M., PHILLIPS, I., ANTHONY, R., OWENS, J. A. & MCMILLEN, I. C. 1998. Prolactin receptor gene expression and foetal adipose tissue. *J Neuroendocrinol,* 10, 4.

SYMONDS, M., POPE, M., SHARKEY, D. & BUDGE, H. 2012. Adipose tissue and fetal programming. *Diabetologia,* 55, 1597-1606.

SYMONDS, M. E. 2007. Integration of physiological and molecular mechanisms of the developmental origins of adult disease: new concepts and insights. *Proceedings of the Nutrition Society,* 66, 442-450.

SYMONDS, M. E. 2013. Brown adipose tissue growth and development. *Scientifica,* 2013.

SYMONDS, M. E., PEARCE, S., BISPHAM, J., GARDNER, D. S. & STEPHENSON, T. 2004. Timing of nutrient restriction and programming of fetal adipose tissue development. *Proceedings of the Nutrition Society,* 63, 397-403.

SYMONDS, M. E., POPE, M. & BUDGE, H. 2015. The ontogeny of brown adipose tissue. *Annual Review of Nutrition,* 35, 295-320.

SYMONDS, M. E., SEBERT, S. & BUDGE, H. 2011. The obesity epidemic: from the environment to epigenetics–not simply a response to dietary manipulation in a thermoneutral environment. *Frontiers in genetics,* 2.

TAKAHASHI, A., ADACHI, S., MORITA, M., TOKUMASU, M., NATSUME, T., SUZUKI, T. & YAMAMOTO, T. 2015. Post-transcriptional Stabilization of Ucp1 mRNA Protects Mice from Diet-Induced Obesity. *Cell Rep,* 13, 2756-67.

TAM, C. S., LECOULTRE, V. & RAVUSSIN, E. 2012. Brown Adipose Tissue Mechanisms and Potential Therapeutic Targets. *Circulation,* 125, 2782-2791.

TIERNEY, A. C. & ROCHE, H. M. 2007. The potential role of olive oil-derived MUFA in insulin sensitivity. *Molecular nutrition & food research,* 51, 1235-1248.

TIMMONS, J. A., WENNMALM, K., LARSSON, O., WALDEN, T. B., LASSMANN, T., PETROVIC, N., HAMILTON, D. L., GIMENO, R. E., WAHLESTEDT, C. & BAAR, K. 2007. Myogenic gene expression signature establishes that brown and white adipocytes originate from distinct cell lineages. *Proceedings of the National Academy of Sciences,* 104, 4401-4406.

TINAHONES, F. J., ARAGÜEZ, L. C., MURRI, M., OLIVERA, W. O., TORRES, M. D. M., BARBARROJA, N., GOMEZ, R. H., DEL MAR MALAGÓN, M. & EL BEKAY, R. 2012. Caspase induction and BCL2 inhibition in human adipose tissue: a potential relationship with insulin signaling alteration. *Diabetes care*, DC_120194.

TIRABY, C. & LANGIN, D. 2003. Conversion from white to brown adipocytes: a strategy for the control of fat mass? *Trends in Endocrinology & Metabolism,* 14, 439-441.

TSENG, Y.-H., KOKKOTOU, E., SCHULZ, T. J., HUANG, T. L., WINNAY, J. N., TANIGUCHI, C. M., TRAN, T. T., SUZUKI, R., ESPINOZA, D. O. & YAMAMOTO, Y. 2008. New role of bone morphogenetic protein 7 in brown adipogenesis and energy expenditure. *Nature,* 454, 1000-1004.
ULDRY, M., YANG, W., ST-PIERRE, J., LIN, J., SEALE, P. & SPIEGELMAN, B. M. 2006. Complementary action of the PGC-1 coactivators in mitochondrial biogenesis and brown fat differentiation. *Cell metabolism,* 3, 333-341.
VAN BREUKELEN, F., SONENBERG, N. & MARTIN, S. L. 2004. Seasonal and state-dependent changes of eIF4E and 4E-BP1 during mammalian hibernation: implications for the control of translation during torpor. *American Journal of Physiology-Regulatory, Integrative and Comparative Physiology,* 287, R349-R353.
VAN DE VIJVER, L., KARDINAAL, A., COUET, C., ARO, A., KAFATOS, A., STEINGRIMSDOTTIR, L., CRUZ, J. A., MOREIRAS, O., BECKER, W. & VAN AMELSVOORT, J. 2000. Association between trans fatty acid intake and cardiovascular risk factors in Europe: the TRANSFAIR study. *European journal of clinical nutrition,* 54, 126.
VAN MARKEN LICHTENBELT, W. D., VANHOMMERIG, J. W., SMULDERS, N. M., DROSSAERTS, J. M., KEMERINK, G. J., BOUVY, N. D., SCHRAUWEN, P. & TEULE, G. J. 2009. Cold-activated brown adipose tissue in healthy men. *New England Journal of Medicine,* 360, 1500-1508.
VARGAS, D., SHIMOKAWA, N., KANEKO, R., ROSALES, W., PARRA, A., CASTELLANOS, A., KOIBUCHI, N. & LIZCANO, F. 2016. Regulation of human subcutaneous adipocyte differentiation by EID1. *J Mol Endocrinol,* 56, 113-22.
VERGNES, L., DAVIES, G. R., LIN, J. Y., YEH, M. W., LIVHITS, M. J., HARARI, A., SYMONDS, M. E., SACKS, H. S. & REUE, K. 2016. Adipocyte browning and higher mitochondrial function in periadrenal but not SC fat in pheochromocytoma. *The Journal of Clinical Endocrinology & Metabolism,* 101, 4440-4448.
VERNON, R. G., ROBERTSON, J. P., CLEGG, R. A. & FLINT, D. J. 1981. Aspects of adipose-tissue metabolism in foetal lambs. *Biochem. J,* 196, 819-824.
VICENTE-MANZANARES, M., MA, X., ADELSTEIN, R. S. & HORWITZ, A. R. 2009. Non-muscle myosin II takes centre stage in cell adhesion and migration. *Nature reviews. Molecular cell biology,* 10, 778.
VIENGCHAREUN, S., SERVEL, N., FÈVE, B., FREEMARK, M., LOMBÈS, M. & BINART, N. 2008. Prolactin receptor signaling is essential for perinatal brown adipocyte function: a role for insulin-like growth factor-2. *PLoS One,* 3, e1535-e1535.
VIJGEN, G. H. E. J., BOUVY, N. D., G. J. J. TEULE, B. B., SCHRAUWEN, P. & LICHTENBELT, W. D. V. M. 2011. Brown adipose tissue in morbidly obese subjects. *PLoS ONE,* 6.
VIRTANEN, K. A., LIDELL, M. E., ORAVA, J., HEGLIND, M., WESTERGREN, R., NIEMI, T., TAITTONEN, M., LAINE, J., SAVISTO, N.-J. & ENERBÄCK, S. 2009. Functional brown adipose tissue in healthy adults. *New England Journal of Medicine,* 360, 1518-1525.
VOGEL, C. & MARCOTTE, E. M. 2012. Insights into the regulation of protein abundance from proteomic and transcriptomic analyses. *Nature Reviews Genetics,* 13, 227.

WANG, J., LIU, R., WANG, F., HONG, J., LI, X., CHEN, M., KE, Y., ZHANG, X., MA, Q. & WANG, R. 2013. Ablation of LGR4 promotes energy expenditure by driving white-to-brown fat switch. *Nature cell biology,* 15, 1455-1463.
WANG, W. & SEALE, P. 2016. Control of brown and beige fat development. *Nature reviews Molecular cell biology,* 17, 691.
WEGGEMANS, R. M., RUDRUM, M. & TRAUTWEIN, E. A. 2004. Intake of ruminant versus industrial trans fatty acids and risk of coronary heart disease–what is the evidence? *European journal of lipid science and technology,* 106, 390-397.
WELTER, K. C., MARTINS, C. M. D. M. R., DE PALMA, A. S. V., MARTINS, M. M., DOS REIS, B. R., SCHMIDT, B. L. U. & NETTO, A. S. 2016. Canola oil in lactating dairy cow diets reduces milk saturated fatty acids and improves its omega-3 and oleic fatty acid content. *PloS one,* 11, e0151876.
WENE, J. D., CONNOR, W. & DENBESTEN, L. 1975. The development of essential fatty acid deficiency in healthy men fed fat-free diets intravenously and orally. *The Journal of clinical investigation,* 56, 127-134.
WESTERTERP, K. & GORAN, M. 1997. Relationship between physical activity related energy expenditure and body composition: a gender difference. *International journal of obesity,* 21, 184.
WETTENHALL, J. M. & SMYTH, G. K. 2004. limmaGUI: a graphical user interface for linear moduleing of microarray data. *Bioinformatics,* 20, 3705-3706.
WHO. 2015. *http://www.who.int/mediacentre/factsheets/fs311/en/* [Online]. [Accessed 25/06/2015 2015].
WHO 2016. http://www.who.int/topics/obesity/en/.
WILLEMSEN, M., VULTO-VAN SILFHOUT, A., NILLESEN, W., WISSINK-LINDHOUT, W., VAN BOKHOVEN, H., PHILIP, N., BERRY-KRAVIS, E., KINI, U., VAN RAVENSWAAIJ-ARTS, C. & DELLE CHIAIE, B. 2011. Update on Kleefstra syndrome. *Molecular syndromology,* 2, 202-212.
WILLLIAMS, P. 1995. The anatomical basis of medicine and surgery. Gray's Anatomy.
WRIGHT, J. & HARWOOD, V. 2012. *Biopolitics and the'obesity epidemic': governing bodies*, Routledge.
WU, J., BOSTRÖM, P., SPARKS, L. M., YE, L., CHOI, J. H., GIANG, A.-H., KHANDEKAR, M., VIRTANEN, K. A., NUUTILA, P. & SCHAART, G. 2012. Beige adipocytes are a distinct type of thermogenic fat cell in mouse and human. *Cell,* 150, 366-376.
WU, J., COHEN, P. & SPIEGELMAN, B. M. 2013. Adaptive thermogenesis in adipocytes: Is beige the new brown? *Genes & development,* 27, 234-250.
XUE, B., RIM, J.-S., HOGAN, J. C., COULTER, A. A., KOZA, R. A. & KOZAK, L. P. 2007. Genetic variability affects the development of brown adipocytes in white fat but not in interscapular brown fat. *Journal of lipid research,* 48, 41-51.
YADAV, H., QUIJANO, C., KAMARAJU, A. K., GAVRILOVA, O., MALEK, R., CHEN, W., ZERFAS, P., ZHIGANG, D., WRIGHT, E. C. & STUELTEN, C. 2011. Protection from obesity and diabetes by blockade of TGF-β/Smad3 signaling. *Cell metabolism,* 14, 67-79.
YAMADA, Y., WANG, X. D., YOKOYAMA, S., FUKUDA, N. & TAKAKURA, N. 2006. Cardiac progenitor cells in brown adipose tissue repaired damaged myocardium. *Biochem Biophys Res Commun,* 342, 662-70.

YAO, D., SHI, W., GOU, Y., ZHOU, X., AW, T. Y., ZHOU, Y. & LIU, Z. 2005. Fatty acid-mediated intracellular iron translocation: a synergistic mechanism of oxidative injury. *Free Radical Biology and Medicine,* 39, 1385-1398.

YEOH, E.-J., ROSS, M. E., SHURTLEFF, S. A., WILLIAMS, W. K., PATEL, D., MAHFOUZ, R., BEHM, F. G., RAIMONDI, S. C., RELLING, M. V. & PATEL, A. 2002. Classification, subtype discovery, and prediction of outcome in pediatric acute lymphoblastic leukemia by gene expression profiling. *Cancer cell,* 1, 133-143.

YONESHIRO, T., AITA, S., MATSUSHITA, M., OKAMATSU-OGURA, Y., KAMEYA, T., KAWAI, Y., MIYAGAWA, M., TSUJISAKI, M. & SAITO, M. 2011. Age-Related Decrease in Cold-Activated Brown Adipose Tissue and Accumulation of Body Fat in Healthy Humans. *Obesity,* 19, 1755-1760.

YONESHIRO, T., OGAWA, T., OKAMOTO, N., MATSUSHITA, M., AITA, S., KAMEYA, T., KAWAI, Y., IWANAGA, T. & SAITO, M. 2013. Impact of UCP1 and β3AR gene polymorphisms on age-related changes in brown adipose tissue and adiposity in humans. *International journal of obesity,* 37, 993-998.

ZHANG, B. & HORVATH, S. 2005. A general framework for weighted gene co-expression network analysis. *Statistical applications in genetics and molecular biology,* 4.

ZHANG, G., SUN, Q. & LIU, C. 2016. Influencing factors of thermogenic adipose tissue activity. *Frontiers in physiology,* 7.

9 Appendix

9.1 Supplementary data

All the supplementary dataset, including the statistical results of gene expression, gene co-expression modules, gene ontogeny, and the lipids composition details, have been published and uploaded by DR. Hernan P. Fainberg here: https://doi.org/10.1038/s41598-018-27376-3.

9.2 RNA concentration and Bioanalyzer data.

Table 9-1 RNA concentration extracted from subcutaneous adipose tissue.

Sample number	Sex	Group	Age	concentration ng/ul
105	M	control	7 day	1367
117	M	control	7 day	2660
130	M	control	7 day	822
122	F	control	7 day	1886
115	F	control	7 day	1704
136	M	control	28 day	2833
141	M	control	28 day	2651
146	M	control	28 day	2453
153	F	control	28 day	2455
155	F	control	28 day	2833

Table 9-2 RNA concentration extracted from omental adipose tissue.

sample number	Sex	Group	Age	concentration (ng/ul)
105	M	control	7 day	1534
117	M	control	7 day	1656
130	M	control	7 day	1396
122	F	control	7 day	1677
115	F	control	7 day	821
141	F	control	28 day	1263
146	M	control	28 day	1276
153	M	control	28 day	2176
155	M	control	28 day	1029
159	F	control	28 day	3433

Table 9-3 RNA concentration extracted from perirenal adipose tissue.

Sample number	Sex	Group	Age	concentration (ng/ul)
105	M	control	7 day	1408
117	M	control	7 day	1584
130	M	control	7 day	1769
109	F	control	7 day	753
115	F	control	7 day	660
146	M	control	28 day	1541
153	M	control	28 day	1371
150	F	control	28 day	1215
141	F	control	28 day	1678
155	F	control	28 day	1773
137	M	canola	28 day	1579
142	M	canola	28 day	1050
145	M	canola	28 day	1177
158	F	canola	28 day	1897
160	F	canola	28 day	1857

Table 9-4 RNA concentration extracted from epicardial adipose tissue.

Sample number	Sex	Group	Age	concentration (ng/ul)
105	M	control	7 day	676
117	M	control	7 day	1332
130	M	control	7 day	663
122	F	control	7 day	978
115	F	control	7 day	320
146	M	control	28 day	2455
151	M	control	28 day	2833
155	M	control	28 day	2651
141	F	control	28 day	2453
159	F	control	28 day	3113

Table 9-5 RNA concentration extracted from sternal adipose tissue

sample number	Gender	Group	Age	concentration (ng/ul)
105	M	Control	7 days	713
109	F	Control	7 days	858
117	M	Control	7 days	810
122	F	Control	7 days	843
130	F	Control	7 days	846
141	F	Control	28 Days	2117
146	M	Control	28 Days	1329
153	M	Control	28 Days	994
155	M	Control	28 Days	2081
159	F	Control	28 Days	1536
106	F	Canola	7 days	858
119	M	Canola	7 days	810
124	M	Canola	7 days	843
139	M	Canola	7 days	846
133	M	Canola	28 Days	3239
137	M	Canola	28 Days	2131
142	F	Canola	28 Days	1410
152	F	Canola	28 Days	2052

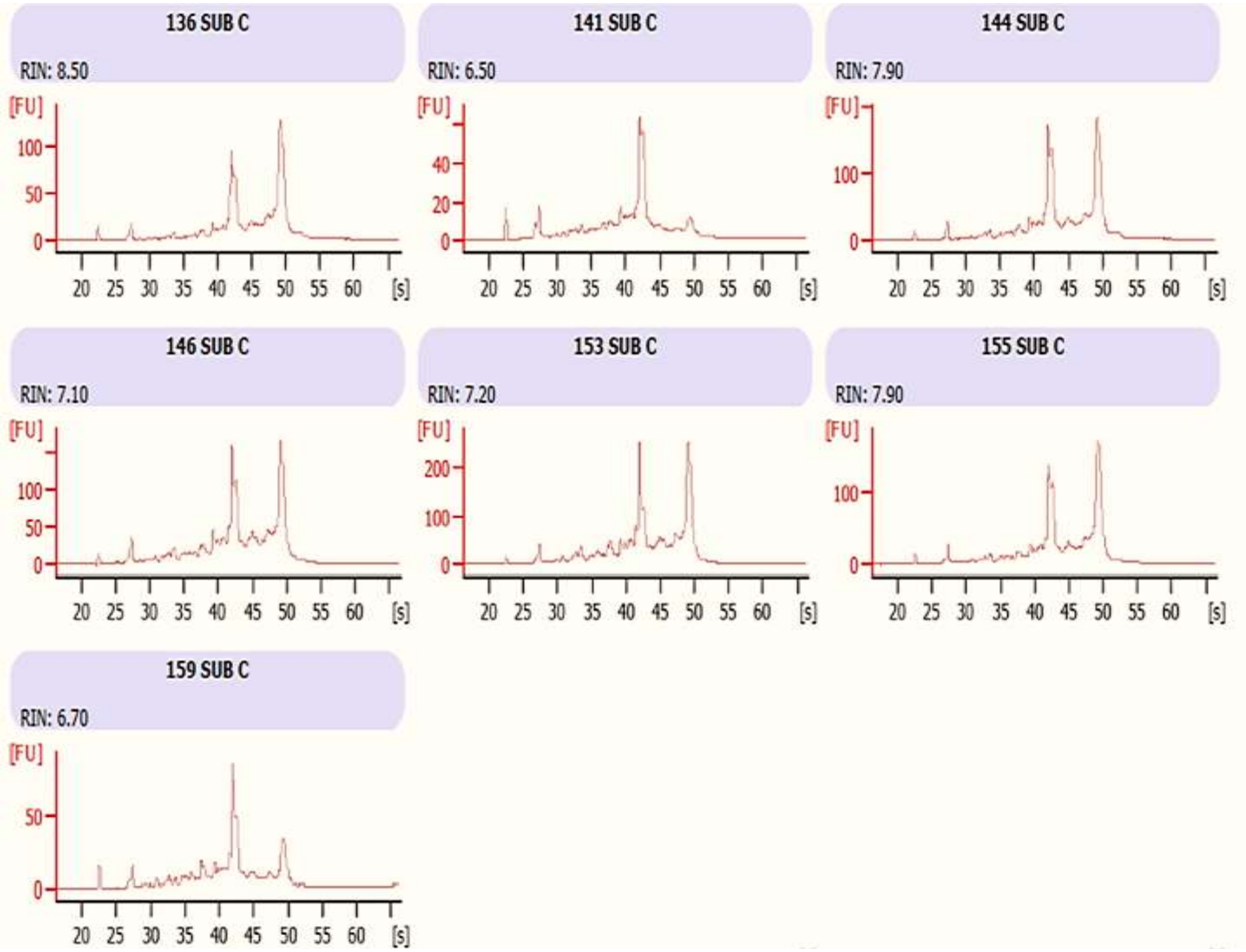

Figure 9-1 Chromatograms of micro-capillary electrophoresis in subcutaneous fat

RNA samples (in numbers) of subcutaneous fat (SUB) in control group (C) at 28 days of age showing different degrees of integrity indicated by multiple peaks in the electropherogram and Fluorescent Unite (FU) by time in seconds.

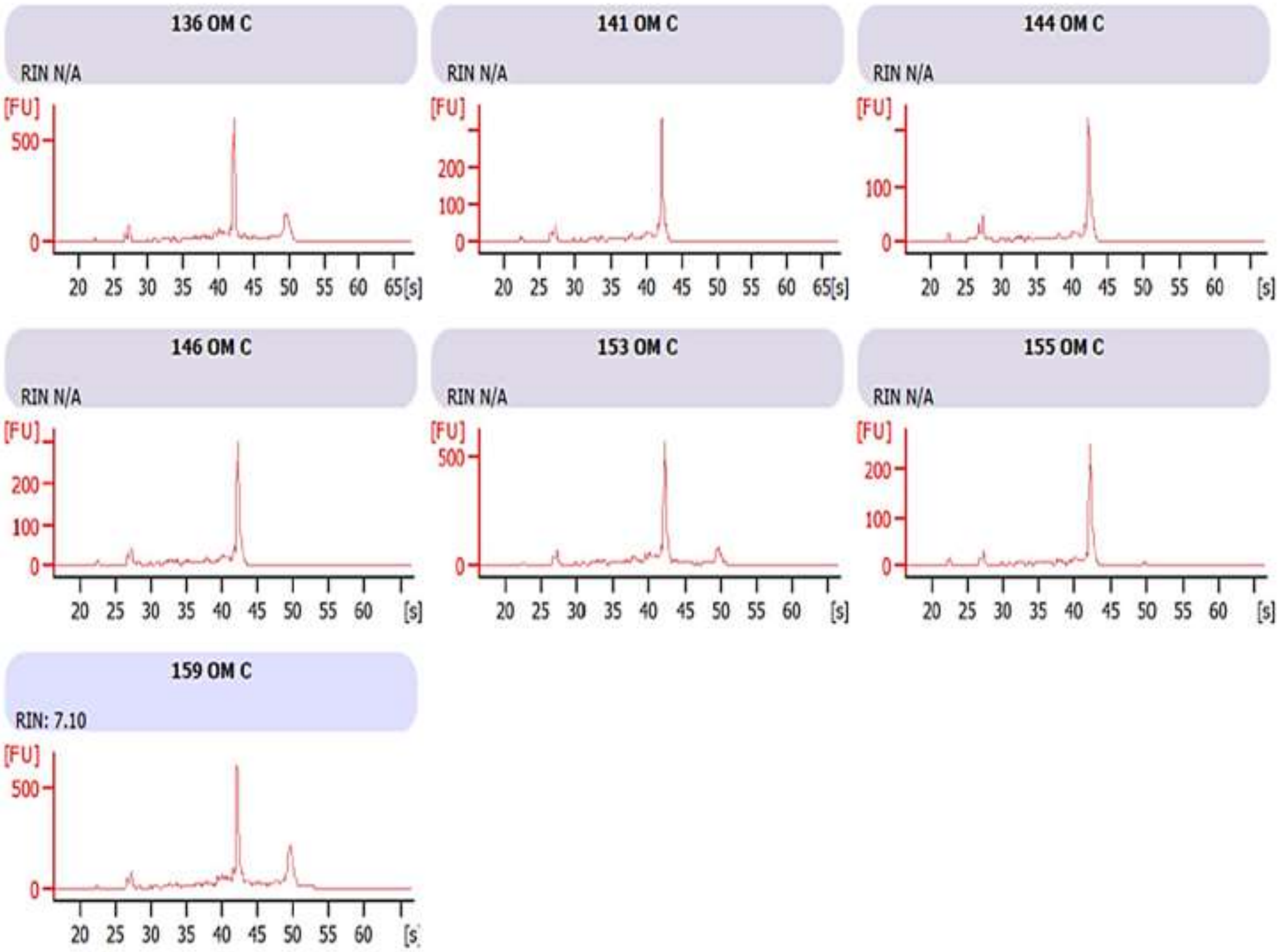

Figure 9-2 Chromatograms of micro-capillary electrophoresis in omental fat

RNA samples (in number) of omental fat (OM) in control group (C) at 28 days of age showing different degrees of integrity indicated by multiple peaks in the electropherogram and fluorescent signal (FU) by time in seconds.

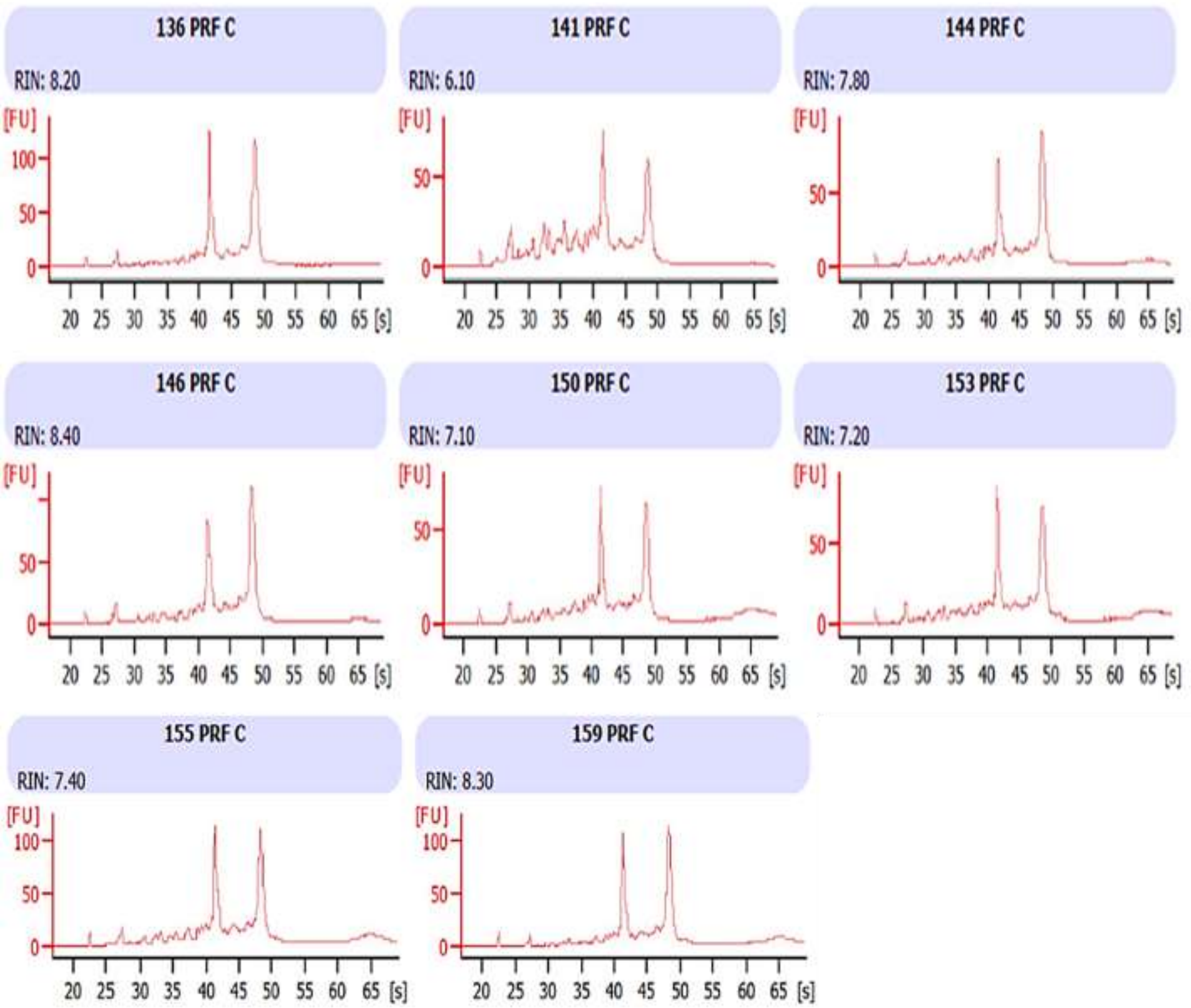

Figure 9-3 Chromatograms of micro-capillary electrophoresis in perirenal fat

RNA samples (in number) of perirenal fat (PRF) in control group (C) at 28 days of age showing different degrees of integrity indicated by multiple peaks in the electropherogram and fluorescent signal (FU) by time in seconds.

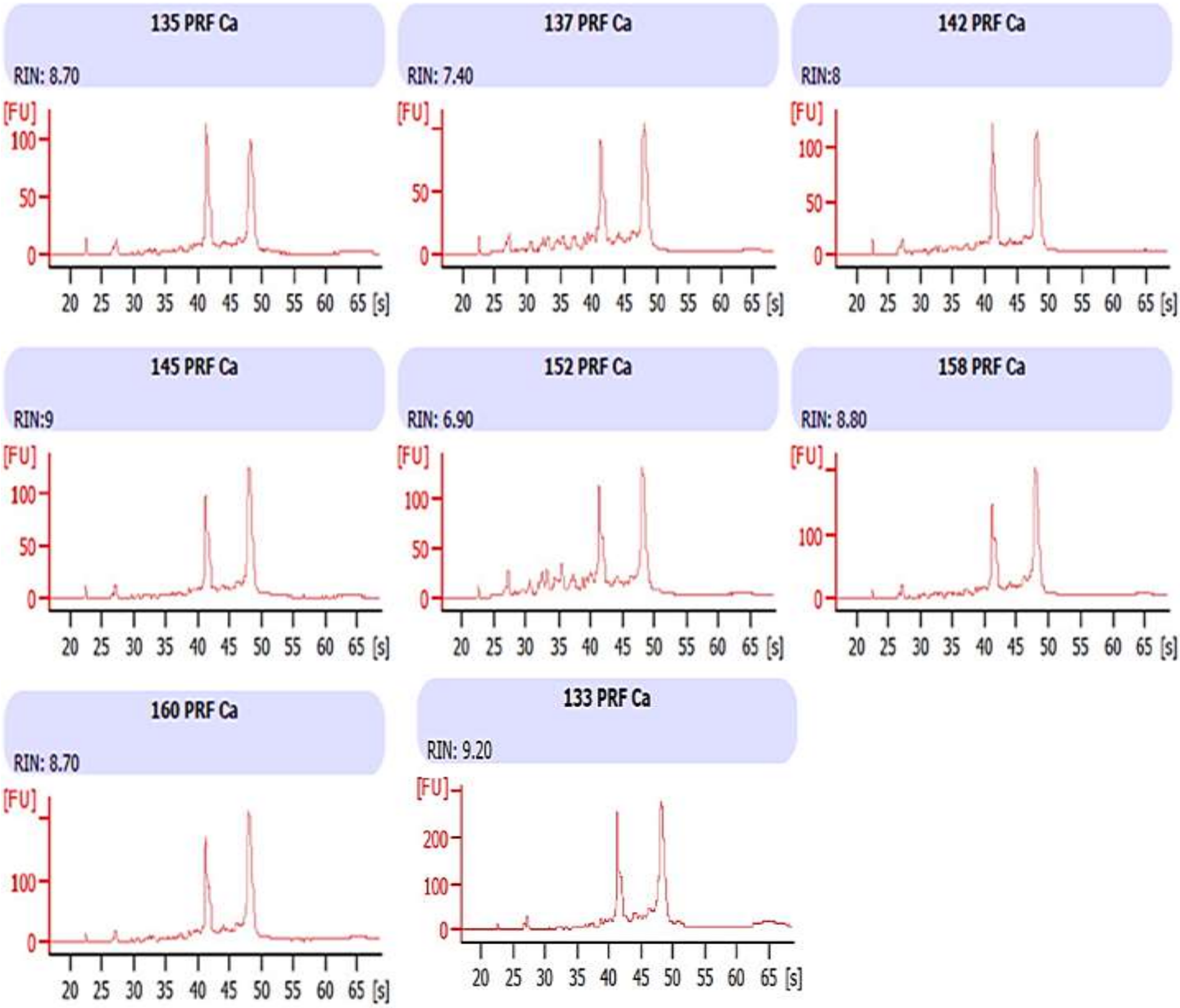

Figure 9-4 Chromatograms of micro-capillary electrophoresis in perirenal fat

RNA samples (in number) of perirenal fat (PRF) in canola diet group (Ca) at 28 days of age showing different degrees of integrity indicated by multiple peaks in the electropherogram and fluorescent unite (FU) by time in seconds.

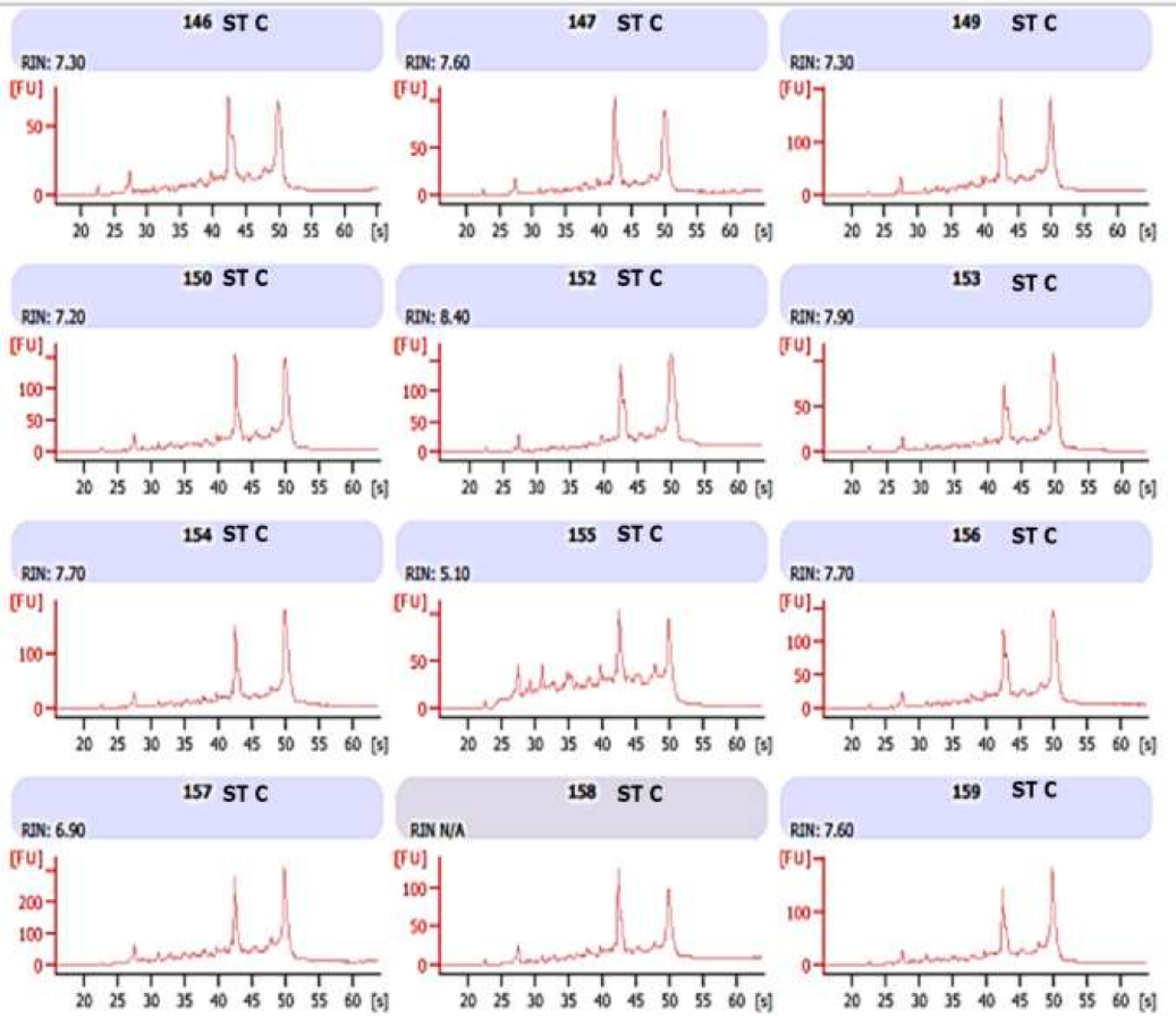

Figure 9-5 Chromatograms of micro-capillary electrophoresis in Sternal fat

RNA samples (in number) of Sternal fat (ST) in control group (C) at 28 days of age showing different degrees of integrity indicated by multiple peaks in the electropherogram and fluorescent signal (FU) by time in seconds.

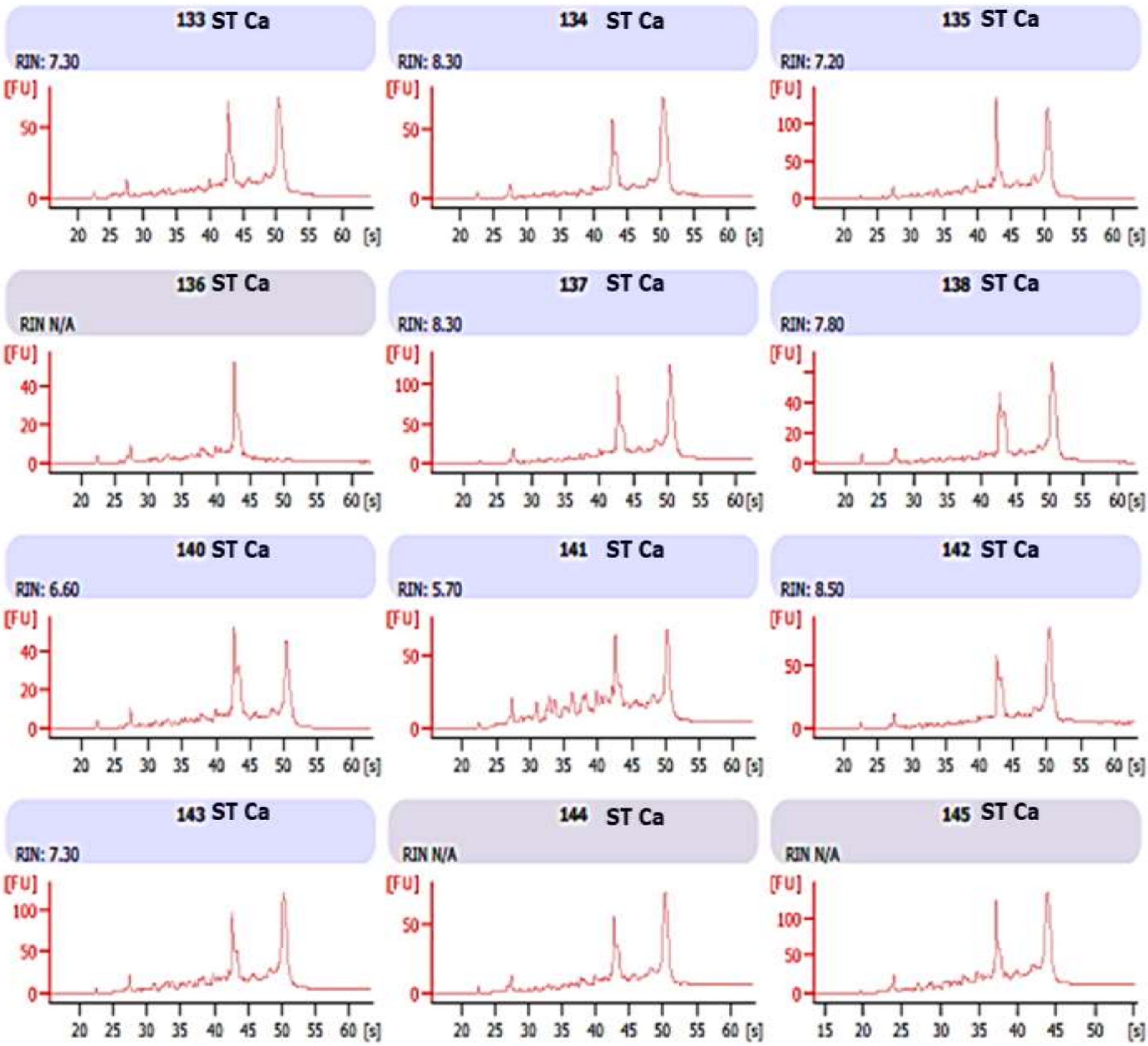

Figure 9-6 Chromatograms of micro-capillary electrophoresis in Sternal fat

RNA samples (in number) of Sternal fat (ST) in canola group (Ca) at 28 days of age showing different degrees of integrity indicated by multiple peaks in the electropherogram and fluorescent signal (FU) by time in seconds.

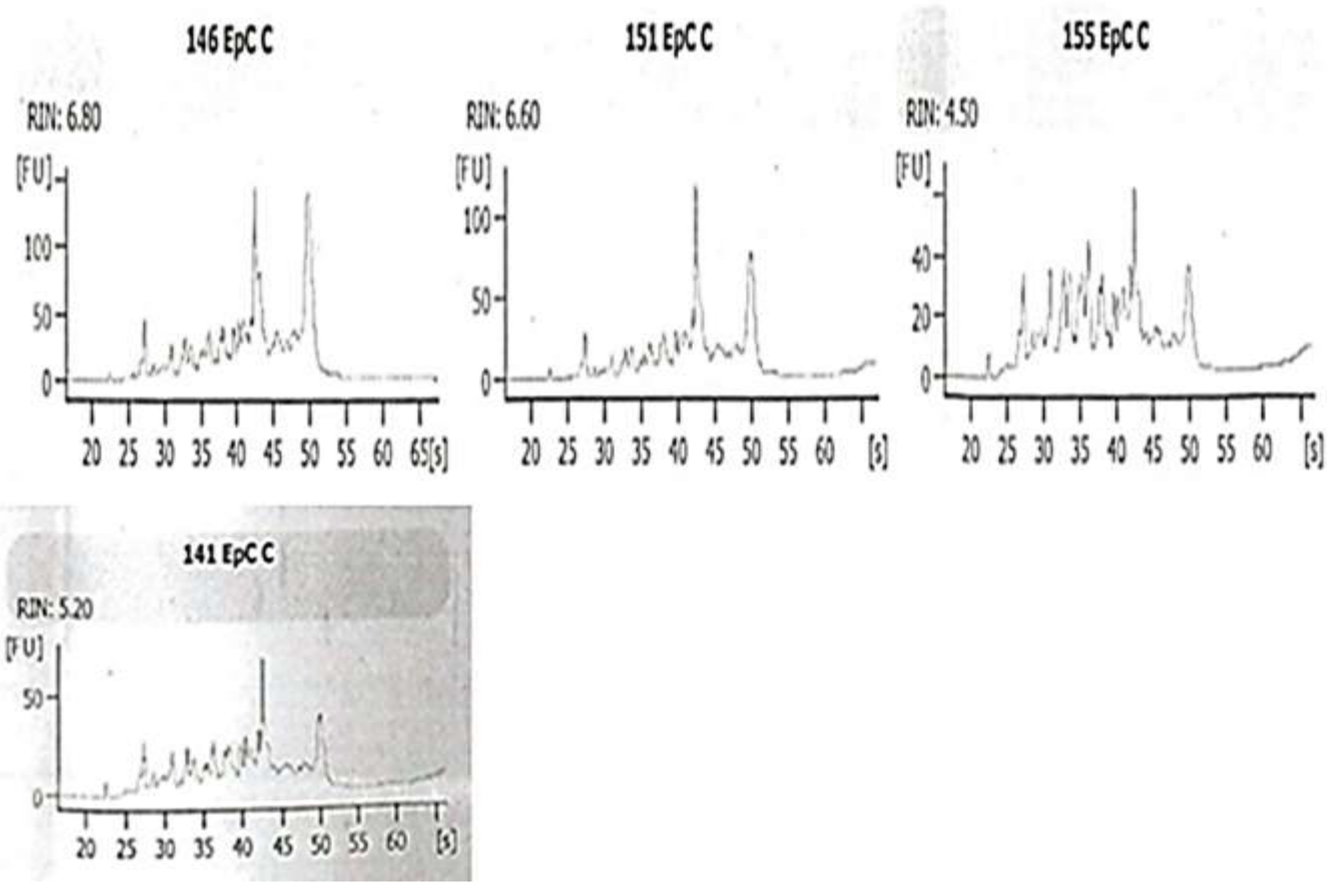

Figure 9-7 Chromatograms of micro-capillary electrophoresis in epicardial fat

RNA samples (in number) of epicardial fat (EpC) in control group (C) at 28 days of age showing different degrees of integrity indicated by multiple peaks in the electropherogram and fluorescent signal (FU) by time in seconds.

9.3 Area under the curve (AUC) values in ROC curve

The validity of each interaction module with age was tested using the power of different statistical measurements obtained from the area under the curve (AUC) and ROC plot. This included false and true positive rate in the performance of the specificity and sensitivity of the classification, assessed by a range from 0 to 1 where 1 indicates high efficiency (see Table 9-6).

Table 9-6 Criterion values and coordinates of the ROC curve from seven to 28 days of adipose tissue

Measure	Overall depot	Epc	Per	Ste	Ome	Sub
Error Rate	0	0	0	0	0	0
Accuracy	1	1	1	1	1	1
Specificity	1	1	1	1	1	1
Sensitivity	1	1	1	1	1	1
Negative Predictive Value	1	1	1	1	1	1
Positive Predictive Value	1	1	1	1	1	1
False Positive Rate	0	0	0	0	0	0
False Negative Rate	0	0	0	0	0	0
Power	1	1	1	1	1	1
Likelihood Ratio Negative	0	0	0	0	0	0
Naïve Error Rate	0.4	0.1	0.1	0.2	0.2	0.1

*Epicardial (EPC), Perirenal (Per), Sternal (Ste), Omental (Ome), Subcutaneous (Sub)

9.4 List of suppliers

ABgene	Abgene House, Blenheim Road, Epsom, KT19 9AP, UK. www.abgene.com
Affymetrix UK Ltd	Wycombe Lane, High Wycombe HP10 0HH, UK. www.thermofisher.com
Agilent Technologies	5301 Stevens Creek Blvd, Santa Clara, CA 95051, USA. www.agilent.com
Alpha Diagnostic International	6203 Woodlake Center, San Antonio, TX 78244, USA. www.4adi.com
Alpha Laboratories Ltd	40 Parham Dr, Eastleigh, SO50 4NU, UK. www.alphalabs.co.uk
Ambion	850 Lincoln Centre Drive, Foster City, CA 94404, USA. www.ambion.com
Anglia Scientific	850 Lincoln Centre Drive, Foster City, CA, 94404, USA. www.appliedbiosystems.com
Applied Biosystems	Lingley House 120 Birchwood Boulevard, Warrington, Cheshire, WA3 7QH, Uk. www.appliedbiosystems.com
BD	Becton Dickinson and Company, Belliver Industrial Estate, Belliver Way, Plymouth, Devon PL6 7BP, UK. www.bd.com

Bio-Rad Ltd.	Life Science Research, Education, Process Separations, Food Science, 2000 Alfred Nobel Drive, Hercules, California 94547, USA. www.bio-rad.com
Dako	Cambridge House, St Thomas Place, Ely, Cambridgeshire, CB7 4EX, UK. www.dako.com
Fisher Scientific UK Ltd	Bishop Meadow Road, Loughborough, LE11 5RG, UK. www.fishersci.co.uk
GE Healthcare	Amersham Place, Little Chalfont, Buckinghamshire, HP7 9NA, UK. www.gehealthcare.co.uk
GraphPad Software	7825 Fay Avenue, Suite 230, La Jolla, CA, USA. www.graphpad.com
Greiner Bio-One	Brunel Way, Stroudwater Business Park, Stonehouse, GL10 3SX, UK. www.greinerbioone.com
Hamamatsu Photonics (UK) Ltd	10 Tewin Rd, Welwyn Garden City, Hertfordshire, AL7 1BW, UK. www.hamamatsu.com
Hoefer Inc. MA	84 October Hill Rd, Suite 10, Holliston, 01746, USA. www.hoeferinc.com
Improvision Ltd	Coventry, UK www.improvision.com
Leica Biosystems	Balliol Business Park West, Newcastle Upon Tyne, NE12 8EW, UK. www.leicabiosystems.com

Leica Microsystems	Larch House, Woodland Business Park, Breckland, Linford Woods, Milton Keynes, MK14 6FG, UK. www.leica-microsystems.com
Manor Farm Feeds	Green Lane, Owston, Oakham, Leicestershire LE15 8DH, UK. www.manorfarmfeeds.co.uk
Media Cybernetics	401 N Washington Street, Rockville, 20850, MD, USA. www.mediacy.com
Menzel-Gläser	Glasbearbeitungswerk GmbH & Co., Saarbrückener Str. 248, D-38116, Braunschweig, Germany. www.menzel.de
Merial Animal Health Ltd	Sandringham House, Harlow Business Park, Harlow, Essex, CM19 5QE, UK. http://merial.com/